UNIVERSIDAD COMPLUTENSE DE MADRID
FACULTAD DE MEDICINA

TESIS DOCTORAL

Hacia nuevas estrategias terapéuticas basadas en cannabinoides para el síndrome de Dravet

Towards new therapeutic strategies based on cannabinoids for Dravet syndrome

MEMORIA PARA OPTAR AL GRADO DE DOCTOR

PRESENTADA POR

Cristina Alonso Gómez

Directores

Javier Fernández Ruiz
Onintza Sagredo Ezkioga

Madrid

UNIVERSIDAD COMPLUTENSE DE MADRID

FACULTAD DE MEDICINA

TESIS DOCTORAL

HACIA NUEVAS ESTRATEGIAS TERAPÉUTICAS BASADAS EN CANNABINOIDES PARA EL SÍNDROME DE DRAVET

TOWARDS NEW THERAPEUTIC STRATEGIES BASED ON CANNABINOIDS FOR DRAVET SYNDROME

MEMORIA PARA OPTAR AL GRADO DE DOCTOR

PRESENTADA POR:

Cristina Alonso Gómez

DIRIGIDA POR:

Javier Fernández Ruiz
Onintza Sagredo Ezkioga

Madrid, 2021

UNIVERSIDAD COMPLUTENSE DE MADRID
FACULTAD DE MEDICINA

TESIS DOCTORAL

HACIA NUEVAS ESTRATEGIAS TERAPÉUTICAS BASADAS EN CANNABINOIDES PARA EL SÍNDROME DE DRAVET

TOWARDS NEW THERAPEUTIC STRATEGIES BASED ON CANNABINOIDS FOR DRAVET SYNDROME

MEMORIA PARA OPTAR AL GRADO DE DOCTOR

PRESENTADA POR

CRISTINA ALONSO GÓMEZ

DIRECTORES

JAVIER FERNÁNDEZ RUIZ
ONINTZA SAGREDO EZKIOGA

SUMMARY/RESUMEN

SUMMARY

Towards new therapeutic strategies based on cannabinoids for Dravet syndrome

Dravet syndrome (DS) is a rare genetic epileptic encephalopathy affecting children which, in approximately 70-80% of patients, is caused by loss-of-function mutations in the *Scn1a* gene, which encodes the α1 subunit of the voltage-gated sodium channel ($Na_V1.1$). Clinically, these patients present different types of epileptic seizures, which are frequently accompanied by some comorbidities such as developmental delay, cognitive impairment, hyperactivity, autistic traits and a rate of premature mortality of around 20%. Therapeutic strategies typically involve a complex polytherapy, with antiepileptic drugs whose action mechanisms are focused on correcting hyperexcitability, i.e., the imbalance between excitation and inhibition occurring in epilepsy. Current treatment algorithms often lead to tolerance issues as well as adverse effects, and around 30% of patients remain refractory. Therefore, there is an urgent need for new and effective therapeutic approaches.

Together with hyperexcitability, oxidative stress and neuroinflammation comprise a pathogenic triad that plays a key role within the pathophysiology of diverse forms of epileptic syndromes, including DS. These pathological processes occur as a consequence of epileptic activity, and contribute to increase the susceptibility to subsequent seizures as well as associated comorbidities. Thus, compounds able to modulate these mechanisms may represent a promising disease-modifying strategy. In this context, the non-psychotropic phytocannabinoid cannabidiol (CBD) has been recently approved for the treatment of DS and other forms of pediatric epilepsy. In addition to its anticonvulsant potential in these patients, CBD exerts beneficial effects against excitotoxicity, inflammation and oxidative stress in several experimental conditions, thus positioning this molecule as a compound with therapeutic potential beyond epileptic activity. Moreover, several preclinical studies have revealed that other compounds in the cannabis plant also represent a promising strategy to modulate both epileptic activity and associated behavioral disturbances. Among these molecules, in this Doctoral Thesis we have focused on β-caryophyllene (BCP), a cannabis-derived sesquiterpene that has shown anticonvulsant effects in experimental models of acute epilepsy, as well as effectiveness against inflammation and oxidative stress in a wide variety of preclinical studies in several diseases. Interestingly, in certain situations, phytocannabinoids and terpenes can act synergistically according to the so-called

"entourage" effect and exert additional positive effects, which would enable to improve current therapeutic strategies.

Based on this background, the **general aim** of this Doctoral Thesis is to deepen the knowledge and validate the therapeutic potential of cannabinoids in DS. This general aim can be divided into three **specific aims**:

- **Aim 1:** Neuropathological characterization of a novel DS mouse model.
- **Aim 2:** Analysis of BCP as an anticonvulsant and disease-modifying agent in DS.
- **Aim 3:** Evaluation of the effectiveness of a combination of BCP and CBD as a potential therapeutic approach in DS.

To address **Aim 1,** in Chapter 1 we performed several behavioral and molecular analysis to validate *Scn1a*-A1783V conditional knock-in mice as a suitable experimental model for DS. Mice recapitulated the main features of DS progression, including developmental delay, hyperactivity, autistic traits, cognitive impairment, seizuring susceptibility and premature death. Of note, these alterations were maximal at postnatal day 25, which correlates with the greater severity of the disease that is observed at early ages in DS patients. However, phenotype was not as aggressive and severe as previous DS models, which enabled us to validate our model as a good experimental tool for long-term studies. Biochemical and histological analysis revealed a partial dysregulation of the endocannabinoid system and the hippocampal neurogenesis, as well as neuroinflammatory events characterized by a prominent reactive gliosis and a partially disrupted blood-brain barrier.

Regarding **Aim 2,** in Chapter 2 we studied BCP effects on epileptic activity and behavioral disturbances in our DS mice. The acute administration of BCP 100 mg/kg was able to attenuate seizure activity induced by the proconvulsant agent pentylenetetrazol (PTZ). Along with these findings, the chronic administration of BCP 10 mg/kg exerted effectiveness against developmental delay, hyperactivity, autistic traits and cognitive impairment. Moreover, BCP was able to attenuate reactive gliosis in both experimental paradigms, thus positioning this molecule as a promising anticonvulsant and disease-modifying agent for DS. Therefore, these results also confirm the importance of modulating neuroinflammatory processes rather than just focusing on epileptic activity.

In Chapter 3, we addressed **Aim 3** with the purpose of evaluating the possible positive effects of a combination of BCP and CBD. *In vitro* experiments with BV2 cells revealed that this combination attenuates more efficiently microglial activation and the expression of different inflammatory markers. *In vivo* procedures with our DS mice

similarly showed more potent effects on modulating DS progression and glial reactivity. Overall, these findings suggested the pharmacological interaction of both molecules and their ability to increase treatment efficacy.

In summary, as **conclusions**, results presented in this Doctoral Thesis have allowed us to validate a novel DS mouse model which faithfully recapitulates disease progression and is useful for long-term studies. Moreover, pharmacological studies have positioned BCP as a promising molecule for DS treatment, not only against epileptic activity, but also against associated comorbidities. Interestingly, combination with CBD adds additional effects, so that this evidence could serve as a basis for improving current therapeutic strategies for DS.

RESUMEN

Hacia nuevas estrategias terapéuticas basadas en cannabinoides para el síndrome de Dravet

El síndrome de Dravet (SD) es una encefalopatía epiléptica rara y genética que afecta a niños y que, en alrededor del 70-80% de los pacientes, está causado por mutaciones con pérdida de función en el gen *Scn1a*, que codifica la subunidad α1 del canal de sodio dependiente de voltaje ($Na_V1.1$). En cuanto a la clínica, estos pacientes presentan diversos tipos de crisis epilépticas, que a menudo se acompañan por algunas comorbilidades tales como retraso en el desarrollo, alteraciones cognitivas, hiperactividad, rasgos autistas y una tasa de muerte prematura de alrededor del 20%. Las estrategias terapéuticas normalmente implican una compleja politerapia, con fármacos antiepilépticos cuyos mecanismos de acción se centran en corregir la hiperexcitiblidad, es decir, el desequilibrio entre excitación e inhibición que ocurre en situaciones de epilepsia. Los algoritmos de tratamiento actuales a menudo conllevan problemas de tolerancia, así como efectos adversos, y alrededor del 30% de los pacientes permanecen refractarios. Por ello, es urgente la búsqueda de nuevas aproximaciones terapéuticas eficaces.

Junto con la hiperexcitabilidad, el estrés oxidativo y la neuroinflamación conforman una triada patogénica que juega un papel clave en la patofisiología de diversos síndromes epilépticos, incluyendo el SD. Estos eventos patológicos ocurren como consecuencia de la actividad epiléptica, y contribuyen a su vez a aumentar la susceptibilidad a la aparición de nuevas crisis, así como de las comorbilidades asociadas. Por ello, compuestos capaces de modular estos mecanismos representan una prometedora estrategia modificadora de la enfermedad. En este contexto, el fitocannabinoide no psicoactivo cannabidiol (CBD) se ha aprobado recientemente para el tratamiento del SD y otras formas de epilepsia pediátrica. Además de su potencial anticonvulsivante en estos pacientes, el CBD ha demostrado efectos beneficiosos frente a la excitotoxicidad, la inflamación y el estrés oxidativo en varias condiciones patológicas a nivel experimental, lo que posiciona a esta molécula como un compuesto con potencial terapéutico más allá de la actividad epiléptica. Además, varios estudios preclínicos han revelado que otros componentes de la planta del cannabis también representan una estrategia prometedora para modular tanto la actividad epiléptica como las alteraciones comportamentales asociadas. Entre estas moléculas, en esta Tesis Doctoral nos hemos centrado en el β-cariofileno (BCP), un sesquiterpeno derivado del cannabis que ha demostrado efectos anticonvulsivantes en modelos agudos de epilepsia experimental, así como eficacia frente a la inflamación y el estrés oxidativo en una gran variedad de estudios preclínicos en diversas patologías.

Interesantemente, bajo determinadas circunstancias, los fitocannabinoides y los terpenos pueden actuar de manera sinérgica de acuerdo al conocido como efecto "séquito" y ejercer así efectos positivos adicionales, lo que permitiría mejorar las estrategias terapéuticas actuales.

Con estos antecedentes, el **objetivo global** de esta Tesis Doctoral es profundizar en el conocimiento y validar el potencial terapéutico de los cannabinoides en el SD. Este objetivo global se puede dividir en tres **objetivos específicos**:

- **Objetivo 1:** Caracterización neuropatológica de un nuevo modelo murino de SD.
- **Objetivo 2:** Análisis del BCP un agente anticonvulsivante y modificador de la enfermedad para el SD.
- **Objetivo 3:** Evaluación de la eficacia de la combinación de BCP y CBD como un posible abordaje terapéutico para el SD.

Para abordar el **Objetivo 1**, en el Capítulo 1 llevamos a cabo diversos análisis comportamentales y moleculares para validar los ratones knock-in condicionales *Scn1a*-A1783V como un buen modelo experimental para el estudio del SD. Los ratones recapitularon las principales características del progreso del SD, incluyendo retraso en el desarrollo, hiperactividad, rasgos de tipo autista, alteraciones cognitivas, susceptibilidad epiléptica y muerte prematura. Es de destacar que estas alteraciones fueron especialmente acentuadas en el día postnatal 25, lo que coincide con la mayor severidad de la enfermedad que se observa a etapas tempranas en los pacientes. Sin embargo, el fenotipo no resultó ser tan agresivo y severo como el de los modelos experimentales anteriores, lo que permitió validar nuestro modelo como una buena herramienta experimental para llevar a cabo estudios a largo plazo. Los análisis bioquímicos e histológicos pusieron de manifiesto una desregulación parcial del sistema endocannabinoide y de la neurogénesis hipocampal, así como eventos neuroinflamatorios caracterizados por una acentuada gliosis reactiva y una disrupción parcial de la barrera hematoencefálica.

Con respecto al **Objetivo 2**, en el Capítulo 2 evaluamos los efectos del BCP en relación a la actividad epiléptica y las alteraciones comportamentales de nuestro modelo murino del SD. La administración aguda de BCP a 100 mg/kg fue capaz de atenuar la actividad epiléptica inducida por el agente proconvulsivante pentilenotetrazol (PTZ). Junto con estos resultados, la administración crónica de BCP a 10 mg/kg demostró eficacia frente al retraso en el desarrollo, la hiperactividad, la conducta de tipo autista y el deterioro cognitivo. Además, el BCP fue capaz de atenuar la gliosis reactiva en ambos paradigmas

experimentales, lo que posiciona a esta molécula como un prometedor agente modificador del progreso de la enfermedad y anticonvulsivante para el SD. Por lo tanto, estos resultados también confirman la importancia de modular los procesos de inflamación en lugar de centrarse únicamente en la actividad epiléptica.

En el Capítulo 3, abordamos el **Objetivo 3** con el fin de evaluar los posibles efectos positivos de la combinación de BCP y CBD. Los experimentos *in vitro* con las células BV2 indicaron que esta combinación atenúa de manera más eficaz la activación microglial y la expresión de diferentes marcadores inflamatorios. Procedimientos *in vivo* con el modelo animal del SD demostraron de manera similar efectos más potentes a la hora de modular el progreso de la enfermedad y la reactividad glial. En conjunto, estos resultados sugirieron la interacción farmacológica de ambas moléculas y su capacidad de aumentar la eficacia del tratamiento.

En resumen, como **conclusiones**, los resultados presentados en esta Tesis Doctoral han permitido la validación de un nuevo modelo murino del SD que recapitula fielmente la progresión de la enfermedad y que es apropiado para estudios a largo plazo. Además, los estudios farmacológicos han posicionado al BCP como una molécula prometedora para el tratamiento del SD, no solo frente a la actividad epiléptica, sino también contra las comorbilidades asociadas. De manera interesante, su combinación con CBD añade efectos adicionales, por lo que estas evidencias podrían servir como base para mejorar las estrategias terapéuticas actuales para el SD.

ABBREVIATIONS

2-AG	2-arachidonoylglycerol
2-OG	2-oleoylglycerol
2-PG	2-palmitoylglycerol
AA	Arachidonic acid
AAR	Alternate arm returns
ABHD	α/β-hydrolase domain
AC	Adenylate cyclase
ACEA	Arachidonyl-2-chloroethylamide
AEA	Anandamide
Akt	Protein kinase B
AMPA	α-amino-3-hydroxy-5-methyl-4-isoxazolepropionic acid
BBB	Blood-brain barrier
BCP	beta-caryophyllene
BM	Bone marrow
BSA	Bovine serum albumin
cAMP	Cyclic adenosine monophosphate
CB_1	Cannabinoid receptor type-1
CB_2	Cannabinoid receptor type-2
CBD	Cannabidiol
CBDV	Cannabidivarin
CBC	Cannabichromene
CBG	Cannabigerol
CBN	Cannabinol
CBV	Cannabivarin
CD70	Cluster of differentiation 70
cdc42	Cell division control protein 42 homolog
CNS	Central Nervous System
COX	Cyclooxygenase
CREB	cAMP response element-binding
CYP	Cytochrome P450
DAG	Diacylglycerol
DAGL	Diacylglycerol lipase
DAPI	4’,6-diamidino-2-phenylindole
DMEM	Dulbecco’s modified Eagle’s medium
DMSO	Dimethyl sulphoxide
DPBS	Dulbecco's phosphate-buffered saline
DS	Dravet syndrome
DSE	Depolarization-induced suppression of excitation
DSI	Depolarization-induced suppression of inhibition
ECS	Endogenous cannabinoid system
EDTA	Ethylenediaminetetraacetic acid
EEG	Electroencephalography
EMA	European Medicines Agency
EO	Essential oil

ERK1/2	Extracellular signal-regulated kinase 1/2
FAAH	Fatty acid amide hydrolase
FACS	Fluorescence-activated cell sorting
FBS	Fetal bovine serum
FDA	Food and Drug Administration
GABA	Gamma-aminobutyric acid
GAPDH	Glyceraldehyde-3-phosphate dehydrogenase
GCL	Granule cell layer
GEFS+	Generalized epilepsy with febrile seizures plus
GFAP	Glial fibrillary acidic protein
GPCR	G protein-coupled receptor
HER2	Human epidermal growth factor receptor 2
ICEGTC	Intractable childhood epilepsy with generalized tonic-clonic seizures
IL1β	Interleukin 1 beta
ILAE	International League Against Epilepsy
IPC	Intermediate progenitor cell
IPSC	Induced pluripotent stem cell
JNK	c-Jun N-terminal kinase
KA	Kainic acid
LGS	Lennox-Gastaut syndrome
LOX	Lipoxygenase
LPI	Lysophosphatidylinositol
LPS	Lipopolysaccharide
LTD	Long-term depression
MAGL	Monoacylglycerol lipase
MAPK	Mitogen-activated protein kinase
MDM	Monocyte-derived macrophage
NADA	*N*-arachidonoyldopamine
nAChR	Nicotinic acetylcholine receptor
NAGly	*N*-arachidonoylglycine
NAPE	*N*-arachidonoyl phosphatidylethanolamine
NAPE-PLD	*N*-arachidonoyl phosphatidylethanolamine phospholipase D
NAT	*N*-acyltransferase
NMDA	N-methyl-D-aspartate
NSC	Neural stem cell
OEA	*N*-oleoylethanolamine or oleoylethanolamide
PBS	Phosphate-buffered saline
PCR	Polymerase chain reaction
PE	Phosphatidylethanolamine
PEA	*N*-palmitoylethanolamine or palmitoylethanolamide
PI	Phosphatidylinositol
PI3K	Phosphoinositide 3-kinase
PKA	Protein kinase A
PLC	Phospholipase C
PMSF	Phenylmethylsulfonyl fluoride

PND	Postnatal day
PNS	Peripheral Nervous System
PPAR	Peroxisome-proliferator activated receptor
PTZ	Pentylenetetrazol
PV	Parvalbumin
PVDF	Polyvinylidene fluoride
Rac1	Ras-related C3 botulinum toxin substrate 1
RGC	Radial glia-like cell
RhoA	Ras homolog family member A
RIPA	Radioimmunoprecipitation assay
RNS	Reactive nitrogen species
ROS	Reactive oxygen species
RXR	Retinoid X receptor
SAP	Spontaneous alternation performance
SAR	Same arm returns
SDS	Sodium dodecyl sulfate
SE	Status epilepticus
SEA	*N*-stearoylethanolamine or stearoylethanolamide
SGZ	Subgranular zone
SMEI	Severe myoclonic epilepsy of infancy
SMEIB	Severe myoclonic epilepsy of infancy - borderline
SST	Somatostatin
SUDEP	Sudden unexpected death in epilepsy patients
SVZ	Subventricular zone
Syn1	Synapsin 1
TBS	Tris-buffered saline
Δ⁹-THC	Δ⁹-tetrahydrocannabinol
Δ⁹-THCV	Δ⁹-tetrahydrocannabivarin
TLR4	Toll-like receptor 4
TNFα	Tumor necrosis factor alpha
TRP	Transient receptor potential channel
WHO	World Health Organization

INTRODUCTION

1. DRAVET SYNDROME

1.1. Background and epidemiology

The word "epilepsy" derives from the Greek and means to be taken, seized or attacked. According to the World Health Organization (WHO), it is a serious chronic neurological condition that affects around 50 million people, which represents 1% of the population worldwide (Thurman *et al.*, 2011). Additionally, it is one of the most common disorders in childhood, including epileptic encephalopathies such as West, Dravet (DS), Doose and Lennox-Gastaut (LGS) syndromes, among others (Wirrell, 2016). According to the International League Against Epilepsy (ILAE), the term epileptic encephalopathy "embodies the notion that the epileptic activity itself may contribute to severe cognitive and behavioral impairments above and beyond what might be expected from the underlying pathology alone, and that these can worsen over time" (Berg *et al.*, 2010). Around 30% of these children remain refractory to current treatments, which means that they do not achieve seizure freedom after adequate trials of two antiepileptic drugs, leading to devastating implications for their proper development (Dale *et al.*, 2019). For a description of some common terms related to epilepsy, see Box 1.

DS is a rare epileptic encephalopathy that is accompanied by psychomotor and neurological developmental delay, which occurs in the first year of life in children that prior diagnosis are apparently normal (Dravet, 2011). It was first described in 1978 by the French psychiatrist and epileptologist Charlotte Dravet under the name of severe myoclonic epilepsy of infancy (SMEI) in order to distinguish it from LGS, which was at that moment considered as the most common and severe pediatric epilepsy (Dravet, 1978). She reported various early-onset epilepsy severe cases that, despite some similarities, could not be diagnosed with LGS due to some clinical differences, especially the existence of a higher frequency of myoclonic seizures and the absence of axial tonic seizures. From that moment, other authors reported similar cases in Europe and Japan (Dalla Bernardina *et al.*, 1982; Ogino *et al.*, 1986). Soon afterwards, many children were reported to develop similar symptoms to SMEI patients, but without myoclonic seizures or generalized spike-wave activity; thus, these cases were included in the same disorder as atypical or borderline cases (severe myoclonic epilepsy of infancy - borderline, SMEIB) (Oguni *et al.*, 2001). Furthermore, a subgroup of SMEIB patients was reported to exhibit mainly generalized tonic-clonic seizures rather than myoclonic seizures; these seizures were referred to as intractable childhood epilepsy with generalized tonic-clonic seizures (ICEGTC) (Fujiwara *et al.*, 2003). Generally, children with SMEIB or ICEGTC have fewer cognitive deficits and/or lack myoclonic seizures (Fukuma *et al.*, 2004).

Box 1. Epilepsy and seizures

Epilepsy is defined as "a disorder of the brain characterized by an enduring predisposition to generate epileptic seizures, and by the neurobiological, cognitive, psychological and social consequences of this condition". This definition requires the occurrence of at least one epileptic seizure, which is considered a "transient occurrence of signs and/or symptoms due to abnormal excessive or synchronous neuronal activity" (Fisher *et al.*, 2005, 2014).

According to behavioral observations and electroencephalography (EEG) activity, seizures are defined by onset as: (1) focal onset, (2) generalized onset and (3) unknown onset (Fisher *et al.*, 2017):

- Focal onset seizures are those in which the abnormal electrical activity begins locally on one hemisphere of the brain. They can be subdivided in:
    - Simple partial seizures, if consciousness is present.
    - Complex partial seizures, if consciousness is reduced or absent.

  Sometimes, the abnormal electrical activity can evolve quickly from a focal seizure to a tonic-clonic seizure affecting both hemispheres of the brain, known as a focal to bilateral tonic-clonic seizure.
- Generalized onset seizures are those in which the abnormal electrical activity originates simultaneously on both hemispheres of the brain, and they are characterized by a complete loss of consciousness. Six different types of generalized seizures can be distinguished:
    - Absence seizures are short periods of sudden loss of consciousness lasting only a few seconds, with no - or only minimal - motor manifestations.
    - Myoclonic seizures are sudden, abrupt and brief involuntary muscle contractions occurring either in one limb, or more widespread and bilateral.
    - Clonic seizures are repetitive, rhythmic and jerky flexing and stretching of the limbs.
    - Tonic seizures are sustained muscle contractions with a marked stiffness in a strained position.
    - Tonic-clonic seizures are characterized by a generalized stiffness (tonic phase) followed by violent muscle jerking (clonic phase). The patient typically falls down and becomes cyanotic, and when regains consciousness, he usually feels tiredness, headache and confusion. They are the most dramatic type of seizure, and are normally referred to as convulsive seizures.
    - Atonic seizures are sudden and short loss of muscle tone causing head or limbs drop, in which the patient often falls down but rapidly stands up and continues what he was doing.
- Unknown onset seizures are those which cannot be classified because inadequate/incomplete data, or limited access to EEG studies or other techniques.

Whenever a seizure persists for at least 30 minutes, or is repeated so frequently that recovery between attacks does not exist, status epilepticus (SE) occurs, which is defined as "a condition resulting either from the failure of the mechanisms responsible for seizure termination or from the initiation of mechanisms, which leads to abnormally, prolonged seizures. It can have long-term consequences, including neuronal death, neuronal injury, and alteration of neuronal networks, depending on the type and duration of seizures" (Trinka *et al.*, 2015). SE can be categorized as convulsive or nonconvulsive, depending on the presence or absence of prominent motor symptoms and the degree of impaired consciousness, but it is always considered both a neurologic and a medical emergency with the potential for significant morbidity and mortality (Pichler & Hocker, 2017).

Moreover, it was observed that epileptic activity was not limited to childhood but persisted into adulthood. For these reasons, the ILAE recognized it as a syndrome in 1989 (Commission on Classification and Terminology of the International League Against Epilepsy, 1989), and the eponym "Dravet syndrome" was proposed in honor to Charlotte Dravet. Under this eponym, not only SMEI, but also SMEIB and ICEGTC, are now considered.

Despite recognition and diagnosis tools having increased in the last years, DS is still considered a rare disease (classified as ORPHA 33069 according to the Orphanet classification). Its actual frequency is not well known, but it is estimated at 1 per 15.700-40.000 (1.4% of children with epilepsy) based on demographic studies in the United Kingdom, Denmark and the United States (Bayat *et al.*, 2015; Brunklaus *et al.*, 2012; Krueger & Berg, 2015). About sex differences, first studies reported that males were more often affected than females in a ratio of 2:1, but subsequent studies revealed that DS affects equally to both genders (Skluzacek *et al.*, 2011).

1.2. Clinical features and prognosis

According to Charlotte Dravet, three different stages can be identified in the course of DS (Dravet & Oguni, 2013; Gataullina & Dulac, 2017; Genton *et al.*, 2011) (Figure I1): (1) the febrile stage, (2) the worsening stage and (3) the stabilization stage.

In the first stage, the "febrile stage", the first seizure usually appears in the first year of life in an apparently normal child without previous neurological history. Normally, this first seizure occurs between 4 and 8 months of age triggered by mild fever (infection, vaccination, etc.) or a hot bath. It is typically a convulsive clonic seizure, generalized or unilateral, often longer than 15 minutes and evolving into SE. Shortly thereafter, other febrile - and also afebrile - seizures occur, simultaneously with a delay in psychomotor and neurological development.

Between 1 and 5 years of age, during the "worsening stage", different seizure types start to appear with a high frequency: generalized convulsive clonic or tonic-clonic seizures, myoclonic seizures, atypical absences and focal seizures. In contrast to the febrile context of the first stage, in this period seizures normally occur without fever. Moreover, the developmental delay becomes more evident, and cognitive deficit, motor disturbances, hyperactivity and autistic traits also appear.

After 5 years of age, the "stabilization stage" often begins, in which convulsive seizures decrease, are brief, and occur mainly in sleep; atypical absences and myoclonic seizures tend to disappear or attenuate. Although seizures become less common during adolescence and adulthood, they rarely disappear completely. Despite little improvements in psychomotor development and behavior, cognitive impairment often persists throughout the whole life of the patient, with a severe intellectual disability, autistic behavior, motor disturbances, personality disorders and stereotypes.

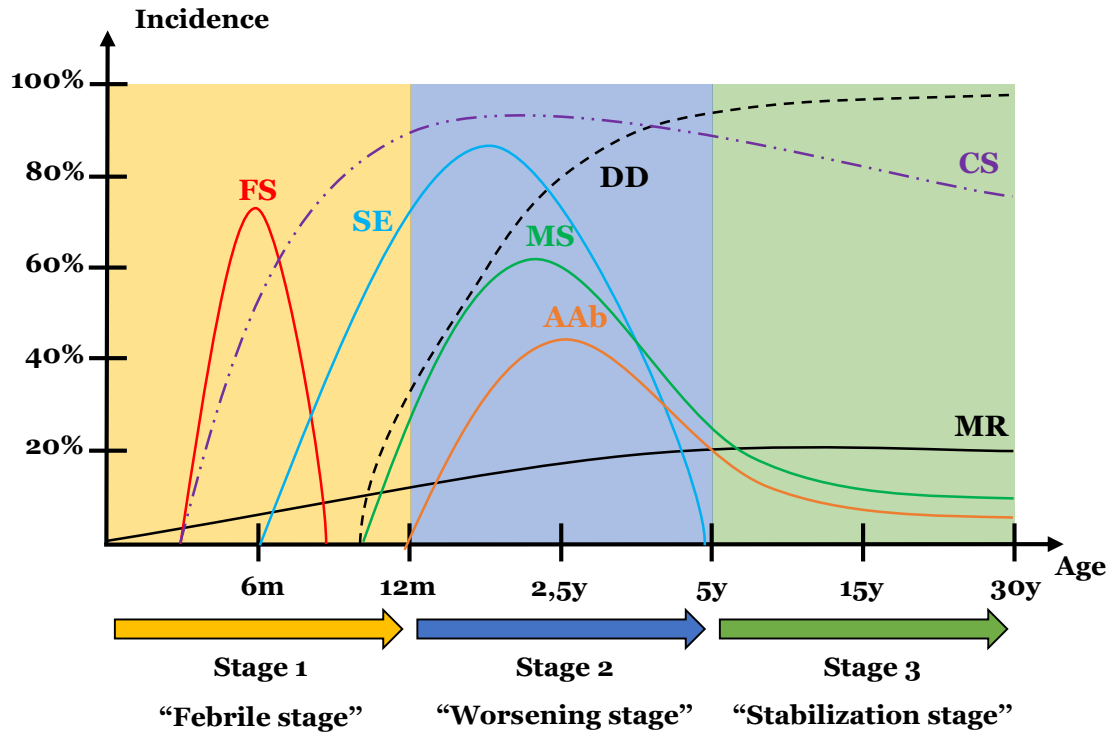

Figure I1. Clinical manifestations of DS and their relative incidence according to age. AAb, atypical absences; CS, convulsive seizures; DD, developmental delay; FS, febrile seizures; MR, mortality rate; MS, myoclonic seizures; SE, status epilepticus (adapted from Gataullina & Dulac, 2017).

Therefore, it seems clear that the DS outcome is poorly favorable. Different large-scale studies have been done in DS patients who were followed from childhood to adulthood, and findings are convergent (Akiyama *et al.*, 2010; Dravet *et al.*, 2009; Jansen *et al.*, 2006). Moreover, a major issue in DS is the high premature mortality and the marked young age at death; it ranges from 3.7-17.5% and occurs more often in young children with a peak at 3-7 years (Skluzacek *et al.*, 2011). Primary causes of premature death include accidental death or drowning, SE and sudden death. Sudden death, known as sudden unexpected death in epilepsy patients (SUDEP), is the main cause of early mortality, accounting for nearly 50% of cases (Shmuely *et al.*, 2016). Overall, the risk of premature death in DS, which is extremely higher than the rates in other refractory epilepsies, is one of the major concerns among patients and families.

Although long-term outcome and comorbidities are highly similar, there is some degree of phenotypic variability between patients; therefore, relative incidences can be defined (Figure I1). Moreover, a better prognosis is associated with having had less than three episodes of SE during childhood, whereas EEG abnormalities during the first year of life, motor disturbances, tonic seizures, as well as an early appearance of myoclonic seizures and absences are associated with a poor prognosis (Brunklaus *et al.*, 2012; Gataullina & Dulac, 2017).

1.3. Etiology and genetics

DS is a genetic disorder whose pathogenesis includes a deep imbalance in neuronal excitability, which leads to hyperexcitability and seizures. Since ion channels are essential for neuronal excitability, it is not surprising that many DS mutations have been identified in genes encoding ion channels subunits. Therefore, DS is considered a channelopathy (Brunklaus & Zuberi, 2014). Approximately 80% of patients carry a mutation in the *Scn1a* gene. In the remaining 20% of cases, additional genes like *Scn2a*, *Scn8a*, *Scn9a*, *Scn1b*, *Hcn1*, *Kcna2*, *Gabra1*, *Gabrg2*, *Cacnb4*, *Pcdh19*, *Stxbp1* and *Chd2* are potentially implicated (Table I1) (Akiyama *et al.*, 2012; Steel *et al.*, 2017).

Table I1. Genes implicated in DS (adapted from Akiyama *et al.*, 2012; Steel *et al.*, 2017).

Gene (location)	**Product**
Sodium channels subunits	
Scn1a (2q24)	Voltage-gated sodium channel α1 subunit
Scn2a (2q24)	Voltage-gated sodium channel α2 subunit
Scn8a (12q13)	Voltage-gated sodium channel α8 subunit
Scn9a (2q24)	Voltage-gated sodium channel α9 subunit
Scn1b (19q13)	Voltage-gated sodium channel β1 subunit
Potassium channels subunits	
Hcn1 (5p12)	Potassium/sodium hyperpolarization-activated cyclic nucleotide-gated channel 1
Kcna2 (1p13)	Voltage-gated potassium channel subfamily A member 2
Chloride channels subunits	
Gabra1 (5q34)	$GABA_A$ receptor α1 subunit
Gabrg2 (5q34)	$GABA_A$ receptor γ2 subunit
Calcium channels subunits	
Cacnb4 (2q22-q23)	Voltage-gated calcium channel β4 auxiliary subunit
Non-channels	
Pcdh19 (Xq22)	Protocadherin 19
Stxbp1 (9q34)	Syntaxin-binding protein 1
Chd2 (15q26)	Chromodomain helicase DNA-binding protein 2

Undoubtedly, one of the most remarkable features of DS is its strong association with mutations in *Scn1a*. This gene contains 26 exons encoding the α1 subunit of the voltage-gated sodium channel, $Na_V1.1$. The $Na_V1.1$ protein is a single polypeptide chain of 260 kDa that folds to four homologous domains (DI to D4) of six transmembrane segments each (S1 to S6). Specific elements within this protein are associated with different essential functions within the channel: (1) S4 segments act as voltage sensors and promote channel opening upon changes in membrane potential, (2) the four loops between segments S5 and S6 form the pore and confer selectivity for sodium and (3) the cytosolic loop connecting domains III and IV is involved in channel inactivation (Figure I2) (Sula *et al.*, 2017). Thus, depending on the location and properties of the amino acid affected, mutations in *Scn1a* will affect the function of $Na_V1.1$ differently.

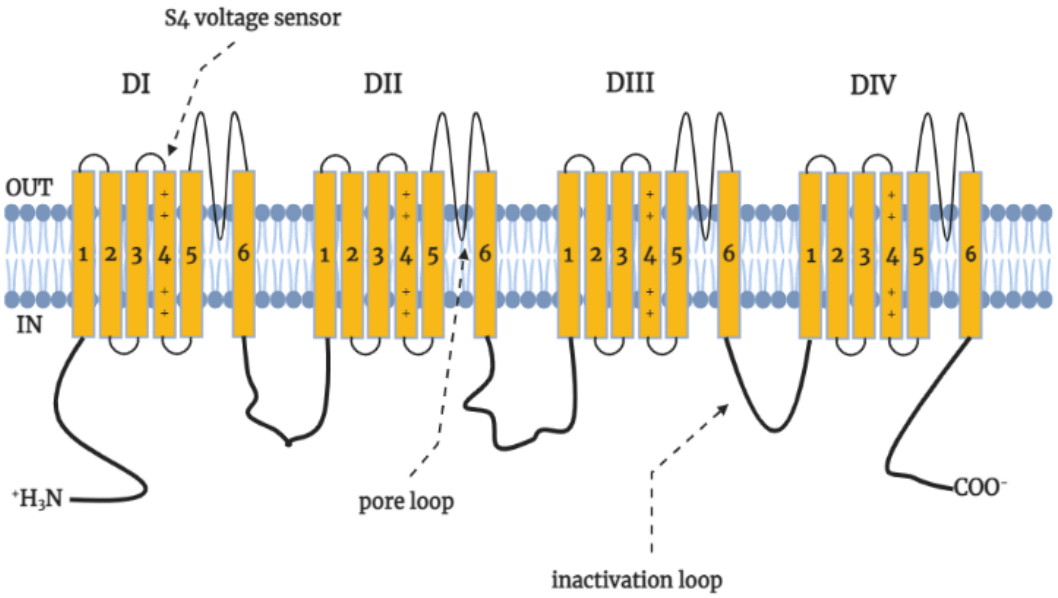

Figure I2. Secondary structure of the α1 subunit of the voltage-gated sodium channel, $Na_V1.1$.

Scn1a mutations were first identified in two large families affected by generalized epilepsy with febrile seizures plus (GEFS+) (Escayg *et al.*, 2000), now renamed as "genetic epilepsy with febrile seizures plus". Soon afterwards, *de novo* mutations in this gene were identified in seven children affected by DS (Claes *et al.*, 2001). Since then, subsequent genetic studies have been performed revealing that around 80% of DS patients carry a mutation in this gene. Therefore, *Scn1a* mutations form a spectrum from mild clinical epilepsy (GEFS+) to severe intractable epilepsy (DS), with borderline clinical syndromes (SMEIB and ICEGTC) presenting an intermediate severity but closer to the severe end (Catterall *et al.*, 2010; Fujiwara *et al.*, 2003; Stafstrom, 2009) (Figure I3).

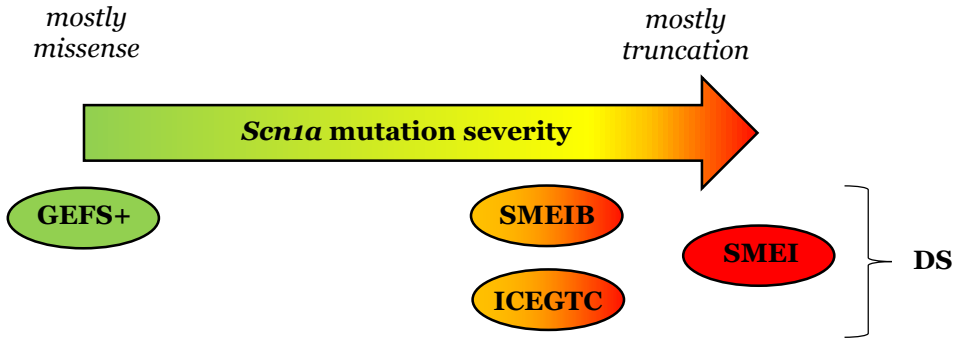

Figure I3. Spectrum of clinical syndromes resulting from *Scn1a* mutations (adapted from Stafstrom, 2009).

The variable severity of mutations in this gene appears to explain the spectrum of severity of *Scn1a*-related epileptic disorders, thus existing a genotype-phenotype correlation. Approximately, 30 *Scn1a* mutations have been described in GEFS+ patients; these are typically missense mutations that are spread throughout the gene, but most frequently outside the pore-forming region, suggesting that these mutations alter partially - but do not completely abolish - *Scn1a* activity (Escayg & Goldin, 2010; Gambardella & Marini, 2009). In contrast, most of the more than 600 *Scn1a* mutations that have been described in DS patients are nonsense or frameshift truncating mutations that result in a non-functional protein product (Marini *et al.*, 2011); missense mutations occur in about one-third of DS patients, and normally result in polarity change of an amino acid located in the S4 voltage sensors or the S5-S6 pore loop region (Zuberi *et al.*, 2011). Since individuals are heterozygous for these mutations, the *Scn1a* gene exhibit haploinsufficiency, which results from a 50% reduction of functional $Na_V1.1$ protein. These findings support the existence of a genotype-phenotype correlation, since mutations resulting in greater alterations in the properties of the channel are relatively associated with a more severe phenotype (Figure I3).

As mentioned before, most *Scn1a* mutations in DS patients arise *de novo*, but familial mutations occur in around 5-10% of cases and are usually missense in nature. Interestingly, in these familial cases, the pathogenic variant is inherited in a dominant manner from other family members who have a missense mutation in *Scn1a* and mild phenotypes consistent with GEFS+ spectrum (Marini *et al.*, 2011).

Despite being a congenital genetic syndrome, clinical manifestations do not begin from birth but start later on, during the first year of life (Dravet & Oguni, 2013; Gataullina & Dulac, 2017), a phenomenon that can be explained attending to the expression and maturation pattern of voltage-gated sodium channels. In neonates, $Na_V1.1$ expression is

very low, but compensated by $Na_V1.3$. With increasing age, $Na_V1.3$ normally declines and $Na_V1.1$ progressively increases, reaching adult levels over the first four weeks of life in rodents, which corresponds to the first year of life in humans (Cheah *et al.*, 2013). Thus, the timing of DS onset is a result of the failure of $Na_V1.1$ to fully replace the natural loss of $Na_V1.3$ (Mashimo *et al.*, 2010; Ogiwara *et al.*, 2007).

1.4. Pathophysiology

To fully understand DS pathophysiology, it is important to define the specific subcellular localization of $Na_V1.1$, as well as the main cell substrates affected.

On the one hand, $Na_V1.1$ is primarily localized in the neuronal soma and proximal dendrites, where the synaptic impulses are integrated in order to control neuronal excitability for action potential initiation and propagation. On the other hand, although mutations are not limited to specific cell types, different studies have revealed that some cell populations are more affected than others. Particularly, GABAergic interneurons are those mainly affected in this disorder. Therefore, loss-of-function mutations severely impair sodium currents and action potential firing in these cells, thus leading to a decreased GABAergic inhibitory tone and, subsequently, marked hyperexcitability in neuronal circuits (Catterall *et al.*, 2010, 2018). In addition, although $Na_V1.1$ is expressed throughout the brain, reduced sodium currents are specifically observed in hippocampal, cortical and cerebellar GABAergic interneurons (Han *et al.*, 2012; Ogiwara *et al.*, 2007; Yu *et al.*, 2006). Taking into account all these considerations and thanks to different experimental DS models, we are currently able to explain - at least in part - the underlying mechanisms of the complex DS phenotype, which is mainly characterized by epileptic seizures, comorbidities and premature death (Dravet & Oguni, 2013; Gataullina & Dulac, 2017).

Epileptic seizures are due to reduced sodium currents in GABAergic parvalbumin (PV)- and somatostatin (SST)-positive interneurons in the hippocampus and cerebral cortex; since pyramidal glutamatergic excitatory neurons are not affected, this leads to hyperexcitability and epileptic seizures. This was first elucidated using a heterozygote *Scn1a* knock-out mouse model (*Scn1a*$^{+/-}$) (Yu *et al.*, 2006), and has been supported by further studies carried out with other mouse models (Martin *et al.*, 2010; Mashimo *et al.*, 2010; Ogiwara *et al.*, 2007). Furthermore, GABA is a neurotransmitter importantly involved in thermoregulation; however, GABAergic transmission is also decreased in situations of hyperthermia (Qu *et al.*, 2007), which would explain the fact that DS children usually have seizures by elevated body temperature (febrile seizures) as their first symptom (Gataullina & Dulac, 2017; Oakley *et al.*, 2009). With DS progression,

other types of spontaneous seizures start to appear (Figure I1). Interestingly, fever impairs trafficking and/or accelerates endocytosis of surface $GABA_A$ receptors in those DS patients carrying a mutation in the *Gabrg2* gene, encoding the $GABA_A$ receptor γ2 subunit (Kang *et al.*, 2006). Therefore, genetics can explain the appearance of epileptic seizures in these patients, since a deep imbalance among excitatory and inhibitory synapses is established in brain networks.

Moreover, it is pivotal to remark several particularities of the immature developing brain that make children particularly susceptible to seizures compared with later life (Huntsman *et al.*, 2020; Rakhade & Jensen, 2009). Seizure threshold is reduced in children, since there is a tendency towards an increased neuronal excitation over inhibition. It is due to an over expression of N-methyl-D-aspartate (NMDA) and α-amino-3-hydroxy-5-methyl-4-isoxazolepropionic acid (AMPA) receptors, and to the fact that GABA neurotransmitter is excitatory in early life (Jensen, 2002). Moreover, calcium homeostasis is altered in the immature brain; calcium influx can result in GABA receptors endocytosis, which increases this neuronal hyperexcitability (Rakhade & Jensen, 2009). In addition, the immature brain exhibits increased susceptibility to oxidative stress and inflammation (Johnston *et al.*, 2011), which together with excitotoxicity, represent the pathogenic triad that characterizes the pathophysiology of many brain disorders, including epilepsy (Ambrogini *et al.*, 2019) (Box 2). This evidence might help to explain why children diagnosed with epilepsy have significantly higher rates of associated comorbidities (Russ *et al.*, 2012).

Regarding the main comorbidities, some pathophysiological correlates related to specific DS symptoms have been also partially described as follows: (1) autistic-like behaviors are due to impaired action potential firing in GABAergic PV-positive interneurons in the hippocampus and cerebral cortex (Han *et al.*, 2012), (2) hyperactivity and stereotyped movements are due to impaired action potential firing in GABAergic SST-positive interneurons in the hippocampus and cerebral cortex (Rubinstein *et al.*, 2015), (3) cognitive deficits, such as attention and learning problems, are due to impaired action potential firing in GABAergic PV- and SST-positive interneurons in the hippocampus and cerebral cortex (Rubinstein *et al.*, 2015) and (4) movement abnormalities, such as ataxia and impaired motor reflexes, are due to impaired action potential firing in GABAergic Purkinje neurons in the cerebellar cortex (Kalume *et al.*, 2007).

Finally, the high premature death rate is one of the most serious and devastating issues regarding the long-term outcome of DS, with SUDEP as the main cause of this early mortality. It was initially suggested that SUDEP is more likely to be triggered by a neurological cause rather than by a cardiac one. First studies showed that loss of $Na_V1.1$

channel in GABAergic forebrain neurons was sufficient to reproduce the main phenotypic features of DS, including SUDEP. In these studies, SUDEP was proposed to be caused by a seizure-associated hyperactivity of the parasympathetic activity, leading to lethal bradycardia and dysfunction of the ventricle (Cheah *et al.*, 2012; Kalume *et al.*, 2013). However, since $Na_V1.1$ channel is expressed in heart as well as in brain (Mishra *et al.*, 2015), alterations in cardiac excitability contributing to SUDEP have been further analyzed. In this sense, more recent studies reveal that failing ventricular myocytes, in addition to seizures, are likely to primarily contribute to SUDEP (Frasier *et al.*, 2018). However, this issue is still controversial, so further studies are needed.

Box 2. Pathogenic mechanisms associated with epilepsy

Some additional pathogenic mechanisms associated with epilepsy may include (1) oxidative stress, (2) excitotoxicity and (3) neuroinflammation. These mechanisms represent a pathogenic triad which characterizes the pathophysiology of different brain disorders, including epilepsy (Ambrogini *et al.*, 2019).

- Oxidative stress is defined as an imbalance between pro- and antioxidants. In epilepsy, there is an excessive production of reactive oxygen (ROS) and nitrogen (RNS) species, which trigger tissue toxicity, harming DNA, proteins and fatty acids (Borowicz-Reutt & Czuczwar, 2020). Moreover, the brain is particularly susceptible to oxidative stress, since the activity of antioxidant enzymes, such as catalase or glutathione peroxidase, is around ten times lower in this organ (Puttachary *et al.*, 2015). Interestingly, antioxidant enzymes can be diminished in different pathologies, including epilepsy (Munguía-Martínez *et al.*, 2019).
- Excitotoxicity is characterized by an overactivation of postsynaptic glutamate receptors (mainly ionotropic) due to an excessive glutamate release. Toxic concentrations of glutamate increase calcium influx in postsynaptic terminals, mainly through NMDA receptor activation. This uncontrolled influx of calcium activates a wide variety of phospholipases, endonucleases and proteases, which eventually damage cell components and trigger degeneration of postsynaptic neurons (Ambrogini *et al.*, 2019). Additionally, NMDA receptor activation also induces reduced nicotinamide adenine dinucleotide phosphate (NADPH) oxidase 2 (NOX2) assembly and activity, producing ROS, NOS and oxidative stress (Kovac *et al.*, 2017).
- Neuroinflammation has been demonstrated to be a hallmark of epilepsy. Seizures normally lead to the activation of microglial cells and astrocytes, which consequently overproduce and release an array of inflammatory mediators, such as interleukin 1β (IL1β), tumor necrosis factor α (TNFα) and prostaglandins, among others (Steinborn *et al.*, 2014). As a result, these molecules activate specific signalling cascades in neurons and affect their excitability (Vezzani, 2011; Vezzani *et al.*, 2019).

Current therapies for epilepsy are predominantly anticonvulsant and do not modify this pathogenic triad, resulting in an insufficient ability to ameliorate symptoms and disease progression. Targeting these mechanisms may represent a promising tool for the treatment of these patients, since therapeutic strategies must include disease-modifying paradigms focused not only on the epileptic activity, but also on these pathological events and subsequent long-term comorbidities. As it will be further discussed in this Doctoral Thesis, cannabinoids represent an example of this promising therapeutic strategy.

1.5. Neuroinflammation, blood-brain barrier and epilepsy

Although epilepsy has been classically addressed focusing on brain hyperexcitability, neuroinflammation has proven to be a key hallmark within its pathophysiology (Vezzani, 2011; Vezzani *et al.*, 2019). It is defined as a chain of inflammatory events in the Central Nervous System (CNS) triggered by intruders of homeostasis, including infections, toxins, autoimmunity or other insults such as epileptic seizures. This persistent inflammatory response is associated with the production of cytokines, chemokines and ROS, which are mainly released by resident CNS glial cells, but also by infiltrating peripheral immune cells and other mediators (DiSabato *et al.*, 2016).

Seizures often lead to prominent gliosis, which includes a broad spectrum of changes in glial cells (particularly astrocytes and microglia). Main features of gliosis include (1) hypertrophy of cell bodies and processes, (2) increased cell proliferation and (3) upregulated expression of several proteins, such as intermediate filament proteins (glial fibrillary acidic protein (GFAP) and vimentin) in astrocytes and ionized calcium-binding adaptor molecule 1 (Iba-1) and cluster of differentiation 68 (Cd68) in microglia. Reactive glia may exert beneficial effects; however, when persistent, it may cause network hyperexcitability and tissue damage (Patel *et al.*, 2019).

As mentioned above, neuroinflammation can be also triggered by infiltrating peripheral inflammatory mediators and even immune cells, since seizures might promote a breakdown and an increased permeability in the blood-brain barrier (BBB) (see Box 3 for a brief overview on BBB structure). Under normal conditions, the brain is considered an immune-privileged site, since the BBB is relatively impermeable. However, BBB dysfunction has been reported in many CNS pathological conditions, including epileptic disorders (Kadry *et al.*, 2020; Remy & Beck, 2006). Changes in BBB permeability typically result from loss of tight complexes and degradation of basement membranes (Moya *et al.*, 2020). Additionally, several studies have demonstrated that during an inflammatory process, vascular endothelial cells might upregulate the expression of some cell adhesion molecules, such as vascular cell adhesion molecule 1 (VCAM-1) and intercellular adhesion molecule 1 (ICAM-1), thus facilitating the infiltration of immune cells into the brain parenchyma (Carman & Martinelly, 2015). Overall, this increased permeability often promotes extravasation to the brain of peripheral immune cells (macrophages, monocytes, neutrophils, B cells and T cells, among others), chemokines and other components (such as serum albumin or IgG), thus contributing to reactive gliosis (Figure I5) (Librizzi *et al.*, 2012).

Box 3. Blood-brain barrier: structural overview

The BBB is a highly specialized physical and biological barrier which is situated at the interface between blood and brain parenchyma, thus contributing to CNS protection and homeostasis maintenance. It is a multicellular structure comprised by a monolayer of endothelial cells in capillary walls, pericytes, a basement membrane surrounding the endothelial cells and astrocytic foot processes (Figure I4A) (Kadry *et al.*, 2020).

BBB properties are primarily determined by junctional complexes between adjacent endothelial cells, which are comprised of tight junctions and adherent junctions (Figure I4B). On the one hand, tight junctions (TJs) consist of (1) three transmembrane proteins, namely, claudins, occludins and junction adhesion molecules (JAMs) and (2) several cytosolic accessory proteins, including zonula occludens (ZO) proteins, cingulins and others. Transmembrane proteins physically associate with their counterparts of adjacent endothelial cells, whereas cytosolic accessory proteins link transmembrane proteins to actin cytoskeleton and participate in intracellular signalling. On the other hand, adherent junctions are mainly composed of cadherins, transmembrane proteins which also participate in the adhesion between adjacent endothelial cells and join the actin cytoskeleton through catenins. All these junctions contribute to maintain the structural and functional integrity of the BBB (Stamatovic *et al.*, 2008, 2016).

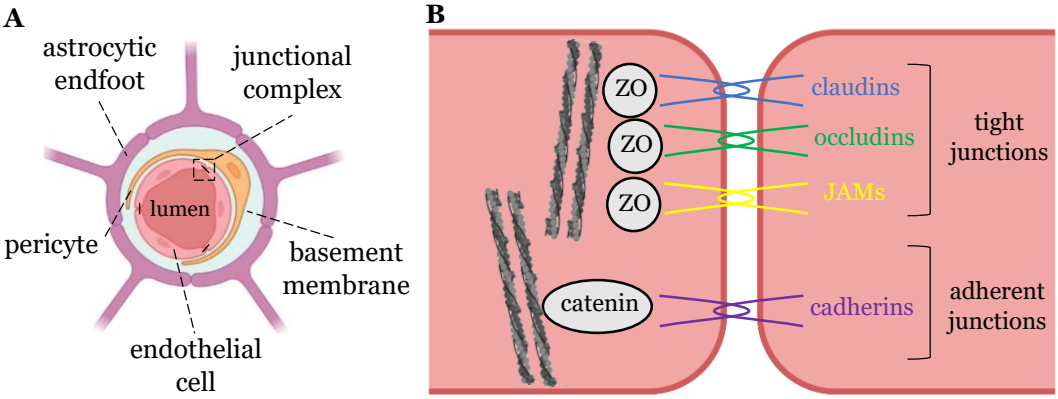

Figure I4. Schematic overview of BBB structure. Representation of **(A)** cell types and **(B)** junctional complexes within the BBB.

Consequently, these central and peripheral neuroinflammatory processes lead to a decrease in the seizure threshold which exacerbates and contributes to the onset of subsequent seizures, thus establishing a vicious pathological cycle of inflammation and seizures. Concurrently with seizures, long-term neuroinflammation may also contribute to the development of some of the comorbidities of epilepsy, such as cognitive deficits and autism (Kanner *et al.*, 2014).

Although little is known regarding the role of neuroinflammation in DS, some clinical evidence is currently available. In this context, some inflammation-related markers have been found to be upregulated in lymphocytes of patients, including CB_2 receptor,

peroxisome proliferator-activated receptor γ (PPARγ), cluster of differentiation 70 (Cd70, a marker of lymphocyte proliferation and activation) and pro-inflammatory cytokines (Rubio *et al.*, 2016). However, these data were obtained by studying peripheral blood, thus representing indirect evidence of what may be happening in the brain. Therefore, further research is needed to shine light on the role of inflammation in DS.

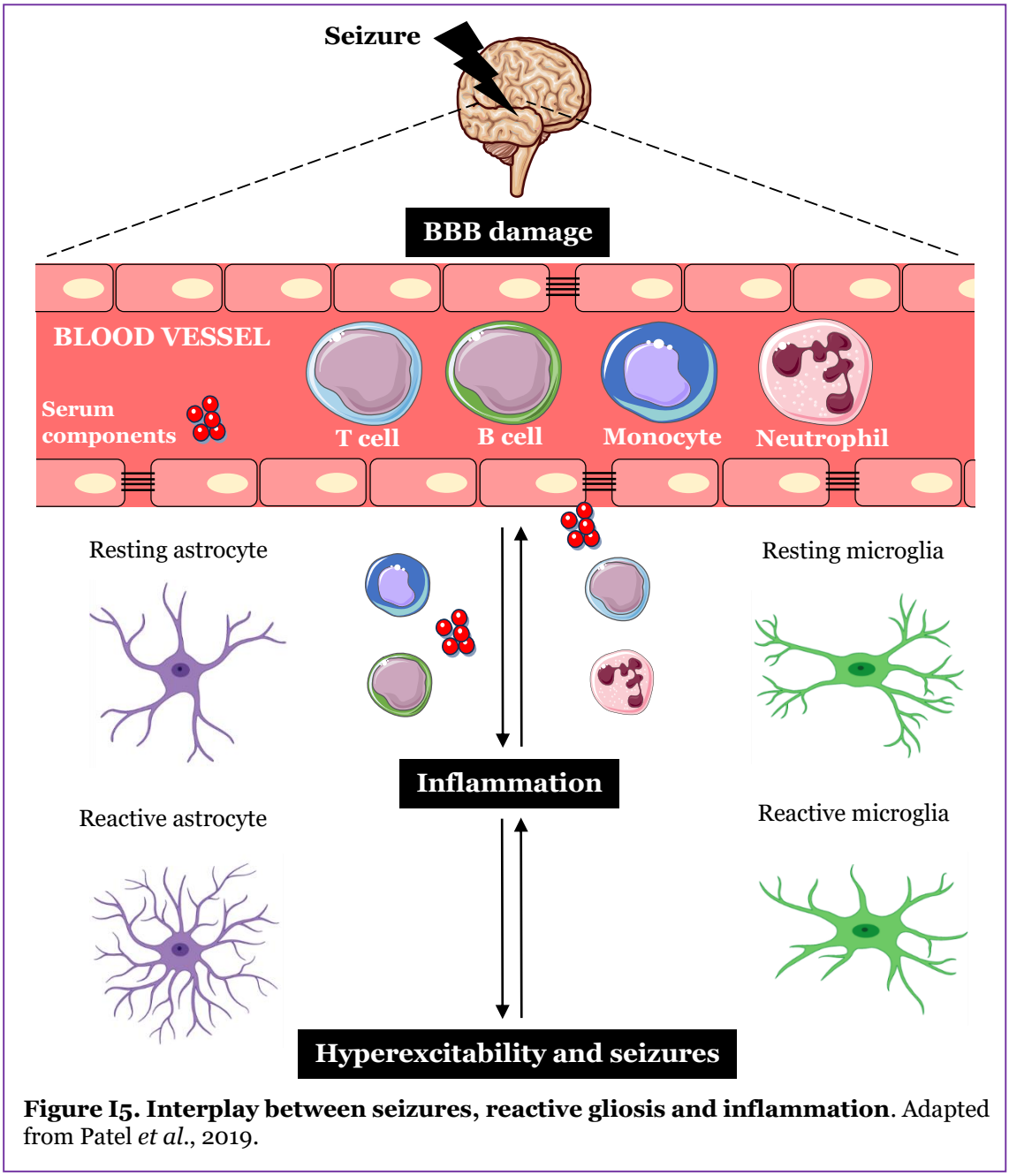

Figure I5. Interplay between seizures, reactive gliosis and inflammation. Adapted from Patel *et al.*, 2019.

1.6. Adult hippocampal neurogenesis and epilepsy

Another event that might play a key role in epilepsy is the so-called aberrant adult hippocampal neurogenesis (Bielefeld *et al.*, 2019; Chen *et al.*, 2020) (for further general insights about neurogenesis, see Box 4).

Box 4. Adult neurogenesis

Adult neurogenesis is a dynamic process which is restricted under normal conditions to two specialized niches in the adult mammalian brain: (1) the subventricular zone (SVZ) at the walls of the lateral ventricles, where newly generated neurons migrate through the rostral migratory stream to the olfactory bulb to become interneurons (Luskin, 1993), and (2) the subgranular zone (SGZ) of the hippocampal dentate gyrus, where new dentate granule cells are generated and integrated into the local granule cell synaptic circuitry (Kaplan & Hinds, 1977). Attending to the context of this Doctoral Thesis thesis, the focus will be on the SGZ.

The SGZ is a thin band located between the granule cell layer (GCL) and the hilus of the hippocampal dentate gyrus. Apart from the neural stem cells (NSCs) population, this niche is comprised by a dense vascular network and other cellular components, including endothelial cells, ependymal cells, astrocytes, microglia and mature neurons. All these components are tightly associated with the neural precursors, thus supporting and regulating neurogenesis both in physiological and pathological conditions (Gonçalves *et al.*, 2016).

NSCs are radial glia-like cells (RGCs, type 1 cells) that, like astrocytes, express GFAP. Under normal circumstances, NSCs remain quiescent, but after certain neurogenic stimuli, they get activated and enter into the cell cycle. They typically divide asymmetrically, producing one new NSC (to maintain the NSCs population) and a subsequent neural precursor, known as proliferating intermediate progenitor cell (IPCs, type 2 cells) with transient amplifying characteristics, which can give rise to neuroblasts (type 3 cells). These neuroblasts - and subsequent newborn and immature neurons - migrate into the inner granule cell layer and differentiate into mature granule cell neurons, which extend dendrites towards the molecular layer (ML) and project axons through the hilus towards the CA3, thus being integrated into the pre-existent synaptic network and contributing to spatial memory and learning abilities. This timeline of cell maturity can be assessed by the expression of different stage-specific molecular markers (Figure I6) (Gonçalves *et al.*, 2016; Ming & Song, 2011).

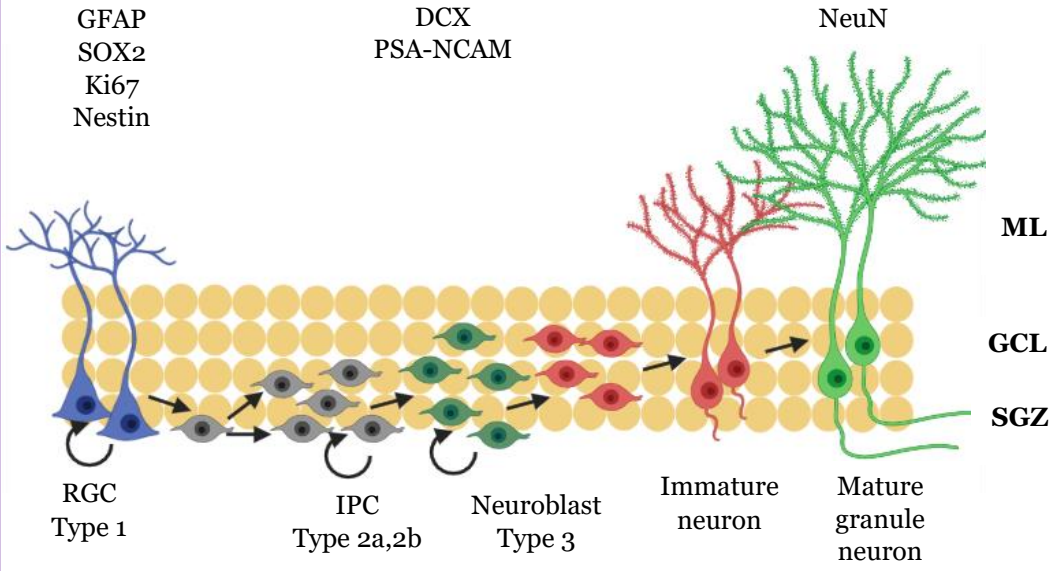

Figure I6. Stages of adult neurogenesis in the dentate gyrus of the hippocampus. Schematic view of cells at various stages of maturation contributing to neurogenesis and stage-specific molecular markers sequentially expressed during the process.

Neurogenesis in the hippocampal SGZ is a complex process that is chiefly regulated by neuronal activity in the surrounding hippocampal networks. Therefore, it can be affected under pathological situations of neuronal hyperactivation and excitotoxicity, such as epilepsy, thus resulting in the so-called aberrant neurogenesis. This aberrant process is characterized by a wide variety of cellular and molecular changes, including an increased proliferation of NSCs, production of ectopic granule neurons and neuronal hypertrophy, among others (Parent *et al.*, 1997). Moreover, this aberrant process may contribute to exacerbate epileptic seizures and associated comorbidities, since hippocampal neurogenesis participates in memory and learning (Cho *et al.*, 2015).

It is well-demonstrated that seizure activity induces a proliferative response in the dentate gyrus, which provokes NSCs hyperproliferation (Sierra *et al.*, 2015). Several experimental models suggest that this increased proliferation of precursor cells initially accelerates neuronal maturation and integration of newborn granule neurons. However, these cells typically present morphological abnormalities (such as hilar basal dendrites) as well as an ectopic migration (Scharfman *et al.*, 2000). When epilepsy is persistent, NSCs transform into reactive-NSCs that divide symmetrically. These reactive-NSCs then transform into reactive astrocytes which contribute to hippocampal reactive gliosis and neuroinflammation (Martín-Suárez *et al.*, 2020; Miro-García *et al.*, 2019; Sierra *et al.*, 2015; Valcárcel-Martín *et al.*, 2020). This is possible due to the fact that NSCs do not only have neurogenic (Seri *et al.*, 2001) but also gliogenic potential under certain circumstances, such as this context (Encinas *et al.*, 2011).

Moreover, not only seizures but also inflammatory signals related to the epileptic context, affect NSCs proliferation, migration and maturation. Specifically, NSCs constitutively express receptors for cytokines and other inflammatory factors, which allow them to sense the surrounding inflammatory responses typically occurring in epilepsy (Covacu & Brundin, 2015; Green *et al.*, 2012). Therefore, it seems clear that neurogenesis should be considered within the vicious pathological cycle of inflammation and seizures (Figure I7).

Of note, populations of NSCs and adult hippocampal neurogenesis are maximal in postnatal-juvenile stages and minimal in the aged brain, since NSCs get depleted over time in an activation-dependent manner (Sorrells *et al.*, 2018). Therefore, the impact of seizures on hippocampal neurogenesis is particularly severe in pediatric-onset epileptic syndromes, such as DS. In this sense, first studies in a DS mouse model have shown that DS mice present an altered neurogenic niche and a significant aberrant neurogenesis (Martín-Suárez *et al.*, 2020). According to this evidence, it seems clear that alterations

in adult hippocampal neurogenesis (together with neuroinflammation) may play a key role in DS pathogenesis.

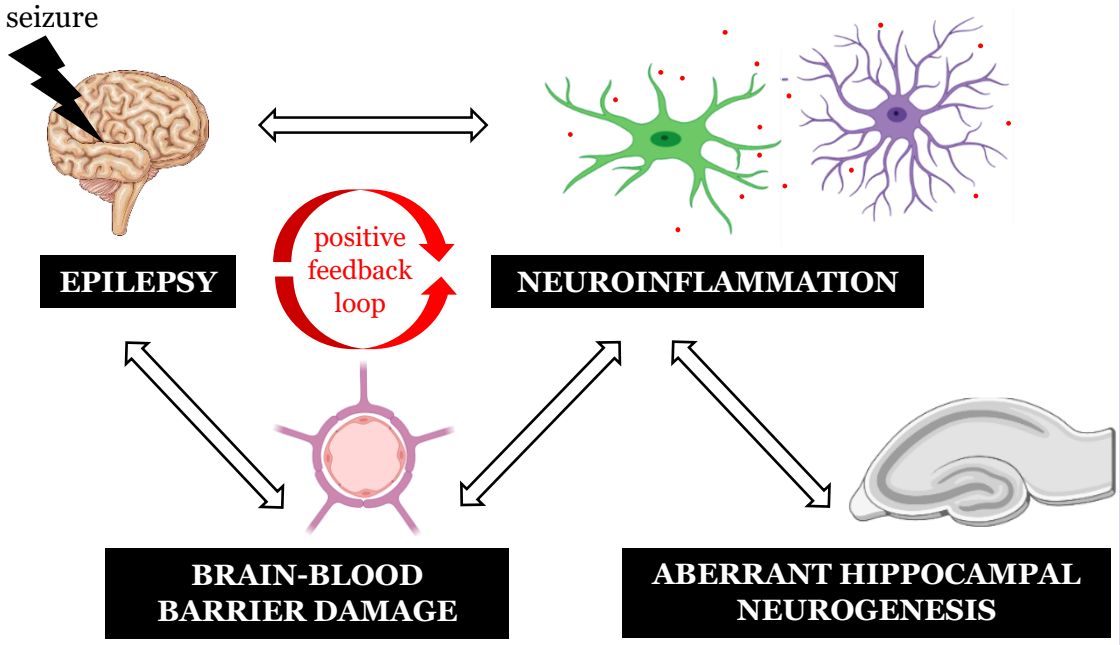

Figure I7. Relationship between epilepsy, blood-brain barrier integrity, neuroinflammation and hippocampal neurogenesis.

1.7. Management and therapeutic strategies

When making a diagnosis of DS, it is essential to define early appropriate therapeutic strategies, since it is a chronic, progressive and devastating disorder. Reasonably, the main therapy goal involves complete seizure cessation. Thus, the main focus is usually on preventing long-lasting seizures, reducing seizure frequency and improving cognitive and motor development.

The last proposed treatment guidance for DS included both pharmacological and non-pharmacological approaches, and considered three lines of treatment (Villanueva *et al.*, 2021; Wirrell *et al.*, 2017) (Figure I8).

Just after diagnosis, first-line therapies typically include valproic acid and clobazam. Normally, treatment is initiated with valproic acid, which reports a mean seizure reduction of 40% (Dressler *et al.*, 2015). It is a broad-spectrum drug with multiple mechanisms of action, such as increasing GABA synthesis and decreasing its degradation, inhibiting T-type calcium channels and decreasing glutamate synthesis (Wirrell & Nabbout, 2019). However, since seizure control is not fully effective, clobazam

is usually added, a benzodiazepine-derivative drug that acts as a partial agonist of $GABA_A$ receptors, thus potentiating GABAergic neurotransmission and providing additional benefits (Morimoto *et al.*, 2017).

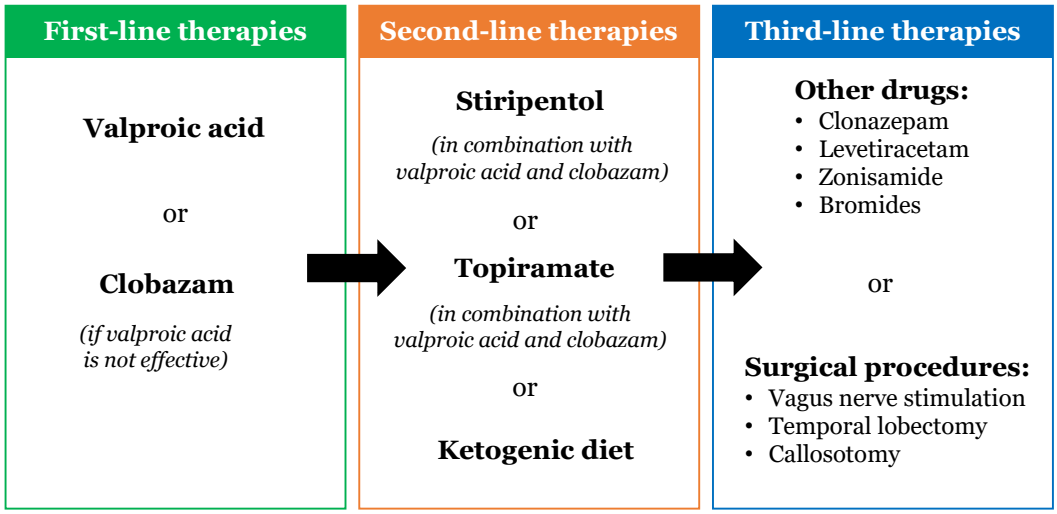

Figure I8. Treatment guidance for DS patients. Adapted from Villanueva *et al.*, 2021; Wirrell *et al.*, 2017.

Second-line therapies include topiramate and stiripentol. Topiramate has a broad spectrum of action, including enhancement of GABAergic neurotransmission, inhibition of kainate and AMPA glutamate receptors and blockade of voltage-gated calcium channels. Stiripentol has also multiple mechanisms of action, since it enhances GABAergic neurotransmission, as well as acts as a positive allosteric modulator of $GABA_A$ receptors (Wirrell & Nabbout, 2019). One of these agents is typically used in combination with valproic acid and clobazam if seizures remain refractory (Wirrell *et al.*, 2017). In fact, the most commonly used treatment is a combination of valproic acid, clobazam and stiripentol (Schubert-Bast *et al.*, 2019). In those patients with a suboptimal response to first- and second-line agents, third-line therapeutic options are implemented, including drugs such as clonazepam, levetiracetam, zonisamide or bromides (Wirrell *et al.*, 2017). However, in some countries such as Germany or Japan, the use of bromides is more frequent (Schubert-Bast *et al.*, 2019).

Apart from pharmacological agents, there are non-pharmacological strategies for those patients highly pharmacorresistant and with a poor prognosis. These strategies include the ketogenic diet (second-line agent) and surgical procedures (third-line agent). The ketogenic diet comprises a high-fat, low-carbohydrate and adequate-protein diet, whose action mechanism is still actively investigated and debated. However, several studies suggest that higher ketone bodies levels could promote a decrease in neuronal

excitability (Meira *et al.*, 2019). The efficacy of the ketogenic diet in epilepsy is variable, but there are reports of highly pharmacorresistant children in which, after diet initiation, a mean seizure reduction of up to 50% is experienced (Liu *et al.*, 2019; Yan *et al.*, 2018). Regarding surgical procedures, the risk/benefit ratio must be carefully evaluated before considering any surgery, and just when other therapies have failed. These procedures include vagus nerve stimulation, temporal lobectomy and complete corpus callosotomy. However, the benefits of these invasive procedures remain unclear, so that clinicians often discard surgery as an option for DS management (Dlouhy *et al.*, 2016).

In recent years, new drugs have undergone clinical trials and been approved as novel therapeutical tools for DS; among them, the most remarkable ones are fenfluramine and cannabidiol (CBD). Fenfluramine is an amphetamine derivative whose antiepileptic potential involves an increase in serotonin brain levels by disrupting its vesicular storage and inhibiting its reuptake (Zaccara *et al.*, 2018). CBD is the main non-psychotropic component in the cannabis plant; its specific properties and insights will be deeply discussed below.

In addition to all these strategies, all DS patients require a seizure rescue medication for home use (rectal diazepam for children under 6 years, and nasal or buccal midazolam for older children, teenagers and adults), as well as a detailed emergency protocol to be carried out at their local hospital (Camfield *et al.*, 2012).

Overall, it seems clear that DS therapeutic management is highly complex, and despite all the currently available strategies, around 30% of patients remain poorly controlled. Moreover, DS patients usually undergo changeable polytherapy, with limited benefits and typically associated with important side effects. Therefore, it is highly necessary the search for new and effective therapies acting at both seizure activity and long-term associated comorbidities. While molecular mechanisms of conventional antiepileptic drugs often involve the modulation of neurotransmitter levels aimed at reducing brain excitability, new pharmacological targets are being proposed. Accordingly, compounds able to modulate oxidative stress and inflammation (such as cannabinoids) may prove to be useful in order to overcome therapeutic failure.

1.8. Preclinical animal models

Validation of DS experimental models is essential, not only to efficiently discover new therapies for these patients, but also to fully understand the cellular and molecular mechanisms underlying this disorder. Thanks to genetic engineering techniques, *Scn1a* loss-of-function typically occurring in DS has been successfully modelled in heterologous

expression systems, induced pluripotent stem cell (IPSC)-derived neurons, zebrafish, fruit flies and mice (Escayg & Goldin, 2010; Schutte *et al.*, 2016). Undoubtedly, the genetic and physiologic similarities between mice and humans, and the huge amount of genetic engineering tools currently available in order to introduce disease-cause mutations or to make gene knock-outs, have made mice incredibly useful in modelling human genetic diseases, such as DS. To date, several genetic mouse models for *Scn1a*-associated DS have been published (Table I2).

Table I2. List of mouse models of DS based on *Scn1a* gene modifications.

Mouse model	Genetic approach	Reference
Scn1a^{tm1Wac}	Knock-out	Yu *et al.*, 2006
Scn1a$^{tm1.1Kzy}$	Knock-in (R1407X)	Ogiwara *et al.*, 2007
Scn1a$^{tm1.1.Aesc}$	Knock-in (R1648H)	Martin *et al.*, 2010
Scn1a$^{tm2.1Wac}$	Conditional knock-out	Cheah *et al.*, 2012
Scn1a^{tm2Kzy}	Conditional knock-out	Ogiwara *et al.*, 2013
Scn1a$^{tm2.1Aesc}$	Conditional knock-out	Dutton *et al.*, 2013
Scn1a^{tm1Kea}	Knock-out	Miller *et al.*, 2014
Scn1a$^{tm1.1Swl}$	Knock-in (E1099X)	Tsai *et al.*, 2015

These models have greatly enabled a better understanding of DS. However, their use has limitations due to two major issues: (1) constitutive models have an aggressive phenotype and die before maturity, which leads to breeding and shipping difficulties, as well as (2) the lack of open access to most of these models, generally owned by specific laboratories. To overcome both issues, an open-access DS mouse model has been developed by the Dravet Syndrome Foundation Spain and is available through the repository of Jackson Laboratories (Bar Harbor, ME, USA). It is a conditional knock-in mouse (B6(Cg)-*Scn1a*$^{tm1.1Dsf}$/J, The Jackson Laboratory, stock no. 026133) expressing the *Scn1a*-A1783V missense mutation, which is one of the most frequent in DS patients (Lossin *et al.*, 2009), upon Cre-driven recombination. The affected amino acid is located in the domain IV S6 segment of the protein, which is important for ion selectivity (Figure I2). To date, several studies have been already published using this conditional *Scn1a*-A1783V mouse model. In these studies, conditional mice have been crossed with mice expressing Cre-recombinase under different promoters, including (1) CMV, the constitutive human cytomegalovirus promoter (Almog *et al.*, 2021; Fadila *et al.*, 2020; Ricobaraza *et al.*, 2019) and (2) *Slc32a1*, the gene that encodes the vesicular GABA transporter Vgat (Kuo *et al.*, 2019). These models have resulted to be excellent tools for the study of different pathogenic aspects of DS. However, they generally present high rates of mortality, which again limits their use for long-term studies.

Despite it is technically possible, logistics for measuring spontaneous seizure events in these genetic mouse models require labour-intensive EEG monitoring. In this context, a wide variety of chemoconvulsants have proven utility to exogenously evoke acute seizures, including pentylenetetrazol (PTZ), kainic acid (KA) or pilocarpine (Kandratavicius *et al.*, 2014; Löscher, 2011). PTZ has been used for such purpose in this Doctoral Thesis; PTZ is a non-competitive antagonism of the $GABA_A$ receptor, which impairs GABA-mediated inhibition and leads to generalized tonic-clonic seizures (Bialer & White, 2010). This compound has been widely used in different experimental paradigms to study seizure-like behaviours and the efficacy of antiepileptic drugs (Fallah & Eubanks, 2020; Löscher, 2009, 2011).

2. CANNABINOIDS AND THE ENDOGENOUS CANNABINOID SYSTEM

Cannabis sativa, native from Central Asia, is one of the world's oldest cultivated plants, and preparations such as marijuana and hashish have been used for millennia by ancient civilizations for recreational, religious and medicinal purposes. The oldest written description regarding its medical use dates back to 2350 B.C. in Ancient Egypt, which is generally recognized as an early civilization with an advanced medical system. Since then, several pieces of evidence suggest that cannabis has remained in active use for medicinal purposes throughout ages and societies (Mechoulam *et al.*, 2014), which led to attempts to isolate the active constituents of the plant. Key events regarding this field of research occurred in the mid-20th century, when the development of novel chromatography methods enabled the isolation of the main non-psychotropic cannabinoid, CBD (Mechoulam & Shvo, 1963), and the main psychotropic constituent, Δ^9-tetrahydrocannabinol (Δ^9-THC) (Gaoni & Mechoulam, 1964). However, it was not until 30 years later that the endogenous molecular targets for cannabinoids action were characterized, as it will be further described below. This opened a new field of research related to an endogenous system of intercellular communication, the so-called endogenous cannabinoid system (ECS) (Mechoulam & Parker, 2013).

Traditionally, the term "cannabinoids" has referred to a group of terpenophenolic compounds predominantly found in the *C. sativa* plant. However, since the discovery of the ECS, this term refers to a heterogeneous family divided into three categories of compounds according to their source of production: (1) phytocannabinoids (plant-derived cannabinoids), (2) endocannabinoids (endogenous cannabinoids synthesized by animals - mainly mammals - including humans) and (3) synthetic cannabinoids designed and generated by chemical synthesis in the laboratory (Ligresti *et al.*, 2016).

2.1. The endogenous cannabinoid system

As indicated before, the ECS was identified while trying to elucidate the mechanisms of action of phytocannabinoids. It is an intercellular communicating system that plays a key role in different physiological and pathological processes. Overall, major ECS components include the cannabinoid receptors, their endogenous ligands (endocannabinoids) and the enzymatic machinery for endocannabinoid biosynthesis and inactivation. Importantly, all these elements can be selectively modulated, thus positioning the ECS as a potential target with pharmacological applications in different contexts. Although they will be described in the following sections, a schematic overview of major ECS elements can be seen in Figure I9.

2.1.1. Cannabinoid receptors

To date, CB_1 and CB_2 are considered the canonical receptors within this communication system. Both receptor types belong to the superfamily of class A G protein-coupled receptors (GPCRs), which are integral membrane proteins with seven transmembrane domains, and coupled to specific G proteins leading to a wide variety of intracellular signalling pathways. They share 44% protein identity, although this percentage is higher (around 68%) in transmembrane regions, which are involved in ligand binding (Montero *et al.*, 2005). However, some effects cannot be fully explained by the activation of these major and classic receptors. In this sense, more recent studies have shown that beyond CB_1 and CB_2, non-canonical cannabinoid receptors can be involved in this complex signalling, including other GPCRs, ion channels and nuclear receptors (Pertwee, 2015).

Cannabinoid receptor type-1

At the pharmacological level, the CB_1 receptor was first discovered using the radiolabeled THC analog [^{3}H]CP-55,940 (Devane *et al.*, 1988). Soon afterwards, it was cloned in rats (Matsuda *et al.*, 1990) and humans (Gerard *et al.*, 1991), which completed its molecular characterization. However, it has not been until recently that its crystal structure has been obtained (Hua *et al.*, 2016). It consists of 472 amino acids in humans, with a sequence identity well-conserved among vertebrate species (97-99% among humans and rodents). Moreover, it has been found not only in vertebrates, but also in different invertebrates, thus indicating a long presence in the phylogeny (Alexander, 2015; Elphick, 2012).

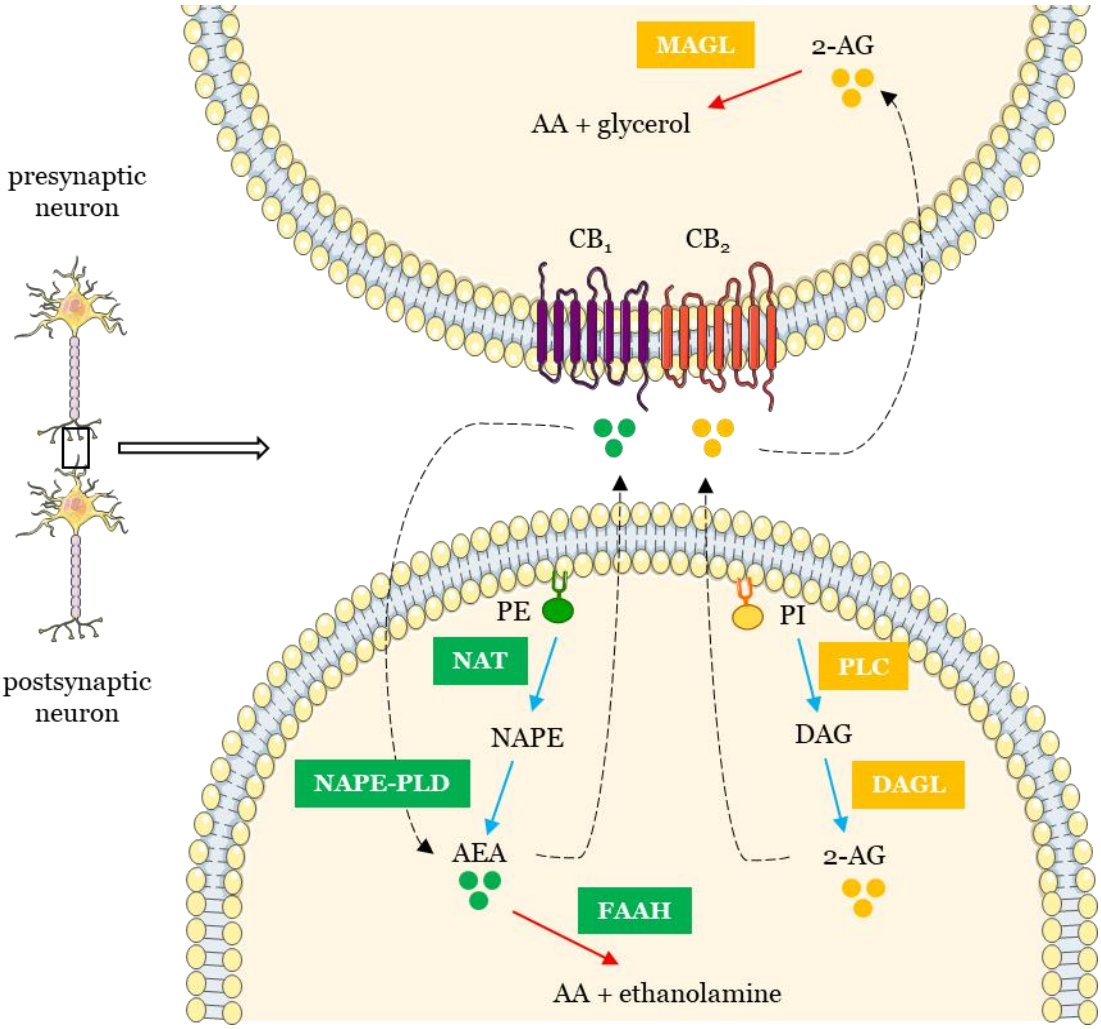

Figure I9. Schematic overview of main ECS elements, including cannabinoid receptors (CB_1 and CB_2), endocannabinoids (2-AG and AEA), biosynthetic enzymes (DAGL and NAPE-PLD, as well as additional enzymes typically involved in lipid metabolism, such as NAT and PLC) and inactivating enzymes (MAGL and FAAH). 2-AG, 2-arachidonoylglycerol; AA, arachidonic acid; AEA, anandamide; CB_1, cannabinoid receptor type-1; CB_2, cannabinoid receptor type-2; DAG, diaclyglycerol; DAGL, diaclyglycerol lipase; FAAH, fatty acid amide hydrolase; MAGL, monoacylglycerol lipase; NAPE, *N*-arachidonoyl phosphatidylethanolamine; NAPE-PLD, NAPE phospholipase D; NAT, *N*-acyltransferase; PE, phosphatidylethanolamine; PI, phosphatidylinositol; PLC, phospholipase C. Blue arrows indicate biosynthesis processes and red arrows indicate inactivation processes.

CB_1 receptor is widely expressed in the CNS and has proven to be the most abundant GPCR in the brain (Herkenham *et al.*, 1991). It is highly expressed in inhibitory GABAergic terminals and, to a lesser extent, in excitatory glutamatergic terminals; in both locations it modulates the inhibition of neurotransmitter release through its retrograde signalling, one of the major functions of the ECS (Dudok *et al.*, 2015). It has been also found postsynaptically, as well as in astrocytes, oligodendrocytes, microglia and neural precursors. Subcellularly, CB_1 receptor is localized in plasma membranes, and also in intracellular organelles, such as mitochondria outer membranes (mainly in neurons) (Bénard *et al.*, 2012). It is particularly abundant in the hippocampus, basal

ganglia, cerebellum and cerebral cortex, whereas lower levels have been found in amygdala, thalamus, hypothalamus, brainstem and spinal cord. This wide distribution is consistent with the important role of this receptor in different neurobiological processes (Mackie, 2005).

Outside the CNS, it is also expressed in the Peripheral Nervous System (PNS), as well as in non-neural peripheral tissues including spleen, liver, pancreas, lung, vascular endothelium, skeletal muscle, reproductive system or gastrointestinal tract, among others (Mackie, 2005).

As for its intracellular signalling, the CB_1 receptor belongs to the GPCRs superfamily, which are coupled to heterotrimeric G proteins through their cytoplasmic carboxyl-terminal domain. It has been classically associated with the activation of $G_{i/o}$ proteins; signal transduction via $G\alpha_{i/o}$ inhibits adenylate cyclase (AC) activity and decreases cyclic adenosine monophosphate (cAMP) intracellular concentration, which consequently suppresses the cAMP-dependent protein kinase (PKA) activity, thus affecting the activity of effector proteins that are regulated by the phosphorylation/dephosphorylation balance, as well as the expression of genes whose transcription is regulated by the cAMP response element-binding (CREB) (Davis *et al.*, 2003). However, depending on the cell context, CB_1 receptor may also signal through other different intracellular pathways. In this way, activation of $G_{i/o}$ (in part, through released βγ subunits) also triggers the (1) inhibition of Ca^{2+} influx by blocking N-type and P/Q-type voltage-activated Ca^{2+} channels, (2) enhancement of K^+ outflux by opening of inwardly-rectifying K^+ channels (Guo & Ikeda, 2004), (3) activation of mitogen-activated protein kinases (MAPKs) cascades, including extracellular signal-regulated kinase 1/2 (ERK1/2), c-Jun N-terminal kinase (JNK) and p38 (Bouaboula *et al.*, 1995), and (4) stimulation of the phosphoinositide 3-kinase (PI3K)/ protein kinase B (Akt) signalling (Galve-Roperh *et al.*, 2002). In addition to the classical $G_{i/o}$ coupling, CB_1 can also bind to G_s and G_q proteins in certain circumstances. $G\alpha_s$, contrary to $G\alpha_{i/o}$, activates AC and increases cAMP levels (Glass *et al.*, 1997). On the other hand, $G\alpha_q$ activates phospholipase C (PLC), which releases Ca^{2+} from the endoplasmic reticulum and increases its cytosolic levels (Lauckner *et al.*, 2005). All these pathways are schematically summarized in Figure I10.

This complex pattern of possible intracellular pathways can be explained by a phenomenon known as “biased signalling” or “functional selectivity”, a concept that describes the ability of an agonist to stabilize the receptor in such a conformation that selectively activates one specific signalling cascade over another, thus triggering distinct physiological responses (Wouters *et al.*, 2019). This phenomenon has recently gained

increasing attention, especially since the elucidation of crystal tridimensional structures which will help to fully understand this complexity (Hua *et al.*, 2016; Li *et al.*, 2019). In addition, "biased signalling" can be also a consequence of the ability of CB_1 receptor to form oligomers, thus affecting the manner in which this receptor responds to ligands and enriching the signalling repertoire. It can form both homodimers (Wager-Miller *et al.*, 2002) and heterodimers in association with other GPCRs such as CB_2 (Callén *et al.*, 2012), GPR55 (Martínez-Pinilla *et al.*, 2014), D2 dopamine receptor (Kearn *et al.*, 2005), A_{2A} adenosine receptor (Moreno *et al.*, 2018) and 5-HT_{2A} serotonin receptor (Viñals *et al.*, 2015), as well as with other non-GPCR receptors (Moreno *et al.*, 2018).

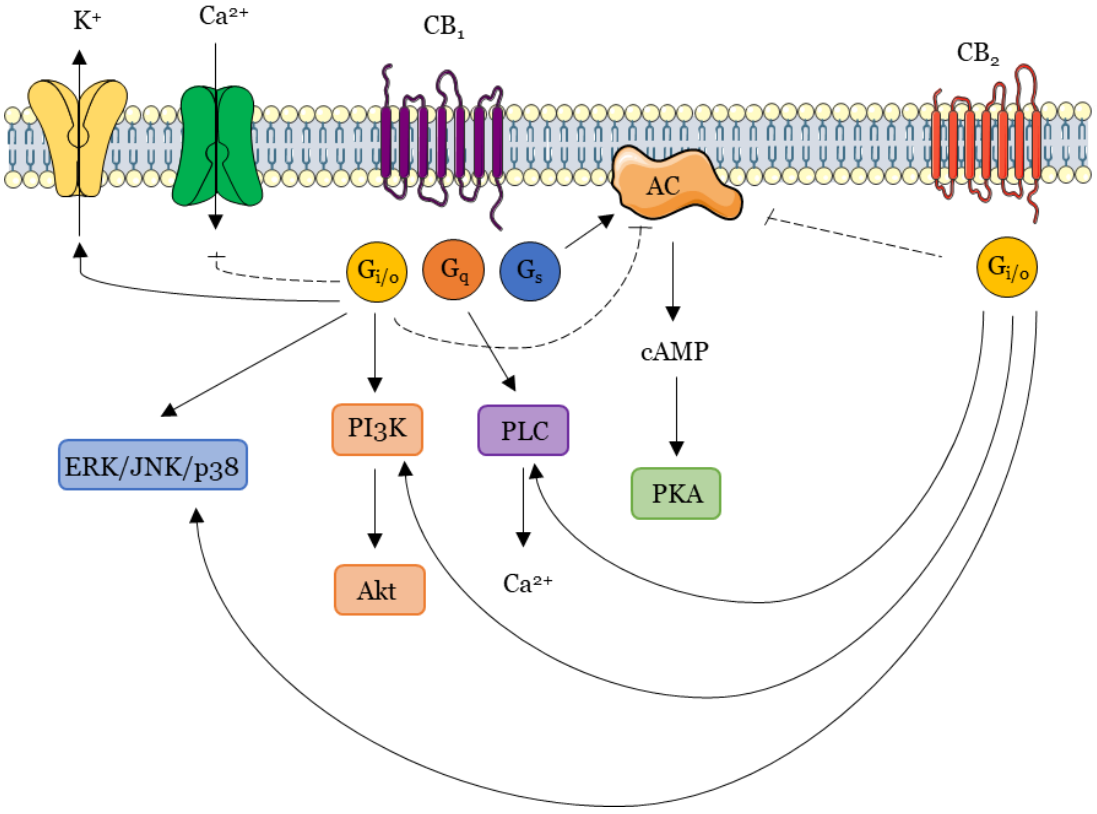

Figure I10. Main signalling pathways triggered by CB_1/CB_2 activation. Upon ligand binding, depending on the G protein coupled, CB_1/CB_2 receptors trigger different intracellular cascades. Arrows indicate stimulation and blunted arrows indicate inhibition

Cannabinoid receptor type-2

CB_2 receptor was the second cannabinoid receptor identified, and it was first detected in spleen macrophages (Munro *et al.*, 1993). It consists of 360 amino acids in humans, with greater variations in the sequences of different species in comparison to CB_1 receptor (around 80% identity among humans and rodents) (Zhang *et al.*, 2015). As with CB_1 receptor, CB_2 receptor crystal structure has been recently published (Li *et al.*, 2019). Originally, it was considered the "peripheral" cannabinoid receptor, with a predominant

expression in immune cells. However, it has now been identified throughout the CNS, particularly in microglial cells (Núñez *et al.*, 2004), astrocytes (Fernández-Trapero *et al.*, 2017), oligodendrocytes (Molina-Holgado *et al.*, 2002) and neural progenitors (Palazuelos *et al.*, 2012). In addition, although this is an issue under intense debate due to the lack of good experimental tools for its cellular detection, some studies have shown CB_2 receptor expression in neurons (Stempel *et al.*, 2016). Despite controversial, what seems clear is that CB_2 receptor expression in the CNS is much lower in comparison to CB_1 receptor or the peripheral immune system.

In the CNS, the role of CB_2 receptor in healthy conditions is not well demonstrated, but many studies have shown that under some pathological conditions, especially those that occur with neuroinflammation, CB_2 receptor expression is enhanced. Therefore, this receptor is proposed to be part of a protective system (Pacher & Mechoulam, 2011), as it will be discussed.

Intracellular signalling mechanisms associated with the activation of CB_2 receptor are quite similar to those described for CB_1, except for effects on Ca^{2+} and K^+ conductance. CB_2 receptor activation triggers $G_{i/o}$ coupling, but not G_s and G_q. Signalling through $G_{i/o}$ inhibits AC activity and cAMP production, activates MAPKs cascades and stimulates PI3K/Akt signalling (Davis *et al.*, 2003). It has no effect on Ca^{2+} and K^+ ion channels, although βγ subunits can activate PLC and increase Ca^{2+} cytosolic levels (Zoratti *et al.*, 2003). All these pathways are also schematically summarized in Figure I10. Although less investigated, CB_2 receptor can also form homodimers (Singh *et al.*, 2012), as well as heterodimers with CB_1 (Callén *et al.*, 2012), GPR55 (Moreno *et al.*, 2014), 5-HT_{1A} serotonin receptor (Pazos *et al.*, 2013), CXCR4 chemokine receptor (Coke *et al.*, 2016) and human epidermal growth factor receptor 2 (HER2) (Blasco-Benito *et al.*, 2019), contributing to the phenomenon known as "biased signalling" or "functional selectivity".

Other cannabinoid receptors

As mentioned above, in addition to CB_1 and CB_2 canonical cannabinoid receptors, non-canonical receptors include other GPCRs, ion channels and nuclear hormone receptors (Pertwee, 2015). This variability shows the emerging complexity that involves this communication system.

Regarding GPCRs, we may distinguish three orphan GPCRs: GPR55, GPR18 and GPR119. The main endogenous ligand of GPR55 is a PI-derivative known as lysophosphatidylinositol (LPI) (Oka *et al.*, 2009); GPR55 has been shown to display G-protein coupling promiscuity, since it can associate with G_{12}, G_{13} and G_q. Downstream

signalling cascades mainly include an increase of cytosolic Ca^{2+} levels and activation of monomeric G proteins such as Ras homolog family member A (RhoA), cell division control protein 42 homolog (Cdc42) and Ras-related C3 botulinum toxin substrate 1 (Rac1), involved in actin dynamics (Lauckner *et al.*, 2008; Ryberg *et al.*, 2007). *N*-arachidonoylglycine (NAGly), an oxidized metabolite of the endocannabinoid *N*-arachidonoylethanolamine (anandamide, AEA) (Bradshaw *et al.*, 2009) is proposed as the main endogenous ligand for GPR18 (Kohno *et al.*, 2006). Lastly, *N*-oleoylethanolamine (Overton *et al.*, 2006) and 2-oleoylglycerol (Hansen *et al.*, 2011), analogs of the endocannabinoids AEA and 2-AG, respectively, have been proposed to be GPR119 ligands. Although intracellular cascades and cell functions are less studied, evidence shows that GPR18 couples $G_{i/o}$ and G_q (Console-Bram *et al.*, 2014), while GPR119 couples G_s (Godlewski *et al.*, 2009). Therefore, the strong link between these GPCRs with endocannabinoid-like molecules is clear. In addition, several studies suggest that specific phytocannabinoids or synthetic cannabinoids could also bind these receptors, although some results are still controversial and must be confirmed by further studies (Alexander, 2015).

Among ion channels, there is evidence for certain transient receptor potential channels (TRPs), mainly TRPV1-TRPV4, TRPA1 and TRPM8, to be regulated by several cannabinoids (De Petrocellis *et al.*, 2011; Muller *et al.*, 2019). Responses associated with TRP channel activation typically lead to an increase of cytosolic Ca^{2+} levels, which trigger different signalling pathways involved in somatosensory sensations (De Petrocellis *et al.*, 2011). Although less characterized, certain cannabinoids also modulate other ion channels, including ligand-gated ion channels (such as 5-HT_3 receptors) as well as voltage-gated Ca^{2+} and K^+ channels (Pertwee, 2015).

Additionally, cannabinoids can modulate nuclear hormone receptors, particularly PPARs (Pistis & Melis, 2010). Upon ligand activation, PPARs form heterodimers with retinoid X receptors (RXR) and become transcription factors that regulate target genes related to lipid metabolism, glucose homeostasis, cell differentiation or inflammation (Mirza *et al.*, 2019). Certain cannabinoids are able to activate mainly PPARα and PPARγ, an activation that has been related to anti-inflammatory effects (O'Sullivan, 2016).

2.1.2. Endocannabinoids and their metabolism

Endocannabinoids, identified after the discovery of CB_1 and CB_2 receptors, are small lipids defined as the endogenous ligands for cannabinoid receptors. The most relevant and best-studied endocannabinoids include AEA and 2-AG, which are analogs of arachidonic acid (AA), a long-chain polyunsaturated fatty acid (Fezza & Maccarrone,

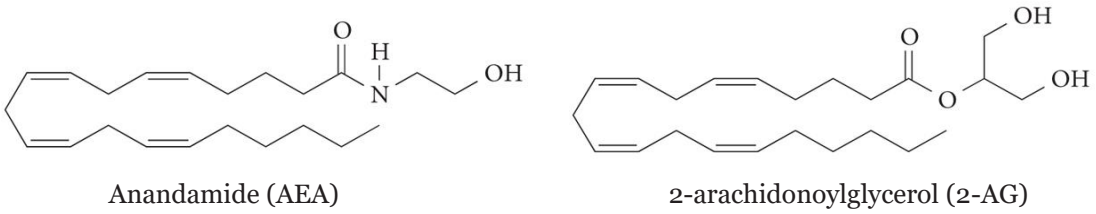

Anandamide (AEA) 2-arachidonoylglycerol (2-AG)

Figure I11. Chemical structures of endocannabinoids, anandamide (AEA) and 2-arachidonoylglycerol (2-AG).

2014) (Figure I11). In the CNS, AEA levels are relatively low (Bisogno *et al.*, 1999), whereas 2-AG is more abundant (Fezza & Maccarrone, 2014). AEA is a CB_1 partial agonist and a weak CB_2 partial agonist; in contrast, 2-AG is a CB_1 and CB_2 full agonist (Howlett *et al.*, 2002; Pertwee *et al.*, 2010), thus being proposed as the main endogenous agonist for both receptors. Based on differences in endogenous concentrations and receptor binding properties, both endocannabinoids can exert distinct effects. Although less studied, there are other AA analogs that are also considered endocannabinoids, including 2-arachidonoylglycerylether (noladin ether), *O*-arachidonoylethanolamine (virodhamine) and *N*-arachidonoyldopamine (NADA) (Zoerner *et al.*, 2011).

Interestingly, endocannabinoids are typically accompanied in a physiological context by structurally similar compounds, the so-called endocannabinoids-like compounds. The best known are chemically related to AEA; these are the *N*-acyl ethanolamines of palmitic (*N*-palmitoylethanolamine, PEA), oleic (*N*-oleoylethanolamine, OEA) and stearic acid (*N*-stearoylethanolamine, SEA). 2-AG has also some structurally similar compounds, such as 2-palmitoylglycerol (2-PG) and 2-oleoylglycerol (2-OG) (Murataeva *et al.*, 2016). The majority of these molecules have no affinity for cannabinoids receptors. However, they are able to modulate endocannabinoid action, since they share some metabolic enzymes (Di Marzo & Piscitelli, 2015).

Differently from classical neurotransmitters, endocannabinoids are produced and released de novo and "on-demand" rather than stored in secretory vesicles. Specifically, they are synthesized from cell membrane phospholipids in response to specific stimuli, which normally trigger an elevation of intracellular Ca^{2+} levels, and are immediately released extracellularly to act at nearby cell receptors (paracrine action) (Sugiura, 2008).

Main pathway of 2-AG biosynthesis engages sequential action of PLC and DAGL (Figure I9). First, PLC hydrolyzes membrane PI to generate the intermediate DAG. Subsequently, DAGL converts DAG to 2-AG (Bisogno *et al.*, 2005). Alternative biosynthetic pathways have been proposed, but they only act under certain

circumstances (Piomelli, 2003). AEA biosynthesis is much more complex, because it involves multiple enzymes and there are several alternative pathways, even in a Ca^{2+}-independent manner (Piomelli, 2003). Main pathway engages sequential action of NAT and NAPE-PLD (Figure I9). First, NAT produces the intermediate NAPE from membrane PE, and then NAPE-PLD hydrolyzes NAPE to AEA (Di Marzo *et al.*, 1994).

Both endocannabinoids are immediately released to the extracellular space upon synthesis, and exert their biological function mainly throughout CB_1 or CB_2 receptors located in cells that are in the vicinity, although other cannabinoid receptors can be also activated. As any other endogenous mediators, they require mechanisms for their rapid removal from their molecular targets. This signal termination involves a two-step process: (1) removal from the extracellular space by membrane trafficking followed by (2) intracellular hydrolysis by catabolic enzymes or oxidation (biotransformation).

The internalization process across the plasma membrane is still controversial. A variety of mechanisms have been proposed, including: (1) passive diffusion across the plasma membrane, which is driven by an inward concentration gradient created by their immediate hydrolysis and facilitated by the hydrophobic nature of lipids (Kaczocha *et al.*, 2006), (2) facilitated transport by lipid-carrier proteins, given existing evidence of pharmacological blockade of this process without affecting inactivation enzymes (Hillard *et al.*, 1997) and (3) caveolae-dependent endocytosis (Rimmerman *et al.*, 2008). There are numerous studies on AEA uptake, whereas few data on 2-AG are available. However, evidence is inconclusive, so further research is needed (Nicolussi & Gertsch, 2015).

Once inside the cell, endocannabinoids can be processed by hydrolysis or oxidation. The two major serine hydrolases responsible for the hydrolysis and resulting inactivation of AEA and 2-AG are FAAH (Cravatt *et al.*, 1996) and MAGL (Dinh *et al.*, 2002), respectively. Two additional enzymes, α/β-hydrolase domain types 6 and 12 (ABHD6, ABHD12), have been shown to contribute to 2-AG hydrolysis (Navia-Paldaius *et al.*, 2012). In the brain, FAAH and ABHD6 expression is mainly localized in postsynaptic dendrites, MAGL in presynaptic axons and ABHD12 in microglial cells (Baggelaar *et al.*, 2017; Navia-Paldaius *et al.*, 2012). Enzymatic hydrolysis of the AEA and 2-AG release AA and ethanolamine or glycerol, respectively.

In addition, since both AEA and 2-AG contain AA as fatty acid, they can be susceptible to oxidative metabolism by lipoxygenases (LOX), cyclooxygenases (COX) and cytochrome P450 (CYP) oxidases. In contrast to hydrolysis, oxidation represents biotransformation rather than inactivation, since oxygenated derivatives (such as prostaglandins, prostamides and glycyl esters, among others) are biologically active,

although their physiological relevance must be still clarified (Guindon & Hohmann, 2008; Zelasko *et al.*, 2015).

Figure I12 shows a schematic view of the aforementioned enzymatic pathways.

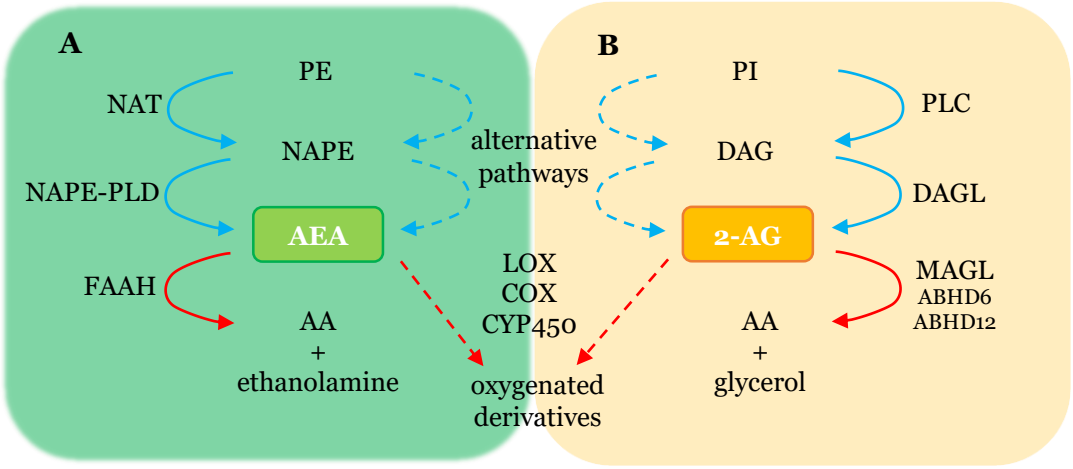

Figure I12. Summary of the different routes for the synthesis and inactivation of the endocannabinoids. Enzymatic pathways for **(A)** AEA and **(B)** 2-AG, including their role as precursors for the synthesis of active oxygenated derivatives. Blue arrows indicate biosynthesis processes and red arrows indicate inactivation processes.

2.1.3. Roles of the ECS

The ECS controls an endless repertoire of physiological processes due to its wide expression throughout the body. The most important roles have been described in the CNS, but it also regulates multiple processes in different peripheral tissues, including the cardiovascular system, gastrointestinal tract, kidneys, pancreas, immune system, skeletal muscle, retina and ocular tissues, bone, reproductive system and skin, among others (Ligresti *et al.*, 2016).

Perhaps, the most important physiological role of the ECS in the CNS is the modulation of the synaptic transmission by the CB_1 receptor, which ultimately maintains a correct homeostasis and integrity in cells and tissues. Briefly, the ECS exerts a protective role aimed at preserving synaptic homeostasis, attenuating both excessive neuronal excitation and inhibition (Castillo *et al.*, 2012; Dudok *et al.*, 2015) (see Box 5 for further information). This property has been recently extended to the CB_2 receptor, although in a more restricted manner (Zhang *et al.*, 2021).

These homeostatic responses are involved in a great variety of neurobiological processes controlled by CNS regions in which the ECS is expressed. Interestingly, selectively enhancing or reducing cannabinoid signalling in these regions may serve as a potential

therapeutic approach to manage pathologies affecting these CNS regions and processes (Fernández-Ruiz *et al.*, 2010) (Table I3).

Box 5. The ECS as a modulatory system in the CNS

The most important role of the ECS in the CNS is the modulation of the synaptic transmission by retrograde signalling (Figure I13A). Endocannabinoids can act as retrograde messengers and participate in both short- and long-term forms of synaptic plasticity, including depolarization-induced suppression of inhibition (DSI) (Willson & Nicoll, 2011) and excitation (DSE) (Kreitzer & Regehr, 2001), as well as forms of long-term depression (LTD) at both excitatory (Gerdeman *et al.*, 2002) and inhibitory (Marsicano *et al.*, 2002) currents. Briefly, postsynaptic depolarization elevates cytosolic Ca^{2+} levels and activates Ca^{2+}-sensitive biosynthetic enzymes. Subsequently, endocannabinoids are immediately released to the synaptic cleft and move backwards across the synapse to bind mainly presynaptic CB_1 receptors closely located to the synaptic active zone, which triggers an intracellular signalling aimed at inducing a transient hyperpolarization of the presynaptic membrane and suppressing Ca^{2+}-induced neurotransmitter release. Typically, short-term depression involves G_i βγ subunits, which inhibit Ca^{2+} influx and enhance K^+ outflux. In contrast, long-term depression requires a reduction in AC and PKA activity modulated by $G\alpha_i$. Whether this retrograde signalling is dependent on either or both 2-AG and AEA is controversial, but 2-AG seems to be the main endocannabinoid required (Castillo *et al.*, 2012).

However, synaptic transmission can be also modulated by non-retrograde or autocrine signalling, which involves AEA binding postsynaptic TRPV1 and CB_1 receptors (Figure I13B) (Bacci *et al.*, 2004; Grueter *et al.*, 2010), as well as by neuron-astrocyte signalling (the so-called "tripartite synapse"), in which released endocannabinoids bind astrocytic CB_1 receptor and trigger gliotransmission (Figure I13C) (Oliveira da Cruz *et al.*, 2016).

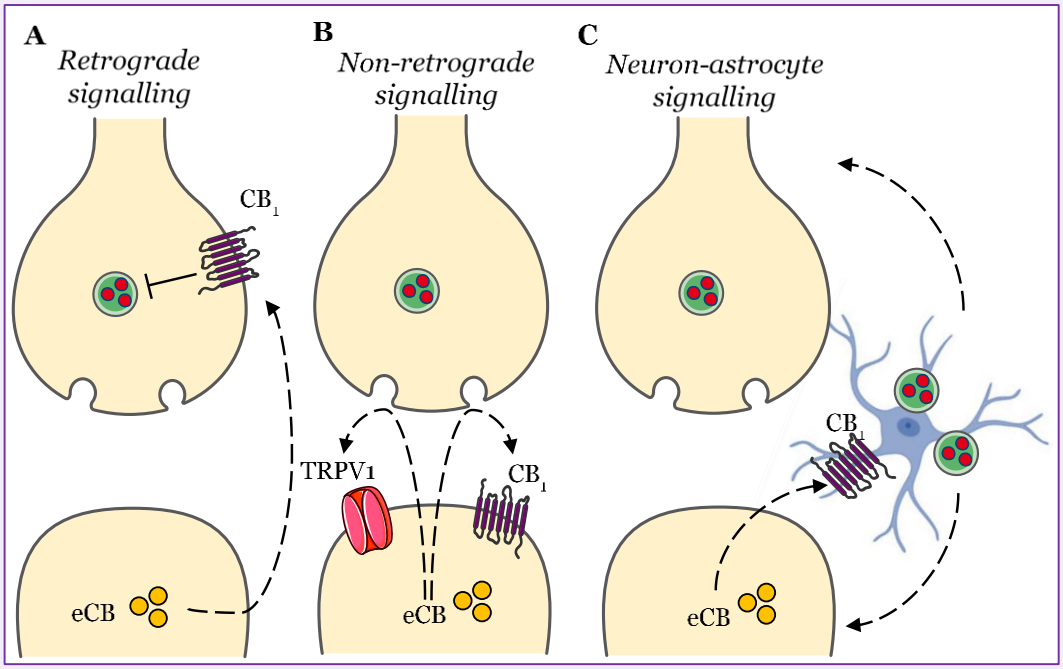

Figure I13. Modulation of the synaptic transmission by the ECS throughout **(A)** retrograde signalling, **(B)** non-retrograde signalling and **(C)** neuron-astrocyte signalling. Adapted from Castillo *et al.*, 2012.

Table I3. Overview of CNS processes and regions in which the ECS and cannabinoid-compounds may represent a novel therapeutic approach to combat related disorders. Adapted from Fernández-Ruiz *et al.*, 2010.

CNS process	CNS region	Neurological disorders for the application of cannabinoids	References
Movement coordination and refinement	Basal ganglia, motor cortex, cerebellum and spinal cord	Huntington's chorea, Tourette's syndrome, Parkinson's disease, dyskinesias	Fernández-Ruiz *et al.*, 2011
Nociception	Spinal and supraspinal structures	Neuropathic pain	Vučković *et al.*, 2018
Memory and learning	Hippocampus	Alzheimer's disease, post-traumatic stress syndrome	Neumeister *et al.*, 2015
Higher cognitive functions	Brain cortex and limbic system	Addiction, psychiatric disorders	Laviolette & Grace, 2006
Emesis	Area postrema	Reduction of nausea and vomiting in cancer patients	Parker *et al.*, 2011
Sleep	Hypothalamus	Insomnia, somnolence	Kesner & Lovinger,2020
Appetite and food intake	Hypothalamus and limbic system	Obesity, anorexia/cachexia	Tarragon & Moreno, 2019
Stress and anxiety	Amygdala and hypothalamus	Anxiety, psychiatric disorders	Sarris *et al.*, 2020
Neuronal excitability	Excitatory glutamatergic and inhibitory GABAergic neurons	Epilepsy	Rosenberg *et al.*, 2015
Neuronal survival	Neuronal and glial subpopulations	Acute brain damage, chronic neurodegenerative disorders	Fernández-Ruiz, 2019

Regarding CB_2 receptor roles in the CNS, it is expressed at low levels in physiological conditions. However, as already mentioned, its expression is enhanced in glial cells under certain pathological neuroinflammatory conditions (Fernández-Ruiz *et al.*, 2007). CB_2 receptors are upregulated in experimental models of neurodegeneration, including Huntington's (Palazuelos *et al.*, 2009; Sagredo *et al.*, 2009), Alzheimer's (López *et al.*, 2018) and Parkinson's (Concannon *et al.*, 2016; Gómez-Gálvez *et al.*, 2016) diseases, as well as amyotrophic lateral sclerosis (Bilsland *et al.*, 2006; Espejo-Porras *et al.*, 2018). This upregulation is believed to be part of a protective system, since direct agonism of CB_2 in these chronic neuroinflammatory contexts often yields neuroprotective effects (Fernández-Ruiz *et al.*, 2007; Pacher & Mechoulam, 2011).

For the purpose of this Doctoral Thesis, the focus will be on the therapeutic potential of the ECS and cannabinoid-related compounds in epilepsy in a following section, with special emphasis on the modulation of neuronal excitability and inflammation.

2.2. Phytocannabinoids and related compounds

Phytocannabinoids are predominantly produced in secretory cells inside glandular trichomes of *C. sativa* female flowers. It is a chemically complex plant due to the vast number of constituents and their possible interaction. Some of these constituents are produced through the primary metabolism (amino acids, fatty acids and steroids) whereas others represent secondary metabolites (phytocannabinoids, flavonoids, stilbenoids, terpenes, lignans and alkaloids) (Flores-Sanchez & Verpoorte, 2008).

Cannabinol (CBN) was the first cannabinoid compound isolated and identified from *C. sativa* (Jacob y Todd, 1940). However, active research on phytocannabinoids started in the 1960s with the isolation and characterization of CBD (Mechoulam & Shvo, 1963) and Δ^9-THC (Gaoni & Mechoulam, 1964), the two major constituents of the plant. To date, more than 100 have been identified in cannabis flowers, in relative concentrations depending on the plant variety and growth conditions. They represent a group of terpenophenolic lipophilic compounds with 21 carbons for neutral forms, 22 carbons for carboxylated forms (acids) and 19 carbons for varin-type derivatives. Although major phytocannabinoids in the plant are Δ^9-THC and CBD, other minor compounds have also generated pharmaceutical interest in the last years, including Δ^8-tetrahydrocannabinol (Δ^8-THC), CBN, cannabigerol (CBG), cannabichromene (CBC), Δ^9-tetrahydrocannabivarin (Δ^9-THCV), cannabivarin (CBV) and cannabidivarin (CBDV), as well as carboxylated precursors (ElSohly & Slade, 2005; Morales *et al.*, 2017).

Beyond the phytocannabinoids, secondary metabolism in *C. sativa* also yields other phytochemicals, including terpenes. However, in contrast to phytocannabinoids, the presence of these constituents is not restricted to *C. sativa*. Typically, they are aromatic volatile compounds responsible for the odor and flavor of the plant. They are produced in glandular trichomes of the plant and form its essential oil (EO), which fulfills an ecological role participating in communication and defense mechanisms (Gonçalves *et al.*, 2020). To date, more than 120 have been identified in *C. sativa*, and some of them (including myrcene, terpinolene, ocimene, limonene, α-pinene, humulene, linalool, and β-caryophyllene) have generated great interest due to their extensive employability (Hanuš & Hod, 2020). In addition, several studies suggest the existence of a phytocannabinoids-terpenes synergistic effect, known as “entourage effect”, which contributes to some of the beneficial effects attributed to this plant (Russo, 2011). Regarding this term, it is important to distinguish between “synergistic effect” and “additive effect”. Whereas the term “additive effect” refers to the sum of individual

effects, a "synergistic effect" refers to the fact that two or more compounds may produce a combined effect greater than their individual effects (García-Fuente *et al.*, 2018).

For the purpose of this Doctoral Thesis, the focus will be done on Δ⁹-THC, CBD and β-caryophyllene (BCP) in the following sections (Figure I14).

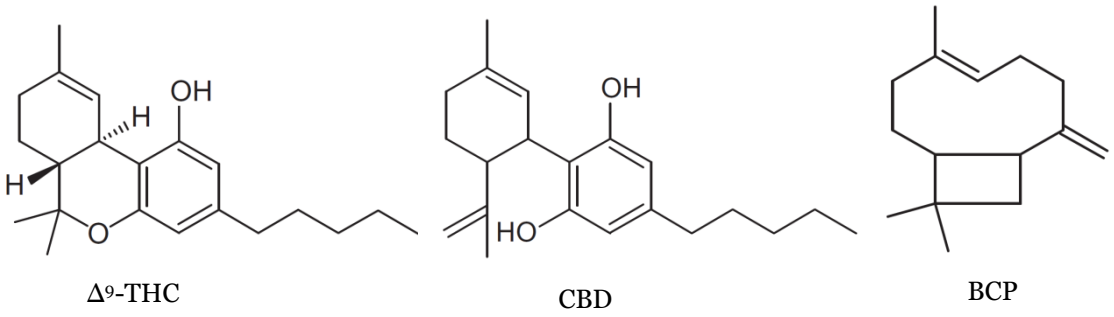

Δ⁹-THC CBD BCP

Figure I14 Chemical structures of the phytocannabinoids Δ⁹-THC and CBD and the terpene BCP.

2.2.1. Δ⁹-tetrahydrocannabinol

Δ⁹-THC is the major component of *C. sativa* and the main responsible for its psychotropic effects. It is classified as a partial agonist for both CB_1 and CB_2 receptors (Howlett *et al.*, 2002; Pertwee *et al.*, 2010). Stimulation of the CB_1 receptor produces most of its central effects, including the well-known tetrad of effects triggered by cannabis: suppression of locomotor activity, hypothermia, catalepsy and antinociception (Martin *et al.*, 1991). In contrast, stimulation of the CB_2 receptor is associated with pain relief and anti-inflammatory effects (Pacher & Mechoulam, 2011).

Additionally, it has been shown to activate orphan receptors (GPR18 and GPR55), TRP channels (TRPV2 and TRPA1) and glycine receptors, and to inhibit serotonin $5\text{-}HT_{3A}$ (Howlett *et al.*, 2002; Pertwee *et al.*, 2010). However, these targets have been validated *in vitro* at micromolar concentrations; taking into account that only low doses of Δ⁹-THC are tolerated in a clinical setting due to psychotropic effects, it remains unclear whether these targets may play a role in a physiological context.

Δ⁹-THC acting on CB_1/CB_2 receptors has shown to exert beneficial effects on analgesia, appetite, nociception, inflammation, neuronal excitability and neuronal survival, among others, thus presenting therapeutic applications in different disorders (Fernández-Ruiz *et al.*, 2020). However, these applications are still limited and hardly translational into clinics, since CB_1 receptor stimulation is not only responsible for some of these beneficial properties, but also for the undesirable psychotropic effect (Ligresti *et al.*, 2016).

2.2.2. Cannabidiol

CBD is the major non-psychotropic constituent of *C. sativa*, showing an almost negligible affinity for CB_1 and CB_2 receptors (Howlett *et al.*, 2002; Pertwee *et al.*, 2010). However, some studies have shown that under certain circumstances CBD is able to behave as a negative allosteric modulator of both CB_1 (Lapraire *et al.*, 2015) and CB_2 receptors (Martínez-Pinilla *et al.*, 2017).

CBD pharmacology is much more complex compared to Δ^9-THC, with multiple targets other than CB_1/CB_2 receptors. CBD has been found to activate GPR18, PPARγ, glycine and serotonin 5-HT_{1A} receptors, as well as TRP channels (TRPV1, TRPV2 and TRPA1), and to inhibit GPR55 receptors (Howlett *et al.*, 2002; Pertwee *et al.*, 2010), among others. Moreover, the presence of two hydroxyl groups and a benzene ring in its chemical structure (Figure I14) is believed to endow CBD with a potent antioxidant profile, even more than common antioxidants such as vitamin C or α-tocopherol (Atalay *et al.*, 2020).

This wide array of molecular targets allows its potential use in different disorders, since CBD has shown to exert beneficial effects on analgesia, appetite, stress, nociception, inflammation, neuronal excitability, oxidative stress and neuronal survival, among others. In addition, the lack of psychotropic effects gives rise to a favorable benefit-to-risk ratio. Therefore, the potential therapeutic use of CBD is being widely investigated (Ligresti *et al.*, 2016; Pisanti *et al.*, 2017).

2.2.3. β-caryophyllene

BCP is a volatile bicyclic sesquiterpene abundantly found in the EOs (about 35%) of *C. Sativa*. In addition, it has been encountered in more than a thousand plants, including dietary plants and spices such as oregano (*Origanum vulgare*), cinnamon (*Cinnamomum spp.*) and black pepper (*Piper nigrum*), among others. Interestingly, it is widely used in food and cosmetics, since it has been designated as "generally recognized as safe" and approved by European and American regulatory agencies as a food additive and flavoring agent. It shows similarities with phytocannabinoids regarding pharmacological properties and chemical structure; therefore, BCP is typically termed as "dietary phytocannabinoid" (Sharma *et al.*, 2016).

BCP was first described as a full and selective agonist with a strong affinity to CB_2 receptors (Gertsch *et al.*, 2008). Further studies revealed that it is also able to activate PPARα/γ and μ-opioid receptors, and to inhibit homomeric nicotinic acetylcholine receptors (α7-nAChRs) and the toll-like receptor complex (CD14/TLR4/MD2) (Sharma

et al., 2016). This polypharmacology allows BCP to exert multiple pharmacological activities, showing antioxidant, anti-inflammatory, anticonvulsant, analgesic and neuroprotective properties, among others. Similar to CBD, BCP is devoid of the psychotropic adverse effects associated with CB_1 stimulation, which, together with its pharmacological properties, makes BCP a novel candidate for a wide variety of therapeutic applications (Gonçalves *et al.*, 2020; Sharma *et al.*, 2016). Moreover, evidence suggests that under certain circumstances BCP can act synergistically with both Δ^9-THC and CBD, taking part in the so-called "entourage effect" (Russo, 2011).

3. CANNABINOIDS, PEDIATRIC EPILEPSY AND DRAVET SYNDROME

3.1. The endogenous cannabinoid system in epilepsy

The ECS is considered a promising target for the treatment of epilepsy, since one of its main functions is acting as an on-demand mechanism protecting the brain against hyperexcitability, inflammation and oxidative stress. As explained above, these three events represent a pathogenic triad that contributes to epilepsy progression (Box 2). Therefore, modulating this triad represents a novel therapeutic approach, and the use of compounds that - directly or indirectly - target the ECS could represent a promising therapeutic strategy to treat epilepsy and related comorbidities.

3.1.1. ECS, cannabinoids and epilepsy: excitotoxicity and hyperexcitability

During an epileptic seizure, an excess of glutamate is released from presynaptic terminals to the synaptic cleft, which triggers brain hyperexcitability (Box 2). In this context, presynaptic CB_1 receptors can be activated and exert a negative feedback mechanism aimed at decreasing the release of excessive glutamate and further neuronal hyperexcitability (Marsicano *et al.*, 2003) (Box 5). However, this signalling is much more complex, since depending on the type of synapse where CB_1 receptor is expressed, its activation might result in totally opposite effects (Figure I15).

CB_1 receptor is expressed in both GABAergic and glutamatergic axon terminals. Although its density in glutamatergic synapses is much lower, several findings suggest that the ECS plays a more effective role in excitatory synapses, thus explaining the protection against epileptiform seizures exerted by this signalling system (Figure I15) (Dudok *et al.*, 2015; Marsicano *et al.*, 2003; Steindel *et al.*, 2013). It can be explained by attending to the so-called "biased signalling" or "functional selectivity" phenomenon that has been mentioned in previous sections.

Likewise, several studies have described an increased production of endocannabinoid levels after an epileptic seizure, which may represent an acute protective response (De Petrocellis *et al.*, 2011). Regarding CB_1 receptor expression, examination of *postmortem* human epileptic brains has revealed that it is decreased in glutamatergic terminals, whereas it is increased in GABAergic ones, which confirm the long-term tendency towards neuronal hyperexcitability (Soltesz *et al.*, 2015). To date, there is no data available regarding the specific implication of CB_1 receptor in DS; therefore, further research is needed.

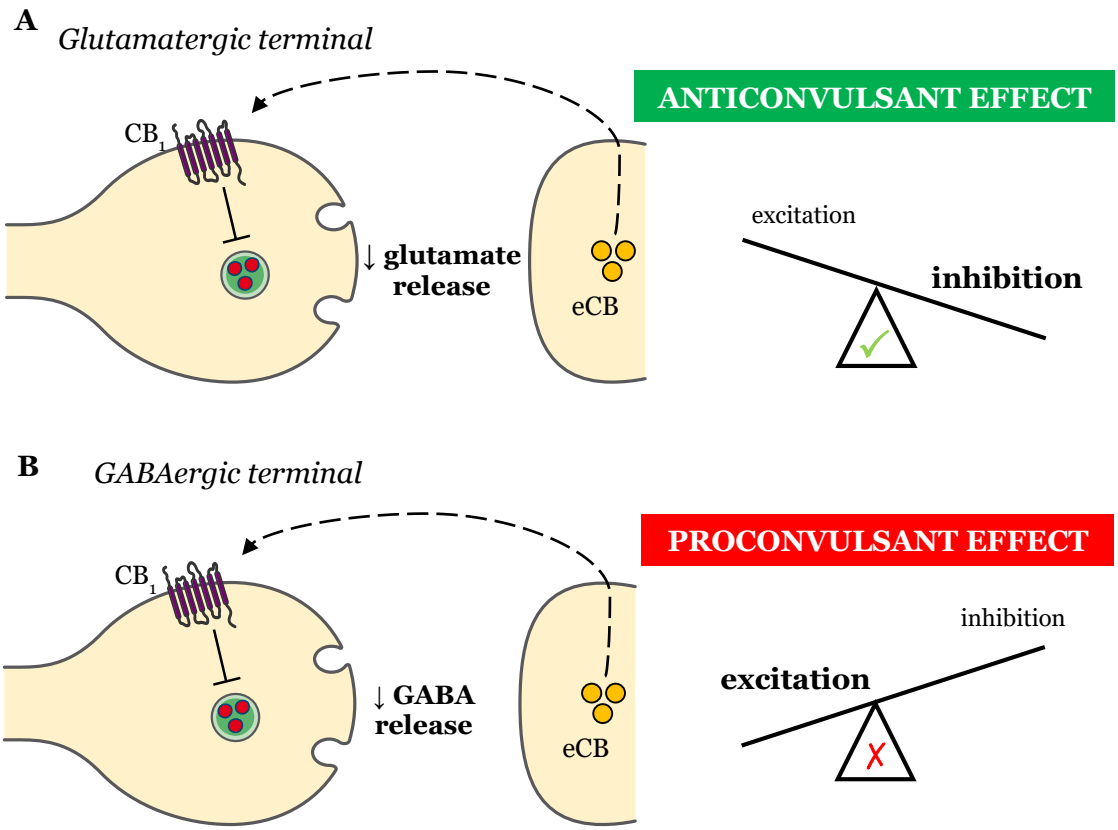

Figure I15. Dichotomy of CB_1 receptor activation on seizure activity. **(A)** CB_1 activation in glutamatergic terminals is anticonvulsant, whereas **(B)** CB_1 activation in GABAergic terminals is proconvulsant.

3.1.2. ECS, cannabinoids and epilepsy: inflammation

As mentioned in previous sections, prolonged seizures and persistent hyperexcitability often lead to the activation of astrocytes and microglia, as well as to the generation of inflammatory events within the CNS (Box 2). Regarding these processes, it is widely accepted that cannabinoids exert potent anti-inflammatory effects by (1) reducing the release of cytotoxic factors by reactive glial cells and (2) increasing the production (mainly by astrocytes) of prosurvival molecules (Fernández-Ruiz *et al.*, 2010).

Even though CB_1 receptor, as well as PPARγ, have been involved in some of these anti-inflammatory effects of cannabinoids, the most solid evidence is related to CB_2 receptor activation (Turcotte *et al.*, 2016). In contrast to CB_1, the role of CB_2 receptor in epilepsy has received much less attention. Although there is a limited number of studies, it is proposed that CB_2 receptor promotes protection against epilepsy. In this sense, a reduction in CB_2 receptor activity has been shown to increase seizure susceptibility in mice (Shapiro *et al.*, 2019). Moreover, its expression has proven to be upregulated on mouse hippocampal neurons following status epilepticus (Wu & Wang, 2018), suggesting that CB_2 receptor may play a protective role following seizures, as it occurs in a wide variety of neurological disorders (Navarro *et al.*, 2016). Interestingly, and together with some inflammatory markers, this receptor has been found to be upregulated in lymphocytes of DS patients (Rubio *et al.*, 2016). Therefore, it is proposed that in an epileptogenic context like DS, where inflammation plays a key role in the neurobiology of the disorder, CB_2 receptor can behave as a protective response aimed at counteracting this inflammatory state.

3.1.3. ECS, cannabinoids and epilepsy: oxidative stress

Seizures also trigger the accumulation of ROS and RNS, which can damage proteins, DNA and membrane lipids (Box 2). When these toxic products are overproduced, endogenous antioxidant mechanisms are not able to maintain a proper homeostasis, which eventually leads to oxidative stress (Borowicz-Reutt & Czuczwar, 2020).

In this context, some cannabinoids (including Δ^9-THC, CBD and BCP) contain certain groups in their chemical structures that allow them to exert antioxidant effects. This potential seems to be cannabinoid receptor-independent, possibly by mere radical scavenging. However, these effects may be also exerted by the regulation of several intracellular signals related to the expression/function of antioxidant mechanisms, such as nrf-2 and phase II antioxidant enzymes (Pazos *et al.*, 2008).

3.2. Cannabinoids for the treatment of epilepsy

C. sativa plant has been used as a potential treatment for drug-resistant epilepsy for many thousands of years. The earliest documented uses were found in an Ancient Sumerian tablet of 1800 B.C. and in an Arabic document of the 12th century (Lozano, 2001; Russo *et al.*, 2008). In Europe, the first evidence was described by the physician William O'Shaughnessy in 1843, who reported successful treatment of seizures using cannabis in childhood epilepsy (O'Shaughnessy, 1843). This idea was supported by other physicians of that time, including the prominent neurologist Sir John Russel Reynolds,

who was Queen Victoria's personal physician (Reynolds, 1868). With the isolation of major phytocannabinoids and the discovery of the ECS in the 20th century, investigations in this field started to increase (Mechoulam *et al.*, 2014).

Δ^9-THC was the first phytocannabinoid to be assessed for its anticonvulsant potential. However, some case reports and multiple animal studies have shown that it can exert either anticonvulsant or proconvulsant effects (Rosenberg *et al.*, 2015). These opposite actions can be explained attending to the location of CB_1 receptor, which is proposed as the main molecular target of Δ^9-THC in these studies. In addition, as already mentioned in previous sections, CB_1 receptor activation can trigger undesirable psychotropic effects; this issue should be carefully considered in the case of infantile or adolescence population, since there are no longitudinal studies assessing the long-term consequences of a treatment with Δ^9-THC at early ages. Hence, it is generally recognized that Δ^9-THC therapeutic potential is hardly limited in these patients (Hofmann & Frazier, 2013; Sagredo *et al.*, 2018). Potential obstacles regarding Δ^9-THC administration led to some researchers starting to look at CBD as an antiseizure treatment, a highly active field that will be independently addressed in the following section.

3.2.1. Cannabidiol in DS and other pediatric epilepsies

Interestingly, the anticonvulsant properties were one of the first effects attributed to CBD (Carlini *et al.*, 1973; Cunha *et al.*, 1980; Mechoulam & Carlini, 1978). Moreover, there is an accumulation of preclinical evidence suggesting anticonvulsant effects of CBD in various *in vitro* and *in vivo* experimental models of epilepsy (Devinsky *et al.*, 2014; Jones *et al.*, 2010, 2012; Shirazi-zand *et al.*, 2013). In the clinical setting, and focusing on treatment-resistant pediatric epilepsies, CBD is reporting great benefits, not only in attenuating seizures, but also regarding the long-term outcome that is typically deteriorated in these patients (Scheffer *et al.*, 2021).

Case reports and clinical data

Thanks to an increased legal availability of medical cannabis in some USA states, and to an easy information transfer via social media platforms, some years ago several parents started to administer CBD-enriched cannabis preparations to their children with severe forms of pediatric epilepsies (Porter & Jacobson, 2013). Perhaps, the most noteworthy example of this promising anticonvulsant potential is represented by Charlotte Figi, a small girl from Colorado who was affected by an intractable form of DS. Her parents started to administer to her a cannabis oil derived from a particular cannabis strain (now named as "Charlotte's Web") with a high CBD:Δ^9-THC ratio, and her seizure frequency

reduced from nearly 50 generalized tonic-clonic seizures per day to 2-3 nocturnal seizures per month (Maa & Figi, 2014).

Almost at the same time, a group of parents of 19 children affected by treatment-resistant pediatric epilepsies (including mainly DS, but also LGS and Doose syndrome, among others), started to use similar cannabis preparations and shared their positive experiences in social media. A follow-up survey collected these data, and 16 (84%) of the 19 parents reported a reduction in seizure frequency (Porter & Jacobson, 2013). Soon afterwards, another follow-up survey collected data from a larger cohort, which also included children with West syndrome, and reported similar results (Press *et al.*, 2015).

This remarkable success in case reports (Devinsky *et al.*, 2014; Jones *et al.*, 2010, 2012; Shirazi-zand *et al.*, 2013), stimulated the British company GW Pharmaceuticals to produce an oral liquid formulation of pharmaceutical-grade 99% pure CBD in strawberry-flavored sesame oil, which is currently known under the brand name of Epidyolex® (Epidiolex® in the USA). In this setting, Epidyolex® obtained the orphan drug designation in 2013 (US Food and Drug Administration, FDA) and 2014 (European Medicines Agency, EMA). Thanks to this designation, five randomized, multi-center, double-blinded and placebo-controlled pivotal trials using CBD have been performed in three pediatric epilepsies, including patients with DS (Devinsky *et al.*, 2017; Miller *et al.*, 2020), LGS (Devinsky *et al.*, 2018; Thiele *et al.*, 2018), and epilepsy associated with tuberous sclerosis complex (TSC) (Thiele *et al.*, 2019). The median percent reduction in seizure frequency in each of these five trials is shown in Figure I16.

Based on these positive results, it received the FDA authorization as a co-adjuvant treatment for seizures in LGS and DS in June 2018, and the EMA approval as a co-adjuvant treatment (specifically with clobazam) in September 2019. For both disorders, it is approved only for patients aged ≥ 2 years. In August 2020, it received FDA approval for the treatment of seizures associated with TSC. Moreover, taking into account its anticonvulsant profile in the preclinical setting, as well as some additional preliminary reports, CBD is likely to be effective in other epileptic syndromes, including focal epilepsy or Doose syndrome, among others (Franco & Perucca, 2019).

Importantly, its safety profile is mostly favorable, having demonstrated good tolerability during the clinical development; reported adverse effects are mild or moderate, including somnolence, decreased appetite, vomiting or fatigue, among others. However, increases in liver transaminases were detected in some cases (8% of patients for the dose of 10 mg/kg/day and 16% of patients for the dose of 20 mg/kg/day) (Devinsky *et al.*, 2017, 2018; Miller *et al.*, 2020; Thiele *et al.*, 2018, 2019); therefore, according to the full

prescribing information provided by GW Pharmaceuticals, transaminases should be measured before, during and after treatment with the purpose of avoiding hepatic impairment, specially in those patients taking a dose of 20 mg/kg/day (Franco & Perucca, 2019).

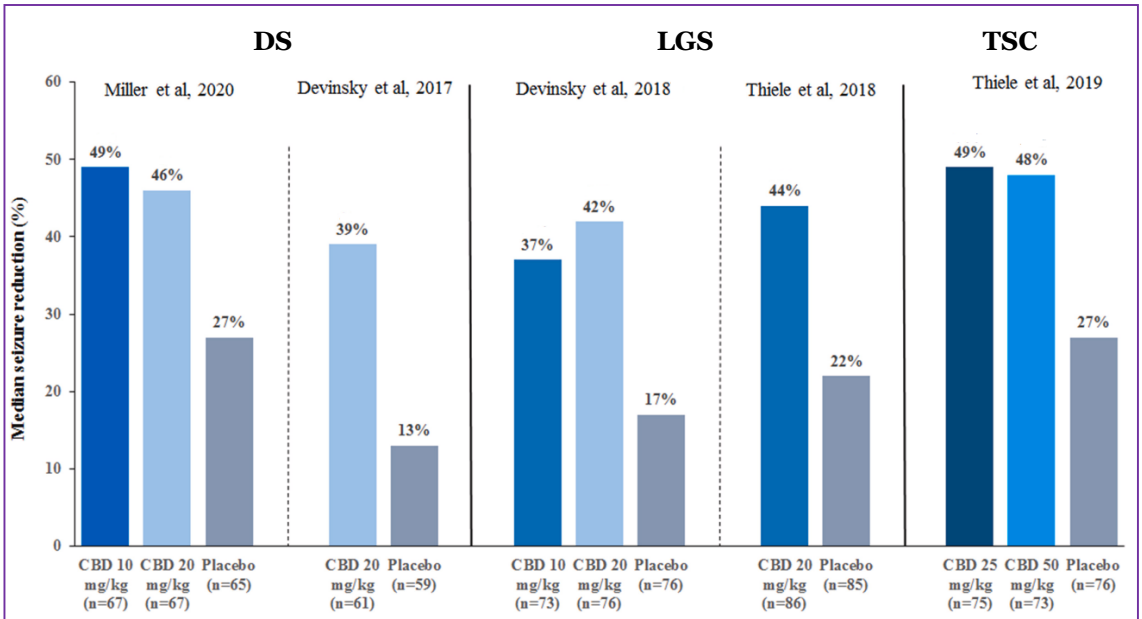

Figure I16. Reduction in seizure frequency in each of the five trials of CBD. Median percent reduction in seizure frequency in patients with DS (Devinsky *et al.*, 2017; Miller *et al.*, 2020), LGS (Devinsky *et al.*, 2018; Thiele *et al.*, 2018), and epilepsy associated with TSC (Thiele *et al.*, 2019). Seizure frequency refers to convulsive seizures for DS patients, drop seizures for LGS patients, and focal and generalized seizures for TSC patients. Taken from Franco *et al.*, 2021.

Proposed molecular mechanisms for cannabidiol in epilepsy

As mentioned, the anticonvulsant profile of CBD is well-documented in a wide variety of experimental paradigms. However, since the pharmacodynamics profile of CBD is extremely complex, its anticonvulsant mechanisms of action are not fully understood. Although further research is needed, it is proposed that CBD might exert a cumulative anticonvulsant effect through the modulation of several endogenous systems (Franco & Perucca, 2019; Gray & Whalley, 2020) (Figure I17).

Within the ECS, CBD has little affinity to $CB_{1/2}$ canonical receptors. However, it has been suggested to indirectly modulate the ECS by blocking the uptake of the endocannabinoid anandamide, as well as by inhibiting its hydrolysis by FAAH (Bisogno *et al.*, 2001; Leweke *et al.*, 2012). In this way, CBD is proposed to increase endocannabinoid levels, which has proven to be protective against seizures, as aforementioned (De Petrocellis *et al.*, 2011). Moreover, it antagonizes the non-canonical cannabinoid receptor GPR55,

which inhibits intracellular calcium release and specifically decreases excitatory currents (Kaplan *et al.*, 2017).

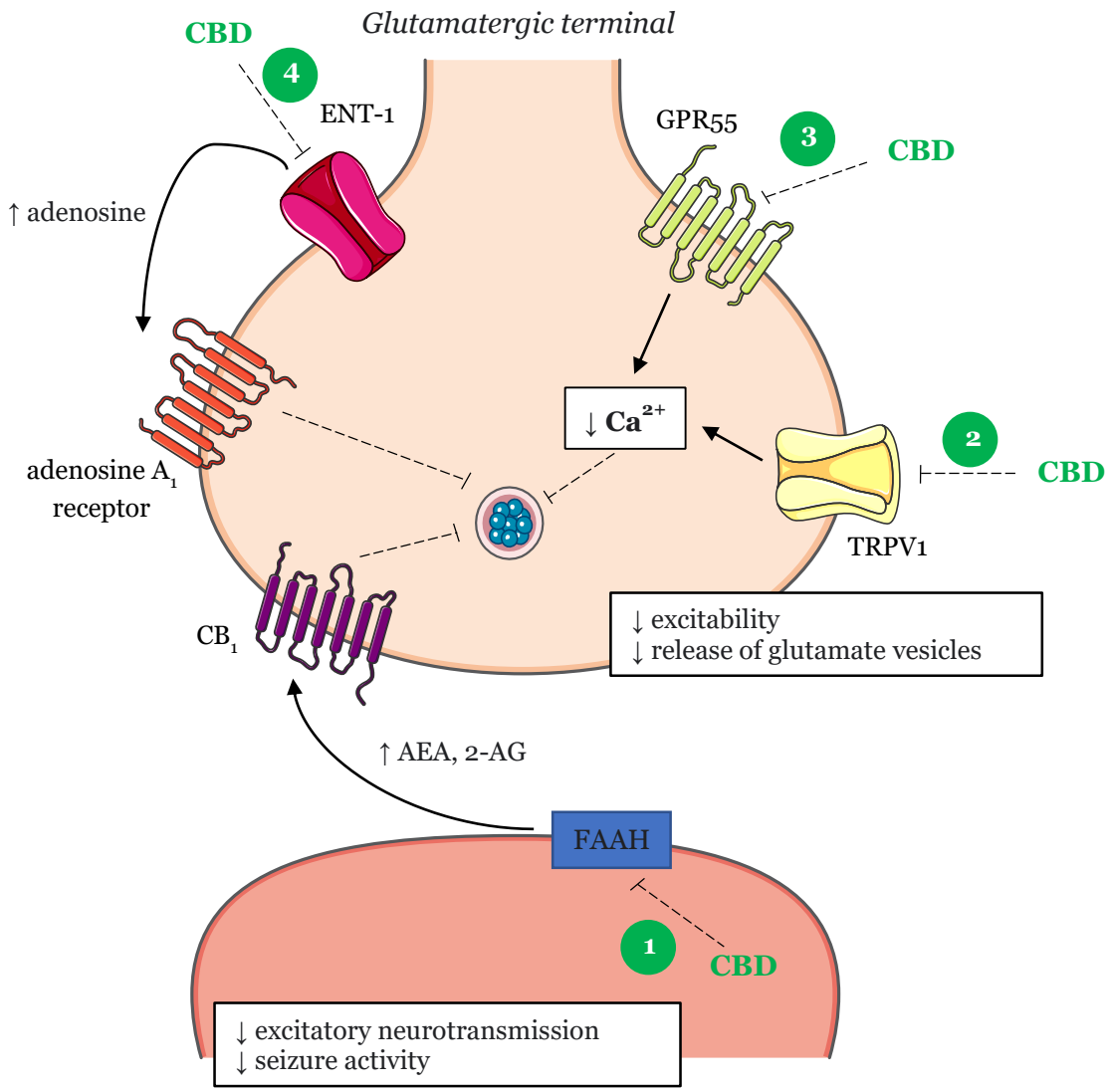

Figure I17. Proposed mechanisms of action for CBD in glutamate excitotoxicity and epilepsy. Effects on (1) FAAH enzyme, (2) $TRPV_1$ channels, (3) GPR55 receptor and (4) ENT-1 transporter. Adapted from Gray & Whalley, 2020.

There are other pharmacological mechanisms that are not directly mediated by the endocannabinoid system. On the one hand, CBD has been shown to desensitize $TRPV_1$ channels, which triggers a decrease in extracellular calcium influx in excitatory terminals and decreases excitatory neurotransmission. Consistent with this effect, the anticonvulsant effects of CBD are attenuated in $TRPV_1$ knock-out mice (Gray *et al.*, 2020). On the other hand, CBD inhibits equilibrative nucleoside transporters (ENT-1), thus reducing adenosine reuptake (Nichol *et al.*, 2019); this increase in extracellular adenosine levels has proven to reduce hyperexcitability and excitatory transmission through adenosine A_1 receptor signalling (Fredholm *et al.*, 2005; Gray & Whalley, 2020).

Although less studied, other CBD mechanisms involved in its anticonvulsant activity may include the activation of 5-HT_{1A} serotonergic receptors, μ-opioid receptors and inhibitory glycine-receptors (dos Santos *et al.*, 2015; Franco & Perucca, 2019; Silvestro *et al.*, 2019).

Apart from the effects of CBD against the hyperexcitability typically occurring during seizure activity, its effects against oxidative stress and neuroinflammation may also contribute to attenuate the overall pathogenic process (Box 2) (Ligresti *et al.*, 2016; Pisanti *et al.*, 2017), which may be beneficial to improve the overall outcome and long-term associated comorbidities.

Another noteworthy mechanism by which CBD improves seizure control is the elevation of plasma concentrations of other anticonvulsants which are concurrently administered. In this sense, the best documented drug-drug interaction has been reported for the concomitant use of clobazam and CBD, with an approximately three-fold increase in plasma levels of *N*-desmethylclobazam, the active metabolite of clobazam (Devinsky *et al.*, 2019; Geffrey *et al.*, 2015). Several studies suggest that this interaction is due to the fact that CBD, at clinically relevant concentrations, is a potent inhibitor of the CYP2C19 enzyme, which is the primary CYP isoform involved in *N*-desmethylclobazam clearance (Gaston *et al.*, 2017; Geffrey *et al.*, 2015). Although few data are still available regarding CBD interaction with other anticonvulsants beyond clobazam, drug-drug interactions have been also proposed for topiramate (Gaston *et al.*, 2017) and stiripentol (Ben-Menachem *et al.*, 2020). Therefore, the influence of CBD on the pharmacokinetics of other concomitantly administered drugs should be taken into account with the purpose of considering dosing adjustments (Franco & Perucca, 2019).

3.2.2. β-caryophyllene as a novel anticonvulsant agent

Recent accumulating evidence indicates that BCP is a promising therapeutic agent in several experimental paradigms, including epilepsy (da Fonseca *et al.*, 2019; Gonçalves *et al.*, 2020; Sharma *et al.*, 2016). In this sense, BCP has been shown to exert anticonvulsant activity in acute seizure models in mice (Table I4).

Interestingly, apart from this anticonvulsant effect, BCP has shown a potent anti-inflammatory and antioxidant profile in a wide variety of experimental paradigms, including neurodegenerative disorders such as Alzheimer's or Parkinson's, cerebral ischemia, depression and anxiety, neuropathic pain, rheumatoid arthritis and gastrointestinal disorders such as ulcerative colitis or peptic ulcer (Machado *et al.*, 2018; Scandiffio *et al.*, 2020). These three properties (anticonvulsant, anti-inflammatory and antioxidant) might constitute a promising therapeutic potential against the overall

pathogenic process and long-term comorbidities, i.e., being disease-modifying, which would represent a major therapeutic advance for epilepsy, including DS.

Table I4. Effects of BCP on epilepsy and acute seizures.

Experimental conditions	Effects	Reference
KA-induced seizures BCP: 30 or 60 mg/kg	Reduction of: mortality by 50%, seizure activity score and severity, lipid peroxidation, oxidative stress markers and pro-inflammatory cytokines.	Liu *et al.*, 2015
PTZ-induced seizures BCP: 10, 30 or 100 mg/kg	Reduction of seizure activity score and severity. Improved performance in the novel object recognition test.	de Oliveira *et al.*, 2016
PTZ-induced seizures KA-induced seizures BCP: 10, 30, 50 or 100 mg/kg	Reduction of: seizure activity score and severity, lipid peroxidation and oxidative stress markers. Improved performance in the Morris water maze test.	Tchekalarova *et al.*, 2018

BCP is proposed to exert its beneficial effects through CB_2 receptor activation (Gertsch *et al.*, 2008), which is tightly related to its anti-inflammatory and antioxidant effects. In addition, other targets, specially PPARγ receptors and the TLR4 complex, might be of interest (Sharma *et al.*, 2016). However, it remains unknown the specific action mechanisms through which BCP exerts its beneficial effects in epilepsy, since available studies do not assess this issue (de Oliveira *et al.*, 2016; Liu *et al.*, 2015; Tchekalarova *et al.*, 2018).

As mentioned, there is evidence that suggests that BCP can act synergistically with both Δ^9-THC and CBD, taking part in the so-called "entourage effect" (Russo, 2011). In the context of epilepsy, this effect could be enormously interesting, since BCP - apart from being beneficial by itself - could potentiate CBD effects, thus enabling a better pharmaceutical management.

AIMS

As mentioned in the Introduction, around 30% of DS patients remain refractory to currently available drugs, thus making it essential the search for additional treatments. Apart from epileptic activity, DS progression is also characterized by a wide range of behavioral comorbidities; therefore, not only anticonvulsant, but also disease-modifying therapeutic approaches, must be considered. In this context, some cannabinoids have been pointed out as promising drugs for the treatment of DS and other pediatric epileptic encephalopathies. In addition to anticonvulsant properties, these compounds have been demonstrated to exert therapeutic effects against oxidative stress and neuroinflammation, which may be beneficial against associated comorbidities. Our **hypothesis** is that a cannabinoid-based treatment may represent a promising therapeutic option to modulate pathogenic mechanisms beyond epileptic activity and modulate DS progression.

In this context, the **global aim** of this Doctoral Thesis is to deepen the knowledge and validate the therapeutic potential of cannabinoids in DS. This general objective was divided into 3 **specific aims**, which are represented in this Doctoral Thesis as 3 different chapters:

1. Neuropathological characterization of a novel DS mouse model.

In order to perform long-term studies focused on disease-modifying therapies, we first characterized a novel *Scn1a*-A1783V mouse model of DS which is particularly useful to investigate the effect of cannabinoids against disease progression. To this end, we initially focused on evaluating survival, seizure susceptibility and associated comorbidities at different postnatal stages. Then, we determined the contribution of different neuropathological processes to DS progression using biochemical and histological tools.

2. Analysis of BCP as an anticonvulsant and disease-modifying agent in DS.

The *Scn1a*-A1783V mouse model previously characterized in Chapter 1 was used to evaluate the therapeutic potential of BCP in DS. In a first study, the anticonvulsant profile of an acute dose of BCP in modulating PTZ-induced seizures was evaluated. In a second study, we assessed its disease-modifying potential by subjecting animals to a chronic pharmacological treatment. In both paradigms, its anti-inflammatory potential was also evaluated.

3. Evaluation of the effectiveness of a combination of BCP and CBD as a potential therapeutic approach in DS.

To this aim, we used both the BV2 microglial cell line and the *Scn1a*-A1783V mouse model. In these two experimental models, we evaluated the therapeutic potential of the combination of BCP and CBD, as well as each compound alone, with the main goal of assessing whether the combination of these compounds may exert additional effective responses. Likewise, there was a special focus on anti-inflammatory effects.

MATERIALS & METHODS

1. *IN VIVO* ANALYSIS

1.1. Animals and genotyping

As mentioned in the Introduction, a conditional knock-in mouse model of DS with *Scn1a* haploinsufficiency was used for the three objectives of this Doctoral Thesis. Specifically, DS was modeled in a C57BL/6J background by expressing a loss-of-function missense mutation (A1783V) in the *Scn1a* gene conditionally expressed in neuronal cells, using the Cre-*loxP* system. Box 6 shows an overview of the genetic construct of these conditional mice.

Box 6. Genetics of B6(Cg)-*Scn1a*$^{tm1.1Dsf}$/J mice

In these mice, one of the *Scn1a* alleles contains a wild-type *Scn1a* exon 26 and a STOP signal, both flanked by Cre-recognition sequences (*loxP* sites). This construct is followed by a humanized mutated *Scn1a* exon 26 containing a C to T change at nucleotide 5348, which will be incorporated in the mature mRNA expressed from this allele. As a result, the amino acid at position 1783 (located in the domain IV S6 transmembrane region of the protein $Na_V1.1$) will change from an alanine to a valine (Figure M1). Therefore, under normal conditions, mice will produce the normal protein $Na_V1.1$. However, when these animals express Cre recombinase, this enzyme will be capable of removing the *loxP* flanked region and express one mutant *Scn1a* copy.

B6(Cg)-*Scn1a*$^{tm1.1Dsf}$/J (stock no. 026133)

Scn1a gene (Chr2):

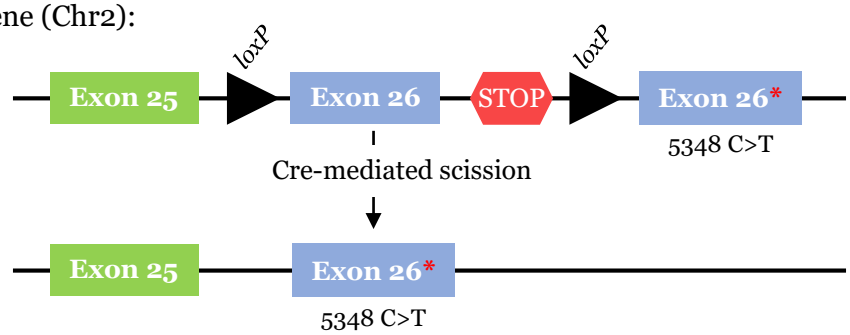

Figure M1. Construct design strategy in B6(Cg)-*Scn1a*$^{tm1.1Dsf}$/J mice. Exon 26 red asterisk makes reference to the mutation resulting in a C to T change at nucleotide 5348.

To this end, breeding colonies of the parental lines B6(Cg)-*Scn1a*$^{tm1.1Dsf}$/J (stock no. 026133) and B6.Cg-Tg(*Syn1-cre*)^{671Jxm}/J (stock no. 003966) were generated based on breeding pairs purchased from The Jackson Laboratory (Bar Harbor, ME, USA). Conditional heterozygous knock-in males with a floxed *Scn1a* (A1783V mutation) were crossed with females hemizygous for Cre recombinase (under the control of the neuronal synapsin 1 (Syn1) promoter), giving rise to four offspring experimental groups as detailed in Table M1.

Table M1. F1 offspring generation of experimental groups upon Cre-mediated recombination.

Experimental group	*Scn1a* missense mutation	Syn1-Cre recombinase	Mutated allele
Scn1a$^{WT/WT}$	-	-	-
Syn1-Cre/Scn1a$^{WT/WT}$	-	+	-
Scn1a$^{WT/A1783V}$	+	-	-
Syn1-Cre/Scn1a$^{WT/A1783V}$	+	+	+

Mice carrying the mutated allele (Syn1-Cre/Scn1a$^{WT/A1783V}$) express the A1783V mutation in neuronal cells expressing Syn1 and will manifest a DS-like phenotype, whereas the other three groups not carrying the mutation will be considered control groups.

During experiments, mice were housed in a climate-controlled animal room (21 ± 2°C temperature, 60% humidity) under a controlled photoperiod of 08:00 -20:00 light, with standard chow and water *ad libitum*. All experiments were conducted according to national and European guidelines (RD 53/2013 and directive 2010/63/EU, respectively), and were approved by the Ethical Committee for Animal Welfare of the Complutense University and the "Comunidad de Madrid" (ref. PROEX 033/17). All possible efforts were made to minimize animal pain and discomfort, as well as to reduce the number of experimental subjects. In all experimental procedures, both males and females were included at similar proportions, given that the incidence and degree of affectation of DS are similar in both genders (Skluzacek *et al.*, 2011).

The genotype of the animals was confirmed by polymerase chain reaction (PCR) using genomic DNA from mouse tail biopsy. Genomic DNA was extracted and amplified using REDExtract-N-Amp Tissue PCR kit (Sigma-Aldrich, Madrid, Spain) and following manufacturer's instructions. Two different PCR amplifications were performed with different primer pairs each; the first one to verify the presence of the floxed insert in the *Scn1a* gene, and the second one to verify the presence of the Syn1-Cre recombinase. Primers sequences and PCR conditions are shown in Table M2. PCR products were separated by electrophoresis in 2% agarose gels and visualized using GelRed. Figure M2 shows a representative agarose gel with the four possible genotypes.

1.2. Drug preparation

For *in vivo* pharmacological experiments, CBD and BCP were purchased from Sigma-Aldrich (Madrid, Spain). Because of classic cannabinoid hydrophobicity, plastic tubes employed in these experiments were pre-treated with Sigmacote (Sigma-Aldrich, Madrid, Spain). BCP and CBD were directly dissolved in ethanol to a final stock

concentration of 50 mg/ml, and stored at -20ºC under a N_2 atmosphere to avoid oxidation. On the day of the experiment, injectable solutions were prepared by further diluting in Tween-80 (Sigma-Aldrich, Madrid, Spain) and 0.9% NaCl to a final proportion of 1:16, and residual ethanol was eliminated under a N_2 flux. Experimental designs and dosage schedules are specifically provided within the Results section.

Table M2. Primers sequences and PCR conditions used in genotyping.

***Scn1a* PCR**		**Cre recombinase PCR**	
Primers sequences (5' → 3')			
Forward	TAC TGG GAT CCA CCT CCA CT	**Forward**	CTC AGC GCT GCC TCA GTC T
Reverse	TAG CTC CGC AAG AAA CAT CC	**Reverse**	GCA TCG ACC GGT AAT GCA
Cycling conditions			
Step	**Temperature (ºC)**	**Time**	
1	94	2 minutes	
2	94	20 seconds	
3	65	15 seconds	
4	68	10 seconds	
5	Repeat steps 2-4 for 10 cycles		
6	94	15 seconds	
7	60	15 seconds	
8	72	10 seconds	
9	Repeat steps 6-8 for 28 cycles		
10	42	2 minutes	
11	10	hold	

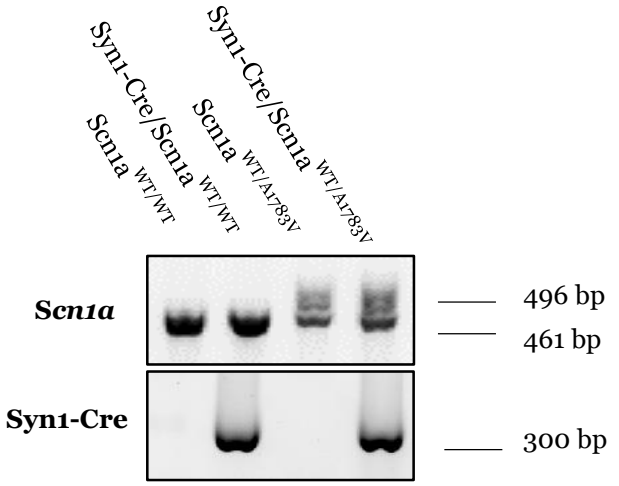

Figure M2. Representative results of genotypes provided by PCR and subsequent agarose gel electrophoresis. Regarding S*cn1a* PCR, the wild-type allele corresponds to a lower 461 bp band, and the mutant allele carrying the missense mutation to an upper 496 bp band. Regarding Cre recombinase PCR, a 300 bp band corresponds to Syn1-Cre.

1.3. Behavioral assessment

In order to evaluate behavioral disturbances and comorbidities in DS mice, different tests were performed at specific postnatal stages, as it will be specified in each experiment.

Before testing, mice were subjected to a 30-minute acclimation period to the test room. Efforts were done to maintain low ambient noise levels during procedures. In addition, researchers were blinded to mouse genotypes and treatment conditions during testing. In those tests requiring specific apparatus, equipment was thoroughly cleaned with 70% alcohol before the next task to remove any residual odor that could interfere with the test outcome.

1.3.1. Reflexes

Limbs grasp reflexes. Front- and hin-limb grasp reflexes were measured as an index of grasping ability and motor development (Blaney *et al.*, 2013). Mice were held on their back and both front- or hindlimbs were touched with a thin rod of 1 mm diameter. A score of 1 was assigned when the stimulation caused the front- or hindlimb to grasp, whereas a score of 0 was assigned if no response was reached.

Vibrissae response. Vibrissae response was measured to analyze the development of the tactile sensory system (Blaney *et al.*, 2013). Mice were held by their tail and approached towards a flat surface. A score of 1 was assigned if mice raised their head to avoid contact with the flat surface due to vibrissae stimulation, whereas a score of 0 was assigned if no response was reached.

Hindlimbs clasping reflex. Hindlimbs clasping behavior was recorded in order to assess dystonia. Mice were suspended by their tail facing downward and the extent of hindlimbs position was observed for 30 sec. If both hindlimbs were entirely retracted and touching the abdomen, a score of 2 was given; if both of them were partially retracted, a score of 1 was assigned, and if both hindlimbs were consistently splayed outward away from the abdomen with splayed toes, a score of 0 was given (adapted from Valdeolivas *et al.*, 2017). Data for each mouse correspond to the average of three trials.

1.3.2. Open-field test

Locomotor activity was analyzed in a computer-aided actimeter (Actitrack, Panlab, Barcelona, Spain) (Figure M3A). This apparatus consisted of a 45 × 45 cm square arena, with infra-red beams all around, spaced 2.5 cm, coupled to a computerized control unit that automatically registered the following parameters, among others: (1) distance run in the actimeter (ambulation); (2) frequency of vertical activity (rearing); (3) resting time; (4) mean velocity during ambulation; and (5) time spent in fast movements (> 5 cm/s) (Palomo-Garo *et al.*, 2016). Measurements were recorded for a period of 30 minutes in characterization studies and 15 minutes in pharmacological studies.

1.3.3. Rotarod test

Motor coordination was measured in a LE8200 device (Panlab, Barcelona, Spain). This apparatus consisted of a horizontally placed rotating cylinder (rod) turning at a constant or accelerated speed, which is mechanically held (Figure M3B). Animals were placed on the rotating rod and after a period of acclimation and training (first session: 0 rpm for 10 sec; second and third sessions: 4 rpm for 10 sec, with periods of 10 min between sessions), mice were tested for three consecutive trials with an acceleration from 4 to 40 rpm over a period of 300 sec, and with a rest period of 30 min between trials. Latency to fall in each trial was recorded, and data for each mouse correspond to the average of the three trials (Palomo-Garo *et al.*, 2016).

1.3.4. Elevated plus maze test

An elevated plus maze was used to assess anxiety-like behavior. This apparatus consisted of two opposite closed (30 cm × 5 cm × 15 cm) and open (30 cm × 5 cm) arms forming a cross-shaped maze (Figure M3C). The structure was elevated to a height of 37.5 cm from the floor and all four arms were connected at a right angle at a central area called start point. At the beginning of a trial, each animal was placed in the start point (facing an open arm) and was left free to explore the maze for 5 min. During this 5 min test period, the following behavioral parameters were recorded: (1) number of open and closed arm entries; and (2) time spent in the open and closed arms. Closed-arm entries (counts/5 min) were considered indicators of locomotor activity, whereas open-arm exploration (% time spent in open arms and % open arm entries) were used as measures of anxiety. An entry was considered when the head and front-limbs of the mouse were in one arm (Satta *et al.*, 2016).

1.3.5. Y-maze test

Y-maze test was used to assess short-term spatial and working memory in mice, based on the capacity of rodents to explore new environments. The apparatus was a polyvinyl plastic horizontal maze formed by 3 identical arms (40 × 12 × 3 cm) placed at 120° angles to each other in the shape of a capital Y, and designated as A, B and C (Figure M3D). Each animal was placed at the end of one arm and was allowed to freely explore the apparatus. The sequence (i.e., ABCCAB, etc.) and the number of arm entries were recorded during 8 min. The spontaneous alternation performance (SAP) is defined as a score of three consecutive different arm entries (ABC, CAB, or BCA) on overlapping triplet sets (% SAP = number of spontaneous alternations/total arm entries x 100). An animal with an intact short-term spatial memory often spends more time exploring new

maze arms. Memory impairments were evaluated by the frequency of same arm returns (SAR) or alternate arm returns (AAR) in the Y-maze (% SAR = number of same arm returns/total arm entries x 100; % AAR = number of alternate arm returns/total arm entries x 100) (Choi *et al.*, 2019).

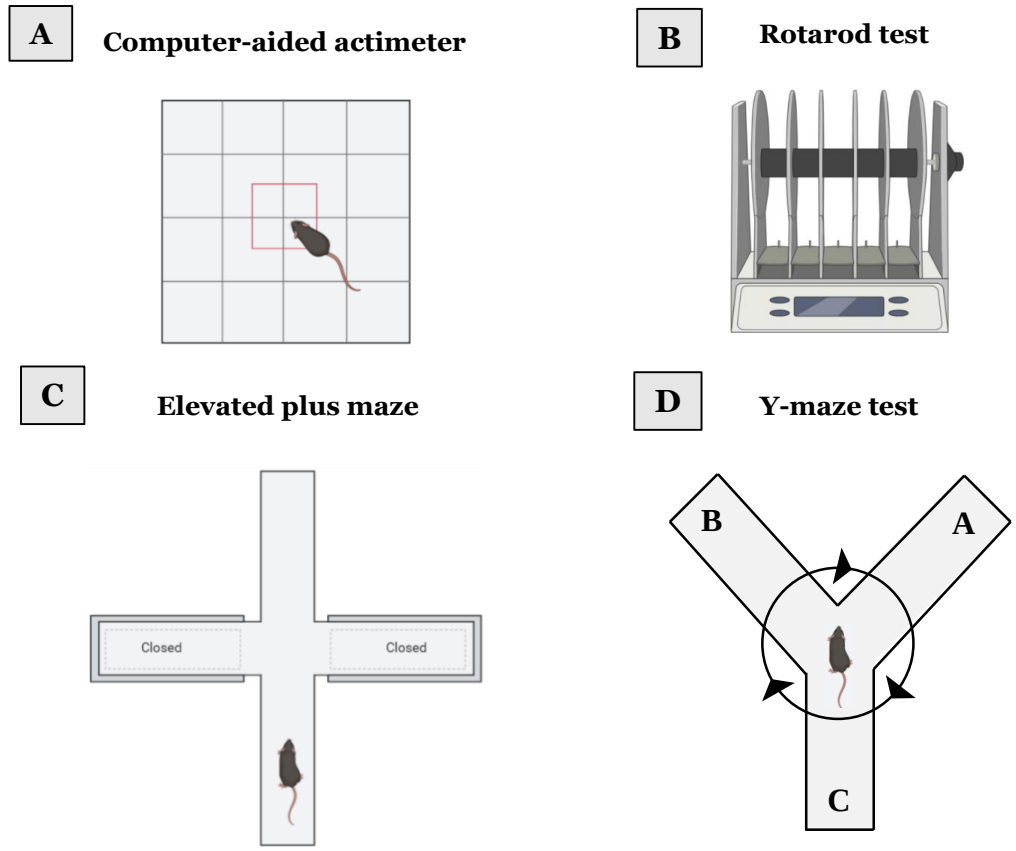

Figure M3. Schematic representation of different behavioral tests. **(A)** Computer aided-actimeter, **(B)** Rotarod test, **(C)** Elevated plus maze and **(D)** Y-maze test.

1.3.6. T-maze test

Similar to the Y-maze test, the T-maze test was also used to assess short-term spatial and working memory in mice, based on the capacity of rodents to explore new environments. Particularly, this test explores their natural tendency to alternate their choice of goal arm and explore new environments (spontaneous alternation without reward). The apparatus was a polyvinyl plastic horizontal maze formed by three arms giving rise to a T-shaped maze. Dimensions are specified in Figure M4A. In each trial, the mouse was placed in the start point and allowed to freely choose one goal arm (A or B), and then confined in the chosen arm with the door down for 30 sec. After 30 sec, the mouse was placed back in the start point and, with doors up, allowed again to freely choose a goal arm. The trial must take one minute and a half maximum (Figure M4B). A score of 1 was assigned if mice chose the opposite arm, whereas a score of 0 was assigned if the same

arm was chosen). Normally, 6 trials per mouse were performed, thus data corresponding to the average of all trials (Deacon & Rawlins, 2006).

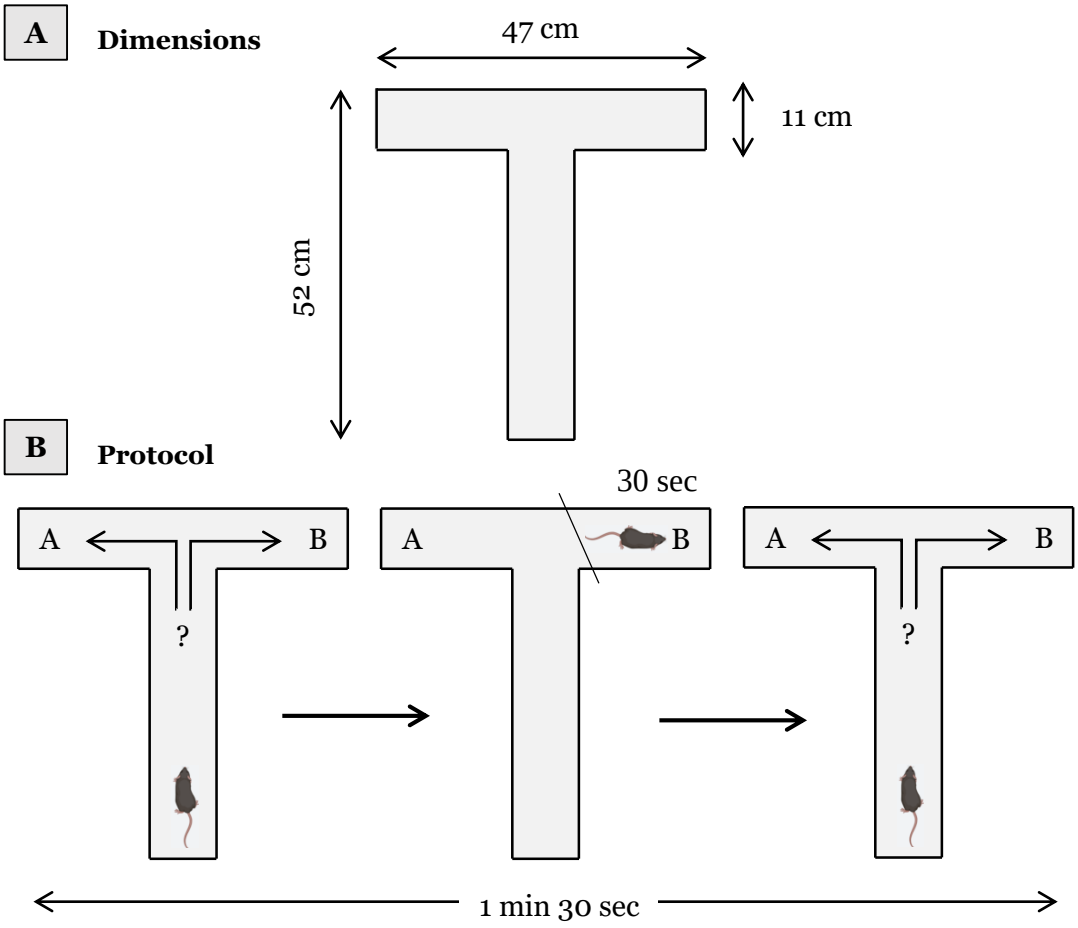

Figure M4. T-maze test. **(A)** Apparatus dimensions and **(B)** schematic diagram of the experimental protocol.

1.3.7. Social interaction test

This test was conducted in an open field arena (50 cm x 26 cm) in which each experimental animal was allowed to freely explore a novel unfamiliar congener of the same sex and of similar weight under dim light. The behaviour was recorded for 20 minutes, and the total time spent by the experimental mouse in nonaggressive social interactions such as sniffing, following or grooming the partner, was monitored (Ricceri *et al.*, 2016). The number of active contacts with the partner was scored as well.

1.3.8. Analysis of PTZ-induced seizuring activity

Seizure activity was induced by administration of the proconvulsant agent PTZ, following a previous method (Alachkar *et al.*, 2020). PTZ (Sigma-Aldrich, Madrid, Spain) was freshly dissolved in sterile saline (0.9% NaCl) to prepare a stock solution with a

concentration of 10 mg/ml. Mice were individually placed in glass boxes and injected with PTZ (50 mg/kg, i.p.) and were then observed for a 30-minute period. During this period, several behavioral parameters were recorded: (1) latency to myoclonic jerks, (2) latency to generalized seizures, (3) the difference between both latencies (calculated as latency to generalized seizures minus latency to myoclonic jerks for each animal) and (4) total duration of generalized seizures. PTZ dose and experimental schedule were selected based on pilot experiments aimed to set those experimental conditions inducing seizuring activity in 100% of control mice.

1.4. Survival analysis

As already mentioned in the Introduction, Dravet syndrome progression is associated with a higher incidence of premature death. Therefore, in both characterization and *in vivo* pharmacological experiments, animal survival was evaluated as a marker of disease severity and/or the effectiveness of a treatment. To this end, time from birth until death was registered, and differences in survival rates between different experimental groups were evaluated using Kaplan-Meier curves.

1.5. Sampling

1.5.1. Sample preparation for histological and molecular biology analysis

Mice were euthanized by rapid decapitation and brains were rapidly removed and divided into the two hemispheres. Left hemispheres were fixed for one day at 4ºC in fresh 4% paraformaldehyde prepared in 0.1 M phosphate-buffered saline (PBS), pH 7.4, then cryoprotected by immersion in a 30% sucrose solution for a further day, and finally stored at -80ºC for immunohistochemical analysis. Right hemispheres were rapidly dissected in different cerebral areas of interest, such as prefrontal cortex, striatum, hippocampus and cerebellum, which were frozen in 2-methylbutane cooled in dry ice and stored at -80ºC until processing for qPCR or Western-blot experiments.

1.5.2. Sample preparation for flow cytometry analysis

Regarding blood and bone marrow (BM) flow cytometry analysis, a different procedure was required (García-Culebras *et al.*, 2019). For this purpose, animals were deeply anesthetized with sodium pentobarbital, and cardiac blood was collected from the right ventricle. Afterwards, transcardiac perfusion was performed with 0.1 M PBS, pH 7.4, for 4 minutes at a rate of 5 ml/min.

Immediately upon collection, blood was thoroughly mixed by several gentle inversions with 5 µl of 0.5 M ethylenediaminetetraacetic acid (EDTA) used as an anticoagulant. Then, red blood cells were lysed in ice-cold lysis buffer (150 mM NH_4Cl, 10 mM $NaHCO_3$, 0.1 mM EDTA) and subjected to centrifugation at 1.000 x *g* for 5 minutes at 4ºC. Cell pellets were flushed with ice-cold 0.1 M PBS, pH 7.4, and subjected to another centrifugation at 1.000 x *g* for 5 minutes at 4ºC. Supernatants were discarded and remaining blood cell pellets were resuspended in fluorescence-activated cell sorting (FACS) buffer for immediate flow cytometry staining. FACS buffer contains 0.1% low endotoxin bovine serum albumin (BSA) in Dulbecco's PBS (DPBS).

BM cells were obtained from tibial and femoral bones. BM stromal cells were washed with FACS buffer and gently homogenized. Cell suspensions were centrifuged at 400 x *g* for 5 minutes at 4ºC, and cell pellets were lysed in lysis buffer. Finally, another centrifugation at 400 x *g* for 5 minutes at 4ºC was performed and remaining BM cell pellets were resuspended in FACS buffer for immediate flow cytometry staining.

2. *IN VITRO* ANALYSIS

2.1. Cell culture and reagents

The immortalized murine BV2 microglial cell line was kindly provided by Dra. Lastres-Becker ("Alberto Sols" Biomedical Research Institute, Madrid, Spain). Cells were maintained in Dulbecco's modified Eagle's medium (DMEM) (Lonza, Verviers, Belgium) supplemented with 10% heat-inactivated fetal bovine serum (FBS) (Sigma-Aldrich, Madrid, Spain), 2 mM ultra-glutamine (Lonza, Verviers, Belgium) and 1% of an antibiotic mixture (penicillin 100 U/ml and streptomycin 100 µg/ml) (Lonza, Verviers, Belgium) in a humidified incubator at 37ºC, 5% CO_2. When cultures reached 70-80% confluency, the cells were serially passaged.

For *in vitro* pharmacological experiments, CBD and BCP were purchased from Sigma-Aldrich (Madrid, Spain). Stock solutions were prepared in 100% DMSO according to manufacturers' solubility instructions and subsequently diluted in culture medium to the desired working concentration, with a final DMSO concentration that did not exceed 0.2%.

2.2. Cell treatments

For cell treatments, BV2 cells were plated at a density of (1) 1×10^6 cells per well in 6-well culture plates for those experiments involving Western-blot, qPCR or

immunocytochemistry, and (2) 6 × 10^4 cells per well in 96-well culture plates for those experiments involving cell viability measurement. In all experiments, cells were incubated in DMEM with a reduction of FBS to 1%, and allowed to attach for four hours after seeding.

In order to study the anti-inflammatory effects of different compounds, cells were treated with 1 µg/ml LPS from *Escherichia coli* 055:B5, (Sigma-Aldrich, Madrid, Spain), alone or in combination with BCP and/or CBD (used at specific concentrations depending on the assay) and added 1 h before LPS. Sixteen hours after the addition of LPS, different experimental procedures were performed, including cell viability assessment by the MTT (3-[4,5-dimethylthiazol-2-yl]-2,5-diphenyltetrazolium bromide) assay, gene expression analysis by qPCR, as well as protein analysis by Western-blot or immunofluorescence (Figure M5).

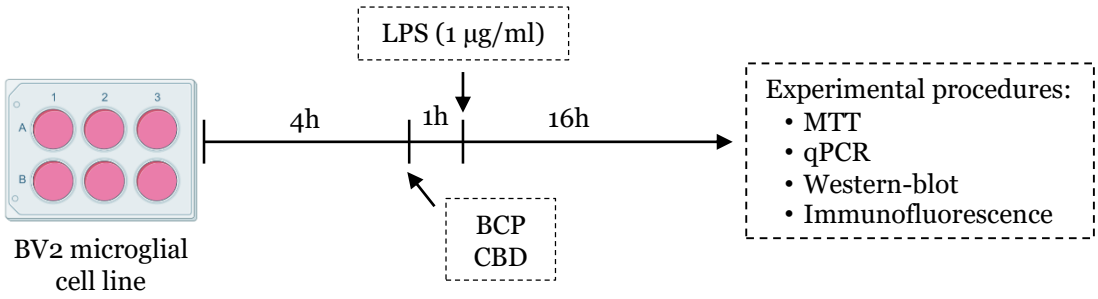

Figure M5. General scheme for cell treatments in BV2 cells. This scheme shows all the possibilities for cell treatments and experimental procedures. Specific adaptations of this scheme for every single experimental design will be provided when required.

Technical specifications for qPCR, Western-blot and immunofluorescence will be provided in a subsequent section. In the case of the cell viability assessment, briefly, MTT (Sigma-Aldrich, Madrid, Spain) was added to each well at a final concentration of 0.5 mg/ml. After 1.5 hours of incubation, the medium was removed and the resultant insoluble formazan crystals were dissolved using 4 mM of HCl in isopropanol. The optical density at 570 nm was recorded using a spectrophotometer, and the amount of formazan formed directly correlates with the cell viability.

3. EXPERIMENTAL PROCEDURES

3.1. Real-time qRT-PCR

Gene expression analysis of specific genes of interest was performed by real-time qPCR. To this aim, total RNA was extracted and purified from brain tissues using SurePrep™ RNA/Protein Purification kit (Fisher BioReagents, FairLawn, NJ, USA). In the case of

cultured cells, total RNA was extracted and purified using Trizol reagent (Sigma-Aldrich, Madrid, Spain). The total amount of RNA extracted was quantitated by spectrometry at 260 nm and its purity was evaluated by the ratio between the absorbance values at 260 and 280 nm, whereas its integrity was confirmed in agarose gels. To prevent genomic DNA contamination, DNA was removed and single-stranded complementary DNA was synthesized from 1 μg of total RNA using a commercial kit (Rneasy Mini Quantitect Reverse Transcription, Qiagen, Izasa, Madrid, Spain). The reaction mixture was kept frozen at -80ºC until enzymatic amplification.

Quantitative real-time PCR assays were performed to quantify mRNA levels, using FastStart TaqMan Probe Master Mix (Roche, Madrid, Spain) and Taqman probes from Applied Biosystems (Madrid, Spain) (Table M3). Glyceraldehyde-3-phosphate dehydrogenase (GAPDH) expression was used as an endogenous control gene for normalization. PCR amplifications were carried out using the 7300 Fast Real-Time PCR System (Applied Biosystems, Foster City, CA, USA) and the threshold cycle (Ct) was calculated by the instrument's software (7300 Fast System, Applied Biosystems, Foster City, CA, USA). Expression levels were calculated using the $2^{-\Delta\Delta Ct}$ method, but, for presentation, data were transformed to the percentage over the mean obtained (1) in the wild-type group for *in vivo* experiments, and (2) in the cells treated with vehicle in absence of LPS for *in vitro* experiments.

Table M3. Taqman probes used in real-time qPCRs assays

Gene	Protein	Applied Biosystems reference
Cnr1	CB1	Mm00432621_s1
Cnr2	CB2	Mm00438286_m1
Gpr55	GPR55	Mm03978245_m1
Pparg	PPARγ	Mm01184322_m1
Faah	FAAH	Mm00515684_m1
Mgll	MAGL	Mm00449274_m1
Dagla	DAGLα	Mm00813830_m1
Napepld	NAPE-PLD	Mm00724596_m1
Tnf	TNFα	Mm99999068_m1
Il1b	IL1β	Mm00434228_m1
Ptgs2	COX-2	Mm00478372_m1
Nos2	iNOS	Mm01309902_m1
Bdnf	BDNF	Mm01334042_m1
Arg1	ARG1	Mm00475988_m1
Gapdh	GAPDH	Mm99999915_g1

3.2. Western-blot

For protein extraction, brain tissues and cultured cells were homogenized in ice-cold radioimmunoprecipitation assay (RIPA) buffer, containing 10 mM Na_2HPO_4, 150 mM NaCl, 1% NP-40, 0.5% sodium deoxycholate, 0.1% sodium dodecyl sulfate (SDS) and 1 mM phenylmethylsulfonyl fluoride (PMSF) as protease inhibitor. Lysates were then subjected to centrifugation at 10.000 x *g* for 15 minutes at 4°C. Bio-Rad DC protein assay kit (Bio-Rad Laboratories, CA, USA) was used to quantify protein concentration, using BSA as the standard protein. Then, 20 µg of protein were boiled for 5 minutes in Laemmli SDS loading buffer (10% glycerol, 5% SDS, 5%-mercaptoethanol, 0.01% bromophenol blue, and 125 mM TRIS-HCl, pH 6.8) and loaded onto a 12% acrylamide gel (TGX Stain-free Gel FastCast; Bio-Rad Laboratories, CA, USA). After electrophoresis, proteins were transferred to polyvinylidene fluoride (PVDF) membranes (Immobilon-P, Millipore, MA, USA) using mini Trans-Blot Electrophoretic transfer cell (Bio-Rad Laboratories, CA, USA). Membranes were then blocked for 1 hour at room temperature with Tris-buffered saline (TBS) containing 5% nonfat dried milk and Tween20 0.1%, and incubated overnight at 4°C with a primary antibody. Primary antibodies used for Western-blot analysis are listed in Table M4.

Table M4. Primary antibodies used in Western-blot analysis

Antibody	Host	Dilution	Company	Reference
CB1	Rabbit	1:500	Frontier Institute	CB1-Rb-Af380
CB2	Rabbit	1:200	Abcam	ab3561
MAGL	Rabbit	1:1000	Frontier Institute	MGL-Rb-Af200
FAAH	Rabbit	1:1000	Cayman	CAY-101600
ZO-1	Mouse	1:200	Santa Cruz	sc-33725
Claudin-5	Mouse	1:200	Santa Cruz	sc-374221
ICAM-1	Mouse	1:200	Santa Cruz	sc-8439
Laminin	Rabbit	1:500	Novus Biologicals	NB300-144
Iba-1	Rabbit	1:500	Wako	019-19741
Catalase	Mouse	1:200	Santa Cruz	sc-271803
TLR4	Mouse	1:500	Santa Cruz	sc-293072

Membranes were finally incubated with the corresponding ECL Horseradish Peroxidase-linked whole secondary antibody (GE Healthcare UK Limited, Buckinghamshire, UK) used at a 1:5000 dilution for 2 hours at room temperature. Reactive bands were detected by chemiluminescence with the Amersham ECL Prime Western Blotting Detection Reagent (GE Healthcare UK Limited, Buckinghamshire, UK). Images were analyzed with ImageLab software (Bio-Rad Laboratories, CA, USA). Data were calculated as the ratio between the optical densities of the specific protein band and the total protein measured

in membranes, and then normalized as percentages over the mean obtained (1) in the wild-type group for *in vivo* experiments, and (2) in the cells treated with vehicle in absence of LPS for *in vitro* experiments.

3.3. Immunofluorescence staining

3.3.1. Immunofluorescence staining of cultured cells

Cultured cells were fixed in 4% PFA for 30 min and washed with PBS. Cells were then permeabilized with PBS containing Triton X-100 0.3% for 15 minutes, and blocked with PBS containing Triton X-100 0.1% and BSA 2% for 30 minutes. After several washes with PBS, cells were incubated for 1 hour at room temperature with the primary antibody rabbit anti-Iba-1 (1:300; Wako Chemicals, Richmond, VI, USA). After incubation, cells were washed in PBS, followed by incubation for 1 hour at room temperature with the secondary antibody Alexa Fluor 488 donkey anti-rabbit (1:200; reference A21206, Life Technologies, Bleiswijk, The Netherlands). Both primary and secondary antibodies were prepared in PBS containing Triton X-100 0.3% and BSA 2%. Finally, preparations were mounted with Dako fluorescent mounting medium (Dako, Carpinteria, CA, USA). Negative control samples were obtained using the same protocol with the omission of the primary antibody. A Leica DMRB microscope and a DFC300FX camera (Leica, Wetzlar, Germany) were used for the observation and photography of the slides, respectively. Immunostaining was quantified by measuring the mean density of labelling in the selected area using the ImageJ software (U.S. National Institutes of Health, Bethesda, Maryland, USA, http://imagej.nih.gov/ij/, 1997-2012). For quantification, high-resolution digital microphotographs were taken under the same conditions of light, brightness and contrast. Data were normalized over the mean obtained in the cells treated with vehicle in absence of LPS.

3.3.2. Immunofluorescence staining of fixed brains

Fixed brains were sliced in coronal sections of 30 µm thick (containing prefrontal cortex, striatum or hippocampus) in a cryostat (Leica CM3050, Leica, Wetzlar, Germany), collected on antifreeze solution (glycerol/ethylene glycol/PBS; 2:3:5) and stored at -20°C until used.

Sections were mounted on gelatin-coated slides and, once adhered, washed with TBS, permeabilized with TBS containing Triton X-100 0.2% for 30 minutes, and blocked with TBS containing Triton X-100 0.1% and BSA 5% for 1 hour. After several washes with TBS, sections were incubated overnight at 4°C with the primary antibody (Table M5). The

different primary antibodies are shown in Table M5. After incubation, sections were washed in TBS, followed by incubation for 2 hours at 37°C with the corresponding secondary antibody, also listed in Table M5. Both primary and secondary antibodies were prepared TBS containing Triton X-100 0.1% and BSA 2%. Nuclear stain Hoechst (H-33258, Fluka, Madrid, Spain) was used to facilitate the localization of the different brain regions on the microscope. Finally, sections were mounted with Dako fluorescent mounting medium (Dako, Carpinteria, CA, USA). Negative control sections were obtained using the same protocol with omission of the primary antibody. For quantification, microphotographs were obtained as indicated in the previous section, and data were normalized over the control mice values.

Endogenous IgG immunostaining was performed to detect BBB disruption by measuring its extravasation from brain blood vessels. To this end, brain sections from perfused mice were analyzed following the same general protocol just described. Specifically, sections were incubated overnight at 4°C with a biotinylated horse anti-mouse IgG secondary antibody (1:200; reference BA-2000, Vector Laboratories, Burlingame, CA, USA). After incubation, sections were incubated for 2 hours at 37°C with Alexa Fluor 546 streptavidin (Molecular Probes, S11225).

Table M5. Primary and secondary antibodies used in immunofluorescence analysis

Primary antibodies				
Antibody	**Host**	**Dilution**	**Company**	**Reference**
Laminin	Rabbit	1:200	Novus Biologicals	NB300-144
NIMP-R14	Rat	1:200	Abcam	ab2557
GFAP	Rabbit	1:200	Dako	Z033429
GFAP	Goat	1:1000	Abcam	ab53554
GFAP-Cy3	Mouse	1:1000	Sigma	MAB3402C3
Iba-1	Rabbit	1:500	Wako	019-19741
Ki67	Rabbit	1:1000	Vector Laboratories	VP-RM04
Secondary antibodies				
Antibody	**Host**	**Dilution**	**Company**	**Reference**
Alexa Fluor 546 anti-rabbit	Goat	1:200	Invitrogen	A11010
Alexa Fluor 647 anti-rabbit	Goat	1:500	Invitrogen	A32733
Alexa Fluor 488 anti-rabbit	Donkey	1:200	Invitrogen	A21206
Alexa Fluor 488 anti-rat	Donkey	1:200	Invitrogen	A21208
Alexa Fluor 568 anti-goat	Donkey	1:500	Invitrogen	A11057

For quantification of cell proliferation in the hippocampal neurogenic niche, immunostaining was carried out following a slightly different protocol. To this end, sections were washed with PBS, and permeabilized and blocked at the same time using PBS containing Triton X-100 0.25% and BSA 3% for 3 hours. After several washes with PBS, sections were incubated overnight at 4°C with the corresponding primary antibody, listed in Table M5. After incubation, sections were washed in PBS, followed by incubation for 3 hours at room temperature with the corresponding secondary antibody, also listed in Table M5. Both primary and secondary antibodies were prepared in PBS containing Triton X-100 0.25% and BSA 3%. 4',6-diamidino-2-phenylindole (DAPI, Sigma-Aldrich) was also added to the sections to counterstain cell nuclei. Finally, sections were mounted on slides with Dako fluorescent mounting medium (Dako, Carpinteria, CA, USA). A Leica SP8 microscope (Leica, Wetzlar, Germany) and LAS X software were used to analyze slides, using a 40x magnification. Densities were normalized for the total volume of the dentate gyrus (SGZ + GCL) obtained using DAPI staining. For Ki67 quantifications, representative numbers ranging from 50 to 300 cells of interest were quantified and classified in randomly selected confocal z-stacks of 30 µm below to 30 µm above the GCL using a 63x oil immersion objective. GCL dispersion was calculated by measuring the thickness of the GCL using DAPI for visualization. Cell circularity was measured using the "Circularity" plugin in ImageJ software (U.S. National Institutes of Health, Bethesda, Maryland, USA, http://imagej.nih.gov/ij/, 1997-2012).

3.4. Flow cytometry analysis

BM and blood cell pellets resuspended in FACS were subjected to flow cytometry analysis. To this end, cell suspensions were transferred to a 96-well plate and Fc fragments blocked by incubation with Fc Blocking Reagent (Miltenyi, Madrid, Spain) for 30 minutes. Then, samples were stained with the corresponding fluorochrome-conjugated monoclonal antibodies (Table M6) used at 1 µg/ml for 1 hour. Plates were then centrifuged at 400 x *g* for 5 minutes, supernatants discarded and cell pellets resuspended in FACS buffer.

Table M6. Antibodies used in flow cytometry analysis

Antibody	Clone	Company
PE/Cy7 anti-mouse/human **B220**	RA3-6B2	Biolegend
PerCP/Cy5.5 anti-mouse **CD3**	17A2	Biolegend
APC/Cy7 anti-mouse/human **CD11b**	M1/70	Biolegend
Pacific Blue™/APC anti-mouse **Ly6G**	1A8	Biolegend
Brilliant Violet 510™ anti-mouse **Ly6C**	HK1.4	Biolegend
APC anti-mouse **CCR2**	-	R&D systems

Data were acquired using a FACScalibur® (Becton Dickinson, USA) and analyzed using FlowJO software (TreeStar Inc., USA). Specific populations of B cells, T cells, neutrophils and monocyte-derived macrophages (MDMs) were analyzed attending to a specific markers pattern, as shown in Table M7.

Table M7. Markers pattern employed to differentiate specific cell populations.

Cell type	Blood	BM
B cells	$B220^+$	$B220^+$
T cells	$CD3^+$ $B220^-$	$CD3^+$ $B220^-$
Neutrophils	$CD11b^+$ $Ly6G^+$	$Ly6G^+$
MDMs	$CD11b^+$ $Ly6G^-$ $CCR2^+$ $Ly6C^+$	$CD11b^+$ $Ly6G^-$ $CCR2^+$ $Ly6C^+$

4. STATISTICAL ANALYSIS

GraphPad Prism® software (version 8.0; GraphPad Software Inc., San Diego, CA, USA) was used for the statistical analysis. Data were normally distributed (tested with the Shapiro-Wilk normality test) and were assessed, as required (see test used and specificities in the figure legends), by the Student's *t*-test, or by one-way or two-way ANOVA followed by the Bonferroni or Tukey test. Kaplan-Meier survival curves were compared by using the Log-Rank test. The significance level was set at p value <0.05 (*p<0.05, **p<0.01, ***p<0.005, ****p<0.001).

RESULTS

CHAPTER 1. NEUROPATHOLOGICAL CHARACTERIZATION OF A NOVEL DS MOUSE MODEL

As already mentioned, the first goal in this Doctoral Thesis was to characterize a novel DS mouse model that faithfully recapitulated most clinical aspects of the disorder, thus enabling the development of future studies based on disease-modifying therapies. Since our main goal has been to investigate therapies for long-term comorbidities, one of our initial main interests was to be able to have a mouse model with higher survival rates than the other models based on *Scn1a*-A1783V mice (Almog *et al.*, 2021; Fadila *et al.*, 2020; Kuo *et al.*, 2019; Ricobaraza *et al.*, 2019). To this end, we first monitored multiple behavioral features at different postnatal ages, as well as animal survival and seizure susceptibility. Then, we aimed to determine the contribution to these behavioral disturbances of different neuropathological alterations, including dysregulations in the endocannabinoid system, inflammatory events and alterations in the hippocampal neurogenesis. Part of these results has been recently published (Satta *et al.*, 2021).

1.1. Behavioral recording of the disease progression

Different tests were performed to evaluate those behavioral comorbidities typically associated with DS progression (Dravet & Oguni, 2013; Gataullina & Dulac, 2017), including possible motor deficits (limb grasp reflexes, rotarod test, computer-aided actimeter), cognitive and emotional impairments (Y-maze and elevated plus maze tests, respectively) and autistic-like traits (social interaction test) at some representative ages after birth: PND10 (only reflexes), PND25, PND40, and PND60 (all tests). These ages were carefully selected with the main purpose of having a long-term characterization with representative ages recapitulating DS progression (from childhood to adulthood) (Dutta & Sengupta, 2016). Animal survival was also analyzed in these mice. The four experimental groups were included in these tests in order to verify if there were differences among the three different control groups (Table M1). Additionally, a different cohort of mice was used for evaluating seizure-related behavior after PTZ administration at PND25. Figure R1 shows a scheme of this experimental design.

Reflexes and body weight

Early reflexes were measured to assess the status of neurological development. Grasp reflexes appear in mice at a range from PND3 to PND15, with a response that is typically earlier in forelimbs than in hindlimbs (Heyser, 2004). In agreement with this statement, forelimb grasping had completely appeared in all mice by PND10 (Figure R2B), in

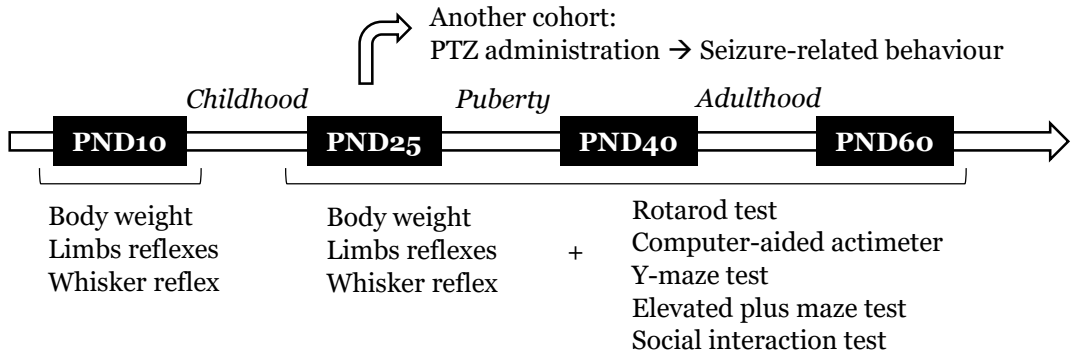

Figure R1. Timeline of experimental procedure for the DS mouse model behavioral characterization.

contrast to hindlimb grasping (Figure R2C), whose development was still not completed at this age. Interestingly, Syn1-Cre/Scn1a$^{WT/A1783V}$ mice exhibited a stronger reduction in hindlimb grasp reflex when compared with control groups (Figure R2C) at PND10. This alteration disappeared at PND25, PND40 and PND60, thus suggesting a delay in early motor development in Syn1-Cre/Scn1a$^{WT/A1783V}$ newborns. About to whisker reflex, no differences were observed (Figure R2D).

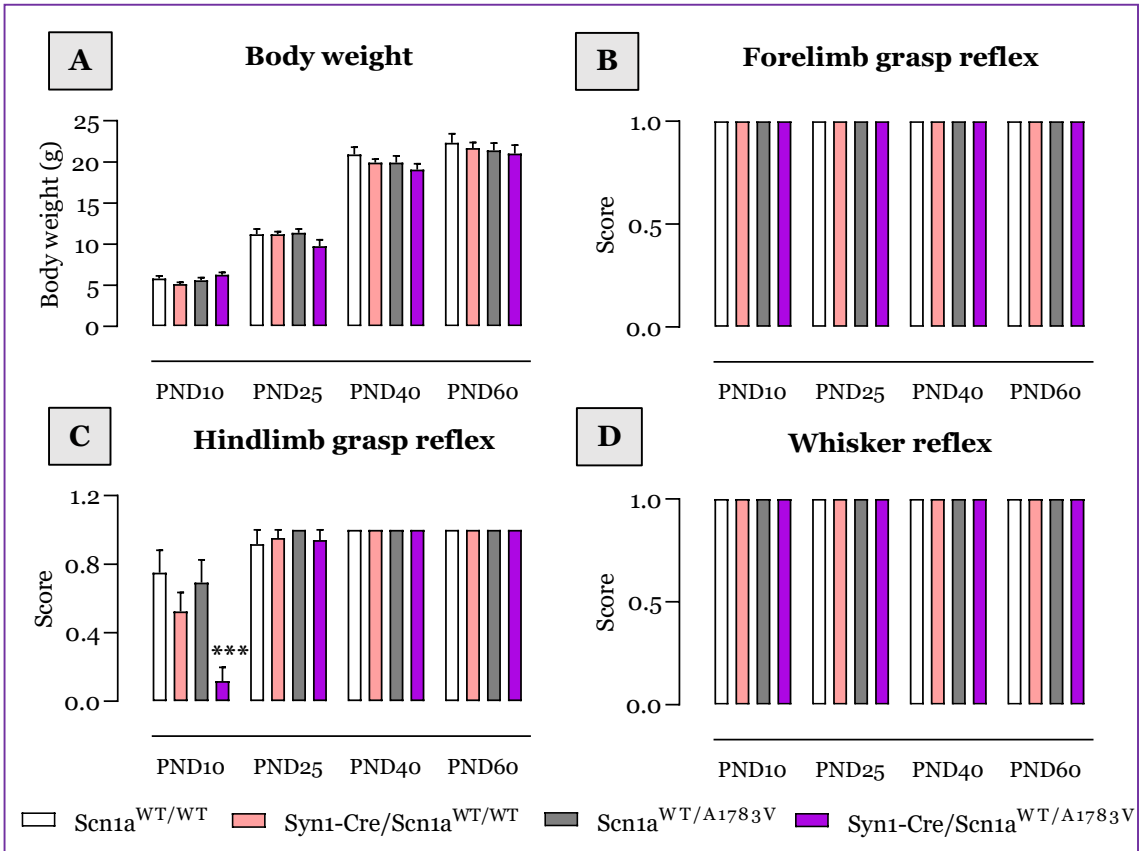

Figure R2. Evolution of different developmental parameters in the DS mouse model. (A) Body weight, **(B)** forelimb grasp reflex, **(C)** hindlimb grasp reflex and **(D)** whisker reflex in Syn1-Cre/Scn1a$^{WT/A1783V}$ mice and their three control groups (Scn1a$^{WT/WT}$, Syn1-Cre/Scn1a$^{WT/WT}$ and Scn1a$^{WT/A1783V}$ mice) measured at different PNDs in the range PND10-PND60. Values are means ± SEM of 12-21 animals per group. Data were assessed by two-way ANOVA for repeated measures followed by the Bonferroni test (***p<0.005 vs. the other three groups).

In parallel, body weight was also recorded at the same timepoints. The progressive increase in body weight revealed differences by age but not by genotype (Figure R2A).

Motor coordination and locomotor activity

Motor coordination and locomotor activity were analyzed in the Rotarod test and in the computer-aided actimeter, respectively. No differences were shown in the Rotarod test, neither by genotype nor by age, thus suggesting a normal motor coordination in all experimental groups (Figure R3).

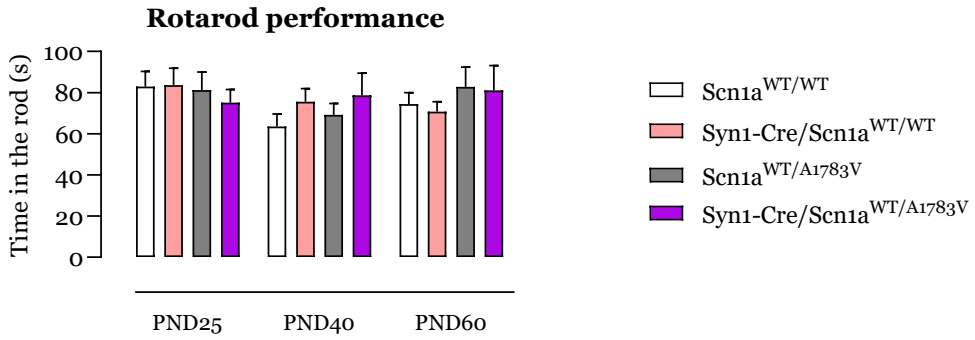

Figure R3. Rotarod performance in the DS mouse model. Rotarod performance in Syn1-Cre/Scn1a$^{WT/A1783V}$ mice and their three control groups (Scn1a$^{WT/WT}$, Syn1-Cre/Scn1a$^{WT/WT}$ and Scn1a$^{WT/A1783V}$ mice) measured at different PNDs in the range PND10-PND60. Values are means ± SEM of 12-21 animals per group. Data were assessed by two-way ANOVA for repeated measures followed by the Bonferroni test.

In contrast, some locomotor alterations were recorded in the computer aided-actimeter (Figures R4A-F). At PND25, Syn1-Cre/Scn1a$^{WT/A1783V}$ mice showed an increase in total ambulation (Figure R4A), frequency of rears (Figure R4B), mean velocity (Figure R4D) and time spent in fast movements (Figure R4E) when compared with the three control groups. On the other hand, they exhibited a marked decrease in the resting time (Figure R4C). Overall, these results suggested the occurrence of a hyperactive behavior in Syn1-Cre/Scn1a$^{WT/A1783V}$ mice at PND25, which can be also appreciated in the representative trajectory plots generated from the Actitrack software (Figure R4F). Faster peak velocities and the higher number of rears may additionally suggest the existence of impulsivity and a stereotyped behavior. Interestingly, these motor alterations completely disappeared at PND40 and PND60, thus indicating that hyperactivity was specifically circumscribed to the pre-adolescent period (PND25).

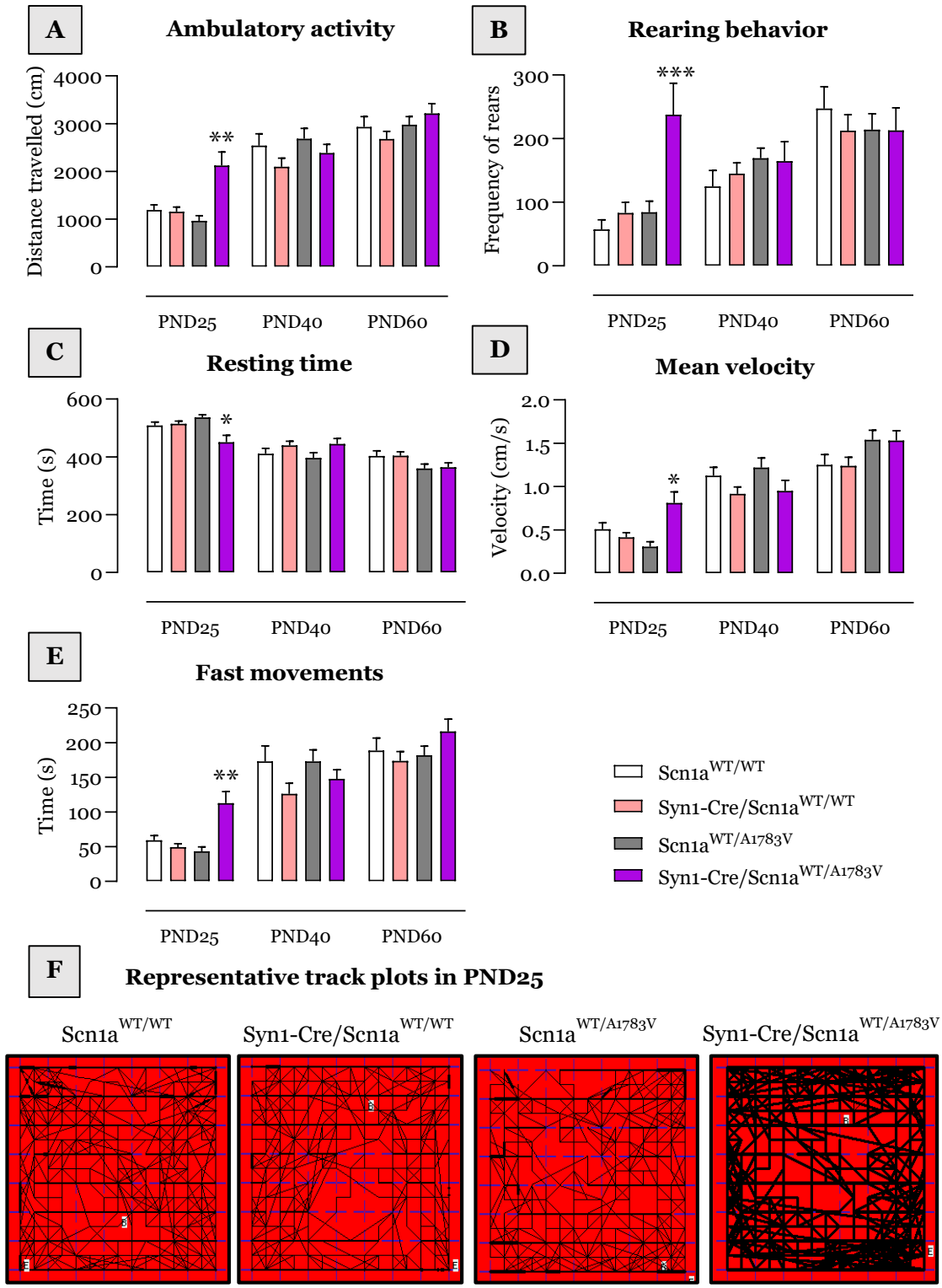

Figure R4. Locomotor activity parameters in the DS mouse model. Measurement of different parameters recorded in the computer-aided actimeter in Syn1-Cre/Scn1a$^{WT/A1783V}$ mice and their three control groups (Scn1a$^{WT/WT}$, Syn1-Cre/Scn1a$^{WT/WT}$ and Scn1a$^{WT/A1783V}$ mice), including **(A)** ambulatory activity, **(B)** rearing behavior, **(C)** resting time, **(D)** mean velocity and **(E)** fast movements, at different PNDs in the range PND25-PND60. Panel **(F)** shows representative track plots in PND25 generated from the Actitrack software. Values are means ± SEM of 13-21 animals per group. Data were assessed by two-way ANOVA for repeated measures followed by the Bonferroni test (*p<0.05, **p<0.01, ***p<0.005 vs. the other three groups).

Spatial working memory

Animals were also subjected to the Y-maze test in order to assess their spatial working memory and spontaneous alteration (Figures R5A-D), given that mice natural curiosity promotes them to alternate between maze arms. Although data did not reach statistical significance at any age, results indicated a slight worsening in Syn1-Cre/Scn1a$^{WT/A1783V}$ mice of the performance in this test at PND25, with trends towards an increase in the number of total entries in the maze arms (p=0.099, Figure R5A) (which further corroborates their hyperactive behavior at PND25), a decreased spontaneous alternation (p=0.151, Figure R5B) and an increased percentage of alternate arm returns (p=0.094, Figure R5C) when compared with the other three control groups. These trends disappeared at PND40 and PND60, thus indicating that this slight impairment in spatial working memory was only apparent in the pre-adolescent period (PND25).

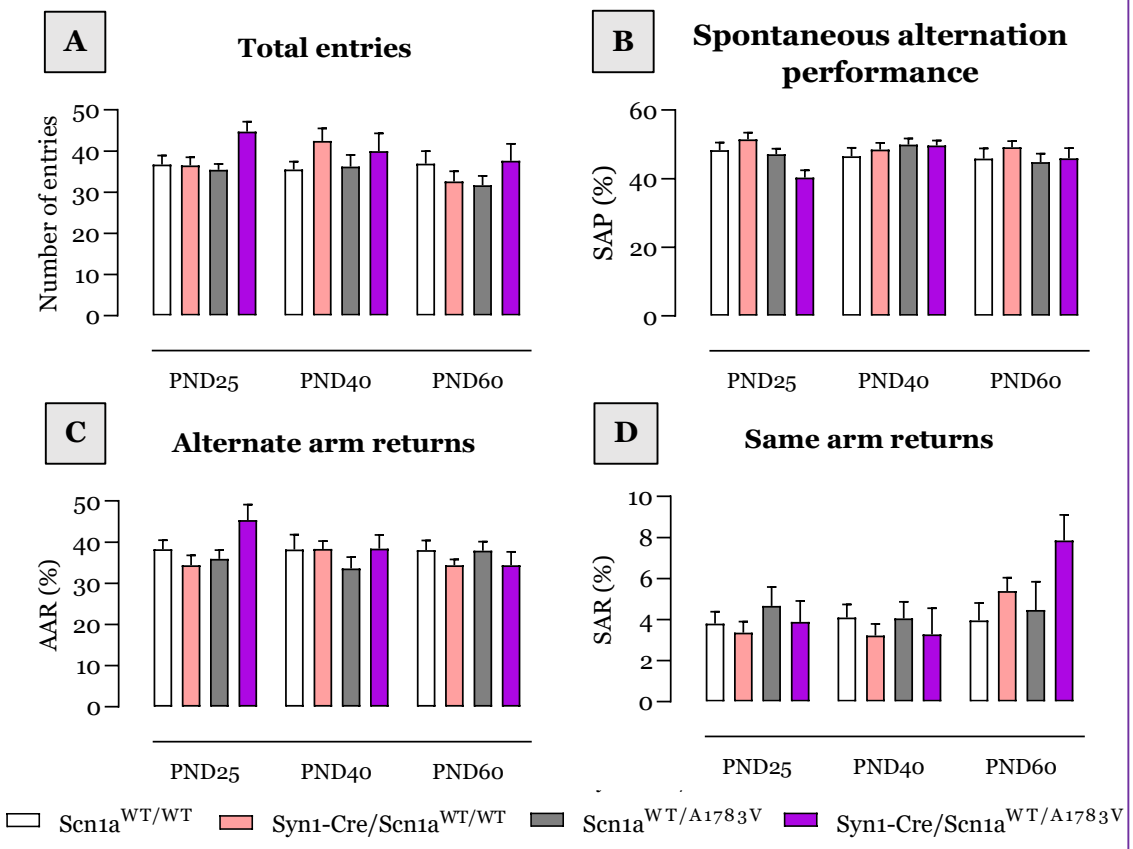

Figure R5. Parameters recorded in the Y-maze test in the DS mouse model. Measurement of different parameters in Syn1-Cre/Scn1a$^{WT/A1783V}$ mice and their three control groups (Scn1a$^{WT/WT}$, Syn1-Cre/Scn1a$^{WT/WT}$ and Scn1a$^{WT/A1783V}$ mice), including **(A)** number of total entries, **(B)** spontaneous alternation performance, **(C)** alternate arm returns and **(D)** same arm returns at different PNDs in the range PND25-PND60. Values are means ± SEM of 13-21 animals per group. Data were assessed by two-way ANOVA for repeated measures followed by the Bonferroni test.

Anxiety

Animal anxiety levels were examined in the elevated plus maze test. At PND25, Syn1-Cre/Scn1a$^{WT/A1783V}$ mice exhibited lower levels of anxiety, with a marked increase in the percentage of time spent in the open arms (Figure R6A) when compared with the other three control groups, despite the number of entries in open arms did not change (Figure R6B). Interestingly, these alterations disappeared a PND40, but differences were again visible at PND60 for both parameters (Figures R6A,B).

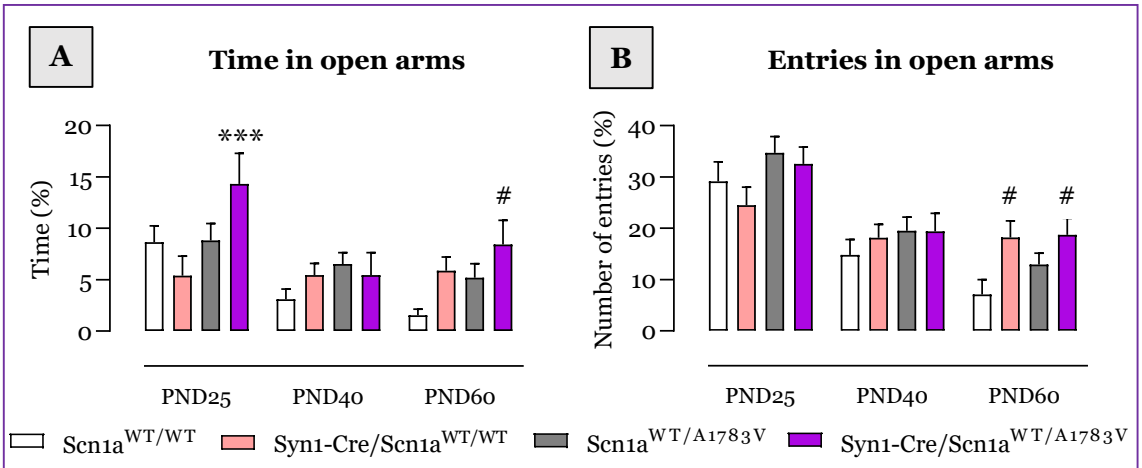

Figure R6. Parameters recorded in the elevated plus maze in the DS mouse model. Measurement of different parameters in Syn1-Cre/Scn1a$^{WT/A1783V}$ mice and their three control groups (Scn1a$^{WT/WT}$, Syn1-Cre/Scn1a$^{WT/WT}$ and Scn1a$^{WT/A1783V}$ mice), including **(A)** time in open arms and **(B)** number of entries in open arms at different PNDs in the range PND25-PND60. Values are means ± SEM of 13-21 animals per group. Data were assessed by two-way ANOVA for repeated measures followed by the Bonferroni test (***p<0.005 vs. the other three groups; $^{\#}p$<0.05 vs. Scn1a$^{WT/A1783V}$ mice).

Social interaction

Social behavior was evaluated in the social interaction test, which revealed a marked autistic-like behavior in Syn1-Cre/Scn1a$^{WT/A1783V}$ mice (Figures R7A,B). In this test, Syn1-Cre/Scn1a$^{WT/A1783V}$ mice spent a significantly lower time in active interaction with a novel unfamiliar partner when compared with the other three groups at PND25, PND40 and PND60 (Figure R7A). In parallel, the total number of total interactions was also lower at PND25 and PND40, and a trend towards a decrease was also observed at PND60 (Figure R7B). Therefore, this is the only behavioral parameter that was drastically altered at the three evaluated ages.

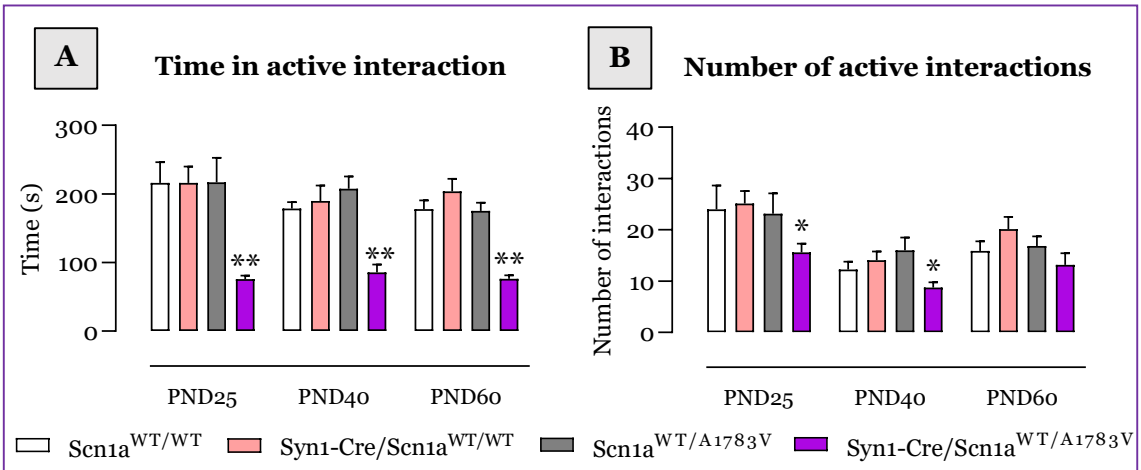

Figure R7. Parameters recorded in the social interaction test in the DS mouse model. Measurement of different parameters in Syn1-Cre/Scn1a$^{WT/A1783V}$ mice and their three control groups (Scn1a$^{WT/WT}$, Syn1-Cre/Scn1a$^{WT/WT}$ and Scn1a$^{WT/A1783V}$ mice), including **(A)** time in active interaction and **(B)** number of active interactions at different PNDs in the range PND25-PND60. Values are means ± SEM of 13-21 animals per group. Data were assessed by two-way ANOVA for repeated measures followed by the Bonferroni test (*p<0.05, **p<0.01 vs. the other three groups).

Seizure-like activity

During animal daily handling, Syn1-Cre/Scn1a$^{WT/A1783V}$ mice were shown to exhibit spontaneous seizures beginning around PND18. Given that these seizures were difficult to record and quantify without specialized tools and devices (and would have caused us to remove animals from long-term behavioral studies and caused animals to incur social isolation stress, which is also known to lower seizure threshold), we measured seizure-like activity induced by acutely injecting the proconvulsant agent PTZ at PND25 (Figures R8A-D). As mentioned, this experiment was performed in a different animal cohort.

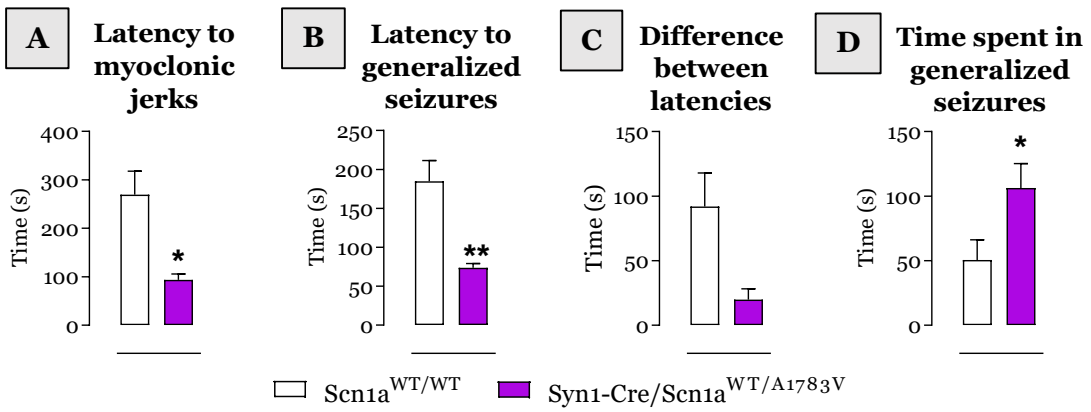

Figure R8. Behavioral evaluation of seizure-related activity in DS mice treated with PTZ. Measurement of different parameters in Syn1-Cre/Scn1a$^{WT/A1783V}$ mice and their control group (Scn1a$^{WT/WT}$) at PND25, including **(A)** latency to myoclonic jerks, **(B)** latency to generalized seizures, **(C)** time between generalized seizures and myoclonic jerks and **(D)** time spent in generalized seizures. Values are means ± SEM of 5-8 animals per group. Data were assessed by Student's t-test (*p<0.05, **p<0.01 vs. Scn1a$^{WT/WT}$ mice).

Syn1-Cre/Scn1a$^{WT/A1783V}$ showed a marked increase in seizure-like activity when compared to the control group (only Scn1a$^{WT/WT}$, given that no differences were found among the three control groups in the previous behavioral analysis). Such increase was reflected by significant reductions in the latency to myoclonic jerks (Figure R8A) and generalized seizures (Figure R8B), a trend towards a decrease in the difference between both latencies (p=0.0575, Figure R8C) and a significant increase in the total time spent in generalized seizures (Figure R8D).

Animal survival

As indicated above, a relevant characteristic expected for this DS mouse model was a reduced premature mortality relative to other knock-outs and conditional models, which may facilitate its use in chronic treatments against long-term comorbidities. To this end, those animals that were subjected to the behavioral tests shown in Figures R2-R7 were also used for measuring animal survival. As shown in Figure R9, survival of Syn1-Cre/Scn1a$^{WT/A1783V}$ mice dropped from around PND14 until PND21, and then remained relatively stable, resulting in approximately 75% long-term survivors. The statistical analysis of these data indicated they resulted significant (χ^2=5.907, p<0.05). It is important to remark that, despite the reduction in animal survival, it is much more moderate if compared with the high mortality rates of other mouse models generated from *Scn1a*-A1783V conditional mice (Almog *et al.*, 2021; Fadila *et al.*, 2020; Kuo *et al.*, 2019; Ricobaraza *et al.*, 2019), as it has been discussed in the Introduction. Overall, this fact makes our model suitable for long-term studies in this disorder.

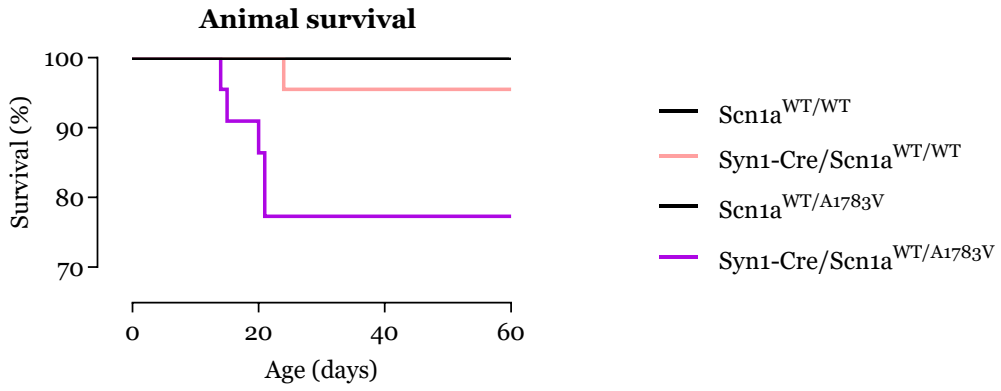

Figure R9. Animal survival in the DS mouse model. Kaplan-Meier plot for the analysis of animal survival in Syn1-Cre/Scn1a$^{WT/A1783V}$ mice and their three control groups (Scn1a$^{WT/WT}$, Syn1-Cre/Scn1a$^{WT/WT}$ and Scn1a$^{WT/A1783V}$ mice). Data correspond to 13-21 animals per group and were assessed by the Log-Rank test.

1.2. Biochemical and histopathological data

Once behaviorally characterized, we next wanted to determine the contribution of different neuropathological events to these behavioral disturbances, including alterations in the endocannabinoid system, inflammatory events and disruptions in the hippocampal neurogenesis. In this second group of experiments comprising this Chapter, neural tissues of Syn1-Cre/Scn1a$^{WT/A1783V}$ mice were compared to those of Scn1a$^{WT/WT}$ mice (hereafter considered as the control group, since no differences were found among the three control groups in the previous behavioral tests). In addition, given that PND25 was the age at which behavioral impairment was maximal, these biochemical and histopathological data - as well as further measurements in the following Chapters - were collected at this stage.

Analysis of the endocannabinoid system

Given that specific elements within the ECS may serve as potential targets for a cannabinoid-based treatment in DS (Gray & Whalley, 2020), our main goal in this study was to detect a possible dysregulation within this signalling system that may explain the efficacy of certain cannabinoids as disease-modifying therapies in this disorder. As discussed, previous data from our laboratory revealed an upregulation of CB_2 receptor in lymphocytes of DS patients (Rubio *et al.*, 2016). Therefore, we next wanted to assess if this signalling system was somehow dysregulated in our DS mouse model. To this end, both mRNA (Figure R10) and protein (Figure R11) levels for different ECS elements were quantified in CNS structures of Syn1-Cre/Scn1a$^{WT/A1783V}$ mice.

Regarding cannabinoid receptors, qPCR analysis revealed a decrease of CB_1 receptor in the cerebellum and a trend towards a downregulation in the hippocampus (p=0,179) (Figure R10A), which was further corroborated by Western-blot analysis (Figure R11A). No changes were found in prefrontal cortex and striatum (Figures R10A, R11A). qPCR analysis of CB_2 receptor did not show any changes in the different CNS structures (Figure R10B). In contrast, Western-blot analysis revealed an upregulation of this receptor in the hippocampus, but not in the prefrontal cortex (Figure R11B). Lastly, we also analyzed GPR55 receptor, which has been proposed as the molecular target for the benefits exerted by CBD in a mouse model of DS (Kaplan *et al.*, 2017). Although data were not statistically significant (probably due to a high variability), qPCR analysis revealed some trends towards a decrease in striatum (p=0.2) and hippocampus (p=0.15) (Figure R10C).

Main enzymes involved in biosynthesis (NAPE-PLD and DAGL) and inactivation (MAGL and FAAH) of endocannabinoids were also evaluated. Regarding biosynthetic enzymes,

qPCR analysis did not reveal any changes in the different CNS structures (Figures R10D,E). However, inactivation enzymes exhibited some changes. Particularly, qPCR analysis found a downregulation in MAGL enzyme in prefrontal cortex and cerebellum (Figure R10G); prefrontal cortex downregulation was further confirmed by Western-blot analysis (Figure R11C). No changes were found in the rest of CNS structures (Figures R10G, R11C). Regarding FAAH enzyme, no statistically significant changes were detected. However, qPCR analysis revealed a trend towards a decrease in hippocampus (p=0.062) and cerebellum (p=0.068) (Figure R10F); this small trend in hippocampus was further confirmed by Western-blot analysis (p=0.052, Figure R11D). No changes were found in the rest of CNS structures (Figures R10F, R11D).

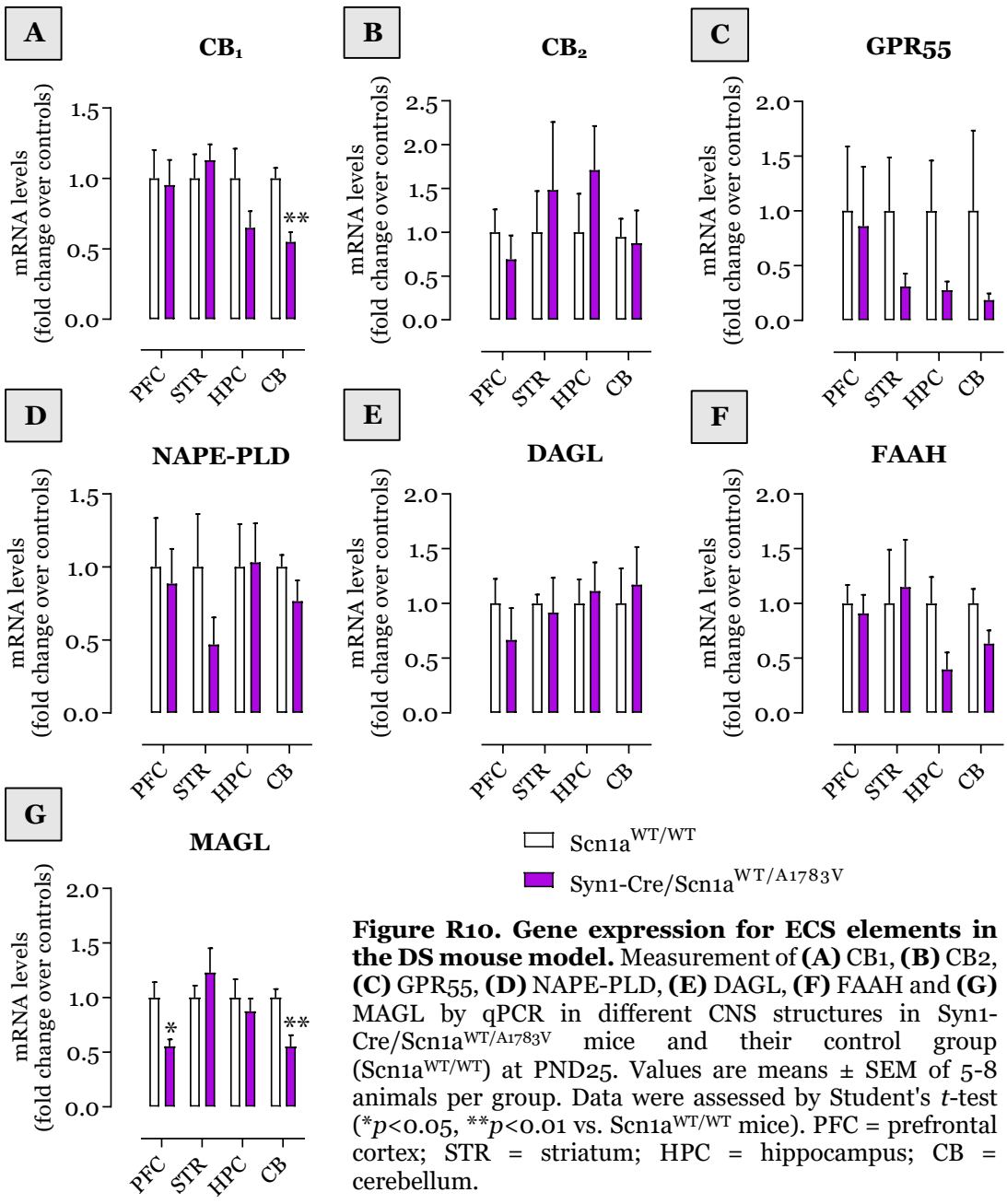

Figure R10. Gene expression for ECS elements in the DS mouse model. Measurement of **(A)** CB1, **(B)** CB2, **(C)** GPR55, **(D)** NAPE-PLD, **(E)** DAGL, **(F)** FAAH and **(G)** MAGL by qPCR in different CNS structures in Syn1-Cre/Scn1a$^{WT/A1783V}$ mice and their control group (Scn1a$^{WT/WT}$) at PND25. Values are means ± SEM of 5-8 animals per group. Data were assessed by Student's t-test (*p<0.05, **p<0.01 vs. Scn1a$^{WT/WT}$ mice). PFC = prefrontal cortex; STR = striatum; HPC = hippocampus; CB = cerebellum.

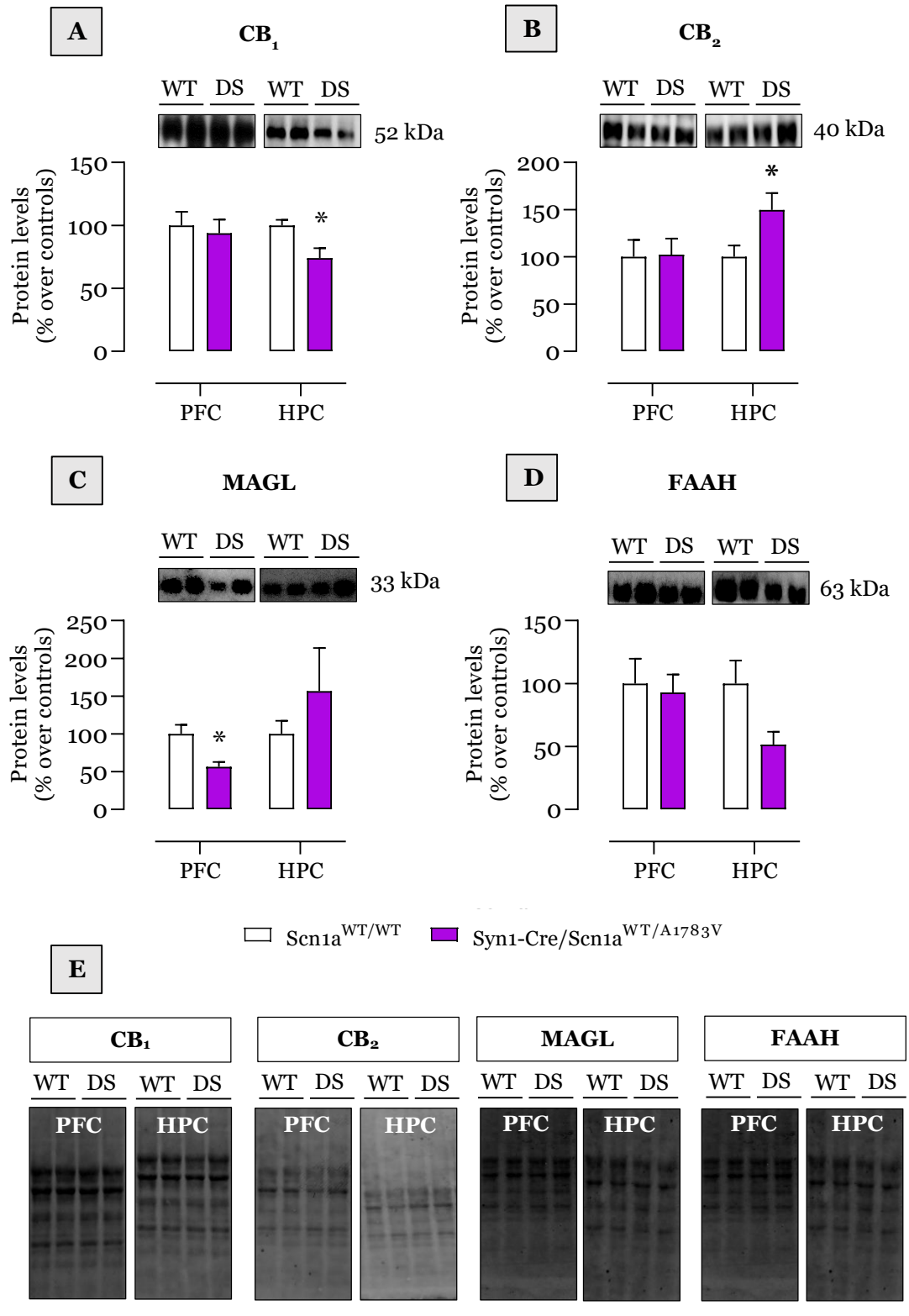

Figure R11. Protein levels for ECS elements in the DS mouse model. Measurement of **(A)** CB_1, **(B)** CB_2, **(C)** MAGL and **(D)** FAAH by Western-Blot in different CNS structures in Syn1-Cre/Scn1a$^{WT/A1783V}$ mice and their control group (Scn1a$^{WT/WT}$) at PND25. Panel **(E)** includes representative images of loading controls. Values are means ± SEM of 5-8 animals per group. Data were assessed by Student's *t*-test (*p<0.05 vs. Scn1a$^{WT/WT}$ mice). WT = Scn1a$^{WT/WT}$, DS = Syn1-Cre/Scn1a$^{WT/A1783V}$. PFC = prefrontal cortex; HPC = hippocampus.

Glial reactivity and neuroinflammation

As discussed above, it is well-documented that neuroinflammatory processes and glial reactivity constitute a hallmark in epilepsy (Vezzani, 2011; Vezzani *et al.*, 2019). Although little is known regarding DS, inflammation-related markers have been found to be upregulated in lymphocytes of DS patients (Rubio *et al.*, 2016), thus supporting the participation of inflammatory events in DS pathogenesis. Based on this idea, we next wanted to assess whether inflammation also occurs in our DS mouse model.

To this aim, we first wanted to analyze glial reactivity in different CNS structures at PND25. Immunofluorescence analysis revealed that Syn1-Cre/Scn1a$^{WT/A1783V}$ mice present higher levels of GFAP (Figure R12) and Iba-1 (Figure R13) immunoreactivity, thus indicating the existence of astrogliosis and microgliosis, respectively. Interestingly, in both cases, gliosis was restricted to the prefrontal cortex (Figures R12A, R13A) and the hippocampal dentate gyrus (Figures R12B, R13B), with no differences in the striatum or the different subfields of the Ammon's horn of the hippocampus (CA1, CA2 and CA3) (Figures R12C, R13C). Although it was not specifically quantified, representative immunofluorescence images showed a marked hypertrophy of cell bodies and processes, as well as an increased cell proliferation, then supporting the occurrence of reactive gliosis.

Additionally, we quantified by qPCR the gene expression of the pro-inflammatory cytokine TNFα in different CNS structures. Although data did not reach statistical significance (probably due to a high variability), this analysis revealed the existence of a trend towards an increase in the hippocampus (p=0.065, Figure R14).

Peripheral inflammation and BBB integrity

Once established that there are neuroinflammatory events occurring within the brain parenchyma in our DS mouse model, we next wanted to assess whether this local neuroinflammation could be driven - at least in part - by peripheral signals. As it has been explained in the Introduction, seizures may promote the mobilization of peripheral inflammatory mediators and even immune cells, as well as a partial breakdown in the BBB, thus resulting in the infiltration of inflammatory signals within the brain parenchyma; as a result, these central and peripheral inflammatory signals may cooperate and give rise to a decrease in the seizure threshold (Librizzi *et al.*, 2016).

To assess whether brain inflammation can be partially triggered by seizure-induced mobilization of peripheral immune cells, we measured B cells, T cells, neutrophils and

MDMs numbers in both BM and blood circulation by flow cytometry in Syn1-Cre/Scn1a$^{WT/A1783V}$ mice at PND25 (Figure R15).

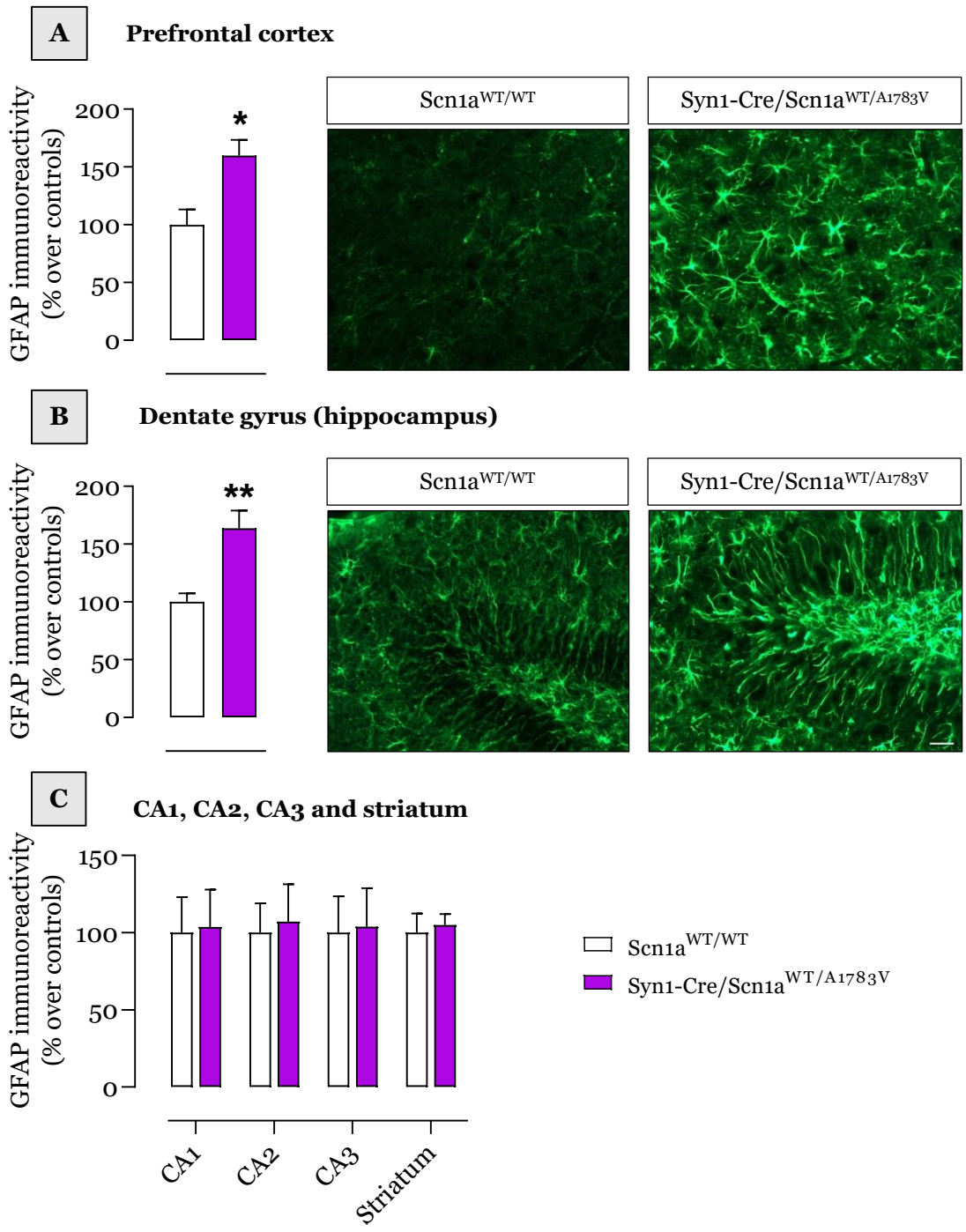

Figure R12. Immunofluorescence for the astroglial marker GFAP in the DS mouse model. Measurement of GFAP immunoreactivity in different CNS structures in Syn1-Cre/Scn1a$^{WT/A1783V}$ mice and their control group (Scn1a$^{WT/WT}$) at PND25. Quantification and representative immunofluorescence images in **(A)** prefrontal cortex and **(B)** hippocampal dentate gyrus, and quantification in other CNS areas, including **(C)** CA1, CA2, CA3 and striatum. Values are means ± SEM of 5-6 animals per group. Data were assessed by Student's *t*-test (*p<0.05, **p<0.01 vs. Scn1a$^{WT/WT}$ mice). Scale bar = 100µm.

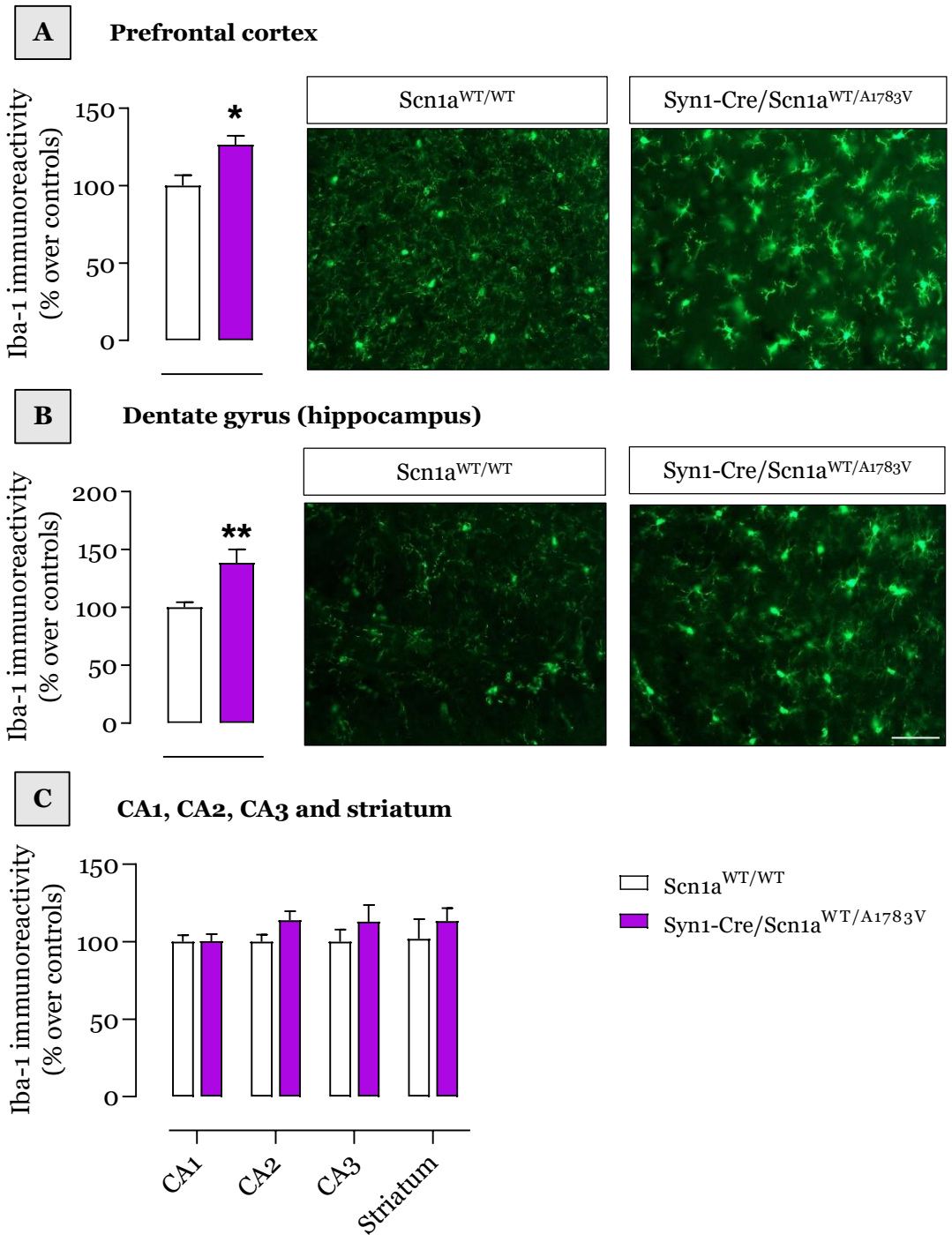

Figure R13. Immunofluorescence for the microglial marker Iba-1 in the DS mouse model. Measurement of Iba-1 immunoreactivity in different CNS structures in Syn1-Cre/Scn1a$^{WT/A1783V}$ mice and their control group (Scn1a$^{WT/WT}$) at PND25. Quantification and representative immunofluorescence images in **(A)** prefrontal cortex and **(B)** hippocampal dentate gyrus, and quantification in other CNS areas, including **(C)** CA1, CA2, CA3 and striatum. Values are means ± SEM of 5-6 animals per group. Data were assessed by Student's *t*-test (*p<0.05, **p<0.01 vs. Scn1a$^{WT/WT}$ mice). Scale bar = 100µm.

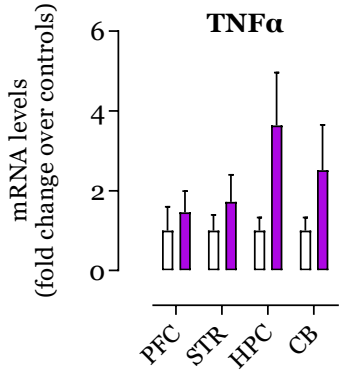

Figure R14. Gene expression for TNFα in the DS mouse model. Measurement of TNFα and by qPCR in different CNS structures in Syn1-Cre/Scn1a$^{WT/A1783V}$ mice and their control group (Scn1a$^{WT/WT}$) at PND25. Values are means ± SEM of 5-8 animals per group. Data were assessed by Student's *t*-test. PFC = prefrontal cortex; STR = striatum; HPC = hippocampus; CB = cerebellum.

Interestingly, Syn1-Cre/Scn1a$^{WT/A1783V}$ mice showed a marked reduction in the number of B cells (Figure R15A), T cells (Figure R15B) and neutrophils (Figure R15C) in the BM. However, no changes were detected in the number of MDMs (Figure 15D). With regard to blood circulation, our data revealed an increase in the number of neutrophils (Figure R15G), whereas no changes were observed in the case of B cells, T cells and MDMs (Figures R15E,F,H). Overall, these results suggested that neutrophils are mobilized from the BM into the peripheral circulation in Syn1-Cre/Scn1a$^{WT/A1783V}$ mice.

Taking into account these findings, we next wondered whether this increase in the number of neutrophils in blood circulation may involve their traffic and infiltration into the brain parenchyma, where they could contribute to the neuroinflammatory processes that have been reported in the previous section. With this idea in mind, we performed a double immunofluorescence staining of endothelial cells (laminin staining) and neutrophils (NIMP-R14 staining) in brain sections containing the hippocampus of perfused Syn1-Cre/Scn1a$^{WT/A1783V}$ mice, in order to study a possible neutrophil infiltration into the brain parenchyma (Figure R16). We initially wanted to focus this study in the hippocampus, particularly in the dentate gyrus, since it was one of the brain areas where gliosis and neuroinflammatory signals were more prominent (Figures R12B, R13B, R14).

To perform this analysis, we used brain sections containing the infarct core of mice subjected to a permanent middle cerebral artery occlusion (pMCAO) as a positive control, which were kindly provided by Dra. García-Culebras (Department of Pharmacology and Toxicology, Faculty of Medicine, Complutense University of Madrid, Madrid, Spain). As expected, positive control showed an increase in neutrophil infiltration into the ischemic brain tissue (Figure R16) (García-Culebras *et al.*, 2019), where neutrophils are not retained within vessels. In contrast, such observation did not occur in Syn1-Cre/Scn1a$^{WT/A1783V}$ mice, indicating that although neutrophils were

probably being mobilized from the BM (Figure R15C) to the systemic circulation (Figure R15G), they did not eventually infiltrate into the brain parenchyma (Figure R16).

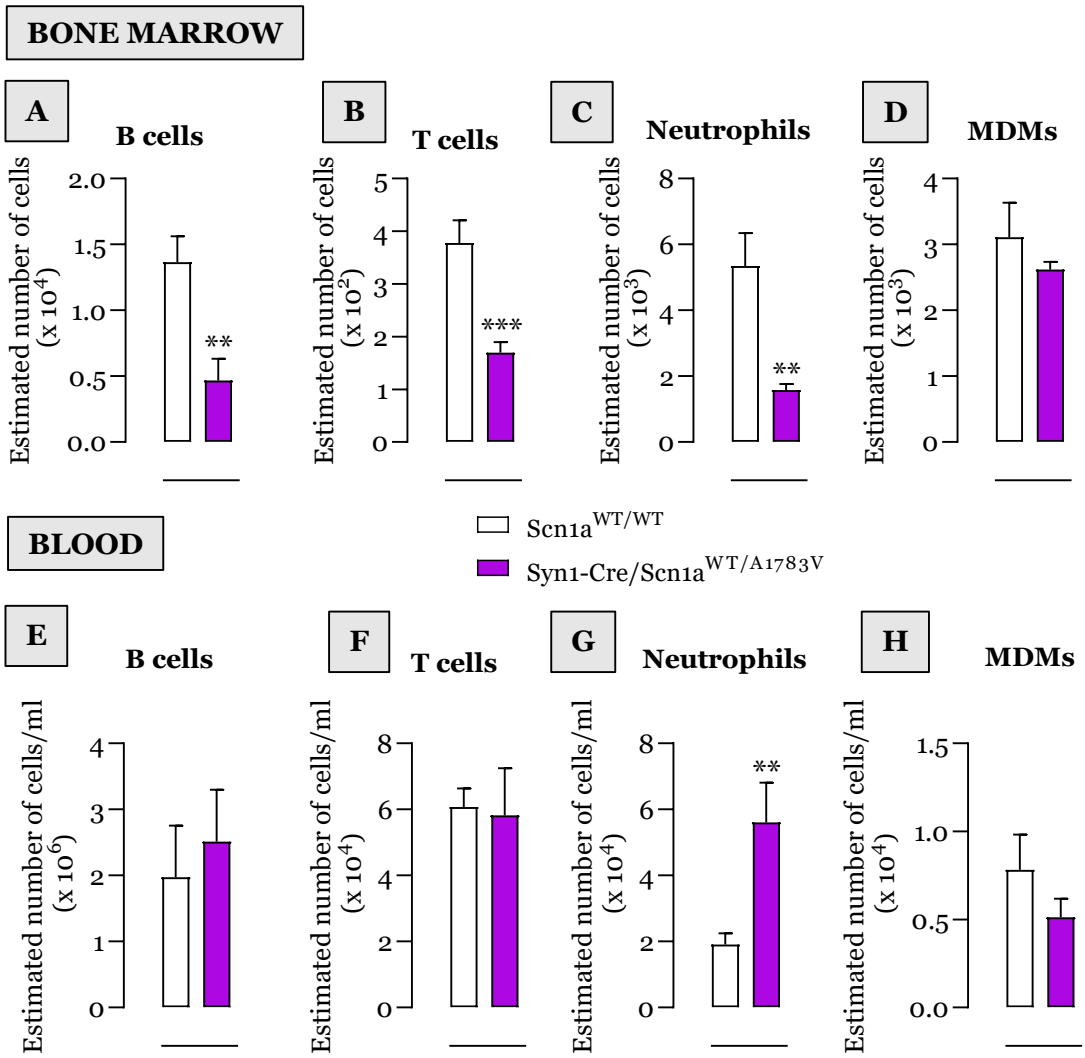

Figure R15. Flow cytometry analysis for different immune cells populations in the DS mouse model. Measurement of B cells, T cells, neutrophils and MDMs in **(A-D)** bone marrow and **(E-H)** blood in Syn1-Cre/Scn1a$^{WT/A1783V}$ mice and their control group (Scn1a$^{WT/WT}$) at PND25. Values are means ± SEM of 5-8 animals per group. Data were assessed by Student's *t*-test (*p<0.05, **p<0.01, ***p<0.005 vs. Scn1a$^{WT/WT}$ mice).

These observations suggested that inflammatory events that were taking part in the pathogenesis of our DS mouse model may not be as severe as those occurring in other pathological conditions where total BBB breakdown and neutrophil infiltration into the CNS is a well-documented phenomenon, including brain ischemia, brain trauma, CNS

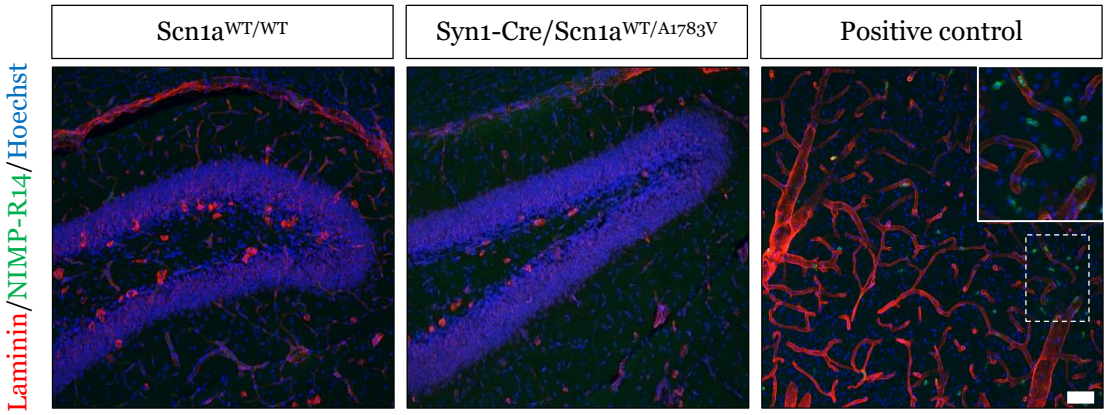

Figure R16 Evaluation of neutrophils infiltration into the brain parenchyma in the DS mouse model. Representative images of a double immunofluorescence of neutrophils (NIMP-R14, green) and the endothelial marker laminin (red) in the hippocampus of Syn1-Cre/Scn1a$^{WT/A1783V}$ mice and their control group (Scn1a$^{WT/WT}$) at PND25. Positive control corresponds to an ischemic brain tissue with proven infiltration of neutrophils into the brain ischemic core. Scale bar = 50 µm.

infections or autoimmune diseases affecting the CNS, among others (Manda-Handzlik & Demkow, 2019). These conditions often involve an acute damage which gives rise to a severe but transient BBB breakdown, which enables the massive infiltration of inflammatory signals. However, the pathogenesis in our DS mouse model may be much more progressive (chronic rather than acute). Therefore, we next wanted to assess whether there was a certain degree of BBB disruption in Syn1-Cre/Scn1a$^{WT/A1783V}$ mice, which may involve the partial contribution of peripheral inflammatory signals.

To this end, we first performed Western-blot analysis of different components of the BBB in hippocampal tissue of Syn1-Cre/Scn1a$^{WT/A1783V}$ mice, including ZO-1 and claudin-5 (tight junction proteins), laminin (basement membrane protein) and ICAM-1 (adhesion molecule controlling cell infiltration) (Figure R17). Results revealed significantly reduced levels of ZO-1 (Figure R17A), as well as small trends towards a decrease in laminin (p=0,1241, Figure R17B) and claudin-5 (p=0,1117, Figure R17D), suggesting a partial loss of BBB integrity. In agreement with the absence of cell infiltrates, levels of ICAM-1 remained unaltered (Figure R17C).

Although the aforementioned results indicated that this partial loss of BBB integrity was not able to induce inflammatory cell infiltration, we wanted to evaluate whether this moderate disruption could be associated with the existence of a leaky BBB that may facilitate the extravasation of inflammatory molecules into the brain parenchyma. To this aim, we performed immunofluorescence analysis of serum IgG extravasation in hippocampal brain sections of perfused Syn1-Cre/Scn1a$^{WT/A1783V}$ mice, which revealed an increase in IgG extravasation (Figure R18).

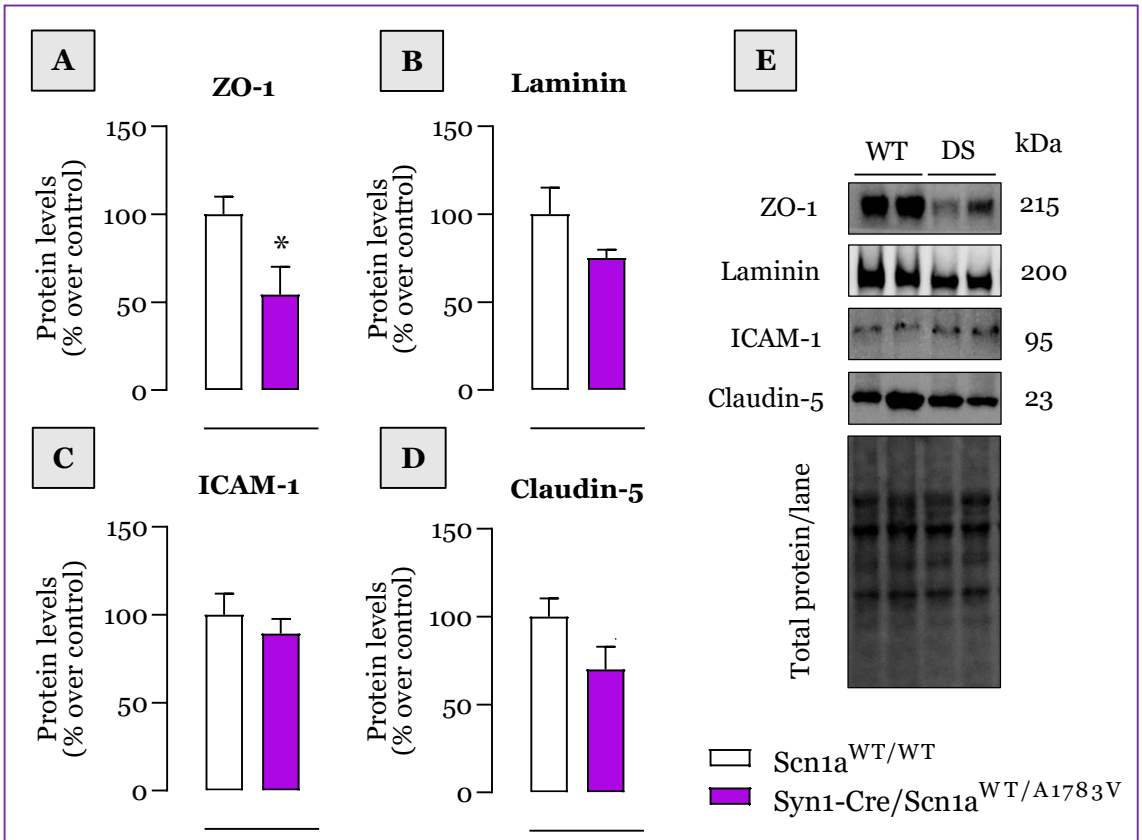

Figure R17. Protein levels for BBB components in the DS mouse model. Measurement of **(A)** ZO-1, **(B)** laminin, **(C)** claudin-5 and **(D)** ICAM-1 in the hippocampus of Syn1-Cre/Scn1a$^{WT/A1783V}$ mice and their control group (Scn1a$^{WT/WT}$) at PND25. Panel **(E)** includes representative images of Western-blots and loading controls. Values are means ± SEM of 5-6 animals per group. Data were assessed by Student's *t*-test (*p<0.05 vs. Scn1a$^{WT/WT}$. WT = Scn1a$^{WT/WT}$, DS = Syn1-Cre/Scn1a$^{WT/A1783V}$.

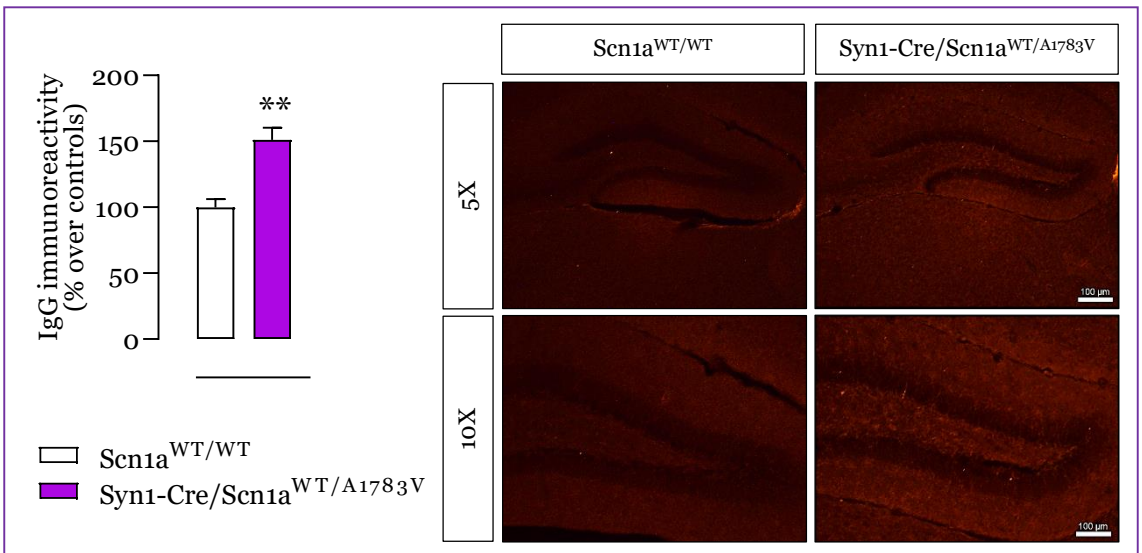

Figure R18. Endogenous IgG extravasation into the brain parenchyma in the DS mouse model. Quantification and representative images of IgG immunostaining in the hippocampus of Syn1-Cre/Scn1a$^{WT/A1783V}$ mice and their control group (Scn1a$^{WT/WT}$) at PND25. Values are means ± SEM of 5-6 animals per group. Data were assessed by Student's *t*-test (**p<0.01 vs. Scn1a$^{WT/WT}$ mice). Scale bar = 100 µm.

Adult hippocampal neurogenesis

As it has been stated in the Introduction, alterations in adult hippocampal neurogenesis have been associated with epilepsy and inflammation (Bielefeld *et al.*, 2019; Chen *et al.*, 2020). Therefore, we were particularly interested in investigating whether adult hippocampal neurogenesis could be disrupted in our Syn1-Cre/Scn1a$^{WT/A1783V}$ mice.

To this end, we performed immunofluorescence analysis focused on the SGZ and the GCL in order to assure NSCs identity (Figure R19). In this analysis, NSCs were defined as those GFAP-expressing cells specifically located in the SGZ and presenting a radial morphology. Although efforts were made in order to minimize the possibility that some astrocytes were also included in the quantification, we cannot exclude it; however, their contribution appeared to be residual.

First, we observed that Syn1-Cre/Scn1a$^{WT/A1783V}$ mice presented a significantly higher GCL dispersion (Figure R19B), as well as a small trend towards an increase in the mitotic marker Ki67 (p=0.13, Figure R19C), thus indicating an increased cell proliferation and mobilization of progenitor cells in Syn1-Cre/Scn1a$^{WT/A1783V}$ mice. As it can be appreciated in representative images of Figure R19A, cell proliferation is mainly restricted to the SGZ.

Next, we performed a double immunofluorescence staining for GFAP and Ki67. We quantified those cells which (1) were positive for both markers, (2) were located in the SGZ and (3) presented a radial morphology, in order to assure NSCs identity. This analysis showed a marked increase in the total number of cells positive for both markers in Syn1-Cre/Scn1a$^{WT/A1783V}$ mice (Figure R19E). When quantifying the percentage of these Ki67^{+} GFAP^{+} cells over the total of GFAP^{+} cells, we also found a small trend towards an increase (p=0.106, Figure R19D). Moreover, as it can be again appreciated in representative images of Figure R19A, these cells were phenotypically different from those of control mice, with basal cytoplasmic expansions and thickened processes, which is consistent with their transformation into a reactive-like phenotype. This reactive neurogenic response may contribute to reactive gliosis.

Lastly, we also measured the nuclei circularity of GCL neurons and found a particularly interesting phenomenon. Whereas control mice presented typical round nuclei, Syn1-Cre/Scn1a$^{WT/A1783V}$ mice showed an abnormal shape with a decreased circularity, with cell nuclei exhibiting an irregular contour with indentations (Figures R19F,G). This characteristic has been related to altered lamin expression and cell damage (Goldman *et al.*, 2004; Vergnes *et al.*, 2004).

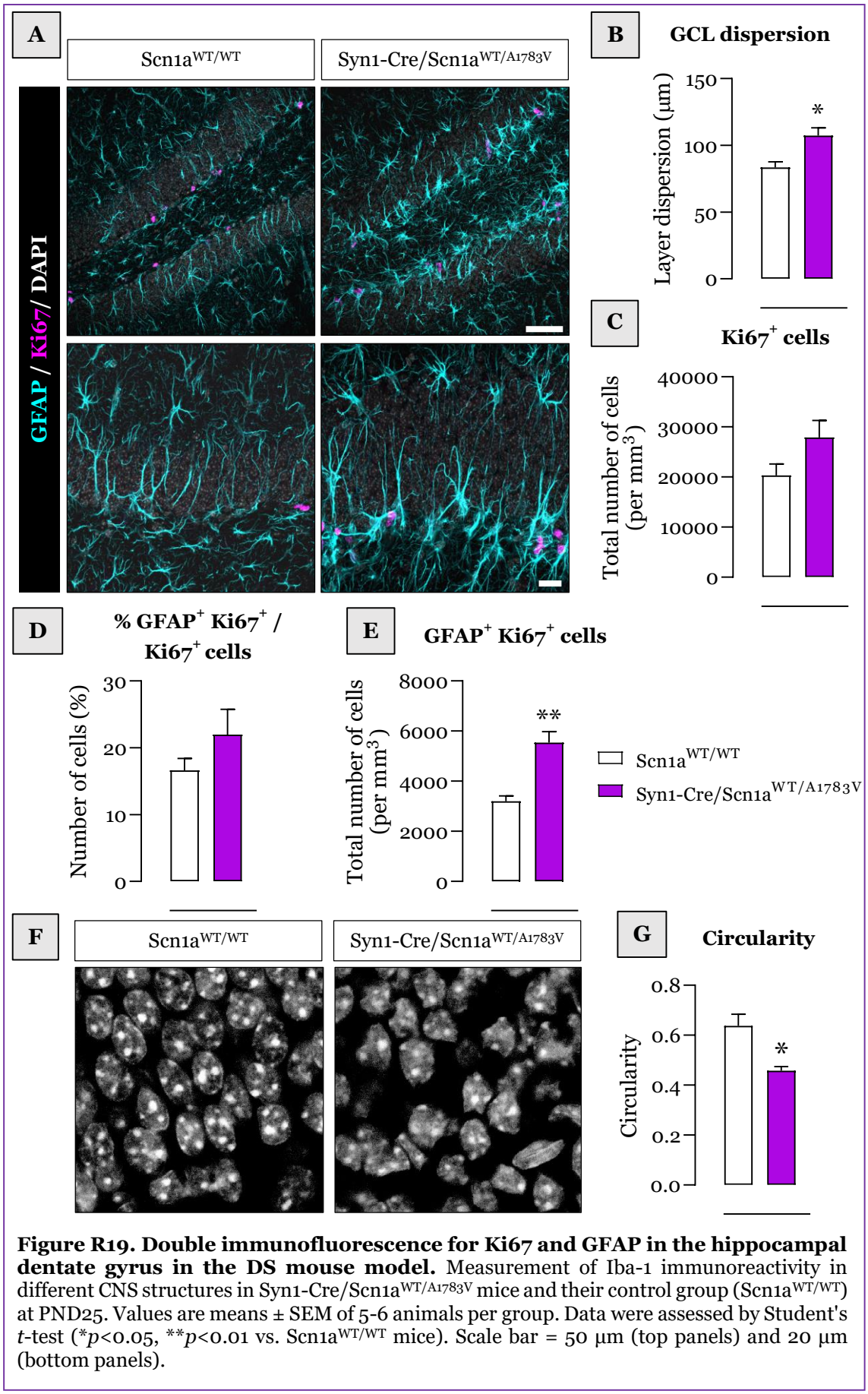

Figure R19. Double immunofluorescence for Ki67 and GFAP in the hippocampal dentate gyrus in the DS mouse model. Measurement of Iba-1 immunoreactivity in different CNS structures in Syn1-Cre/Scn1a$^{WT/A1783V}$ mice and their control group (Scn1a$^{WT/WT}$) at PND25. Values are means ± SEM of 5-6 animals per group. Data were assessed by Student's *t*-test (*p<0.05, **p<0.01 vs. Scn1a$^{WT/WT}$ mice). Scale bar = 50 µm (top panels) and 20 µm (bottom panels).

Summary

To briefly sum up the most important results of this Chapter, we were able to validate a novel DS mouse model with lower mortality rates than previous models, which may serve to further evaluate disease-modifying therapies focused on those long-term comorbidities which are typically associated with DS progression. Moreover, this mouse model recapitulated most behavioral features of DS patients, including hyperactivity, autistic traits, cognitive impairment and seizuring susceptibility, with a particular intensity at PND25. Overall, these findings supported this mouse model as a good experimental tool for long-term studies. Besides, this initial behavioral characterization enabled us to make important decisions regarding subsequent experiments, particularly to (1) consider Scn1a$^{WT/WT}$ as our control group, since no differences were observed in comparison with the other two control groups (mice carrying the mutation in absence of Cre, or mice expressing Cre in absence of the mutation), and (2) focus our measurements on PND25, where behavioral disturbances were found to be maximal.

Apart from this behavioral characterization, we performed several biochemical and histological procedures using this mouse model with the purpose of further exploring DS pathophysiology. These techniques revealed a partial dysregulation of the endocannabinoid system and the hippocampal neurogenesis. Furthermore, we demonstrated that neuroinflammation is a key pathogenic aspect in this DS mouse model, characterized by a prominent gliosis and a leaky BBB which may enable the extravasation of inflammatory molecules into the brain parenchyma.

Importantly, these findings allowed us to focus our following experiments on the main aspects which have been revealed in this Chapter.

CHAPTER 2. ANALYSIS OF BCP AS AN ANTICONVULSANT AGENT AND DISEASE-MODIFYING AGENT IN DS.

As already discussed, previous studies have shown that BCP is able to protect against seizures in preclinical models of acute epilepsy (de Oliveira *et al.*, 2016; Liu *et al.*, 2015; Tchekalarova *et al.*, 2018). Taking into account these findings, our goal was to determine if BCP was similarly protective in DS, not only against seizures, but also against DS-associated comorbidities.

To this end, two different experimental designs were conducted in our previously characterized DS mouse model. In a first study (acute paradigm), we addressed the anticonvulsant effect of BCP against PTZ-induced seizures. In a second study (chronic paradigm), we evaluated BCP effect on the disease progression and associated comorbidities.

Moreover, given that BCP has been demonstrated to display a strong protective role against brain inflammation (Gonçalves *et al.*, 2020; Sharma *et al.*, 2016), in both studies we also evaluated BCP effect on attenuating glial reactivity, since Chapter 1 has revealed that it is a neuropathological hallmark in the progression of the pathological phenotype in Syn1-Cre/Scn1a$^{WT/A1783V}$ mice (Figures R12-14).

2.1. Analysis of BCP as an anticonvulsant agent (acute paradigm)

In order to investigate the effects of BCP on seizure activity induced by PTZ, Syn1-Cre/Scn1a$^{WT/A1783V}$ mice and their controls (Scn1a$^{WT/WT}$) were injected with a single dose of BCP (100 mg/kg, i.p.) or its vehicle at PND24. 30 minutes thereafter, mice were injected with PTZ (50 mg/kg, i.p.) and observed for a 30-minute period. 24 hours after PTZ injection, mice were euthanized and brain tissue was collected for immunofluorescence analysis of glial reactivity. Figure R20 shows a schematic overview of this experimental design.

Effect of BCP on seizure-related activity induced by PTZ

As similarly reported in Chapter 1 characterization (Figure R8), data collected after PTZ administration (Figure R21) corroborated that this proconvulsant agent evokes a more intense seizure-related behavior in vehicle-treated Syn1-Cre/Scn1a$^{WT/A1783V}$ mice when compared with vehicle-treated controls, as particularly reflected as a significantly higher time spent in generalized seizures (Figure R21D). In contrast to those results showed in

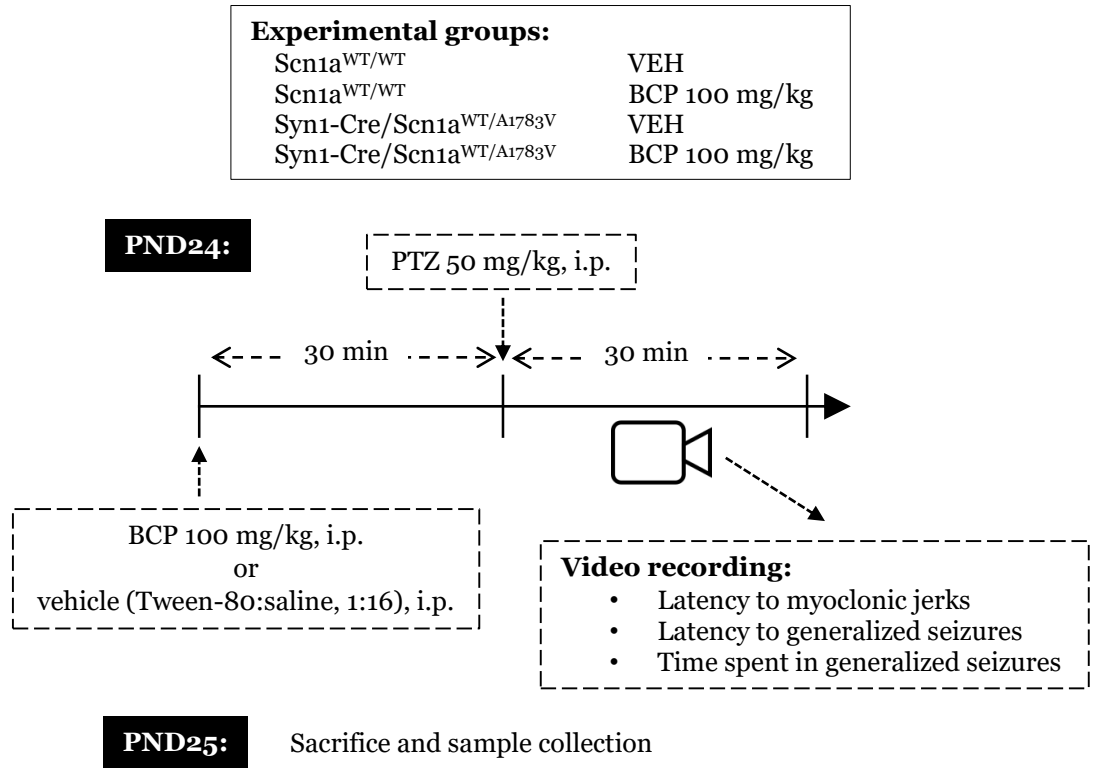

Figure R20. Timeline of the experimental procedure to evaluate BCP potential as an anticonvulsant agent.

Chapter 1 (Figure R8), the other three parameters do not reach statistical significance, probably due to high variability among data. However, trends towards a reduction can be similarly appreciated (Figures R21A,B,C).

When pretreated with BCP, a partial attenuation of seizure activity was detected in both Syn1-Cre/Scn1a$^{WT/A1783V}$ mice and their controls. In the case of control mice, BCP treatment promoted a marked increase in the difference between both latencies, which was not so intense in DS mice (Figure R21C). Regarding Syn1-Cre/Scn1a$^{WT/A1783V}$ mice, BCP drastically decreased the time spent in generalized seizures, an effect much more moderated in control mice (Figure R21D).

Effect of BCP on glial reactivity induced by PTZ

Given that epilepsy is associated with brain inflammation and reactive gliosis (Vezzani, 2011; Vezzani *et al.*, 2019), we next wanted to corroborate whether this response also occurs after PTZ-induced seizures, whether it is different between DS and control mice, and how it is affected by BCP treatment in both genotypes. To this end, we carried out immunofluorescence analysis to evaluate astroglial and microglial reactivity in prefrontal cortex and hippocampal dentate gyrus, the two CNS structures in which we

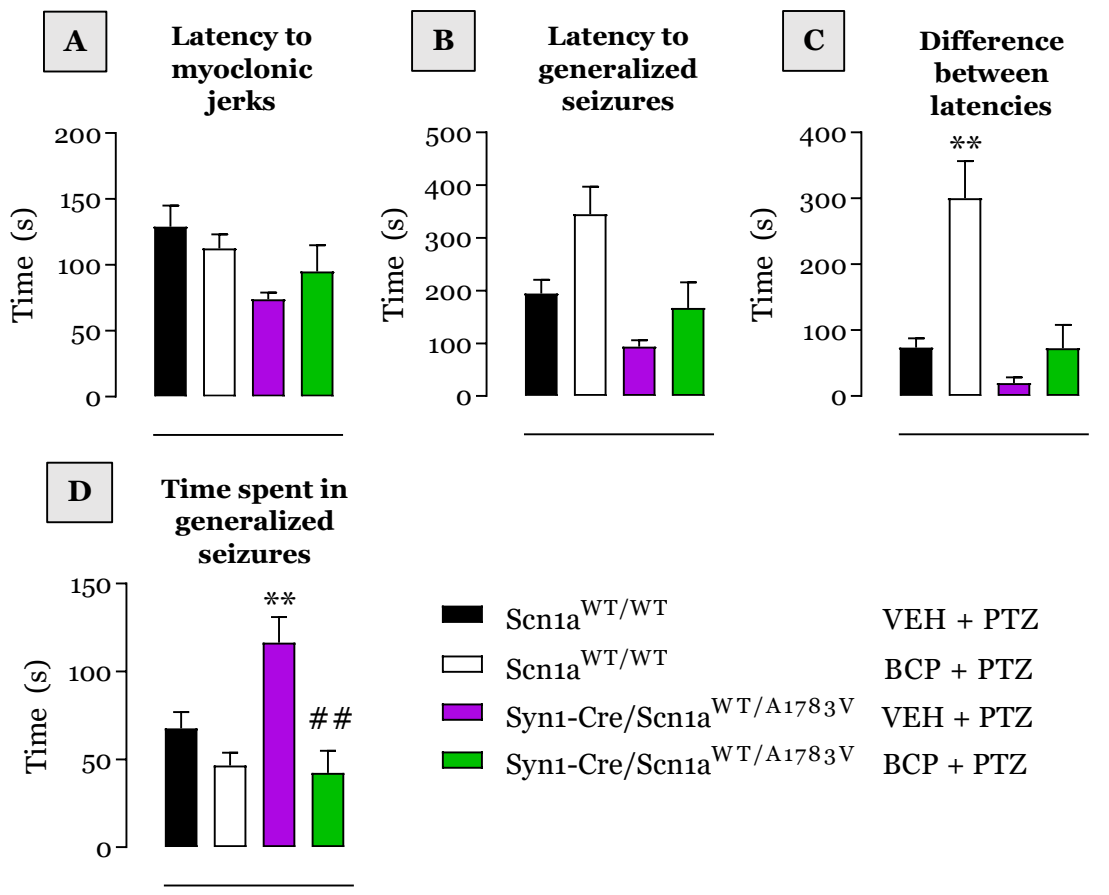

Figure R21. Effect of an acute BCP dose on seizure-related activity in DS mice treated with PTZ. Measurement of different parameters in Syn1-Cre/Scn1a$^{WT/A1783V}$ mice and their control group (Scn1a$^{WT/WT}$ mice) treated with BCP (100 mg/kg) or vehicle, including **(A)** latency to myoclonic jerks, **(B)** latency to generalized seizures, **(C)** time between generalized seizures and myoclonic jerks and **(D)** time spent in generalized seizures. Values are means ± SEM of 6-12 animals per group. Data were assessed by two-way ANOVA followed by the Tukey test (**p<0.01 vs. vehicle-treated Scn1a$^{WT/WT}$ mice; ##p<0.01 vs. vehicle-treated Syn1-Cre/Scn1a$^{WT/A1783V}$ mice).

had previously reported that gliosis is more prominent in our DS mouse model (Figures R12,13). Apart from the four experimental groups that had been behaviorally analyzed, for these immunofluorescence procedures we included two additional experimental groups: non-PTZ treated Syn1-Cre/Scn1a$^{WT/A1783V}$ mice and their controls (Scn1a$^{WT/WT}$), which may serve as a reference to quantify the extent of PTZ effect.

As reported in Chapter 1 (Figures R12,13), non-PTZ Syn1-Cre/Scn1a$^{WT/A1783V}$ animals showed an increase in GFAP immunoreactivity in both prefrontal cortex and hippocampal dentate gyrus (Figures R22A,B) if compared to non-PTZ control mice. Regarding Iba-1 immunoreactivity, we also reported a trend towards an increase in prefrontal cortex and a marked increase in hippocampal dentate gyrus (Figures R23A,B). These prominent levels of astrogliosis and microgliosis occurring in Syn1-Cre/Scn1a$^{WT/A1783V}$ animals were greatly enhanced after PTZ administration.

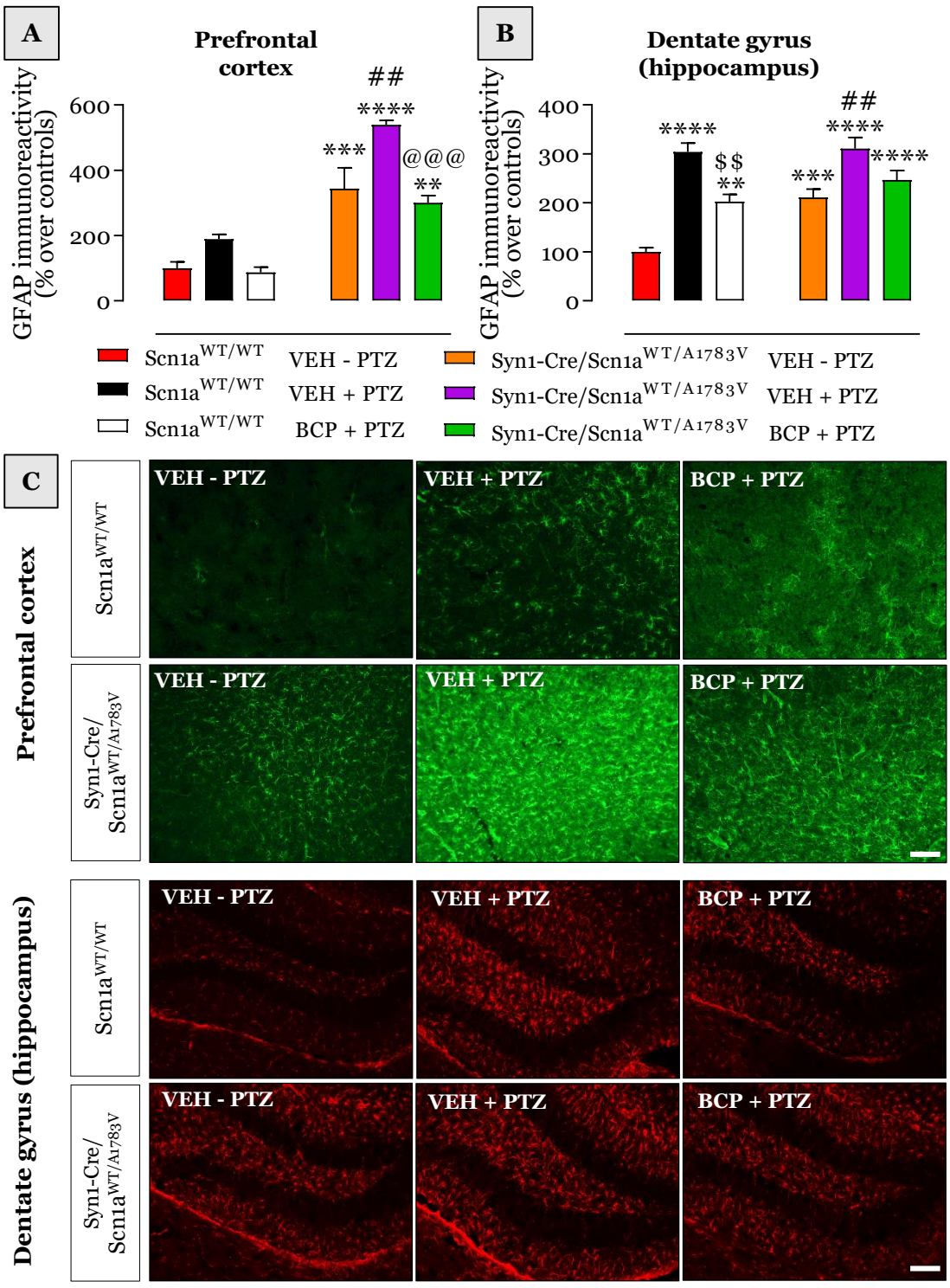

Figure R22. Effect of an acute BCP dose on the astroglial marker GFAP in DS mice treated with PTZ. Quantification of GFAP immunoreactivity in **(A)** prefrontal cortex and **(B)** hippocampal dentate gyrus in Syn1-Cre/Scn1a$^{WT/A1783V}$ mice and their control group (Scn1a$^{WT/WT}$ mice) treated with BCP (100 mg/kg) or vehicle. Panel **(C)** shows representative images of the immunofluorescence staining. Values are means ± SEM of 6-7 animals per group. Data were assessed by two-way ANOVA followed by the Tukey test (**p<0.01, ***p<0.005, ****p<0.001 vs. vehicle-treated Scn1a$^{WT/WT}$ - PTZ mice; $^{\$\$}p$<0.01 vs. vehicle-treated Scn1a$^{WT/WT}$ + PTZ mice; $^{\#\#}p$<0.01 vs. vehicle-treated Syn1-Cre/Scn1a$^{WT/A1783V}$ - PTZ mice; $^{@@}p$ <0.01 vs. vehicle-treated Syn1-Cre/Scn1a$^{WT/A1783V}$ + PTZ mice). Scale bar = 50 µm

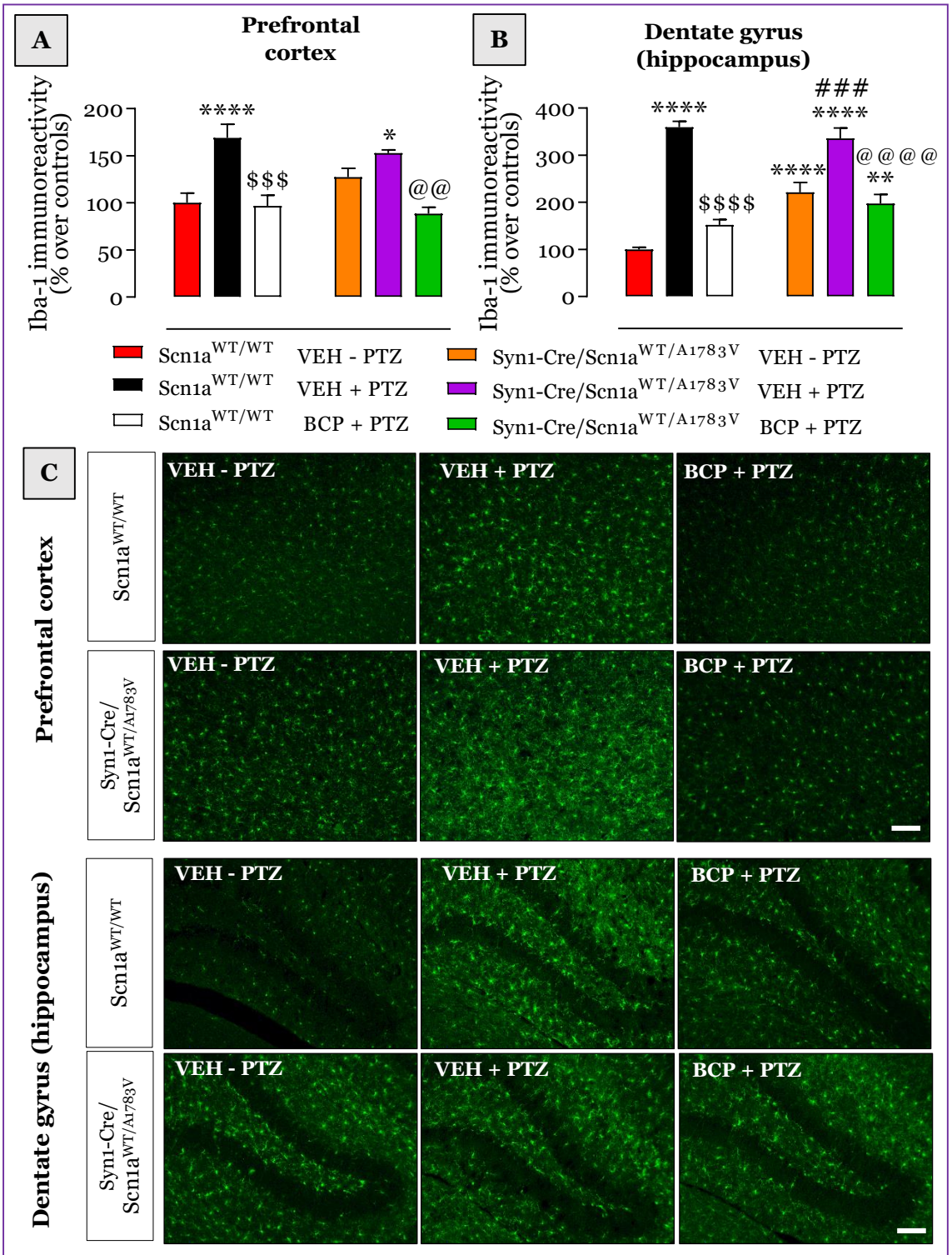

Figure R23. Effect of an acute BCP dose on the microglial marker Iba-1 in DS mice treated with PTZ. Quantification of Iba-1 immunoreactivity in **(A)** prefrontal cortex and **(B)** hippocampal dentate gyrus in Syn1-Cre/Scn1a$^{WT/A1783V}$ mice and their control group (Scn1a$^{WT/WT}$ mice) treated with BCP (100 mg/kg) or vehicle. Panel **(C)** shows representative images of the immunofluorescence staining. Values are means ± SEM of 6-7 animals per group. Data were assessed by two-way ANOVA followed by the Tukey test (*p<0.05, **p<0.01, ****p<0.001 vs. vehicle-treated Scn1a$^{WT/WT}$ - PTZ mice; $^{\$\$\$}p$<0.05, $^{\$\$\$\$}p$<0.001 vs. vehicle-treated Scn1a$^{WT/WT}$ + PTZ mice; $^{\#\#\#}p$<0.005 vs. vehicle-treated Syn1-Cre/Scn1a$^{WT/A1783V}$ - PTZ mice; $^{@@}p$<0.01, $^{@@@@}p$<0.001 vs. vehicle-treated Syn1-Cre/Scn1a$^{WT/A1783V}$ + PTZ mice). Scale bar = 50 µm

In PTZ-injected animals, BCP pretreatment reported promising results, both in Syn1-Cre/Scn1a$^{WT/A1783V}$ and their control mice. In the case of control mice, BCP treatment significantly attenuated astrogliosis in the hippocampal dentate gyrus (Figure R22B), as well as microgliosis in both prefrontal cortex and hippocampal dentate gyrus (Figures R23A,B). Regarding Syn1-Cre/Scn1a$^{WT/A1783V}$ mice, astrogliosis was decreased in prefrontal cortex (Figure R22A) and microgliosis in both prefrontal cortex and hippocampal dentate gyrus (Figures R23A,B).

2.2. Analysis of BCP as a disease-modifying agent (chronic paradigm)

Once demonstrated that BCP was effective against seizure onset, we next wanted to evaluate its effect on modulating the disease progression. For this purpose, we followed the experimental design which is presented in Figure R24. Briefly, Syn1-Cre/Scn1a$^{WT/A1783V}$ mice and their controls were treated with BCP at a dose of 10 mg/kg (i.p.) or its vehicle. The treatment was initiated when the animals were 10 days old, and injections were given every 48 hours (even days) up to PND24. Different neurodevelopmental reflexes were also measured on alternate days (odd days) from the age of 9 days up to 25. Additionally, body weight was recorded daily. At the age of 25 days and at least 24 hours after the last BCP injection, mice underwent behavioral testing (T-maze, Y-maze, social interaction and Actitrack) before being finally sacrificed for sample collection.

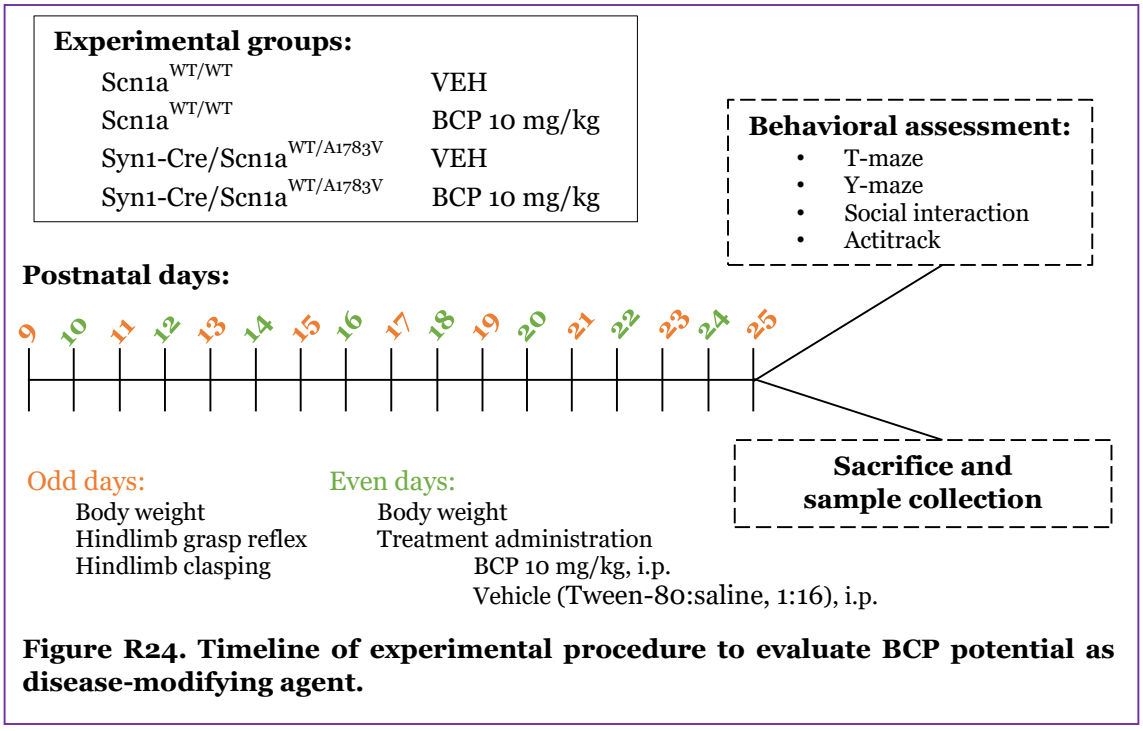

Figure R24. Timeline of experimental procedure to evaluate BCP potential as disease-modifying agent.

Effect of BCP on animal survival, body weight and reflexes

We first analyzed the animal survival in the four experimental groups (Figure R25). At the end of the experiment, the number of both vehicle- and BCP-treated control mice remained unchanged (100% survivors). In contrast, survival of vehicle-treated Syn1-Cre/Scn1a$^{WT/A1783V}$ mice dropped from PND21 to PND23, resulting in 71,5% of survivors at the end of the experiment. BCP treatment slightly improved survival in Syn1-Cre/Scn1a$^{WT/A1783V}$ mice compared with the vehicle-treated group, with 75% of survivors at the end of the experiment. Interestingly, BCP not only improved the survival rate but also extended the age at death, since no mice died before PND23. The statistical analysis of these data indicated they resulted significant (χ^2=5.061, p<0.05).

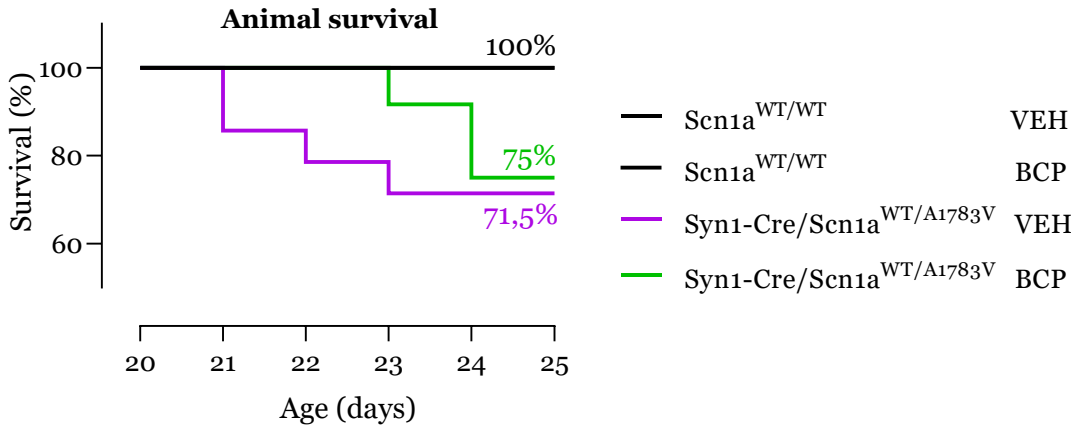

Figure R25. Effect of a BCP treatment on animal survival in DS mice. Kaplan-Meier plot for the analysis of animal survival in Syn1-Cre/Scn1a$^{WT/A1783V}$ mice and their control group (Scn1a$^{WT/WT}$ mice) treated with BCP (10 mg/kg) or vehicle. Data correspond to 6-12 animals per group and were assessed by the Log-Rank test.

Mice were also subjected to analysis of weight gain during the treatment period (Figure R26A). Our results showed that vehicle-treated Syn1-Cre/Scn1a$^{WT/A1783V}$ mice experienced a progressive weight loss beginning in PND21, which was partially attenuated by BCP administration (Figure R26A). This weight loss was not reported in the characterization of the DS mouse model described in Chapter 1 (Figure R2A), and this different trend could be due to the fact that this experimental design (Figure R24) involved daily handling of mice, which could particularly affect Syn1-Cre/Scn1a$^{WT/A1783V}$ mice. Additionally, vehicle-treated Syn1-Cre/Scn1a$^{WT/A1783V}$ mice showed neurodevelopmental anomalies. Particularly, they exhibited a delayed appearance of hindlimb grasping, which was completely acquired a PND19, 6 days later if compared to Scn1a$^{WT/WT}$ mice (Figure R26B). Moreover, they presented a marked clasping behavior from PND9 (Figure R26C). In both cases, our results demonstrated the ability of BCP to attenuate these disturbances.

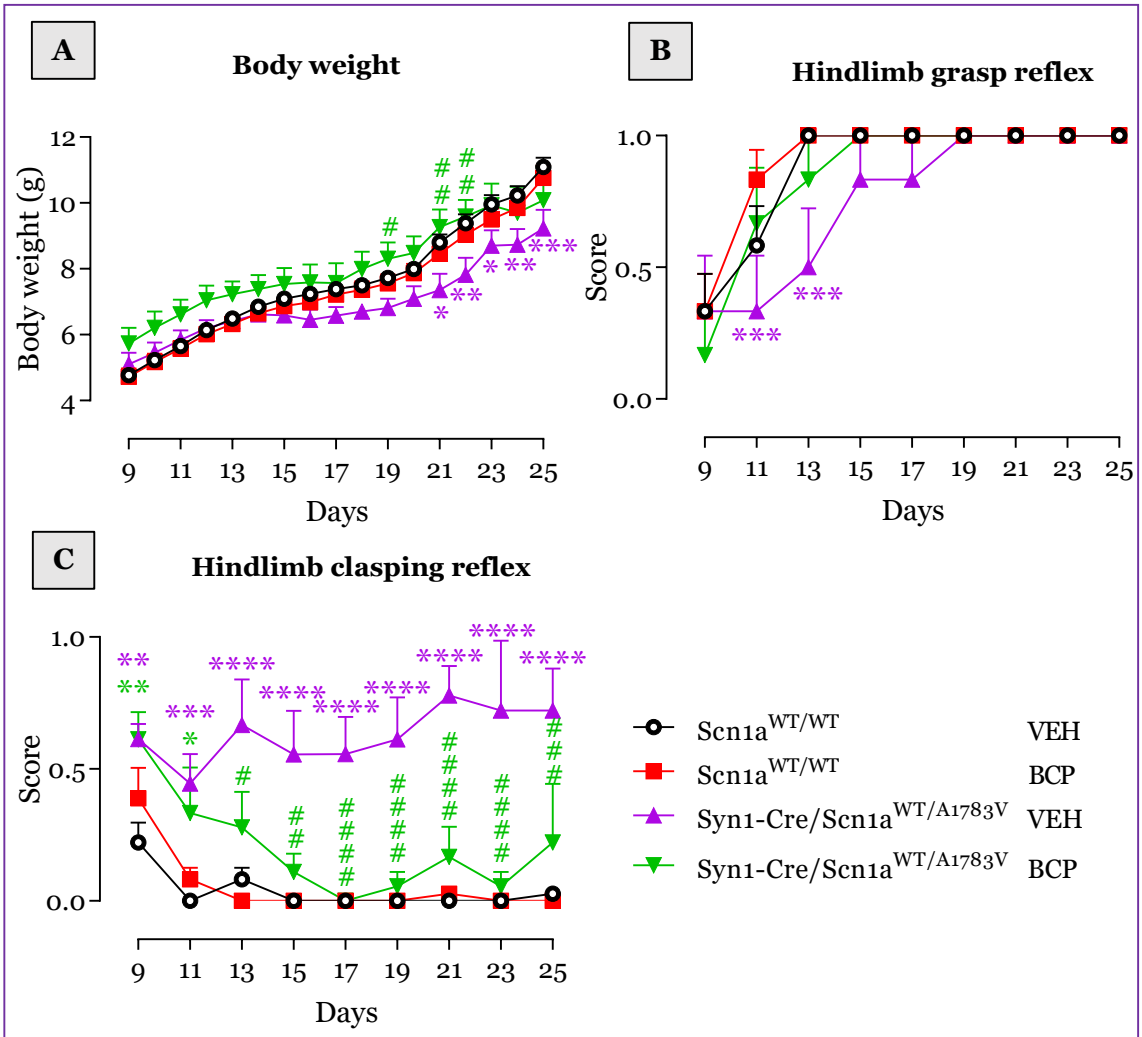

Figure R26. Effect of a BCP treatment on the evolution of different developmental parameters in DS mice. (A) Body weight, **(B)** hindlimb grasp reflex and **(C)** hindlimb clasping reflex in Syn1-Cre/Scn1a$^{WT/A1783V}$ mice and their control group (Scn1a$^{WT/WT}$ mice) treated with BCP (10 mg/kg) or vehicle. Values are means ± SEM of 6-12 animals per group. Data were assessed by two-way ANOVA for repeated measures followed by the Bonferroni test (*p<0.05, **p<0.01, ***p<0.005, ****p<0.001 vs. vehicle-treated Scn1a$^{WT/WT}$ mice; #p<0.05, ##p<0.01, ###p<0.005, ####p<0.001 vs. vehicle-treated Syn1-Cre/Scn1a$^{WT/A1783V}$ mice).

Effect of BCP on locomotor activity

Next, we wanted to study the possible effects of BCP on locomotor activity parameters by using the Actitrack equipment (Figure R27). Again, vehicle-treated Syn1-Cre/Scn1a$^{WT/A1783V}$ mice displayed a significantly more active behavior than control mice, as indicated by their longer distance travelled (Figure R27A), shorter resting time (Figure R27C), increased average velocity (Figure R27D) as well as a significant increase in the time moving fast (Figure R27E). This increased motor activity was also appreciated in the track plots automatically generated by the Actitrack software (Figure R27F).

Treatment with BCP did not produce significant effects, but showed clear trends towards the attenuation of these motor anomalies, which was reflected in the loss of statistical significance of Syn1-Cre/Scn1a$^{WT/A1783V}$ mice if compared to Scn1a$^{WT/WT}$ animals.

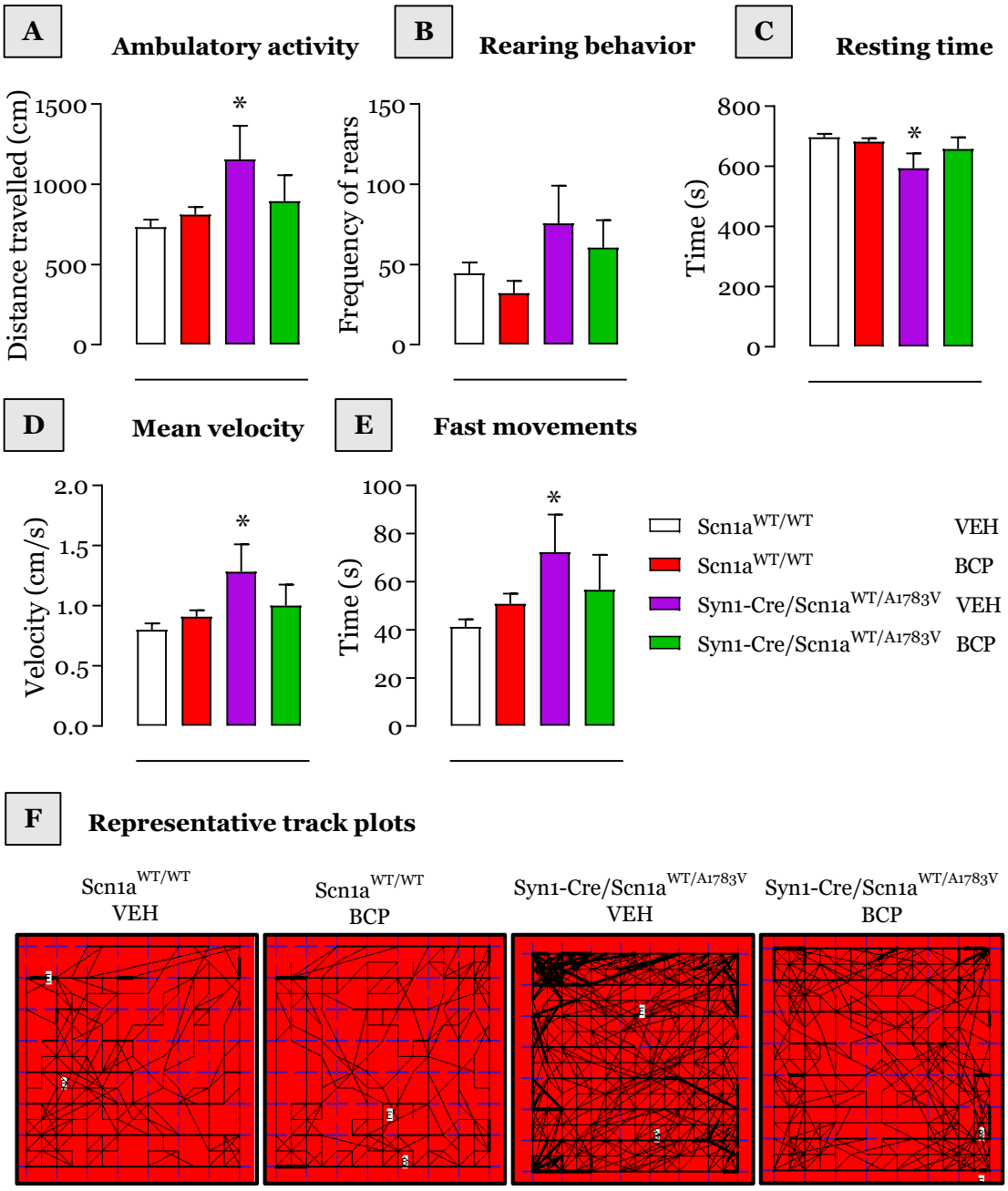

Figure R27. Effect of a BCP treatment on locomotor activity in DS mice. Measurement of different parameters recorded in the computer-aided actimeter in Syn1-Cre/Scn1a$^{WT/A1783V}$ mice and their control group (Scn1a$^{WT/WT}$ mice) treated with BCP (10 mg/kg) or vehicle, including **(A)** ambulatory activity, **(B)** rearing behavior, **(C)** resting time, **(D)** mean velocity and (E) fast movements. Panel **(F)** shows representative track plots generated from the Actitrack software. Values are means ± SEM of 6-12 animals per group. Data were assessed by two-way ANOVA followed by the Tukey test (*p<0.05 vs. vehicle-treated Scn1a$^{WT/WT}$ mice).

Effect of BCP on social interaction

As expected, autism-related behavioral deficits were observed in vehicle-treated Syn1-Cre/Scn1a$^{WT/A1783V}$ mice in the social interaction test (Figure R28), where they showed a significant decrease in the time spent in active interaction (Figure R28A) as well as in the total number of active interactions (Figure R28B) with a novel unfamiliar partner. Again, both deficits were attenuated by BCP administration, in this case, to a greater extent than in those parameters recorded in the actimeter, although effects did not reach statistical significance if compared to vehicle-treated Syn1-Cre/Scn1a$^{WT/A1783V}$ mice.

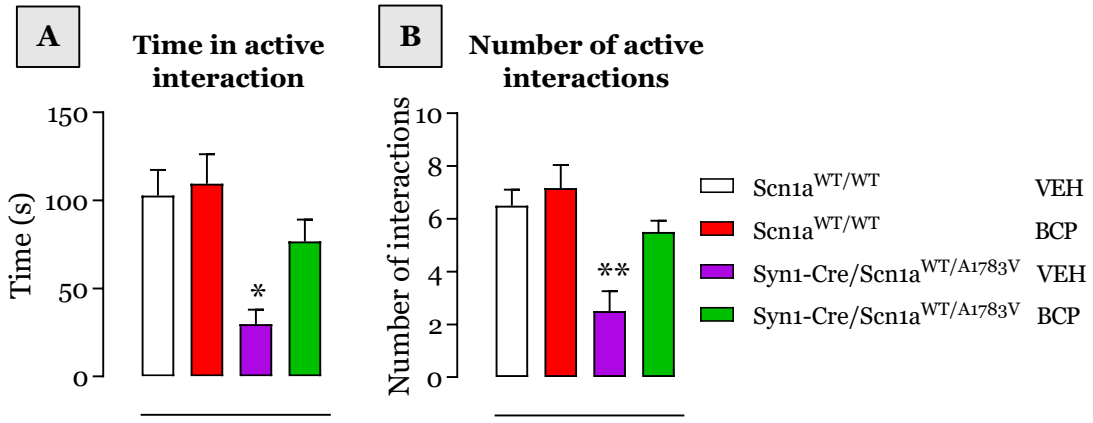

Figure R28. Effect of a BCP treatment on different parameters recorded in the social interaction test in DS mice. Measurement of different parameters in Syn1-Cre/Scn1a$^{WT/A1783V}$ mice and their control group (Scn1a$^{WT/WT}$ mice) treated with BCP (10 mg/kg) or vehicle, including **(A)** time in active interaction and **(B)** number of active interactions. Values are means ± SEM of 6-12 animals per group. Data were assessed by two-way ANOVA followed by the Tukey test (*p<0.05, **p<0.01 vs. vehicle-treated Scn1a$^{WT/WT}$ mice).

Effect of BCP on spatial working memory

In order to assess the effect of BCP on the alterations shown by DS mice in spatial working memory, we used both Y-maze (Figures R29A-D) and T-maze (Figure R29E) tests. As expected, vehicle-treated Syn1-Cre/Scn1a$^{WT/A1783V}$ mice exhibited impaired performance in the Y-maze test, with a marked decrease in the spontaneous alternation (Figure R29B) and small trends towards an increase in the number of total entries in the maze arms (p=0.1222, Figure R29A), as well as in the percentage of alternate arm returns (p=0.1190, Figure R29C). These impairments were also observed in the T-maze task (Figure R29E). In agreement with the aforementioned positive effects, BCP treatment partially attenuated those disturbances recorded in the Y-maze test, specially the number of total entries and the spontaneous alternation (Figures R29A,B). A more potent

beneficial effect was observed in the T-maze test, where BCP totally reversed the low values observed in the task performance (Figure R29E).

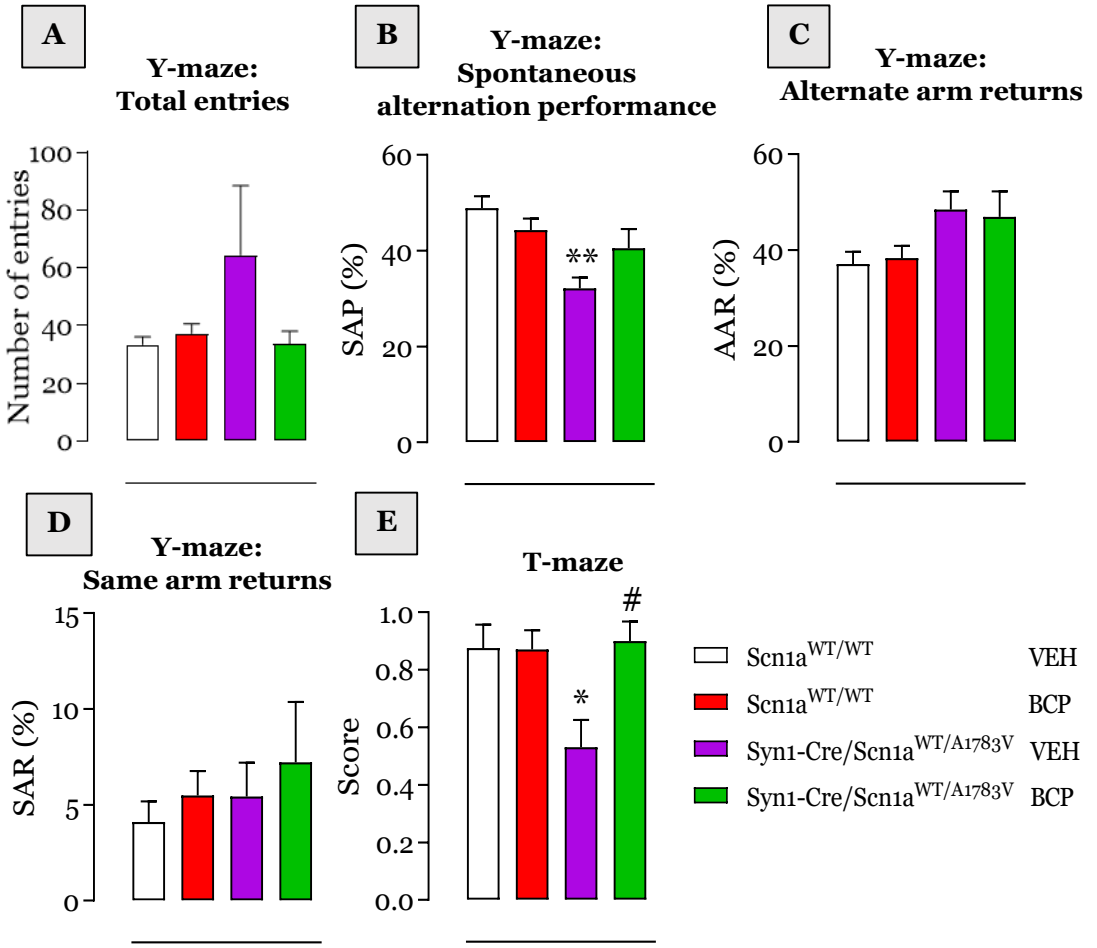

Figure R29. Effect of a BCP treatment on different parameters recorded in the Y-maze and T-maze tests in DS mice. Measurement of different parameters in the **(A-D)** Y-maze test and **(E)** T-maze test in Syn1-Cre/Scn1a$^{WT/A1783V}$ mice and their control group (Scn1a$^{WT/WT}$ mice) treated with BCP (10 mg/kg) or vehicle. Values are means ± SEM of 6-12 animals per group. Data were assessed by two-way ANOVA followed by the Tukey test (*p<0.05, **p<0.01 vs. vehicle-treated Scn1a$^{WT/WT}$ mice; #p<0.05 vs. vehicle-treated Syn1-Cre/Scn1a$^{WT/A1783V}$ mice).

Effect of BCP on glial reactivity

As demonstrated in Chapter 1, behavioral anomalies exhibited by vehicle-treated Syn1-Cre/Scn1a$^{WT/A1783V}$ mice were accompanied by glial reactivity. On the one hand, they presented elevated GFAP immunoreactivity both in prefrontal cortex and hippocampal dentate gyrus (Figures R30A,B). On the other hand, Iba-1 immunoreactivity was also markedly increased in prefrontal cortex and to a lesser extent in the hippocampal dentate gyrus (Figures R31A,B). In accordance with benefits at the behavioral level, and similar to its acute administration, BCP was capable of significantly counteracting astrogliosis in

both prefrontal cortex and dentate gyrus (Figures R30A,B), as well as microgliosis in the prefrontal cortex, and to a lesser extent in the dentate gyrus (Figures R31A,B).

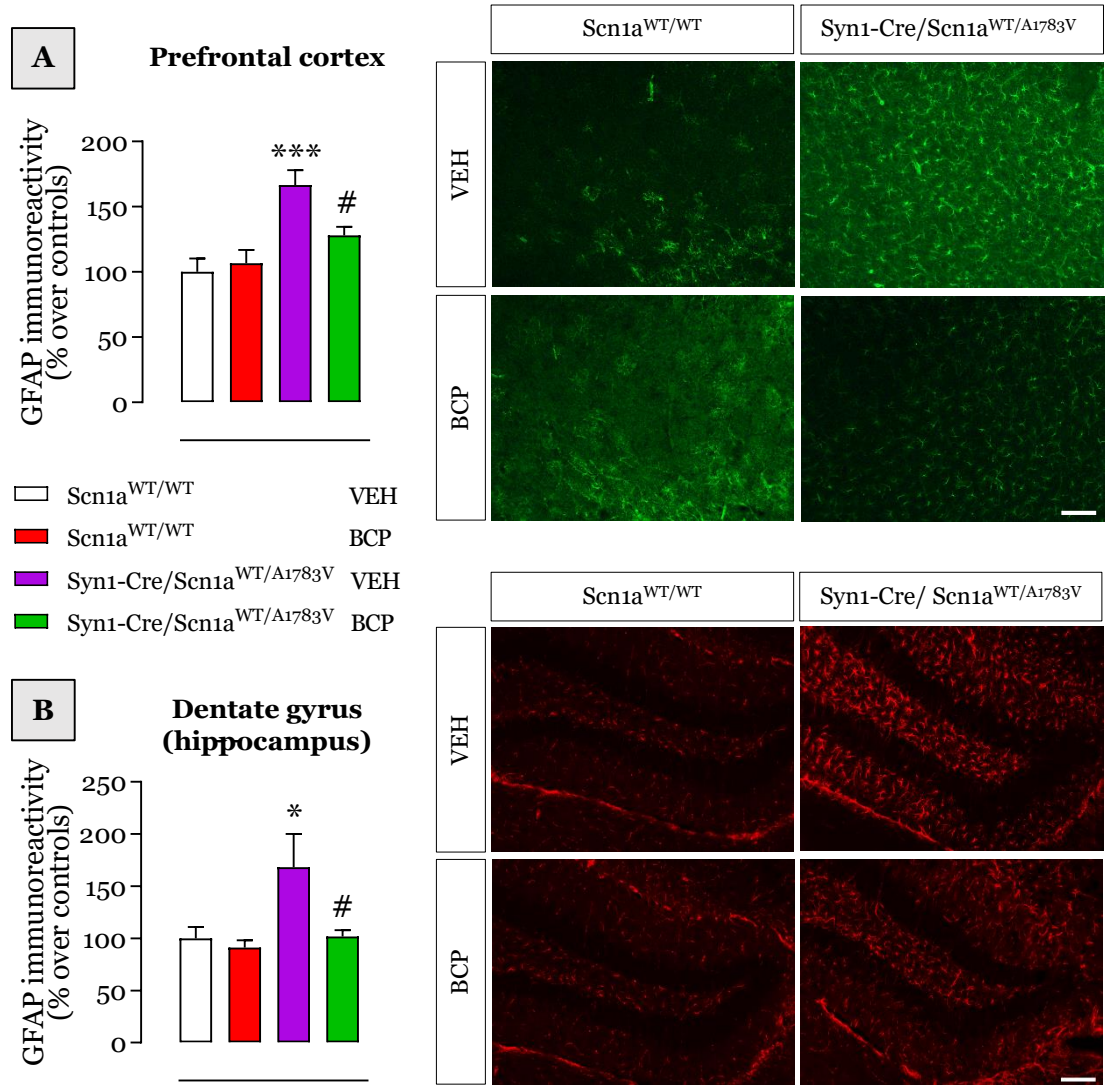

Figure R30. Effect of a BCP treatment on the astroglial marker GFAP in DS mice. Measurement of GFAP immunoreactivity in **(A)** prefrontal cortex and **(B)** hippocampal dentate gyrus in Syn1-Cre/Scn1a$^{WT/A1783V}$ mice and their control group (Scn1a$^{WT/WT}$ mice) treated with BCP (10 mg/kg) or vehicle. Values are means ± SEM of 6-7 animals per group. Data were assessed by two-way ANOVA followed by the Tukey test (*p<0.05, ***p<0.005 vs. vehicle-treated Scn1a$^{WT/WT}$ mice; $^{\#}p$<0.05 vs. vehicle-treated Syn1-Cre/Scn1a$^{WT/A1783V}$ mice). Scale bar = 50 µm.

Summary

To summarize the most important findings of this Chapter, BCP was shown to exert beneficial effects in our DS mice. First, it showed anticonvulsant effects against PTZ-induced seizures in both DS mice and their controls. Second, BCP was also able to attenuate those behavioral disturbances which characterize the progressive comorbidities developed in this mouse model, including the neurodevelopmental delay,

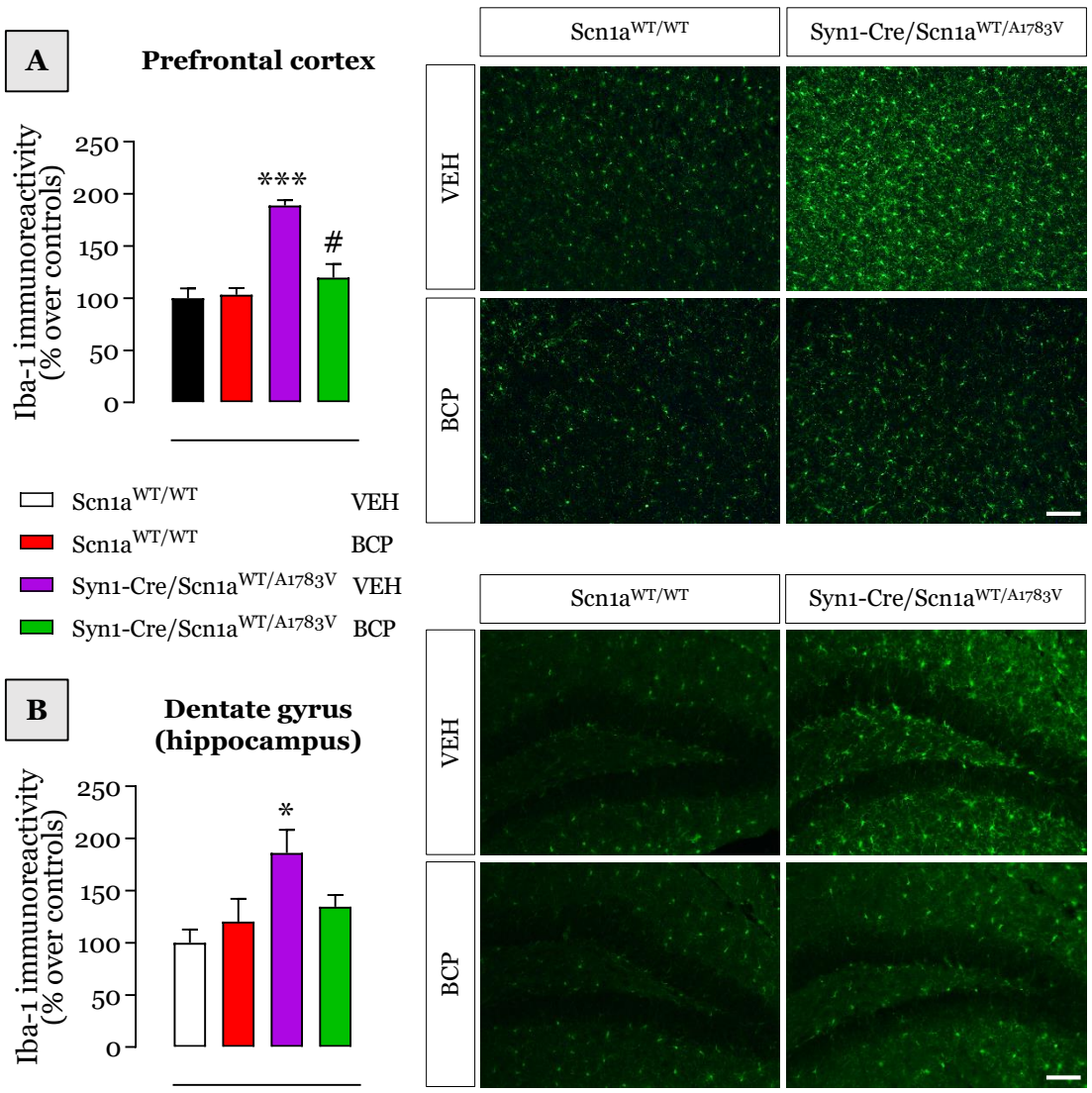

Figure R31. Effect of a BCP treatment on the microglial marker Iba-1 in DS mice. Measurement of Iba-1 immunoreactivity in **(A)** prefrontal cortex and **(B)** hippocampal dentate gyrus in Syn1-Cre/Scn1a$^{WT/A1783V}$ mice and their control group (Scn1a$^{WT/WT}$ mice) treated with BCP (10 mg/kg) or vehicle. Values are means ± SEM of 6-7 animals per group. Data were assessed by two-way ANOVA followed by the Tukey test (*p<0.05, ***p<0.005 vs. vehicle-treated Scn1a$^{WT/WT}$ mice; #p<0.05 vs. vehicle-treated Syn1-Cre/Scn1a$^{WT/A1783V}$ mice). Scale bar = 50 µm.

premature death, motor hyperactivity, cognitive deficits and autistic traits. Besides, it was also able to reduce the elevated glial reactivity found in those CNS structures which are more relevant to these behavioral abnormalities. Therefore, these results provided clear evidence of the promising pharmacological and therapeutic potential of BCP for DS, not only against seizuring activity, but also against long-term behavioral disturbances associated with the proconvulsant activity typical of this disorder. Moreover, these results also provided a theoretical basis for considering anti-inflammatory agents as promising therapeutic strategies for disease modification.

CHAPTER 3. EVALUATION OF THE EFFECTIVENESS OF A COMBINATION OF BCP AND CBD AS A POTENTIAL THERAPEUTIC APPROACH IN DS

As described in the Introduction, CBD has been recently approved as an anticonvulsant agent for the treatment of DS, as well as for other pediatric epileptic encephalopathies (Franco *et al.*, 2021). Results just shown in Chapter 2 revealed that BCP, another *C. sativa* constituent, exhibited a potential value for its further development as a novel candidate for DS treatment. Like CBD, BCP has no affinity for CB_1 receptors (which devoid it from undesirable psychotropic effects) and it is also considered a "multi-target" agent, known to exert positive effects in multiple experimental models by acting on CB_2, PPARγ and/or TLR-4 receptors, among others. Therefore, given that CBD and BCP likely modulate different molecular targets but share common mechanisms of action (e.g., anti-inflammatory and antioxidant), we wondered whether the combination of both *C. sativa* constituents could exert more potent effects than either compound alone. BCP is a food additive and flavoring agent approved by regulatory agencies and with no reported adverse effects, in contrast to some mild or moderate side effects observed after CBD treatment in humans (Devinsky *et al.*, 2017, 2018; Miller *et al.*, 2020; Thiele *et al.*, 2018, 2019), so their combination could facilitate the use of lower doses of CBD, thus reducing possible side effects. Furthermore, according to the "entourage effect", CBD and BCP could act synergistically and exert additional positive effects (Russo, 2011), thus positioning BCP as a compound with future potential to be used in a combination therapy in human pharmaceutics (Gonçalves *et al.*, 2020; Sharma *et al.*, 2016).

Taking into account all this evidence, we performed both an *in vitro* (BV2 cells) and *in vivo* (DS mice) evaluation of possible positive effects exerted by the combination of BCP and CBD, with a focus on anti-inflammatory and antioxidant responses.

3.1. Evaluation of the combination of BCP and CBD in BV2 cells

With the purpose of evaluating the anti-inflammatory potential of BCP and CBD (alone or in combination), LPS-stimulated microglial BV2 cells were used as an *in vitro* model to mimic an inflammatory environment. To this end, we first aimed to identify the optimal concentrations of both BCP and CBD for the remaining *in vitro* experiments. Once identified, we then performed different analysis to assess whether the combination of both compounds could be more beneficial than each compound alone.

Concentration-response analysis for BCP and CBD

In order to establish the optimal concentrations of BCP and CBD which could give rise to anti-inflammatory effects, two concentration-response curves were performed. BV2 cells were treated with different concentrations of BCP (1, 10, 25, 50 or 100 µM) or CBD (0.05, 0.1, 0.5, 1, 5 or 10 µM), and their effects on cell viability and levels of different inflammation-related proteins (TLR-4, catalase and Iba-1) were then evaluated. Figure R32 shows a representative scheme of this experimental design.

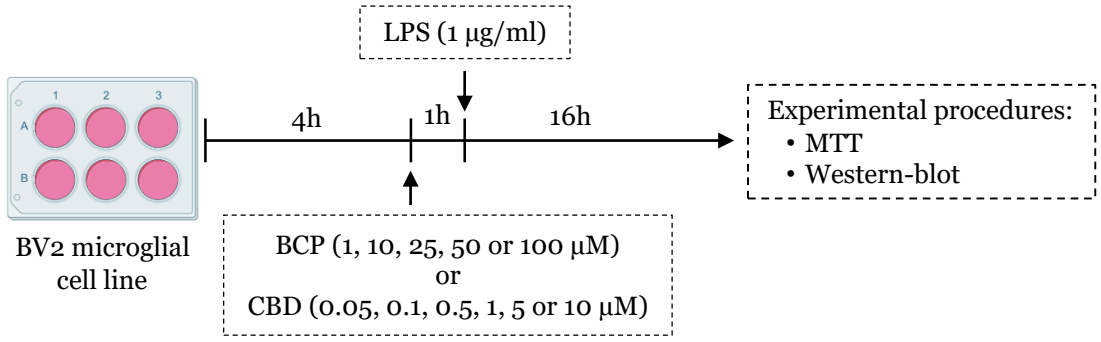

Figure R32. Timeline of experimental procedure to determine optimal BCP and CBD concentrations for BV2 cell treatments.

BCP concentrations of 1, 10 and 25 µM did not affect cell viability when compared to -LPS cells. However, a marked cytotoxic effect was observed for the concentrations of 50 and 100 µM (Figure R33A), as has been also observed in other studies (Guo *et al.*, 2014). Next, we analyzed by Western-blot some inflammation-related proteins, but only with the non-cytotoxic BCP concentrations (1, 10 and 25 µM). Our data indicated that LPS exposure increased TLR-4, catalase and Iba-1 protein levels (Figure R33C), whereas pretreatment with BCP was, in general, effective at attenuating the elevated levels of these three markers in the +LPS group (Figure R33C). However, it is important to remark that only the concentration of 10 µM reported statistically significant effects for the three markers. Therefore, attending to these results, we decided to choose the concentration of 10 µM for the remaining experiments.

Regarding CBD, the concentrations of 0.05, 0.1, 0.5 and 1 µM did not show any cytotoxic effect. In contrast, higher concentrations (5 and 10 µM) drastically decreased cell viability (Figure R34A), as also shown in previous studies (Rimmerman *et al.*, 2013). Therefore, these two concentrations were not included in the Western-blot analysis. Very similar to the BCP concentration-response curve, LPS induced an increase in the expression of TLR-4, catalase and Iba-1 protein levels (Figure R34C). When pretreated with CBD, all non-cytotoxic concentrations (0.05-1 µM) tended to reduce the higher

protein levels for the three markers (except 1 μM for Iba-1), but the most effective concentration was 0.1 μM (reaching statistical significance in all cases except for Iba-1, in which it remained as a trend) (Figure R34C). Therefore, in this case, we decided to continue our following experiments with the concentration of 0.1 μM.

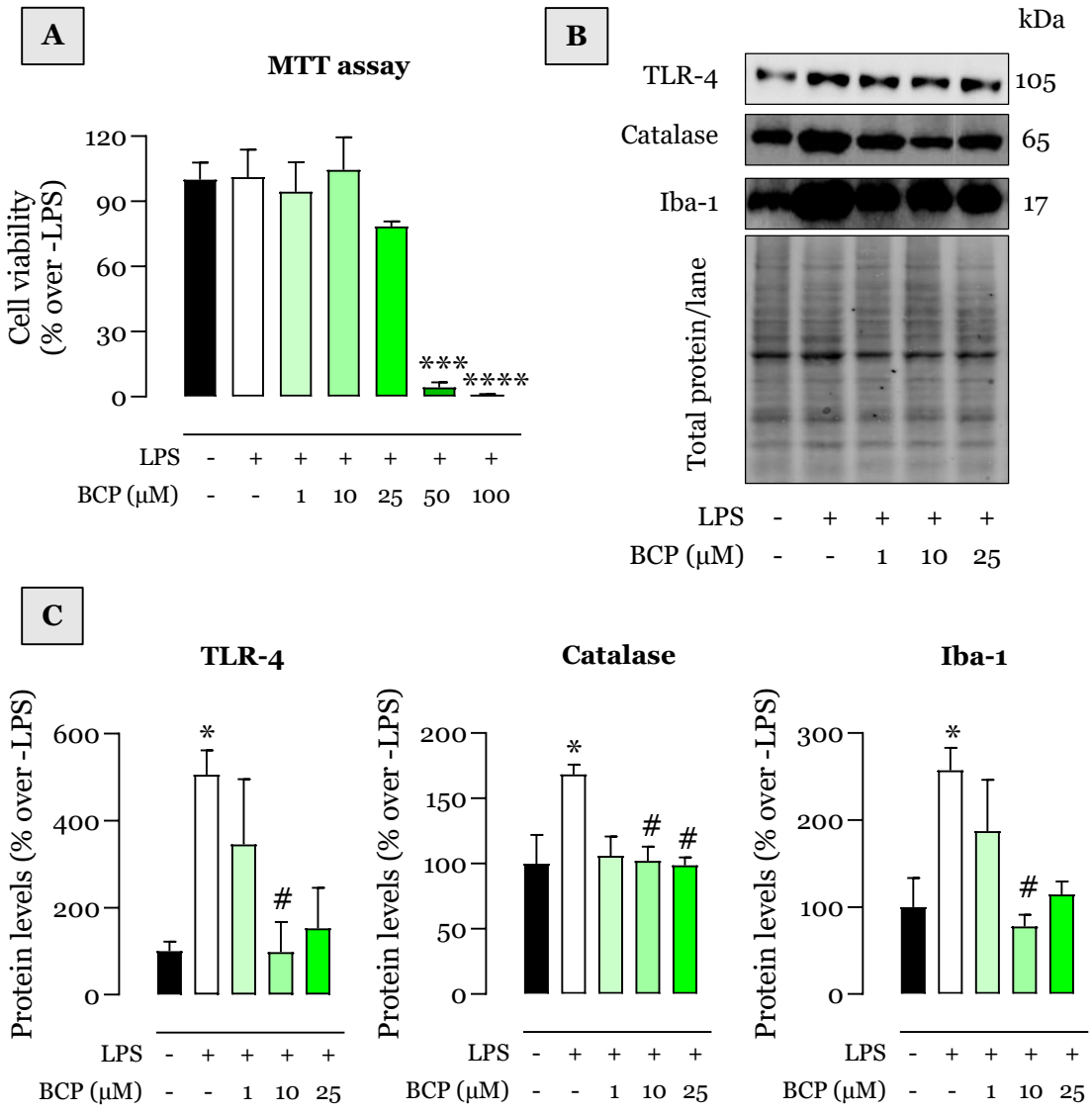

Figure R33. Concentration-response curve of BCP in LPS-stimulated BV2 cells. **(A)** Effect of different concentrations of BCP (1, 10, 25, 50 and 100 μM) in cell viability measured by MTT assay. **(B)** Representative Western-blots with loading controls for TLR-4, catalase and Iba-1 using different concentrations of BCP (1, 10 and 25 μM). **(C)** Quantifications of TLR-4, catalase and Iba-1 protein levels using different concentrations of BCP (1, 10 and 25 μM). Values are the mean ± SEM of at least 4 independent experiments each performed in triplicate. Data were assessed by using one-way ANOVA followed by the Bonferroni test (*p<0.05, ***p<0.005, ****p<0.001 vs. -LPS cells; $^{\#}p$<0.05 vs. +LPS cells).

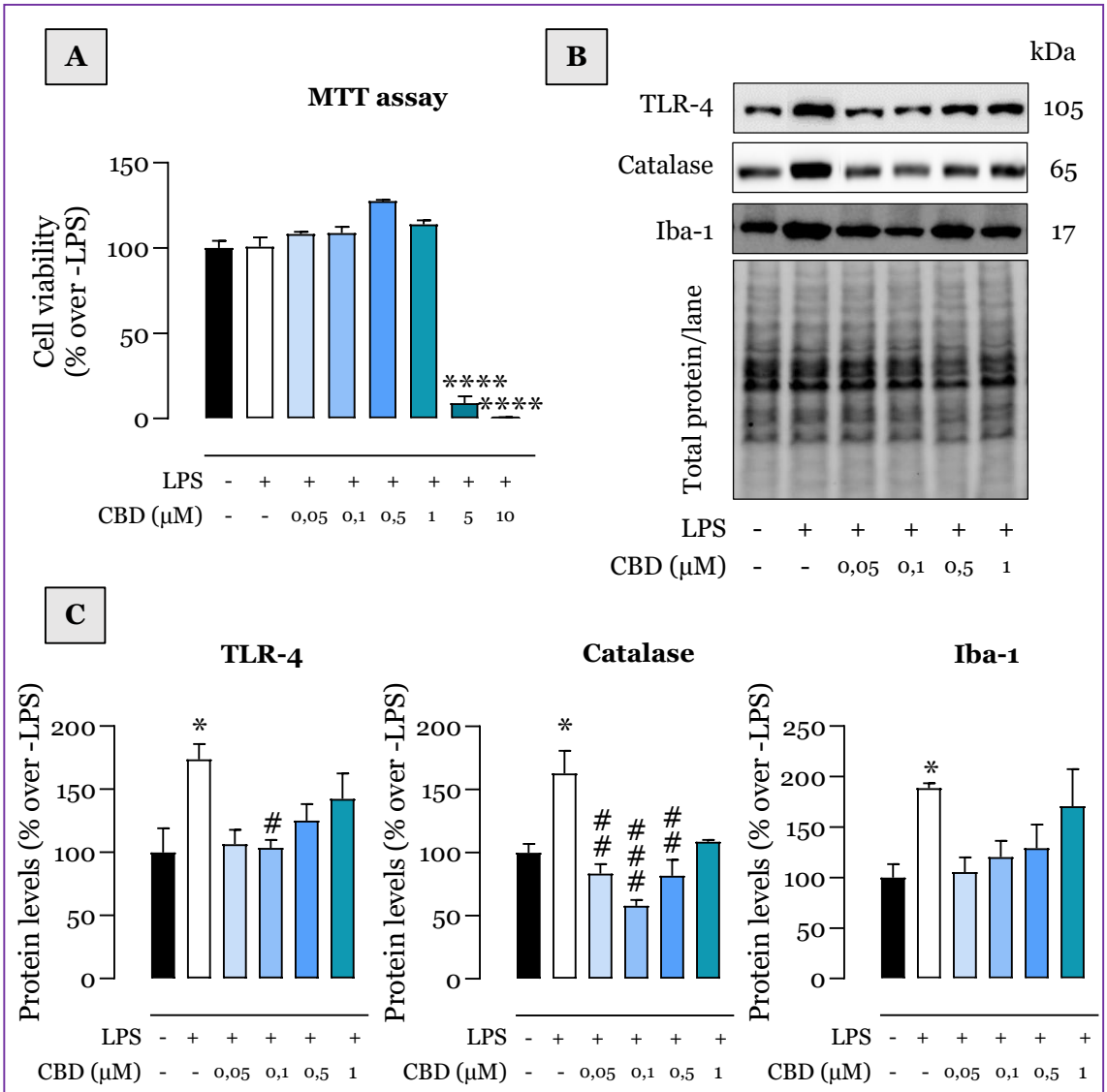

Figure R34. Concentration-response curve of CBD in LPS-stimulated BV2 cells. **(A)** Effect of different concentrations of CBD (0.05, 0.1, 0.5, 1, 5 and 10 μM) in cell viability measured by MTT assay. **(B)** Representative Western-blots with loading controls for TLR-4, catalase and Iba-1 using different concentrations of CBD (0.05, 0.1, 0.5 and 1 μM). **(C)** Quantifications of TLR-4, catalase and Iba-1 protein levels using different concentrations of CBD (0.05, 0.1, 0.5 and 1 μM). Values are the mean ± SEM of at least 4 independent experiments each performed in triplicate. Data were assessed by using one-way ANOVA followed by the Bonferroni test (*p<0.05, ****p<0.001 vs. -LPS cells; #p<0.05, ##p<0.01, ###p<0.005 vs. +LPS cells).

Beneficial effects of the combination of BCP and CBD

Based on the concentration-response curves, we decided to continue our subsequent studies with concentrations of 10 µM of BCP and 0.1 µM of CBD as the most efficacious. As detailed in Figure R35, we followed a similar experimental design and performed several experimental procedures to evaluate the possible positive effects exerted by the combination of BCP and CBD in comparison to the two compounds alone.

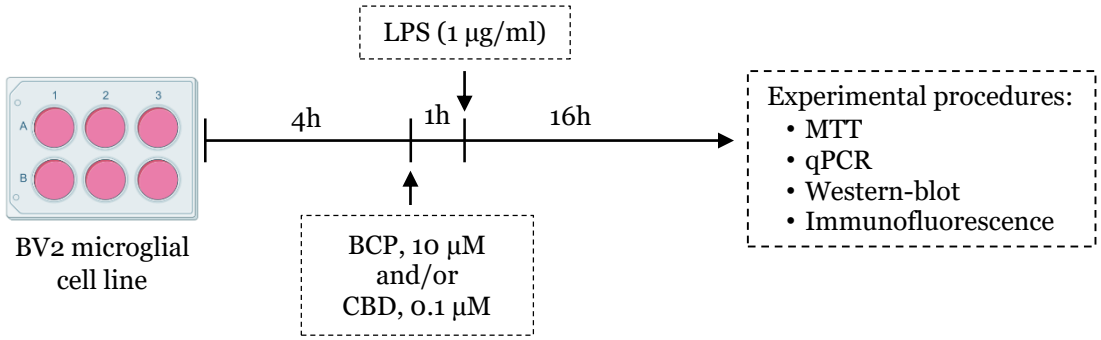

Figure R35. Timeline of experimental procedure to determine the effects of the combination of BCP and CBD on BV2 cells.

First, we wanted to verify that these two concentrations (alone or in combination) did not lead to cell death in this experimental design. As expected, the MTT assay did not show changes in cell viability (Figure R36A). Next, we measured protein levels for the same three markers as in the concentration-response curves. Again, LPS induced an elevated expression of TLR-4, catalase, and Iba-1 when compared to -LPS cells (Figure R36C). In this case, more modest effects were exerted by BCP and CBD compared to +LPS cells when used individually. Thus, BCP treatment led to a trend towards a decrease in TLR-4 (p=0.1129) and catalase (p=0.1248) protein levels; in contrast, no trends were detected in Iba-1 levels. CBD treatment also led to a partial decrease in catalase protein levels (p=0,1763), whereas more modest effects were detected for TLR-4 and no changes for Iba-1. Interestingly, the combination of both compounds revealed interesting synergistic effects, with the maximal reductions for the three markers remaining as trends for TLR-4 (p=0.0721) and Iba-1 (p=0.0753), but reaching statistical significance for catalase (Figure R36C).

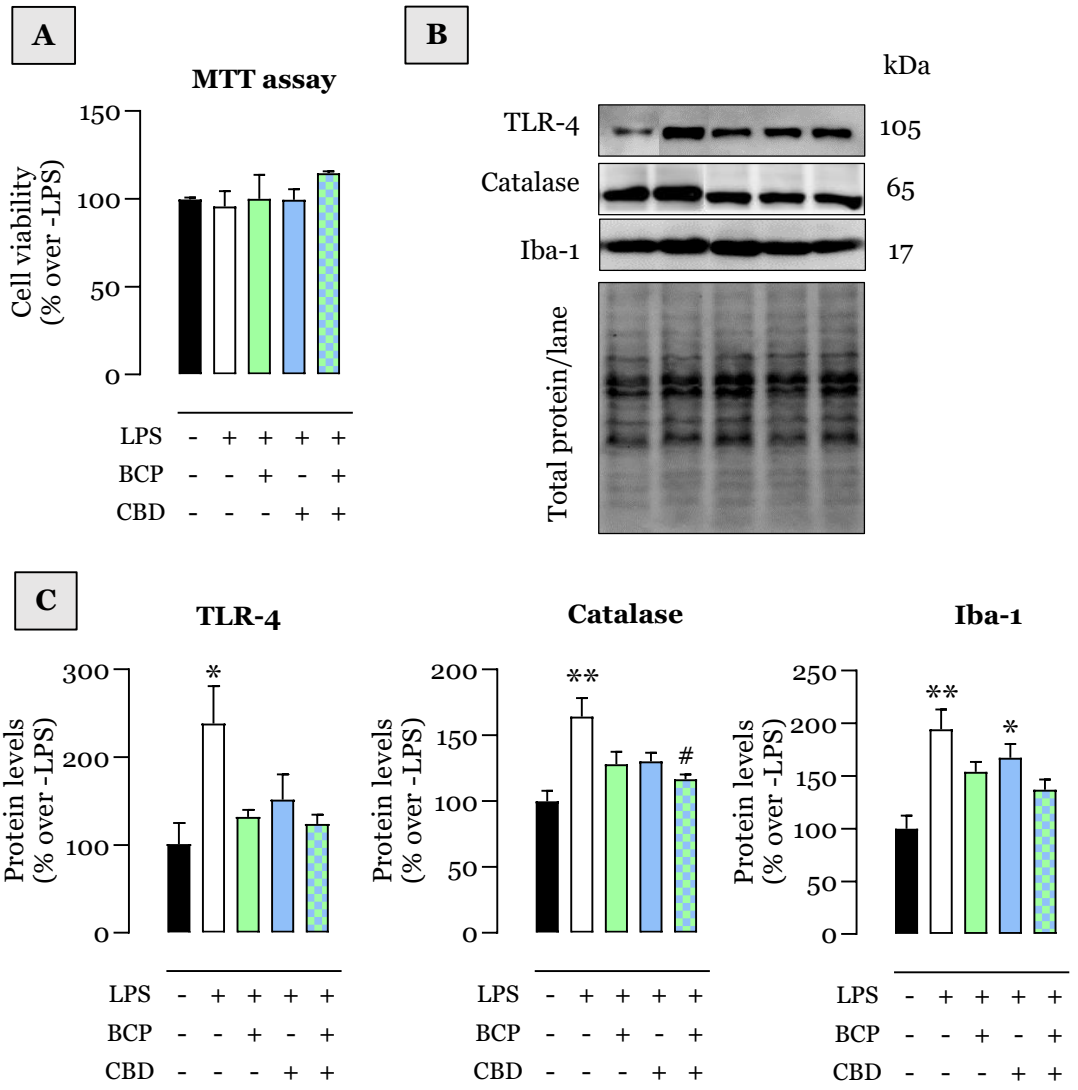

Figure R36. Effect of the combination of BCP and CBD on cell viability and different protein markers. Effect of the treatment with BCP (10 μM) and CBD (0,1 μM), alone or in combination, on **(A)** cell viability and **(C)** TLR-4, catalase and Iba-1 protein levels. Panel **(B)** shows representative Western-blots with loading controls. Values are the mean ± SEM of at least 4 independent experiments each performed in triplicate. Data were assessed by using one-way ANOVA followed by the Bonferroni test (*p<0.5, **p<0.01 vs. -LPS cells; #p<0.05 vs. +LPS cells).

To further explore the beneficial effects of this combination, we also conducted qPCR analysis of genes related to inflammation (Figure R37). As expected, these studies revealed that LPS-stimulated BV2 cells showed an upregulation of the pro-inflammatory genes IL1β, COX-2, TNFα and iNOS, as indicated by their mRNA levels (Figures R37C-F). When administered alone, BCP was able to significantly decrease IL1β and iNOS levels compared to +LPS cells, whereas only a partial reversion was observed for COX-2 and TNFα. Regarding CBD, although less efficiently than BCP, it was also able to decrease IL1β and Inos levels when compared to +LPS cells; again, only partial

reversions were observed for COX-2 and TNFα. In combination, BCP and CBD were able to exert more marked effects, leading to significant decreases of IL1β, TNFα and iNOS levels compared to +LPS cells, and a partial reversion regarding COX-2 (Figures R37C-F). LPS exposure did not result in changes for CB_2 receptor mRNA levels (Figure R37A). However, a small trend towards a downregulation in PPARγ receptor levels (p=0,2806) was shown (Figure R37B), which was partially attenuated by BCP and CBD, alone or in combination.

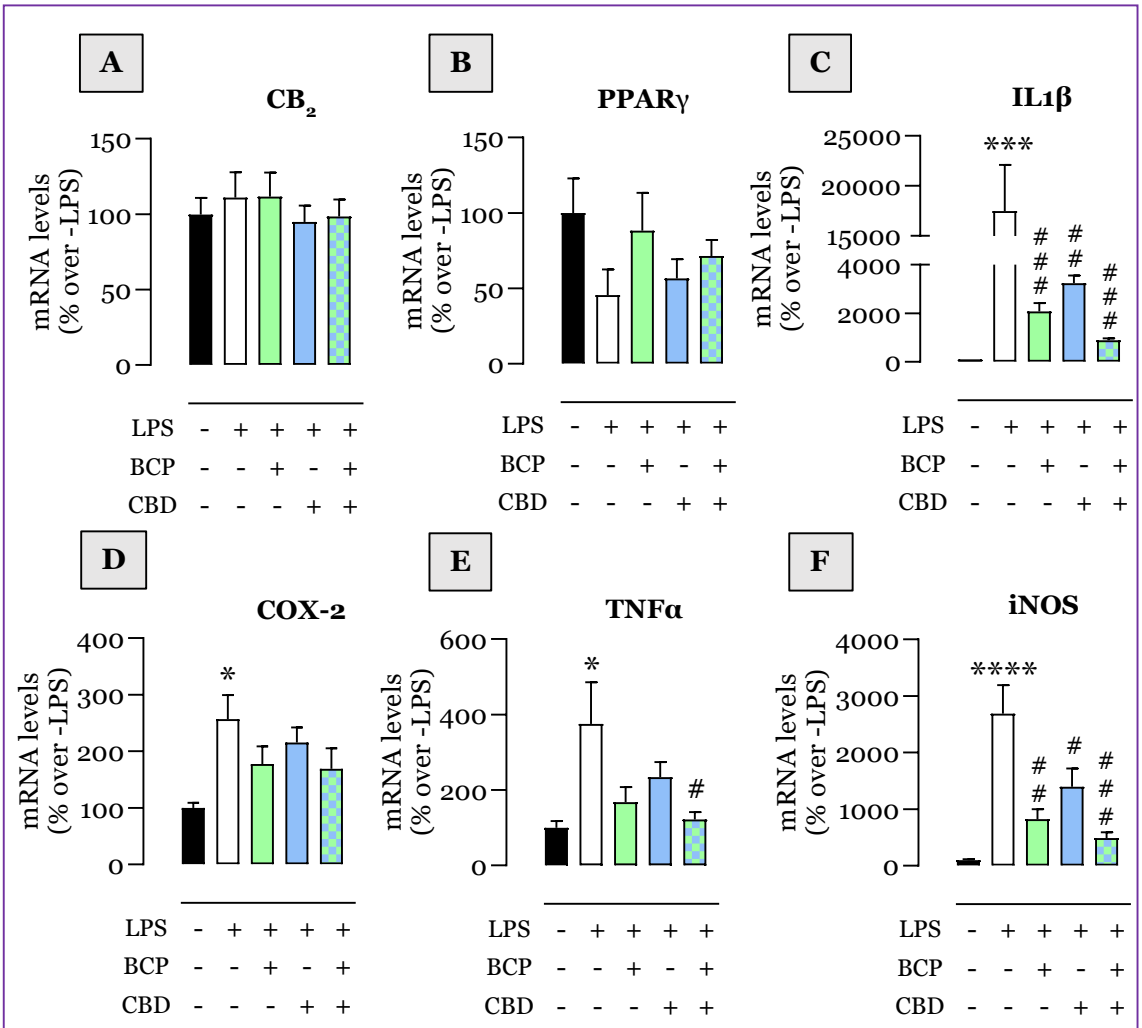

Figure R37. Effect of the combination of BCP and CBD on the gene expression of different inflammatory and oxidative stress markers in LPS-stimulated BV2 cells. Effect of the treatment with BCP (10 µM) and CBD (0,1 µM), alone or in combination, on the gene expression of different markers, including **(A)** CB2 receptor **(B)** PPARγ receptor **(C)** IL1β, **(D)** COX-2, **(E)** TNFα and **(F)** iNOS. Values are the mean ± SEM of at least 4 independent experiments each performed in triplicate. Data were assessed by using one-way ANOVA followed by the Bonferroni test (*p<0.05, ***p<0.005, ****p<0.001 vs. -LPS cells; #p<0.05, ##p<0.01, ###p<0.005 vs. +LPS cells).

Lastly, we carried out an immunofluorescence analysis using the microglial marker Iba-1 to confirm changes of BV2 cells after LPS exposure and BCP/CBD treatments (Figure R38). Our results showed that BV2 cells treated with LPS presented an increase in Iba-1 immunoreactivity (Figure R38A) when compared to -LPS cells, which in part corresponded to a higher number of Iba-1 positive cells (Figure R38B). Although cell morphology was not specifically quantified, representative immunofluorescence images indicated that whereas -LPS cells presented a resting state and showed small cell bodies, +LPS cells appeared to acquire an activated morphology, with some branches emerging from a larger cell body (Figure R38C). Overall, these observations were in agreement with the increase in Iba-1 levels measured by Western-blot in previous experiments (Figures R33,34,36). When pretreated with BCP or CBD alone, a significant attenuation in both parameters when compared to +LPS cells was detected. Interestingly, a more potent effect was found with the combination of both compounds in the case of Iba-1 immunoreactivity (Figure R38A). Moreover, the representative immunofluorescence images of the combination treatment clearly showed BV2 cells with smaller cell bodies, suggesting suppression of cell activation (Figure R38C).

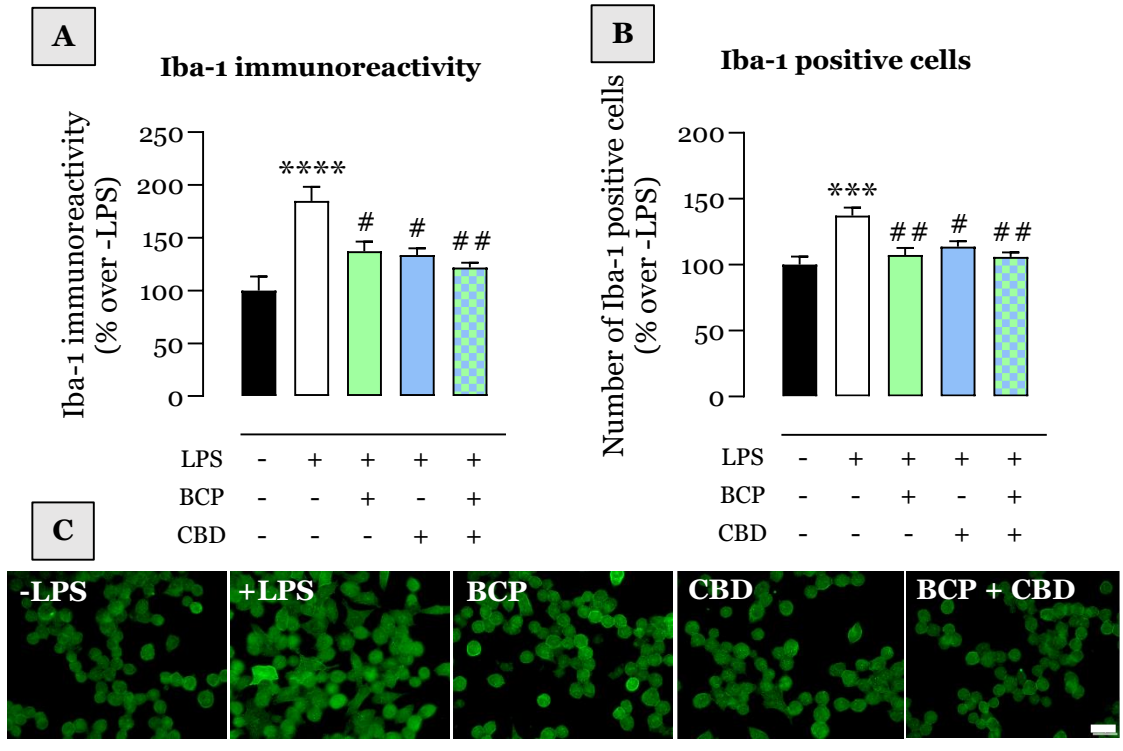

Figure R38. Effect of the combination of BCP and CBD on Iba-1 immunostaining in LPS-stimulated BV2 cells. Effect of the treatment with BCP (10 μM) and CBD (0,1 μM), alone or in combination, on **(A)** the number of Iba-1 positive cells and **(B)** Iba-1 immunoreactivity, including **(C)** representative immunofluorescence images. Values are the mean ± SEM of at least 4 independent experiments each performed in triplicate. Data were assessed by using one-way ANOVA followed by the Bonferroni test (***p<0.005, ****p<0.001 vs. -LPS cells; #p<0.05, ##p<0.01 vs. +LPS cells). Scale bar = 50 μm.

3.2. Evaluation of the combination of BCP and CBD in DS mice

Once demonstrated that the combination of BCP and CBD was more effective than each compound alone at exerting anti-inflammatory effects in BV2 cells, we next wondered whether this combination might be similarly effective in our DS mouse model. To this end, Syn1-Cre/Scn1a$^{WT/A1783V}$ mice were treated with BCP (10 mg/kg, i.p.) or CBD (5 mg/kg, i.p.), alone or in combination, from PND10 up to PND24. Groups of both Syn1-Cre/Scn1a$^{WT/A1783V}$ and Scn1a$^{WT/WT}$ mice treated with vehicle were also included in this experiment. Injections were given every 48 hours (even days). On alternate days (odd days), neurodevelopmental reflexes were measured. Additionally, body weight was daily recorded. At PND25, and at least 24 hours after the last injection, different behavioral tests were performed (Y-maze, social interaction and Actitrack) and mice were finally euthanized for sample collection (Figure R39).

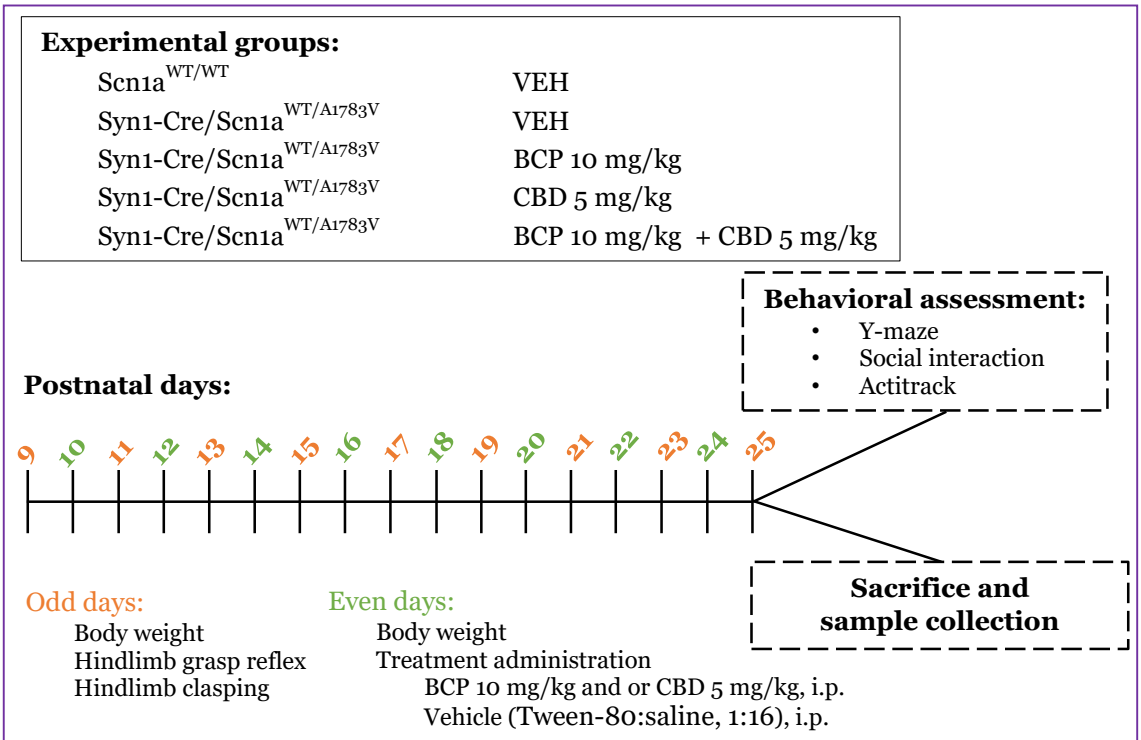

Figure R39. Timeline of the experimental procedure to evaluate the therapeutic potential of a combination of BCP and CBD.

Effect of BCP and CBD combination on animal survival, body weight and reflexes

Survival of vehicle-treated Syn1-Cre/Scn1a$^{WT/A1783V}$ mice started to drop at PND21, and only 53.8% of animals reached PND25. To our surprise, animal mortality in this experiment was higher than in previous cohorts. Possible explanations for this difference

could be (1) the daily handling that this experimental design involved and (2) the fact that the combination treatment required two injections; both aspects could particularly affect Syn1-Cre/Scn1a$^{WT/A1783V}$ mice, which are extremely vulnerable. When administered alone, BCP and CBD were able to increase animal survival and delay the age at death, although BCP demonstrated a more effective response than CBD (75% and 66.7% of survivors, respectively). Interestingly, the combination of BCP and CBD was the treatment that produced the best improvement, with 87.5% of survivors at the end of the experiment. (Figure R40). Although statistical analysis of these data did not reach significance (χ^2=9.097, p=0.0587), Log-Rank test revealed a strong tendency.

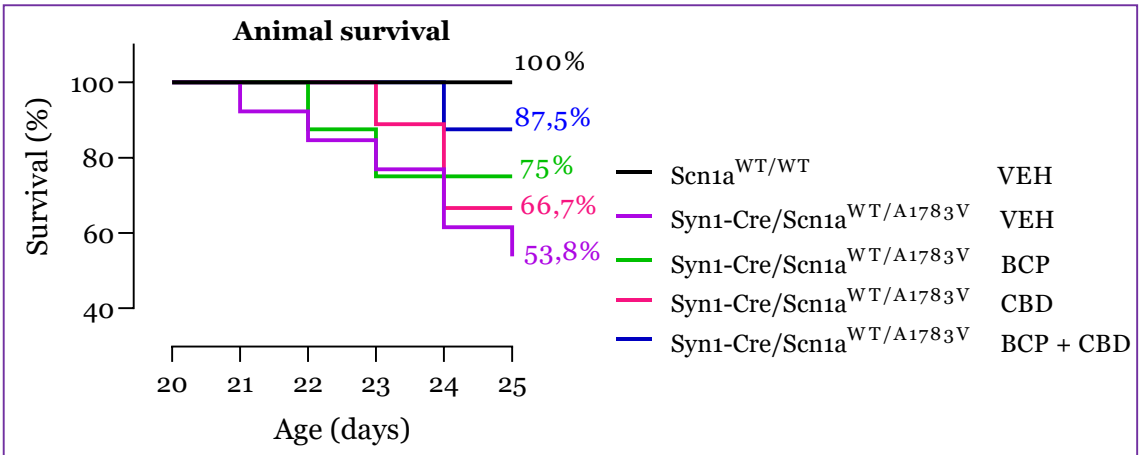

Figure R40. Effect of the combination of BCP and CBD on animal survival in DS mice. Kaplan-Meier plot for the analysis of animal survival in Syn1-Cre/Scn1a$^{WT/A1783V}$ mice and their control group (Scn1a$^{WT/WT}$ mice) treated with BCP (10 mg/kg) and CBD (5 mg/kg), alone or in combination. Data correspond to 6-12 animals per group and were assessed by the Log-Rank test.

Body weight was daily registered in this experiment too. Similar to the chronic BCP treatment of Chapter 2, vehicle-treated Syn1-Cre/Scn1a$^{WT/A1783V}$ mice showed a significant and progressive weight loss beginning in PND22. Although less accentuated, a partial weight loss was also observed in Syn1-Cre/Scn1a$^{WT/A1783V}$ mice treated with CBD. Treatment with BCP alone and the combined treatment of BCP and CBD were effective in partially recovering this characteristic loss of weight, with the combined treatment showing a more effective response (Figure R41A).

As in previous experiments, vehicle-treated Syn1-Cre/Scn1a$^{WT/A1783V}$ mice experienced a significant delay in the appearance of hindlimb grasping (Figure R41B), as well as a marked clasping behavior during the treatment period (Figure R41C). The three treatments options (BCP and CBD alone, as well as in combination) demonstrated the same effectiveness in recovering animals from their deteriorated hindlimb grasping (Figure R41B). Regarding clasping behavior, whereas administration of CBD partially

attenuated this abnormal behavior, BCP was able to produce a more significant effect; however, the combination of both compounds was the treatment option showing better results (Figure R42C).

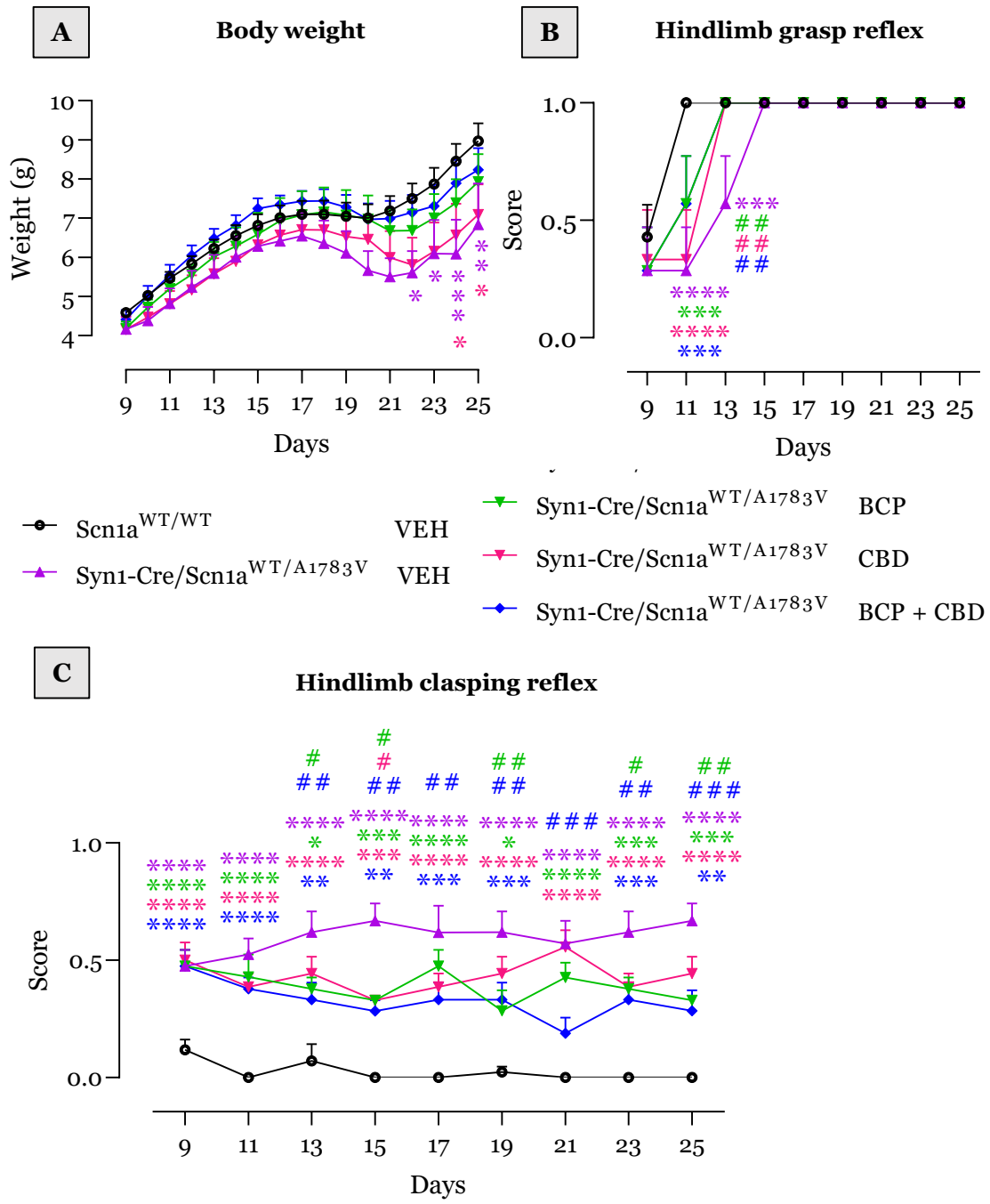

Figure R41. Effect of the combination of BCP and CBD on the evolution of different developmental parameters in DS mice. (A) Body weight, **(B)** hindlimb grasp reflex and **(C)** hindlimb clasping reflex in Syn1-Cre/Scn1a$^{WT/A1783V}$ mice and their control group (Scn1a$^{WT/WT}$ mice) treated with BCP (10 mg/kg) and CBD (5 mg/kg) alone or in combination. Values are means ± SEM of 6-12 animals per group. Data were assessed by two-way ANOVA for repeated measures followed by the Bonferroni test (*p<0.05, **p<0.01, ***p<0.005, ****p<0.001 vs. vehicle-treated Scn1a$^{WT/WT}$ mice; $^{\#}p$<0.05, $^{\#\#}p$<0.01, $^{\#\#\#}p$<0.005, $^{\#\#\#\#}p$<0.001 vs. vehicle-treated Syn1-Cre/Scn1a$^{WT/A1783V}$ mice).

Effect of a BCP and CBD combination on locomotor activity

We also investigated the effect of the three treatment options on locomotor activity. Vehicle-treated Syn1-Cre/Scn1a$^{WT/A1783V}$ mice exhibited their characteristic hyperactive behavior which has been already shown in previous experiments, with a robust increase in the total distance travelled in the actimeter (Figure R42A), an enhanced rearing behavior (Figure R42B), a decrease in the immobility time (Figure R42C) and marked increases in the mean velocity (Figure R42D) and in the time moving fast (Figure R42E). This hyperactive behavior could be clearly appreciated in representative trajectory plots generated by the software (Figure R42F).

Although effects did not reach statistical significance, both BCP and CBD, administered alone or in combination, produced a modest recovery (loss of statistical significance when compared to control mice) of these disturbances (Figures R42A-F). It must be highlighted that in these parameters, no significant differences were observed among treatments, since they produced similar effects. However, in most of these parameters, the administration of CBD alone was the treatment eliciting the higher trends towards normalization of motor hyperactivity.

Effect of a BCP and CBD combination on social interaction

Next, we wanted to study the possible effects of these treatments on autism-related behavioral deficits recorded in the social interaction test. In agreement with previous experiments, Syn1-Cre/Scn1a$^{WT/A1783V}$ mice showed a marked autistic-like behavior, with a strong reduction in the time in active interaction as well as the number of active interactions (Figures R43A,B).

When administered alone, BCP and CBD showed a very similar effect in significantly reducing these alterations. Interestingly, their combination revealed a strong effect at attenuating this social decline, increasing both the time in active interaction and the number of active contacts, thus suggesting that both molecules exert positive effects on social behavior, but they work even better if combined.

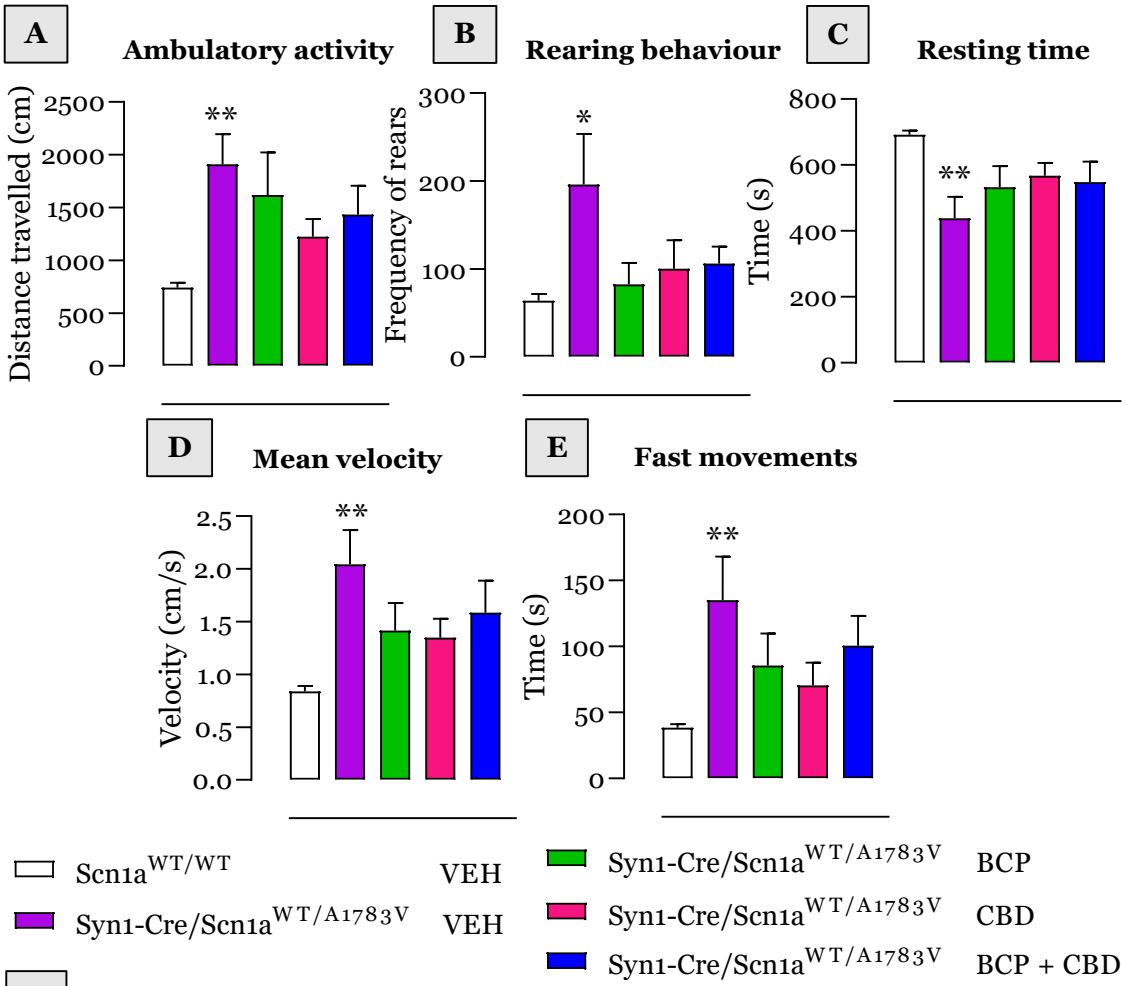

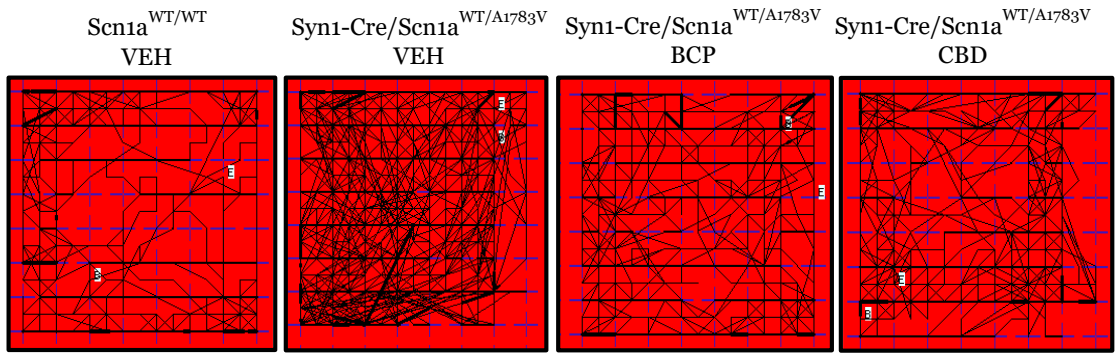

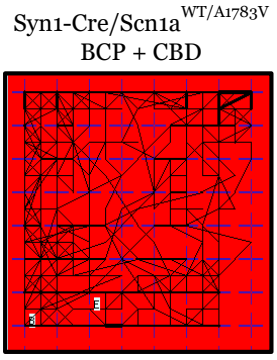

Figure R42. Effect of the combination of BCP and CBD on locomotor activity in DS mice. Measurement of different parameters recorded in the computer-aided actimeter in Syn1-Cre/Scn1a$^{WT/A1783V}$ mice and their control group (Scn1a$^{WT/WT}$ mice) treated with BCP (10 mg/kg) and CBD (5 mg/kg), alone or in combination, including **(A)** ambulatory activity, **(B)** rearing behavior, **(C)** resting time, **(D)** mean velocity and **(E)** fast movements. Panel **(F)** shows representative track plots generated from the Actitrack software. Values are means ± SEM of 6-12 animals per group. Data were assessed by one-way ANOVA followed by the Bonferroni test (*p<0.05, **p<0.01 vs. vehicle-treated Scn1a$^{WT/WT}$ mice).

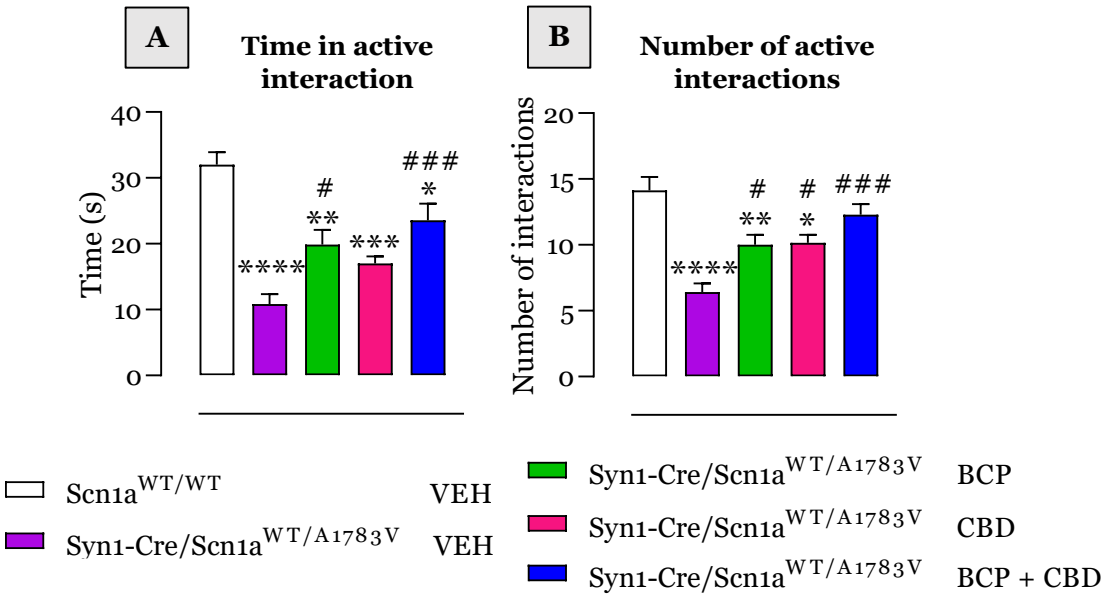

Figure R43. Effect of the combination of BCP and CBD on different parameters recorded in the social interaction test in DS mice. Measurement of different parameters in Syn1-Cre/ Scn1a$^{WT/A1783V}$ mice and their control group (Scn1a$^{WT/WT}$ mice) treated with BCP (10 mg/kg) and CBD (5 mg/kg), alone or in combination, including **(A)** time in active interaction and **(B)** number of active interactions. Values are means ± SEM of 6-12 animals per group. Data were assessed by one-way ANOVA followed by the Bonferroni test (*p<0.05, **p<0.01, ***p<0.005, ****p<0.001 vs. vehicle-treated Scn1a$^{WT/WT}$ mice; $^{\#}p$<0.05, $^{\#\#\#}p$<0.005 vs. vehicle-treated Syn1-Cre/Scn1a$^{WT/A1783V}$ mice).

Effect of a BCP and CBD combination on spatial working memory

In the same way that in previous experiments, Y-maze test was used to explore spatial working memory performance. Results indicated that vehicle-treated Syn1-Cre/Scn1a$^{WT/A1783V}$ mice exhibited a clear alteration in this task, with a marked increase in the total number of explored arms, which further corroborated their hyperactive behavior (Figure R44A), a lower spontaneous alternation (Figure R44B), as well as an increase in alternate arm returns (Figure R44C). However, no changes were detected when measuring the percentage of same arm returns, probably due to high variability in this parameter (FigureR44D). Overall, these results suggested working memory deficits in our DS mouse model, as already described in previous Chapters.

When administered alone, BCP and CBD were able to partially attenuate this abnormal performance. Noteworthy, their combination showed some additional positive effects (Figures R44A-C). In particular, enhanced effectiveness was detected when analysing the alternate arm returns, with the combined treatment exerting a clear additional improvement (Figure R44C).

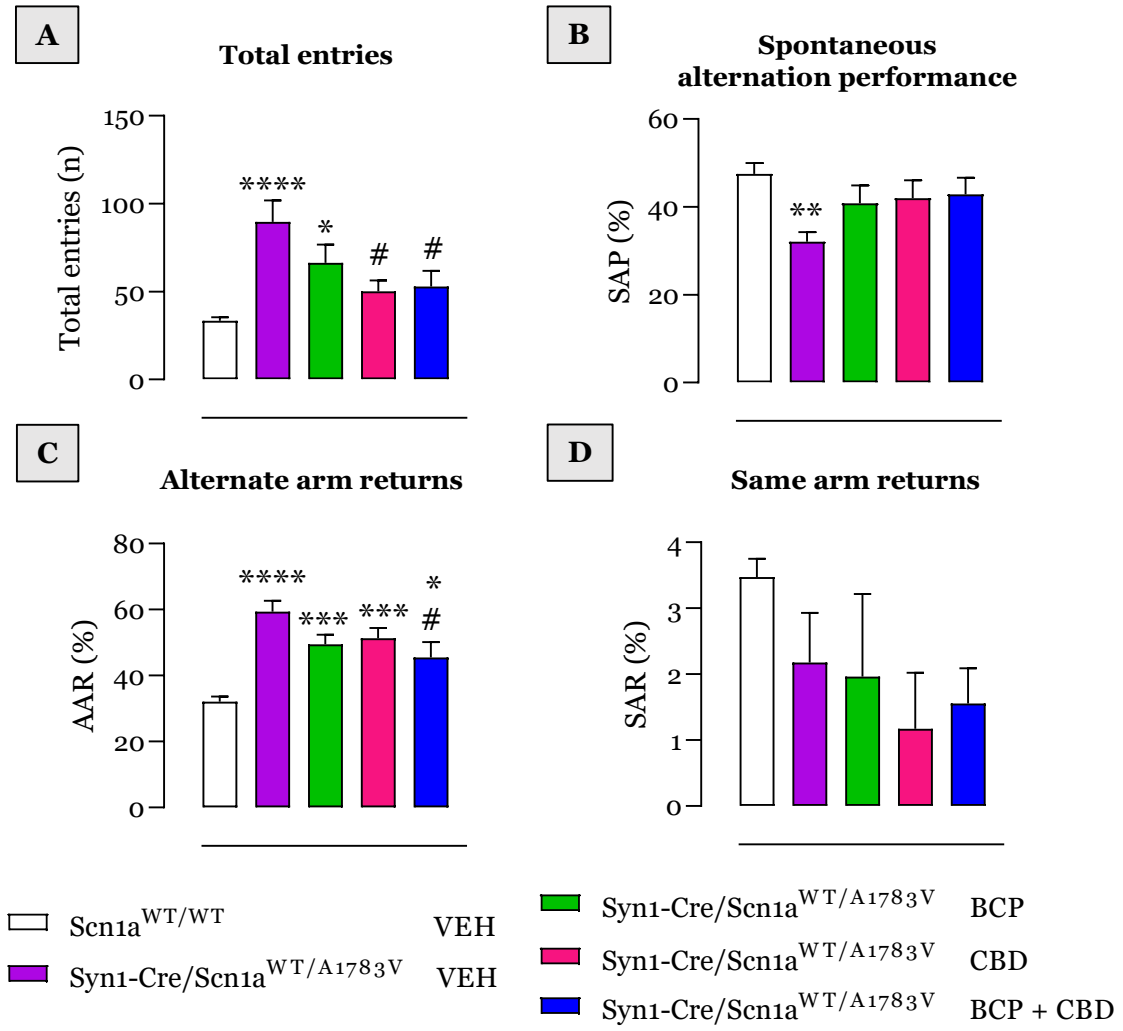

Figure R44. Effect of the combination of BCP and CBD on different parameters recorded in the Y-maze test in DS mice. Measurement of different parameters in the Y-maze test in Syn1-Cre/Scn1a$^{WT/A1783V}$ mice and their control group (Scn1a$^{WT/WT}$ mice) treated with BCP (10 mg/kg) and CBD (5 mg/kg), alone or in combination, including **(A)** number of total entries, **(B)** spontaneous alternation performance, **(C)** alternate arm returns and **(D)** same arm returns. Values are means ± SEM of 6-12 animals per group. Data were assessed by one-way ANOVA followed by the Bonferroni test (*p<0.05, ***p<0.05, ****p<0.001 vs. vehicle-treated Scn1a$^{WT/WT}$ mice; $^{\#}p$<0.05 vs. vehicle-treated Syn1-Cre/Scn1a$^{WT/A1783V}$ mice).

Effect of a BCP and CBD combination on glial reactivity and inflammation

As in the previous experiments, changes in glial reactivity by the treatments were also assessed. In accordance with previous findings, vehicle-treated Syn1-Cre/Scn1a$^{WT/A1783V}$ mice exhibited a prominent gliosis, involving both astrocytes and microglial cells. Thus, as shown by an increase in GFAP immunoreactivity, astrogliosis was evident in prefrontal cortex and the hippocampal dentate gyrus (Figure R45). Likewise, Iba-1 immunoreactivity analysis indicated that microgliosis was also markedly present in both CNS structures (Figure R46).

In agreement with behavioral data, when administered alone, BCP and CBD were able to significantly ameliorate gliosis. However, substantial differences were reported; while modest attenuations were exerted by CBD, BCP showed a more potent effect. Remarkably, mice treated with the combination of both compounds showed greater intense effects than mice treated with each compound alone, showing a significant mitigation of astrogliosis and microgliosis in both prefrontal cortex and hippocampal dentate gyrus (Figures R45,46).

To further investigate the effect of this combination on inflammation and oxidative stress, we measured the hippocampal gene expression of specific markers (Figure R47). In agreement with Chapter 1, vehicle-treated Syn1-Cre/Scn1a$^{WT/A1783V}$ mice showed a trend towards an upregulation in CB_2 receptor (p=0.0617) as well as a significant increase in TNFα. Pharmacological treatment with BCP and CBD, alone or in combination, was able to partially attenuate these changes, with the combination of both compounds showing a statistically significant effect in the case of TNFα (Figures R47A,E). In addition, we also reported increased levels of iNOS (p=0.0782) and COX-2, thus confirming the contribution of oxidative stress and inflammation to the pathogenesis of this DS mouse model. Both single and combined administration of BCP and CBD was able to partially ameliorate these increased levels, with BCP showing a marked effect for COX-2 (Figures R47D,F). Moreover, gene expression of PPARγ, IL1β and Arg1 was also measured, but no significant differences were observed among any experimental group (Figures R47B,C,G).

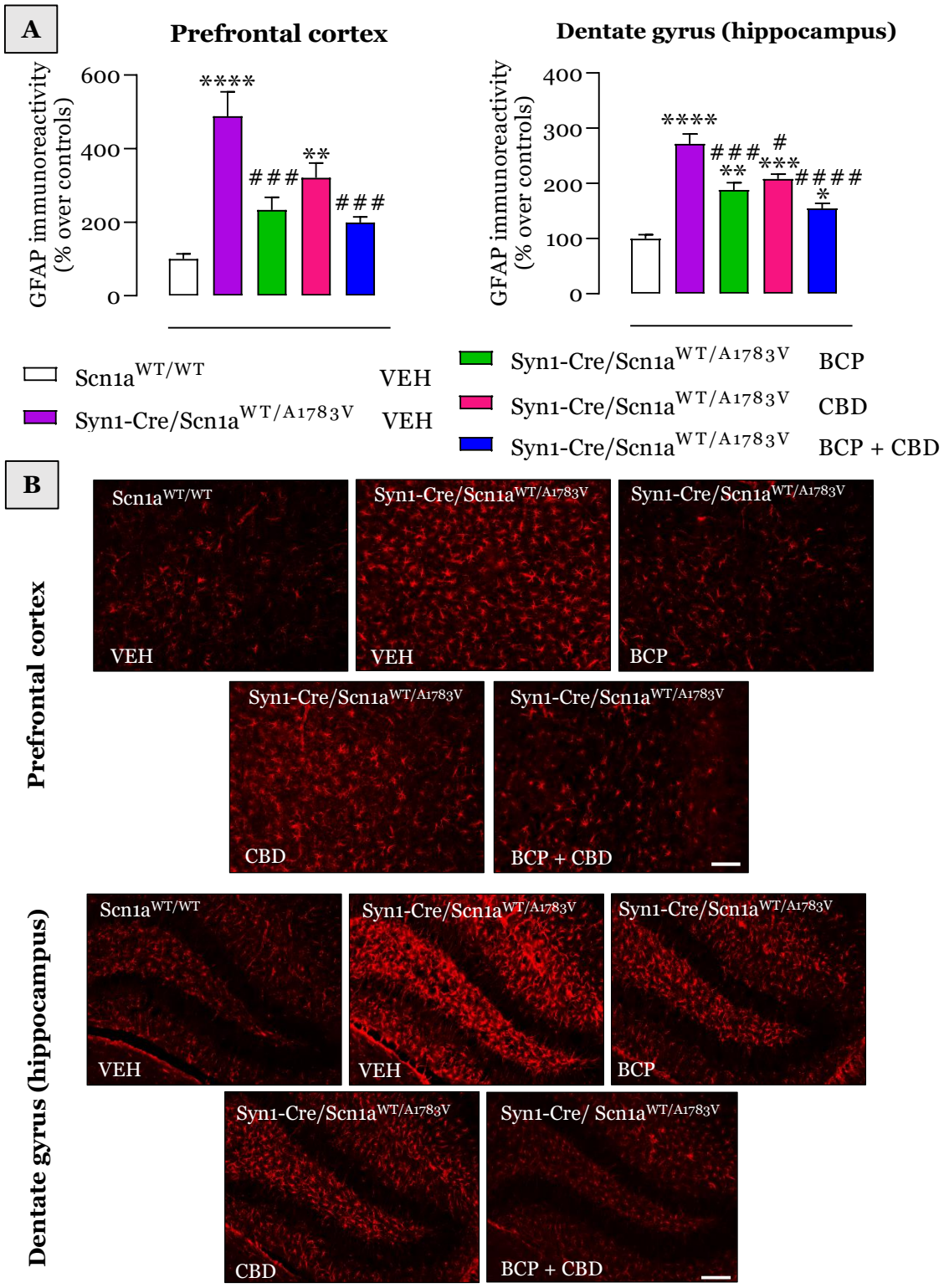

Figure R45. Effect of the combination of BCP and CBD on the astroglial marker GFAP in DS mice. **(A)** Quantification of Iba-1 immunoreactivity in the prefrontal cortex and hippocampal dentate gyrus of Syn1-Cre/Scn1a$^{WT/A1783V}$ mice and their control group (Scn1a$^{WT/WT}$ mice) treated with BCP (10 mg/kg) and CBD (5 mg/kg), alone or in combination. Panel **(B)** shows representative images of the immunofluorescence staining. Values are means ± SEM of 6-7 animals per group. Data were assessed by one-way ANOVA followed by the Bonferroni test. (*p<0.05, **p<0.01 ***p<0.05, ****p<0.001 vs. vehicle-treated Scn1a$^{WT/WT}$ mice; $^{\#}p$<0.05, $^{\#\#\#}p$<0.005 $^{\#\#\#\#}p$<0.001 vs. vehicle-treated Syn1-Cre/Scn1a$^{WT/A1783V}$ mice). Scale bar = 50 µm.

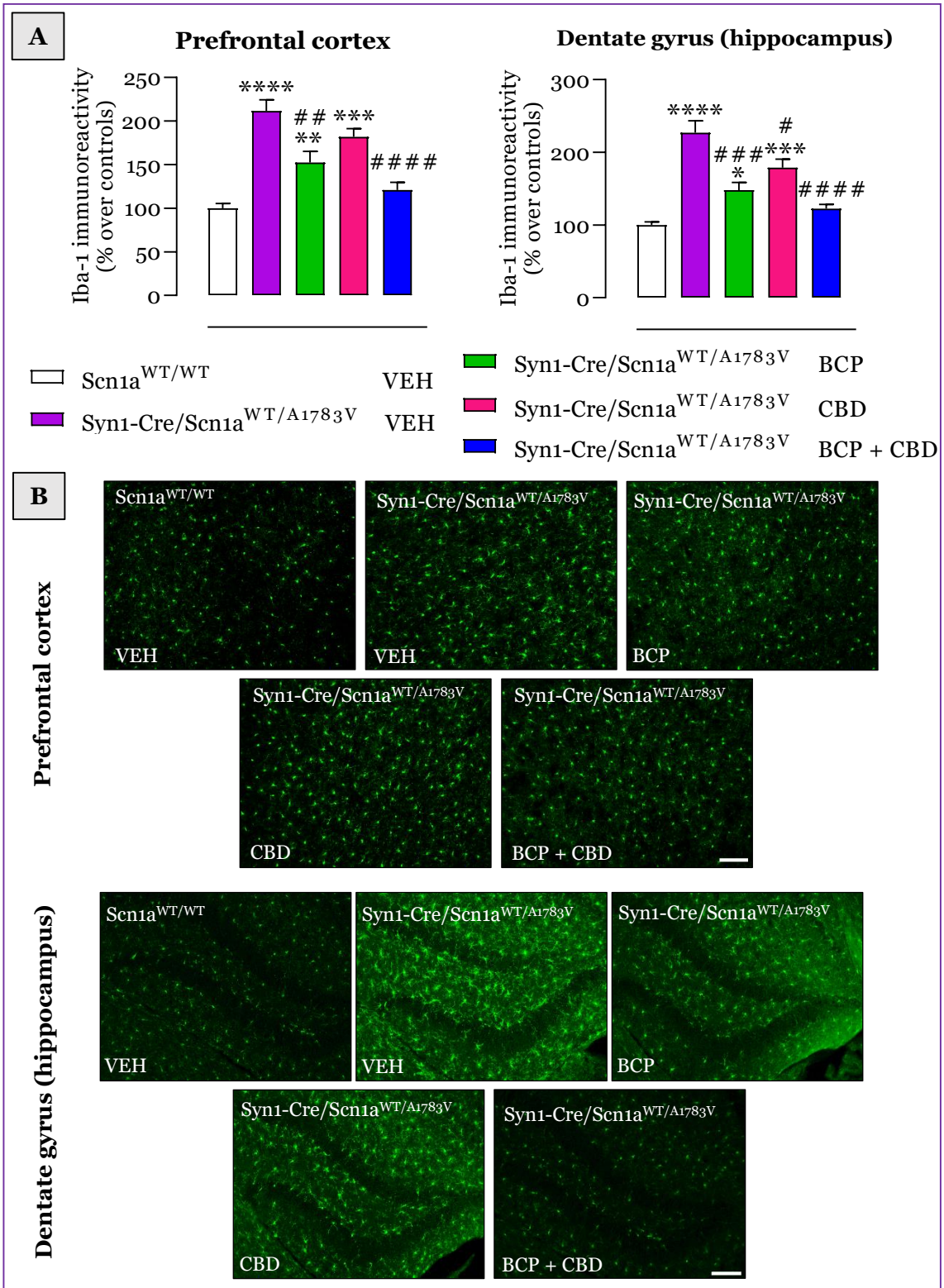

Figure R46. Effect of the combination of BCP and CBD on the microglial marker Iba-1 in DS mice. (A) Quantification of Iba-1 immunoreactivity in the prefrontal cortex and hippocampal dentate gyrus of Syn1-Cre/Scn1a$^{WT/A1783V}$ mice and their control group (Scn1a$^{WT/WT}$ mice) treated with BCP (10 mg/kg) and CBD (5 mg/kg), alone or in combination. Panel **(B)** shows representative images of the immunofluorescence staining. Values are means ± SEM of 6-7 animals per group. Data were assessed by one-way ANOVA followed by the Bonferroni test. (*p<0.05, **p<0.01, ***p<0.05, ****p<0.001 vs. vehicle-treated Scn1a$^{WT/WT}$ mice; #p<0.05, ##p<0.01, ###p<0.005, ####p<0.001 vs. vehicle-treated Syn1-Cre/Scn1a$^{WT/A1783V}$ mice). Scale bar = 50 µm.

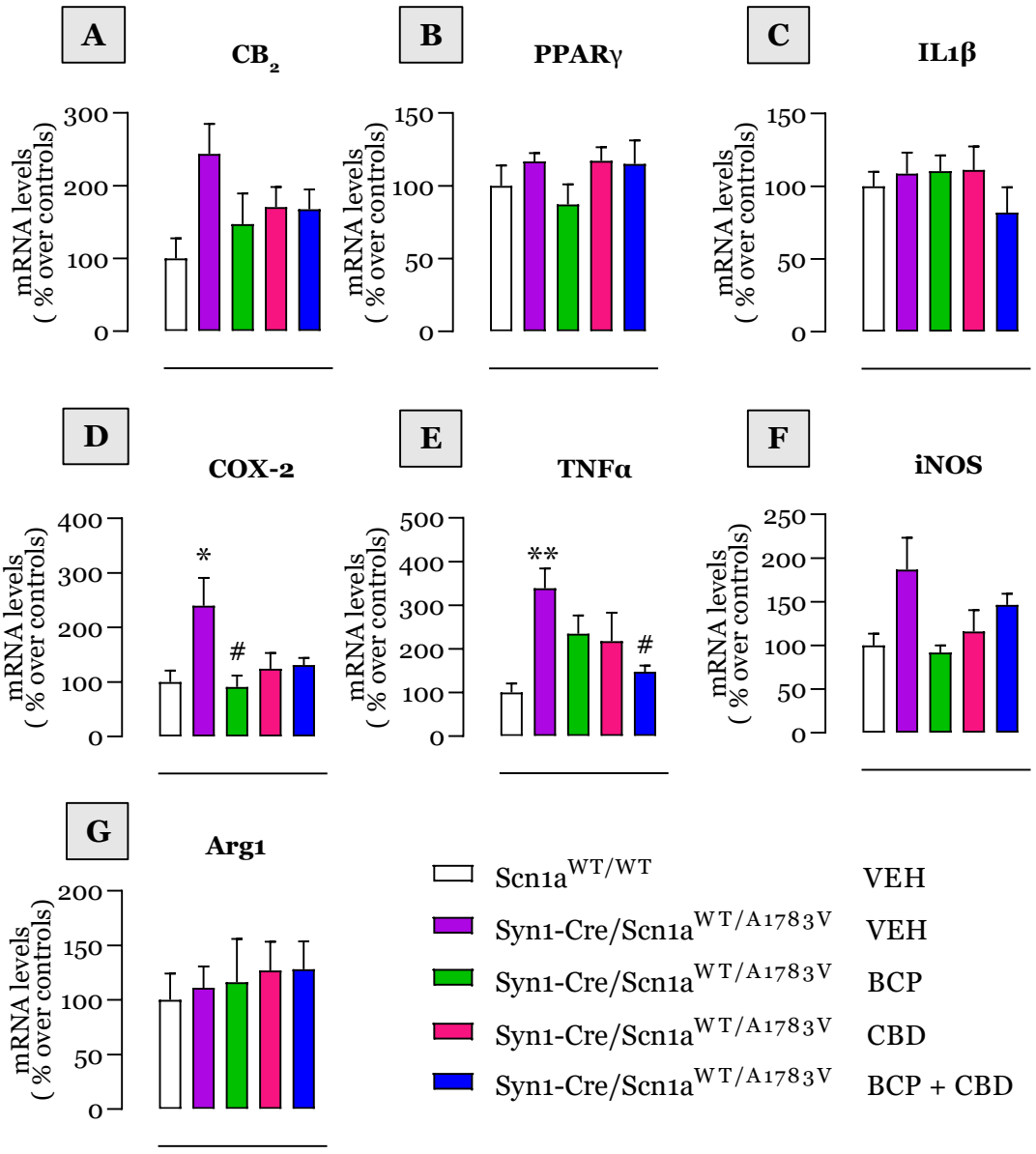

Figure R47. Effect of the combination of BCP and CBD on the gene expression of different inflammatory and oxidative stress markers in DS mice. Measurement by qPCR of the gene expression of different inflammatory markers in the hippocampus of DS mice, including **(A)** CB_2 receptor, **(B)** PPARγ receptor, **(C)** IL1β, **(D)** COX-2, **(E)** TNFα, **(F)** iNOS and **(G)** Arg1. Values are the mean ± SEM of 5-6 animals per group. Data were assessed by using one-way ANOVA followed by the Bonferroni test (*$p<0.05$, **$p<0.01$ vs. vehicle-treated $Scn1a^{WT/A1783V}$ mice; #$p<0.05$ vs. vehicle-treated Syn1-Cre/ $Scn1a^{WT/A1783V}$ mice).

Summary

Taken together, both *in vitro* and *in vivo* experiments performed in Chapter 3 revealed that the combined treatment of BCP and CBD might be a promising therapeutic strategy for the treatment of DS. In terms of efficacy, although BCP and CBD alone exerted positive effects, more potent responses were, in general, observed when combined. Interestingly, the same trend was observed in almost all the experimental procedures

performed. While CBD showed modest effects, BCP demonstrated more robust ones; however, the best improvements were observed when combined.

Specifically, i*n vitro* analysis in LPS-exposed BV2 cells indicated that BCP and CBD combination effectively reduced mRNA and protein levels of different inflammatory markers, as well as suppressing LPS-induced microglial activation. *In vivo* testing in our DS mouse model showed that this combined treatment was effective not only against long-term behavioral disturbances, but also in ameliorating glial reactivity, which are two key aspects in the pathogenesis of these mice.

Therefore, all these findings provided an experimental basis for the further examination of a combined cannabis-based treatment with an anti-inflammatory profile as a therapeutic agent in DS.

DISCUSSION

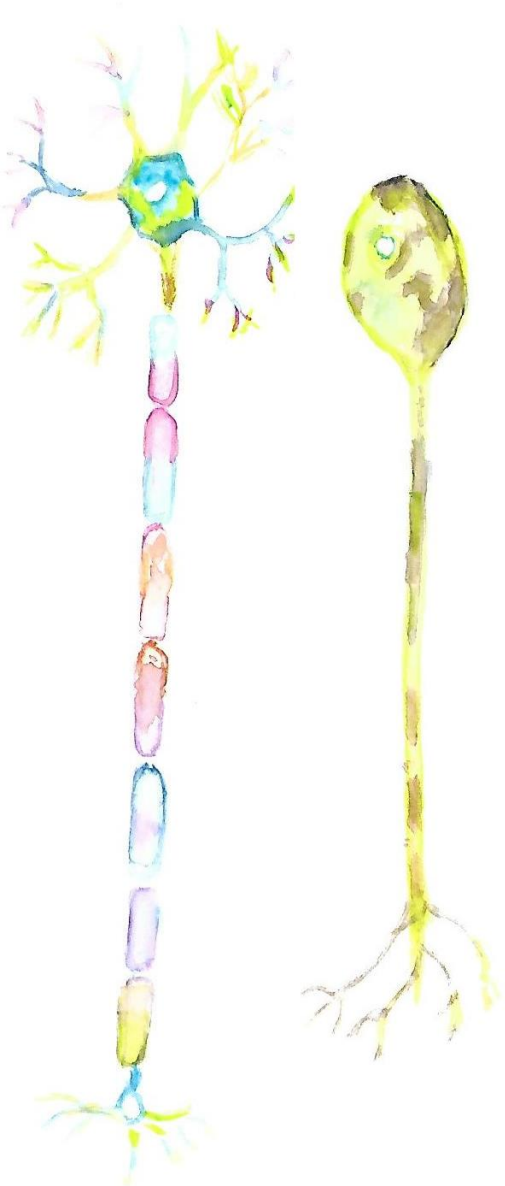

Epilepsy affects around 1% of children worldwide, thus making it one of the most common neurological conditions in childhood (Thurman *et al.*, 2011). About one-third of these children remain refractory to treatment, which means that they do not achieve seizure freedom despite adequate trials of at least two antiepileptic drugs at therapeutic dosages (Dale *et al.*, 2019). Moreover, unremitting epileptic activity during childhood usually triggers a progressive cerebral dysfunction, leading to a condition known as epileptic encephalopathy (Berg *et al.*, 2010). In this context, DS is considered one of the most devastating forms of pediatric epileptic encephalopathy, which is characterized by a wide and complex repertoire of clinical manifestations, including epileptic seizures, behavioral comorbidities and a relatively high rate of premature death. Although seizures tend to decrease both in frequency and severity with age, DS persists throughout adulthood, thus leading to a devastating long-term outcome (Dravet & Oguni, 2013; Gataullina & Dulac, 2017, Genton *et al.*, 2011).

Given that available antiepileptic drugs for DS, as well as other forms of epilepsy, mostly control seizures but not other pathological mechanisms, the burden of behavioral and cognitive comorbidities often remains uncontrolled (Wirrell *et al.*, 2017). To improve patient quality of life, novel therapeutic approaches should extend beyond the direct correction of the imbalance between excitation and inhibition typically occurring in epilepsy, and focus on addressing the major prolonged pathogenic mechanisms associated with epilepsy progression: inflammation, oxidative stress and excitotoxicity (Box 2). In this regard, some cannabinoids have shown beneficial effects against these processes, so they may represent a promising therapeutic strategy not only for seizures, but also for associated comorbidities and long-term outcome (Ambrogini *et al.*, 2019).

Based on this background, one of the main purposes in this Doctoral Thesis has been to develop and characterize a new DS mouse model that faithfully recapitulated disease progression, as well as with high survival rates to enable long-term studies (differently from the majority of mouse models used to date). Once validated, we studied alterations of potential targets (such as ECS elements or inflammatory mechanisms) that may justify pharmacological strategies with cannabinoids. Finally, and considering translating research into clinical practice, we performed pharmacological studies with cannabinoid compounds as possible disease-modifying therapies, with the final purpose of obtaining data that may help to improve the therapeutic management of DS patients.

Validation of *Scn1a*-A1783V mice as a good experimental model for DS

A limited translational impact of basic research is one of the major issues in the clinical practice. Therefore, developing good experimental models that faithfully recapitulate pathological hallmarks and disease progression is a great challenge within biomedical research.

Regarding DS preclinical research, several mouse models have been generated to date (Table I2) and have enabled a better understanding of DS pathogenesis. However, constitutive models based on both homozygous (Ogiwara *et al.*, 2007; Tsai *et al.*, 2015) or heterozygous (Miller *et al.*, 2014; Tsai *et al.*, 2015; Yu *et al.*, 2006) deletion mutations gave rise to aggressive phenotypes and high mortality rates, and consequently breeding and shipping problems. Some of these groups also published the generation of conditional models to prove that the specific deletion of the channel from interneurons was enough to reproduce the phenotype of constitutive models but with less severity (Cheah *et al.*, 2012; Dutton *et al.*, 2013; Ogiwara *et al.*, 2013). However, access to these conditional models has not been granted to any external group. Therefore, it seems clear that aggressive phenotypes with high mortality rates, as well as the generalized lack of open-access to these models, greatly limit DS research.

To overcome these difficulties, a novel DS mouse model has been recently generated by the Dravet Syndrome Foundation Spain and is currently available through the Jackson Laboratory repository. It is a heterozygous conditional knock-in mouse expressing the *Scn1a*-A1783V missense mutation upon Cre-driven recombination. Already published studies using these mice have shown that models with a widespread mutation (expression under CMV promoter) exhibit a profound mortality rate ranging from 50-60% (Almog *et al.*, 2021; Fadila *et al.*, 2020) to 75% (Ricobaraza *et al.*, 2019), and even an extreme 100% mortality when the mutation is expressed exclusively in GABAergic neurons under the *Slc32a1* promoter (Kuo *et al.*, 2019). For the purpose of this Doctoral Thesis, we selected a Cre recombinase under the control of synapsin 1 promoter, so that breeding pairs gave rise to mice expressing the *Scn1a*-A1783V mutation only in CNS neurons. Our DS mice exhibited a remarkably lower mortality rate, around 25%, which has enabled us to perform a long-term characterization focused on behavioral and cognitive alterations, as well as pharmacological studies aimed at evaluating the disease-modifying effects of cannabinoid compounds on DS-associated comorbidities. It is important to remark that those experiments requiring daily handling of mice slightly increased mortality, probably due to the higher vulnerability of DS mice, although this rate was still lower than in the other models. Interestingly, both in our model and in the

rest, the majority of deaths occur within a small window (PND21-24), correlating with sudden death typically occurring in DS patients during the worsening stage (Figure I1) (Skluzacek *et al.*, 2011).

We commonly observed that beginning around PND17 and continuing until approximately PND23, DS mice showed spontaneous seizures during animal handling, which correlates with the marked presence of epileptic activity at early ages both in DS patients (Dravet & Oguni, 2013; Gataullina & Dulac, 2017, Genton *et al.*, 2011) and other DS animal models, including those using these conditional *Scn1a*-A1783V mice (Almog *et al.*, 2021; Fadila *et al.*, 2020; Kuo *et al.*, 2019; Ricobaraza *et al.*, 2019) as well as others previously generated (Ogiwara *et al.*, 2007; Tsai *et al.*, 2015). Since we did not have access to EEG recording systems, we were not able to measure and specifically quantify this spontaneous seizure activity in our DS mice. However, we indirectly quantified seizure susceptibility to the proconvulsant agent PTZ, which is an accepted biomarker of epilepsy (Barker-Haliski *et al.*, 2016; Brandt *et al.*, 2015). These measurements revealed that the seizuring response was markedly more prominent in DS mice.

In addition, DS mice showed a marked absence in the appearance of hindlimb grasp reflex at PND10, suggesting a delayed motor development from very early ages, as occurs in patients (Verheyen *et al.*, 2019). Moreover, hyperactivity and stereotypies were evident at PND25 but disappeared at later stages, which correlates with the hyperactive behavior notably observed in DS patients during childhood but less prominently during juvenile and adult ages (Berkvens *et al.*, 2015; Gataullina & Dulac, 2017). Additionally, DS mice exhibited some cognitive and emotional features, such as a subtle short-term spatial memory impairment and apparently less anxiety, which were again more prominent at PND25. Contrary, autistic-like behaviors were observed at all the evaluated ages, which is in agreement with the persistence of autism spectrum disorders in adult patients with DS (Berkvens *et al.*, 2015). Of note, all these observations are in agreement with the main clinical features of DS patients (Dravet & Oguni, 2013; Gataullina & Dulac, 2017; Genton *et al.*, 2011). In fact, as mentioned in the Introduction, behavioral comorbidities in DS patients are particularly relevant in the worsening stage (although some alterations, such as social deficits, persist during adulthood) which correlates with our results obtained at PND25. Other publications using conditional *Scn1a*-A1783V mice, but with a generalized expression of the mutation, have also reported similar behavioral findings (Fadila *et al.*, 2020; Ricobaraza *et al.*, 2019), which confers reproducibility and robustness to this model. However, our lower mortality has enabled us to detect alterations at later ages, which supports the suitability of this model for long-term studies.

Therefore, we have generated a DS mouse model that recapitulates key phenotypic aspects of the disorder, including epileptic activity, behavioral comorbidities and premature death, thus resembling what occurs in DS patients. Given that PND25 was the age at which behavioral disturbances were particularly prominent, we focused our subsequent studies on this age in order to explore possible neuropathological alterations that could contribute to DS pathophysiology.

As mentioned in the Introduction, five randomized controlled clinical trials have recently demonstrated that the non-psychotropic cannabinoid CBD exerts anticonvulsant effects in DS and other infantile epileptic syndromes (Devinsky *et al.*, 2017, 2018; Miller *et al.*, 2020; Thiele *et al.*, 2018, 2019). Based on these positive results, an oral solution of CBD is currently used (under the trade name of Epidyolex®) as an adjunctive therapy for seizures in children with DS, LGS and TSC. Little is known regarding the mechanisms of action underlying this anticonvulsant effect, but cannabinoids could exert their beneficial effects in drug-resistant epilepsies by directly or indirectly correcting alterations in the ECS, as it has been shown to occur in other neurological disorders (Cristino *et al.*, 2020). In this sense, the evaluation of the ECS status in different CNS structures of our DS mice revealed some alterations within this system.

We have demonstrated that there is a significant decrease in CB_1 receptor in the hippocampus and the cerebellum of DS mice. As already mentioned, CB_1 activation can mediate proconvulsant or anticonvulsant responses depending on whether it is expressed in inhibitory or excitatory presynaptic terminals, respectively (Marsicano *et al.*, 2003, Figure I15). In experimental models of epilepsy, acute seizures have been shown to induce a homeostatic redistribution of CB_1 receptor expression in the short-term, with upregulations in excitatory terminals and downregulations in inhibitory terminals, thus reducing network excitability (Falenski *et al.*, 2007, 2009). Conversely, in situations of prolonged and pharmacoresistant epilepsy, CB_1 receptor homeostasis has proven to be disrupted, with reduced levels in excitatory terminals and increased levels in inhibitory terminals, which triggers a long-term tendency towards neuronal hyperexcitability (Ludányi *et al.*, 2008; Soltesz *et al.*, 2015). Regarding our data, further research is needed in order to evaluate the specific cell type affected by this downregulation in our DS mice, since it could involve different responses.

Although little is known regarding GPR55 role in epilepsy, CBD has been shown to exert anticonvulsant effects in DS mice by antagonism of this receptor (Kaplan *et al.*, 2017). According to this study, blockade of GPR55 receptor results in an enhancement of inhibitory transmission, thus contributing to correcting the imbalance between the inhibition and excitation typically occurring in epilepsy. In our DS model, there is a trend towards a decreased GPR55 expression in striatum, hippocampus and cerebellum, which could represent a compensatory response aimed at enhancing inhibitory signalling.

Another protective mechanism that could partially explain the anticonvulsant properties of CBD involves the enhancement of the endocannabinoid tone by inhibition of the FAAH enzyme (De Petrocellis *et al.*, 2011). Although we have not specifically measured brain endocannabinoid levels in our DS mice, we have evaluated the expression of those enzymes responsible for anandamide and 2-AG degradation, which could be considered as an indirect measurement of the endocannabinoid tone. In this sense, reduction of FAAH expression in the hippocampus and cerebellum, but particularly the significant reduction of MAGL expression in prefrontal cortex and cerebellum, may be compatible with a possible elevation of the endocannabinoid tone, especially for 2-AG. Since 2-AG is the main endogenous ligand of CB_1 receptors, this elevation may be compatible with an acute protective response in situations of brain hyperexcitability (De Petrocellis *et al.*, 2011; Ludányi *et al.*, 2008). Additionally, blockade of endocannabinoid inactivating enzymes in several preclinical models of epilepsy has been demonstrated to be an effective strategy against brain hyperexcitability (Karanian *et al.*, 2007; Naidoo *et al.*, 2011, 2012; von Rüden *et al.*, 2015). This protective response has been also observed in other situations of brain damage, including chronic neurodegenerative disorders (Xu & Chen, 2015) and brain trauma (Panikashvili *et al.*, 2001).

The majority of preclinical research demonstrating the beneficial effects of cannabinoids in epilepsy refers to the ability of some cannabinoid compounds to activate CB_1 receptors (Rosenberg *et al.*, 2017); however, little is known regarding the role that CB_2 receptors may play in the context of epilepsy. In this sense, the upregulation of CB_2 receptor in the hippocampus of our DS model was a remarkable finding that was in agreement with a previous study in which we demonstrated that CB_2 receptor is also upregulated in lymphocytes of DS patients, together with an increase in other inflammatory elements, including proinflammatory cytokines, PPARγ receptor and the lymphocyte activation marker Cd70 (Rubio *et al.*, 2016). This upregulation has been also found in microglia/macrophages in *postmortem* brains of intractable epilepsy patients (Zurolo *et al.*, 2010), as well as in many neurodegenerative diseases typically associated with inflammatory responses (Fernández-Ruiz *et al.*, 2007). In parallel, loss of CB_2 receptor

activity has been shown to increase seizure susceptibility in mice (Shapiro *et al.*, 2019), and administration of both positive allosteric modulators (Shapiro *et al.*, 2021) as well as full agonists (de Oliveira *et al.*, 2016; Liu *et al.*, 2015; Tchekalarova *et al.*, 2018) has shown to exert anticonvulsant effects, which suggest that activation of this receptor may also play a protective effect on seizures. Overall, we suggest that CB_2 receptor upregulation may be an endogenous protective response aimed at attenuating inflammatory responses typically occurring in DS and other forms of epilepsy, as it occurs in other neurological disorders (Fernández-Ruiz, 2019).

With this idea in mind, we further explored the possible existence of events related to inflammation in our DS model, since there is a large body of evidence supporting the link between epilepsy and brain inflammation (Dupuis & Auvin, 2015). Most studies have focused on acquired forms of epilepsies, where brain inflammation caused by viral infections, autoimmune diseases, head trauma and other nongenetic causes can trigger seizures (Aronica *et al.*, 2017). However, little is known regarding those epilepsy forms in which neuroinflammation may be a consequence of seizures, as it is believed to occur in genetic epilepsies such as DS. To our knowledge, very few studies have looked at the role of inflammation in DS, but recently, as it has been already explained, our laboratory has published an article in which we observed an increase in inflammatory markers in lymphocytes of DS patients (Rubio *et al.*, 2016).

In line with previous reports in other DS mouse models (Hawkins *et al.*, 2019; Martín-Suárez et *al.*, 2020; Shen *et al.*, 2020), we have reported the existence of prominent events of reactive astrogliosis and microgliosis in the prefrontal cortex and the hippocampal dentate gyrus in our DS mice. These reactive glial cells can contribute to hyperexcitability and have been described to release pro-inflammatory cytokines and mediators that initiate a cascade of inflammatory responses, which ultimately exert a proconvulsant action (Aronica & Crino, 2011; Vezzani & Granata, 2005; Vezzani *et al.*, 2008). In agreement with this evidence, reactive gliosis was also associated with a strong tendency towards elevated mRNA levels of TNFα in the hippocampus of our DS mice. These local neuroinflammatory events within specific CNS structures, concurrently with seizures, may induce a decrease in the seizure threshold and contribute to the development of some of the behavioral comorbidities of our DS mice. Moreover, it is important to remark that the upregulation of CB_2 receptor in the hippocampus could be associated with the existence of gliosis, since this receptor has been shown to be primarily expressed in these cells (Fernández-Ruiz *et al.*, 2007), which further positions this receptor as a promising therapeutic target in this disorder.

Glia-derived brain inflammation, concurrently with seizures, has been described to affect the permeability properties of the BBB, which in turn may aggravate epilepsy development (Librizzi *et al.*, 2012; Vezzani *et al.*, 2011). We evaluated BBB integrity in our DS mouse model and observed a loss in the tight junction molecules ZO-1 and claudin-5 in the hippocampus, and to a lesser extent in laminin, a basement membrane protein, thus suggesting the existence of BBB leakage in DS mice. This BBB disruption was accompanied by the extravasation of blood-circulating IgG into the hippocampus, accordingly with the well-established blood-to-brain extravasation of serum proteins in situations of BBB compromise (Kassner & Merali, 2015). These findings are in agreement with the hippocampal reactive gliosis and the increased levels of TNFα observed in our DS mice, suggesting that brain inflammation and BBB breakdown are very closely linked in an epileptic context as DS.

In addition, BBB breakdown has been associated with the infiltration of peripheral immune cells into the brain parenchyma under neuroinflammatory conditions in some epilepsy contexts, which may facilitate the activation of brain endogenous glial cells and aggravate brain inflammation and BBB damage (Yamanaka *et al.*, 2021). In fact, seizure activity can promote the mobilization of these peripheral immune cells from the BM and force them out to circulate into the systemic blood, which might facilitate their infiltration into the brain tissue (Marchi *et al.*, 2012). Flow cytometry studies in our DS mice reported a remarkable mobilization of neutrophils, with a decreased number in BM and a parallel increase in circulating blood. However, immunofluorescence analysis revealed that these cells did not finally cross into the brain parenchyma. In agreement with this absence of infiltration, it is not surprising that ICAM-1 levels remain unchanged in our DS mice, since it is an endothelial signalling molecule that facilitates the adhesion and migration of immune cells through the endothelium and subsequent crossing into the CNS (Carman & Martinelly, 2015). In contrast, marked BBB damage and robust infiltrates have been reported in other forms of acute epilepsy, especially temporal lobe epilepsy (Broekaart *et al.*, 2018; Liu *et al.*, 2016; Zattoni *et al.*, 2011). BBB disruption in our DS mice is not severe enough to induce the recruitment of peripheral immune cells, but the observed loss of endothelial tight junctions suggests that BBB alteration in our DS mice is subtle and sufficient to promote extravasation of serum components that aggravate reactive gliosis and consequently increase seizure susceptibility, thus establishing a vicious pathological cycle that is similarly found in neurodegenerative disorders with a chronic and progressive development (Takechi *et al.*, 2010), even during normal aging (Elahy *et al.*, 2015).

Another mechanism by which local neuroinflammatory events may contribute to increase seizure susceptibility and aggravate comorbidities is via seizure-induced aberrant hippocampal neurogenesis (Bielefeld *et al.*, 2019; Chen *et al.*, 2020). Our data are consistent with previous studies reporting an initial increase in the rate of hippocampal neurogenesis after epileptic seizures (Muro-García *et al.*, 2019; Sierra *et al.*, 2015), and accordingly, our DS mice present an elevated cell proliferation of NSCs. Although it was not precisely quantified, these cells are apparently multibranched and present basal prolongations, which is in agreement with their transformation into reactive-NSCs that has been observed in other models of DS (Martín-Suárez *et al.*, 2020) and experimental epilepsy (Muro-García *et al.*, 2019; Sierra *et al.*, 2015). These reactive-NSCs can further differentiate into reactive astrocytes, thus contributing to astrogliosis (Sierra *et al.*, 2015). Of note, data in our DS mice were obtained at PND25, when phenotypic alterations and seizure-activity are maximal, in agreement with the upregulation of the rate of neurogenesis in juvenile stages. However, it would be of great interest to further investigate this process at later ages, since it has been described that after an initial burst of neurogenesis, a long-lasting decline is induced due to NSCs population depletion, thus triggering cognitive deficits associated with an abnormal hippocampal function (Hattiangady *et al.*, 2014; Kralic *et al.*, 2005; Sierra *et al.*, 2015), which could partially explain the behavioral disturbances observed in DS mice at later ages. This NSCs "exhaustion" is tightly associated with long-term inflammation, which has been demonstrated to reduce neurogenesis and promote astroglial differentiation (Zonis *et al.*, 2013).

Overall, it seems clear that an aberrant neurogenic response, together with neuroinflammation and a subtle BBB disruption, may act synergistically and contribute to disease severity and progression, thus establishing a vicious pathological cycle by which seizure susceptibility is increased, which could be potentially responsible, at least in part, for cognitive and memory dysfunctions (Figure D1). In this context, the upregulation of CB_2 receptor may be aimed at counteracting these inflammation-related events, as occurs in other neurological disorders (Fernández-Ruiz, 2019), again supporting the suitability of targeting this receptor as a therapeutic target for DS, and without triggering psychotropic effects associated with CB_1 receptor activation.

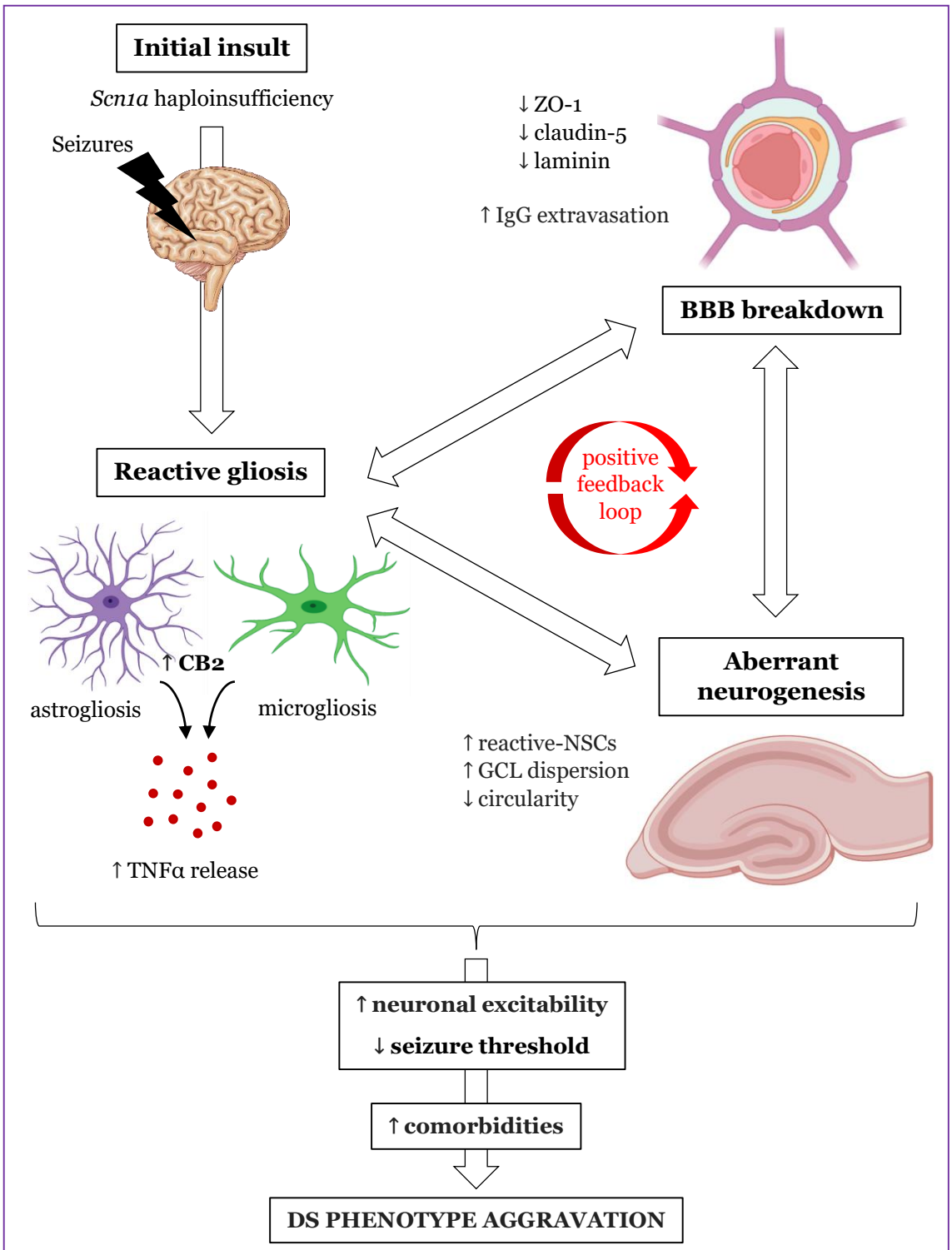

Figure D1. Schematic representation of the proposed neuropathological aspects contributing to DS phenotype. Representation of the cascade of events occurring within the hippocamps and that may be triggered by initial seizures. Neuroinflammation, BBB breakdown and aberrant neurogenesis act synergistically to contribute to DS progression.

Therapeutic potential of cannabinoids for the treatment of DS

Currently available treatments for DS involve antiepileptic drugs that are merely focused on neuronal excitability and seizure control (Wirrell *et al.*, 2017). However, not only neurons, but also glial cells, may play a key role in DS pathogenesis. In addition to hyperexcitability, inflammation and oxidative stress could be targetable hallmarks, thus suggesting that compounds modulating these processes may improve the long-term outcome of the disorder. In this context, cannabinoids have proven to be effective in a wide variety of experimental situations characterized by these neuropathological events (Fernández-Ruiz, 2019). Moreover, our results have revealed that CB_2 receptor could play a key role in this disorder, so that cannabinoids modulating this receptor may represent a promising therapeutic strategy. Importantly, CB_2 receptor is devoid of the psychotropic adverse effects associated with CB_1 receptor stimulation, thus making it a suitable pharmacological target for infantile or adolescence population (when the brain is still undergoing rapid development and change and is particularly sensitive to any effects), as it is the case for DS (Sagredo *et al.*, 2018). However, it is important to remark that some CB_2-selective ligands could trigger immunosuppression as an adverse effect (Basu & Dittel, 2011; Lombard *et al.*, 2007); therefore, this issue should be carefully addressed before considering human application.

In addition to CBD, several preclinical studies have suggested that other components of *C. sativa* could also exert beneficial effects against seizures and associated pathological mechanisms (Rosenberg *et al.*, 2017). Taking into account these considerations, we assessed whether the non-psychotropic cannabis constituent BCP, which has been described as a full agonist of CB_2 receptors (Gertsch *et al.*, 2008), meets this pharmacological profile. Interestingly, we have reported for the first time that BCP is an effective therapeutic strategy for DS treatment, since our results revealed that it is able to alleviate not only seizure activity in our DS mice, but also associated glial reactivity and behavioral disturbances.

To the best of our knowledge, only three studies have previously investigated the anticonvulsant effect of this molecule; in these studies, BCP showed positive effects against both seizure activity and seizure-induced neuroinflammation, oxidative stress and behavioral alterations (de Oliveira *et al.*, 2016; Liu *et al.*, 2015; Tchekalarova *et al.*, 2018). In accordance with these previous studies, an acute dose of BCP (100 mg/kg) showed efficacy against PTZ-induced seizures. However, it is important to remark that this efficacy was much greater in DS mice if compared with controls, since BCP was

capable of attenuating parameters related to a more aggressive seizure-like behavior (such as the time spent in generalized seizures) only in DS mice.

Beneficial effects of the chronically administered BCP dose (10 mg/kg) became apparent from very early stages of development, with great improvements regarding hindlimb grasping and clasping disturbances. Moreover, BCP was also able to reduce locomotor activity and hyperactive behavior in DS mice, in accordance with previous reports (Ogawa *et al.*, 2016). The benefits of the long-term treatment with BCP were not only restricted to motor impairment, but also involved weight gain and improvements in cognition. In this sense, Y-maze and T-maze tests revealed that BCP was able to decrease spatial working memory impairment, as it has been previously shown (Lindsey *et al.*, 2019; Youssef *et al.*, 2019); moreover, more complex cognition tasks (such as the Morris water maze test) have also revealed this capability (Kanojia *et al.*, 2021; Tchekalarova *et al.*, 2018), thus further confirming the capacity of BCP to improve cognitive performance. BCP also demonstrated positive results in the social interaction test; although it is the first time that BCP is demonstrated to be effective in attenuating autistic-like behaviors, it had been already reported to exert beneficial effects in other emotional aspects, such as anxiety or depression (Bahi *et al.*, 2014; Youssef *et al.*, 2019). Perhaps, one of the most striking results was its effects on mortality; although BCP exerted a slight decrease in the mortality rate, it was remarkably capable of delaying the age at death, which undoubtedly has a great translational value. Altogether, this experiment revealed that this molecule is capable of attenuating most of the phenotypic characteristics of the disease progression in our DS mouse model.

A curious aspect is that a high dose of BCP (100 mg/kg) is required to protect against seizures, whereas a much lower dose (10 mg/kg) is enough to improve behavioral disturbances. Although we did not perform *in vivo* dose-response curves, these dosages were defined according to previous studies using BCP (de Oliveira *et al.*, 2016; Hernández-León *et al.*, 2020; Viveros-Paredes *et al.*, 2017). This discrepancy between a high dose required for seizure protection and a lower dose necessary for the improved behavioral outcome is similarly found in studies using CBD (Kaplan *et al.*, 2017) or clonazepam (Han *et al.*, 2012, 2014) in other DS mouse models. This fact could represent a conundrum for defining an appropriate pharmacological approach that both attenuates seizures and long-term outcome. However, in the case of BCP, this issue would be less relevant, since safety of BCP at high doses is well-demonstrated (Sharma *et al.*, 2016). Nevertheless, it should be carefully considered, since different doses could involve different mechanisms of action.

Importantly, in both acute and chronic paradigms, BCP has been shown to attenuate reactive gliosis in our DS mice. This ability of BCP to reduce astroglial and microglial activation has been also reported in experimental models of different CNS conditions, such as normal aging (Chávez-Hurtado *et al.*, 2020), Alzheimer's disease (Cheng *et al.*, 2014), Parkinson's disease (Javed *et al.*, 2016; Ojha *et al.*, 2016; Viveros-Paredes *et al.*, 2017) or stroke (Tian *et al.*, 2019), among others. In these inflammatory states, it is widely demonstrated that BCP-mediated gliosis attenuation is associated with a decrease in pro-inflammatory markers such as TNFα, IL1β or NF-κB (Scandiffio *et al.*, 2020), and it is likely that cognitive and behavioral improvements observed in our DS mice are due to the beneficial effects that BCP exerts on neuroinflammation.

Although we have not investigated the specific molecular targets that may explain BCP effects on our DS mouse model, it is well-established that BCP elicits a full agonist action over CB_2 receptor (Gertsch *et al.*, 2008). In fact, available data suggest that BCP exerts its anti-inflammatory and antioxidant effects through multiple mechanisms normally initiated by the activation of this receptor (Machado *et al.*, 2018; Sharma *et al.*, 2016). In addition, some studies have recently demonstrated BCP activation of PPARs. However, direct binding of BCP has been reported only for PPARα, whereas PPARγ activation depends on the binding of BCP to CB_2 receptors (Wu *et al.*, 2014). Particularly, stimulation of CB_2 receptor by BCP promotes an intracellular signalling cascade which augments MAP kinase activity, that further activates PPARγ via direct phosphorylation (O'Sullivan, 2016). In this way, cross-talk between CB_2 and PPARγ receptors may also contribute to activate anti-inflammatory signals (Picciolo *et al.*, 2020; Youssef *et al.*, 2019) (Figure D2).

It must be highlighted that in addition to displaying important pharmacological activities, other aspects make BCP a promising candidate for pharmacological and clinical development. It is designed as "generally recognized as safe" by American and European regulatory agencies, which supports its safety profile (Gertsch *et al.*, 2008). Importantly, the lack of psychoactivity associated with its negligible activity at the CB_1 receptor, together with the extensive accessibility to this molecule due to its natural availability, make BCP highly suitable for pharmaceutical development. However, despite all these potential advantages, its application into the human biopharmaceutical field must overcome some limitations, since BCP volatility and lipophilicity properties reduce its bioavailability (Sharma *et al.*, 2016). In this sense, some ongoing studies are trying to develop delivery systems (such as inclusion complexes with cyclodextrins, liposomes and nanoparticles, among others) to improve BCP oral bioavailability (Santos *et al.*, 2018).

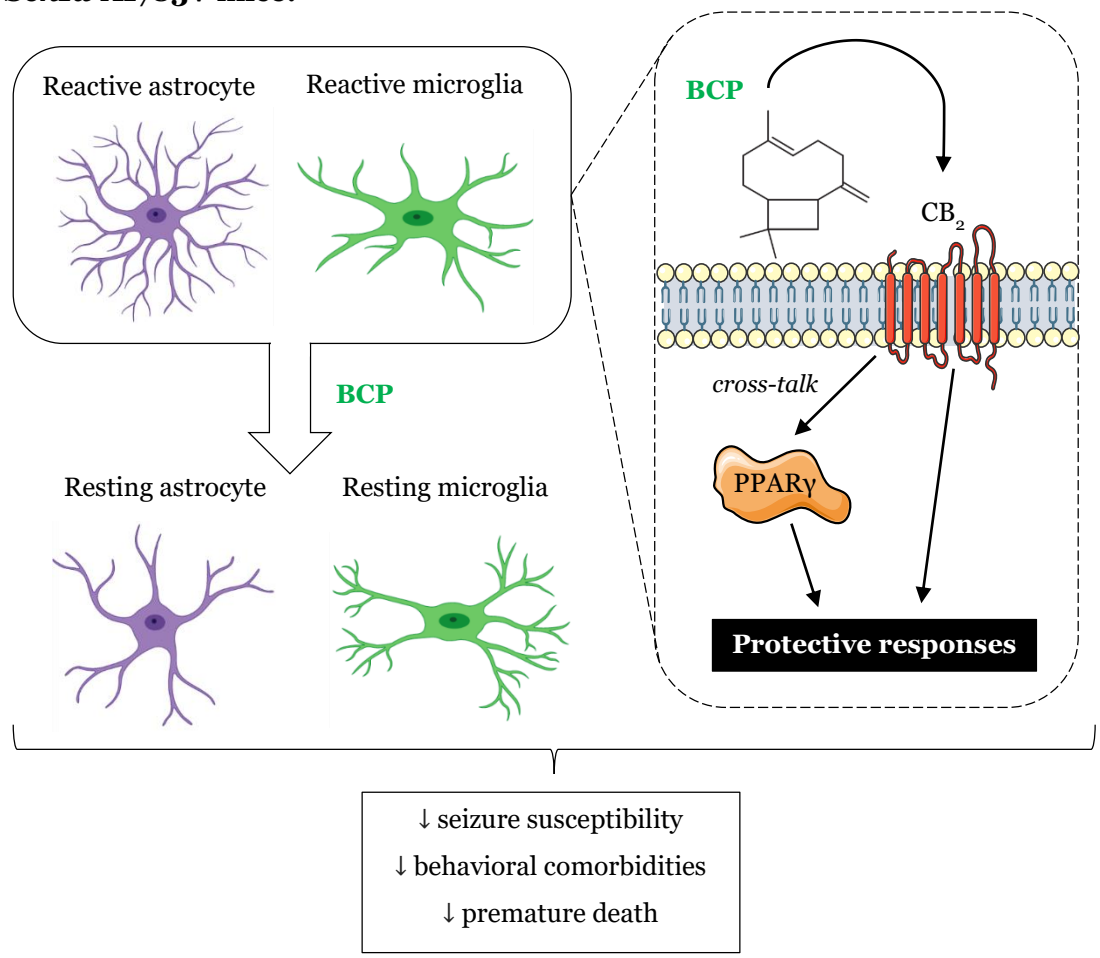

Figure D2. Proposed mechanisms of action for BCP in DS.

Therefore, we have demonstrated for the first time that BCP has a marked efficacy in DS mice, thus holding a great promise for an improved therapy of this devastating disorder. However, although studies on the molecule are promising, these are only preclinical data, so further reports in the clinical setting are required for a possible human application.

Although CBD is already approved for DS treatment and has demonstrated efficacy in mouse models of DS (Kaplan *et al.*, 2017) as well as other models of epilepsy (Patra *et al.*, 2019), beneficial effects observed in our preclinical model of DS opened the possibility of hypothesizing that the combination with BCP may offer additional benefits compared to monotherapy. Some previous evidence pointed to the possibility that cannabinoids and terpenes work better when used in combination according to the so-called "entourage effect" (Russo, 2011), mainly considering potentially common action mechanisms (e.g., anti-inflammatory and antioxidant) shared by both compounds. Moreover, it is important to remark that investigating both molecules in combination is pivotal, since CBD is already used for DS treatment and BCP might not undergo clinical

trials without being combined with pre-existing medication. For this reason, future preclinical research should consider combining BCP with other commonly used drugs, such as valproic acid, clobazam or stiripentol (Wirrell *et al.*, 2017).

In our DS mice, CBD alone exerted positive effects on motor and cognitive alterations. However, BCP was notably more potent than CBD in attenuating the body weight loss and diminishing mortality rate. Besides, BCP was also more effective than CBD in attenuating reactive gliosis in prefrontal cortex and hippocampal dentate gyrus, which correlated with studies carried out in an *in vitro* model of inflammation. The evaluation of BCP and CBD effects on the pro-inflammatory phenotype triggered by the stimulation of BV2 microglial cells with LPS (Kim *et al.*, 2019; Li *et al.*, 2021; Rahimi *et al.*, 2018) revealed that single treatment with the optimal dose of 10 μM of BCP is more effective than single treatment with the optimal dose of 0,1 μM of CBD in terms of attenuating inflammatory and oxidative biomarkers. Although the anti-inflammatory profile of CBD and BCP is highly demonstrated, it appears that BCP is more effective, probably due to the fact that potential molecular targets of BCP (such as CB_2 receptor) may be more relevant in DS pathogenesis than CBD ones.

Interestingly, the combination of both molecules yielded additional benefits, being particularly prominent in some parameters recorded in the Y-maze and social interaction tests, as well as in attenuating reactive gliosis. Importantly, as already widely mentioned, premature mortality is a major problem in DS, and CBD + BCP combination demonstrated a potent ability to decrease mortality rate, as well as to greatly delay the age at death, if compared to their single administration.

Particularly, both previous data (Rubio *et al.*, 2016) and results obtained in this Doctoral Thesis suggest that CB_2 receptor could play a key role in this disorder. Although BCP and CBD share some common mechanisms, agonism of CB_2 is well-established for BCP (Gertsch *et al.*, 2008) but not for CBD, which may explain the additional positive effects exerted by BCP. However, it should be carefully considered, since CBD has been shown to indirectly modulate the ECS under some experimental conditions (Pazos *et al.*, 2013; Vilela *et al.*, 2017), leading to an enhancement of endocannabinoid levels (e.g., FAAH inhibition), which may facilitate cannabinoid signalling and may also be indirectly activating CB_2 receptors (De Petrocellis *et al.*, 2011).

What seems to be clear is that BCP + CBD co-administration exerts additional effects if compared to their individual administration, which is in agreement with the “entourage effect”. This phenomenon could be due to different factors, including multi-target additive effects or increased pharmacokinetic efficiency, among others (Ferber *et al.*,

2020; Russo, 2011). This combination has also yielded promising results in a mouse model of cerebral permanent ischemia (Yokubaitis *al.*, 2021), thus supporting our findings. However, to the best of our knowledge, this is the first report of the efficacy of this unique combination not only in DS, but also in epilepsy as a whole, which confirms the great interest in continuing investigating these effects. Interestingly, in addition to providing an additive effect, BCP might potentially limit CBD dose-related toxicity.

Interestingly, recent studies have reported anticonvulsant effects of CBGA and CBDA (the acid forms of CBG and CBD, respectively), as well as of CBC, in other DS mouse models (Anderson *et al.*, 2019, 2021a, 2021b). Therefore, it seems clear that other cannabinoids beyond CBD might be of great interest for future drug development programs, and should be considered in the context of a cannabinoid-based combined therapy.

As an overall conclusion, results obtained in this Doctoral Thesis have allowed us to validate a novel DS mouse model that faithfully recapitulates the main aspects of the disorder. This mouse model is characterized by particular neuropathological features whose study has served to confirm the importance of designing pharmacological strategies with anti-inflammatory and antioxidant effects, rather than focusing only on preventing seizure activity. Since most patients currently require several antiepileptic drugs, new and effective therapeutic approaches should improve their efficacy, but also reduce side effects of polypharmacy. In this context, a preclinical cannabinoid-based treatment has been demonstrated to be safe and effective against long-term DS-associated comorbidities, thus positioning the ECS as a good therapeutic target to be explored in the context of DS. However, further clinical research is needed, with a focus on the long-term safety of compounds targeting this system, as well as drug-drug interactions.

CONCLUSIONS/ CONCLUSIONES

CONCLUSIONS

The results obtained in this Doctoral Thesis allow us to conclude that:

1. *Scn1a*-A1783V mouse model recapitulates main features of DS progression, including premature death, epileptic activity and behavioral comorbidities such as developmental delay, hyperactivity, cognitive decline and autistic traits.

2. The endogenous cannabinoid system is altered in *Scn1a*-A1783V mice. These changes are focused on cannabinoid receptors, with an increased expression of CB_2 receptor in hippocampus and a decrease in CB_1 receptor in hippocampus and cerebellum, together with a decrease in the inactivation enzyme MAGL in prefrontal cortex and cerebellum.

3. Neuroinflammatatory events may play a key role in the pathogenesis of *Scn1a*-A1783V mice, including a subtle increase in BBB permeability, an enhanced production of proinflammatory cytokines and a prominent reactive gliosis.

4. Adult hippocampal neurogenesis is altered in *Scn1a*-A1783V mice, since neural stem cells with a reactive-like phenotype are present in the neurogenic niche and exhibit high rates of activation and proliferation. However, this process might be induced in an aberrant way, since granule cells nuclei present a distorted morphology.

5. An acute administration of BCP shows anticonvulsant potential in *Scn1a*-A1783V mice, since it is able to attenuate the proconvulsant action of PTZ. This effect is associated with a marked reduction in glial reactivity. Importantly, these benefits are observed in both DS mice and their controls.

6. A chronic treatment with BCP attenuates the long-term behavioral comorbidities associated with DS and delays premature death in *Scn1a*-A1783V mice. Again, these effects are associated with a reduction of glial reactivity.

7. The combination of BCP and CBD shows more positive effects than each compound alone in *Scn1a*-A1783V mice, exerting greater benefits against behavioral abnormalities and reactive gliosis. These findings are also corroborated in microglial BV2 cells, since the combination of both compounds effectively reduces LPS-induced activation. Therefore, this evidence may help to improve cannabinoid-based therapeutic strategies for DS patients.

CONCLUSIONES

Los resultados obtenidos en esta Tesis Doctoral nos permiten concluir que:

1. El modelo animal *Scn1a*-A1783V recapitula las principales características del progreso del SD, incluyendo la muerte prematura, la actividad epiléptica y las comorbilidades comportamentales tales como retraso en el desarrollo, hiperactividad, deterioro cognitivo y rasgos autistas.

2. El sistema cannabinoide endógeno se encuentra alterado en los ratones *Scn1a*-A1783V. Estos cambios implican a los receptores cannabinoides, con un incremento en la expresión del receptor CB_2 en hipocampo y una disminución del receptor CB_1 en hipocampo y cerebelo, así como una disminución de la enzima de inactivación MAGL en corteza prefrontal y cerebelo.

3. Eventos relacionados con la neuroinflamación juegan un papel esencial en la patogénesis de los ratones *Scn1a*-A1783V, lo que incluye un sutil incremento en la permeabilidad de la BHE, una producción eleveada de citoquinas proinflamatorias y una prominente gliosis reactiva.

4. La neurogénesis hipocampal adulta se encuentra alterada en los ratones *Scn1a*-A1783V, dado que las células madre neurales que se encuentran en el nicho neurogénico presentan un fenotipo reactivo y niveles incrementados de activación y proliferación. No obstante, este proceso se induce de una manera aberrante, dado que los núcleos de las células granulares presentan una morfología anormal.

5. La administración aguda de BCP tiene efecto anticonvulsivante en los ratones *Scn1a*-A1783V, ya que es capaz de atenuar la acción proconvulsivante del PTZ. Este efecto se asocia con una potente redución de la reactividad glial. Cabe destacar que estos beneficios se observan tanto en los ratones SD como en sus controles.

6. El tratamiento crónico con BCP atenúa las comorbilidades comportamentales a largo plazo asociadas con el SD y retrasa la muerte prematura en los ratones *Scn1a*-A1783V. De nuevo, estos efectos se asocian con una reducción de la reactividad glial.

7. La combinación de BCP y CBD ejerce efectos positivos adicionales a cada compuesto por separado en los ratones *Scn1a*-A1783V, mostrando mayores beneficios frente a las anomalías comportamentales y la reactividad glial. Estos resultados son corroborados en las células microgliales BV2, ya que la combinación de ambos compuestos reduce de manera eficaz la activación inducida por LPS. Por ello, estas evidencias podrían ayudar a mejorar las estrategias terapéuticas badas en cannabinoides para los pacientes de SD.

REFERENCES

A

Akiyama, M., Kobayashi, K. & Ohtsuka, Y. (2012) Dravet syndrome: a genetic epilepsy disorder. *Acta Med*, **66**, 369-376.

Akiyama, M., Kobayashi, K., Yoshinaga, H. & Ohtsuka, Y. (2010) A longterm follow-up study of Dravet syndrome up to adulthood. *Epilepsia*, **51**, 1043-1052.

Alachkar, A., Ojha, S.K., Sadeq, A., Adem, A., Frank, A., Stark, H. & Sadek, B. (2020) Experimental models for the discovery of novel anticonvulsant drugs: Focus on pentylenetetrazole-induced seizures and associated memory deficits. *Curr Pharm Des*, **26**, 1693-1711.

Alexander, S.P. (2015) Common receptors for endocannabinoid-like mediators and plant cannabinoids. In Di Marzo, V. & Wang, J. (eds) The Endocannabinoidome. Elsevier, pp. 153-175.

Almog, Y., Fadila, S., Brusel, M., Mavashov, A., Anderson, K. & Rubinstein, M. (2021) Developmental alterations in firing properties of hippocampal CA1 inhibitory and excitatory neurons in a mouse model of Dravet syndrome. *Neurobiol Dis*, **148**, 105209.

Ambrogini, P., Torquato, P., Bartolini, D., Albertini, M.C., Lattanzi, D., Di Palma, M., Marinelli, R., Betti, M., Minelli, A., Cuppini, R. & Galli, F. (2019) Excitotoxicity, neuroinflammation and oxidant stress as molecular bases of epileptogenesis and epilepsy-derived neurodegeneration: The role of vitamin E. *Biochim Biophys Acta Mol Basis Dis*, **1865**, 1098-1112.

Anderson, L.L., Ametovski, A., Lin Luo, J., Everett-Morgan, D., McGregor, I.S., Banister, S.D. & Arnold, J.C. (2021a) Cannabichromene, related phytocannabinoids, and 5-fluoro-cannabichromene have anticonvulsant properties in a mouse model of Dravet syndrome. *ACS Chem Neurosci*, **12**, 330-339.

Anderson, L.L., Heblinski, M., Absalom, N.L., Hawkins, N.A., Bowen, M.T., Benson, M.J., Zhang, F., Bahceci, D., Doohan, P.T., Chebib, M., McGregor, I.S., Kearney, J.A. & Arnold, J.C. (2021b) Cannabigerolic acid, a major biosynthetic precursor molecule in cannabis, exhibits divergent effects on seizures in mouse models of epilepsy. *Br J Pharmacol*. Online ahead of print

Anderson, L.L., Low, I.K., Banister, S.D., McGregor, I.S. & Arnold, J.C. (2019) Pharmacokinetics of phytocannabinoid acids and anticonvulsant effect of cannabidiolic acid in a mouse model of Dravet syndrome. *J Nat Prod*, **82**, 3047-3055.

Aronica, E., Bauer, S., Bozzi, Y., Caleo, M., Dingledine, R., Gorter, J.A., Henshall, D.C., Kaufer, D., Koh, S., Löscher, W., Louboutin, J.P., Mishto, M., Norwood, B.A., Palma, E., Poulter, M.O., Terrone, G., Vezzani, A. & Kaminski, R.M. (2017) Neuroinflammatory targets and treatments for epilepsy validated in experimental models. *Epilepsia*, **58**, 27-38.

Aronica, E. & Crino, P.B. (2011) Inflammation in epilepsy: clinical observations. *Epilepsia*, **52**, 26-32.

Atalay, S., Jarocka-Karpowicz, I. & Skrzydlewska, E. (2020) Antioxidative and anti-inflammatory properties of cannabidiol. *Antioxidants*, **9**, 21.

B

Bacci, A., Huguenard, J.R. & Prince, D.A. (2004) Long-lasting self-inhibition of neocortical interneurons mediated by endocannabinoids. *Nature*, **431**, 312–316.

Baggelaar, M.P., Van Esbroeck, A.C.M., Van Rooden, E.J., Florea, B.I., Overkleeft, H.S., Marsicano, G., Chaouloff, F. & Van Der Stelt, M. (2017) Chemical proteomics maps brain region specific activity of endocannabinoid hydrolases. *ACS Chem Biol*, **12**, 852-861.

Bahi, A., Al Mansouri, S., Al Memari, E., Al Ameri, M., Nurulain, S. M. & Ojha, S. (2014) β-Caryophyllene, a CB_2 receptor agonist produces multiple behavioral changes relevant to anxiety and depression in mice. *Physiol Behav*, **135**, 119-124.

Barker-Haliski, M.L., Heck, T.D., Dahle, E.J., Vanegas, F., Pruess, T.H., Wilcox, K.S., & White, H.S. (2016) Acute treatment with minocycline, but not valproic acid, improves long-term behavioral outcomes in the Theiler's virus model of temporal lobe epilepsy. *Epilepsia*, **57**, 1958-1967.

Basu, S. & Dittel, B.N. (2011) Unraveling the complexities of cannabinoid receptor 2 (CB2) immune regulation in health and disease. *Immunol Res*, **51**, 26-38.

Bayat, A., Hjalgrim, H. & Moller, R.S. (2015) The incidence of SCN1A-related Dravet syndrome in Denmark is 1:22,000: A population-based study from 2004 to 2009. *Epilepsia*, **56**, 36-39.

Ben-Menachem, E., Gunning, B., Arenas Cabrera, C.M., VanLandingham, K., Crockett, J., Critchley, D., Wray, L., Tayo, B., Morrison, G. & Toledo, M. (2020) A Phase II randomized trial to explore

the potential for pharmacokinetic drug-drug interactions with stiripentol or valproate when combined with cannabidiol in patients with epilepsy. *CNS drugs*, **34**, 661-672.

Bénard, G., Massa, F., Puente, N., Lourenço, J., Bellocchio, L., Soria-Gómez, E., Matias, I., Delamarre, A., Metna-Laurent, M., Cannich, A., Hebert-Chatelain, E., Mulle, C., Ortega-Gutiérrez, S., Martín-Fontecha, M., Klugmann, M., Guggenhuber, S., Lutz, B., Gertsch, J., Chaouloff, F., López-Rodríguez, M.L., Grandes, P., Rossignol, R. & Marsicano, G. (2012) Mitochondrial CB_1 receptors regulate neuronal energy metabolism. *Nat Neurosci*, **15**, 558-564.

Berg, A.T., Berkovic, S.F., Brodie, M.J., Buchhalter, J., Cross, J.H., van Emde Boas, W., Engel, J., French, J., Glauser, T.A., Mathern, G.W., Moshé, S.L., Nordli, D., Plouin, P. & Scheffer, I.E. (2010) Revised terminology and concepts for organization of seizures and epilepsies: report of the ILAE Commission on Classification and Terminology, 2005-2009. *Epilepsia*, **51**, 676-685.

Berkvens, J.J., Veugen, I., Veendrick-Meekes, M.J., Snoeijen-Schouwenaars, F.M., Schelhaas, H.J., Willemsen, M.H., Tan, I.Y. & Aldenkamp, A.P. (2015) Autism and behavior in adult patients with Dravet syndrome (DS). *Epilepsy Behav*, **47**, 11-16.

Bialer, M. & White, H.S. (2010) Key factors in the discovery and development of new antiepileptic drugs. *Nat Rev Drug Discov*, **9**, 68-82.

Bielefeld, P., Durá, I., Danielewicz, J., Lucassen, P.J., Baekelandt, V., Abrous, D.N., Encinas, J.M. & Fitzsimons, C.P. (2019) Insult-induced aberrant hippocampal neurogenesis: Functional consequences and possible therapeutic strategies. *Behav Brain Res*, **372**, 112032.

Bilsland, L.G., Dick, J.R., Pryce, G., Petrosino, S., Di Marzo, V., Baker, D. & Greensmith, L. (2006) Increasing cannabinoid levels by pharmacological and genetic manipulation delay disease progression in SOD1 mice. *FASEB J*, **20**, 1003-1005.

Bisogno, T., Berrendero, F., Ambrosino, G., Cebeira, M., Ramos, J.A., Fernández-Ruiz, J.J. & Di Marzo, V. (1999) Brain regional distribution of endocannabinoids: implications for their biosynthesis and biological function. *Biochem Biophys Res Commun*, **256**, 377-380.

Bisogno, T., Hanus, L., De Petrocellis, L., Tchilibon, S., Ponde, D. E., Brandi, I., Moriello, A.S., Davis, J.B., Mechoulam, R. & Di Marzo, V. (2001) Molecular targets for cannabidiol and its synthetic analogues: effect on vanilloid VR1 receptors and on the cellular uptake and enzymatic hydrolysis of anandamide. *Br J Pharmacol*, **134**, 845-852.

Bisogno, T., Ligresti, A. & Di Marzo, V. (2005) The endocannabinoid signalling system: Biochemical aspects. *Pharmacol Biochem Behav*, **81**, 224-238.

Blaney, C.E., Gunn, R.K., Stover, K.R. & Brown, R.E. (2013) Maternal genotype influences behavioral development of 3×Tg-AD mouse pups. *Behav Brain Res*, **252**, 40-48.

Blasco-Benito, S., Moreno, E., Seijo-Vila, M., Tundidor, I., Andradas, C., Caffarel, M.M., Caro-Villalobos, M., Urigüen, L., Diez-Alarcia, R., Moreno-Bueno, G., Hernández, L., Manso, L., Homar-Ruano, P., McCormick, P.J., Bibic, L., Bernadó-Morales, C., Arribas, J., Canals, M., Casadó, V., Canela, E.I., Guzmán, M., Pérez-Gómez, E. & Sánchez, C. (2019) Therapeutic targeting of HER2-CB2R heteromers in HER2-positive breast cancer. *Proc Natl Acad Sci USA*, **26**, 3863-3872.

Borowicz-Reutt, K.K. & Czuczwar, S.J. (2020) Role of oxidative stress in epileptogenesis and potential implications for therapy. *Pharmacol Rep*, **72**, 1218-1226.

Bouaboula, M., Poinot-Chazel, C., Bourrie, B., Canat, X., Calandra, B., Rinaldi-Carmona, M., Le Fur, G. & Casellas, P. (1995) Activation of mitogen-activated protein kinases by stimulation of the central cannabinoid receptor CB_1. *Biochem J*, **312**, 637-641.

Bradshaw, H.B., Rimmerman, N., Hu, S.S., Benton, V.M., Stuart, J.M., Masuda, K., Cravatt, B.F., O'Dell, D. K. & Walker, J.M. (2009) The endocannabinoid anandamide is a precursor for the signaling lipid N-arachidonoyl glycine by two distinct pathways. *BMC Biochem*, **10**, 14.

Brandt, C., Töllner, K., Klee, R., Bröer, S. & Löscher, W. (2015) Effective termination of status epilepticus by rational polypharmacy in the lithium-pilocarpine model in rats: Window of opportunity to prevent epilepsy and prediction of epilepsy by biomarkers. *Neurobiol Dis*, **75**, 78-90.

Broekaart, D., Anink, J.J., Baayen, J.C., Idema, S., de Vries, H.E., Aronica, E., Gorter, J.A. & van Vliet, E.A. (2018) Activation of the innate immune system is evident throughout epileptogenesis and is associated with blood-brain barrier dysfunction and seizure progression. *Epilepsia*, **59**, 1931-1944.

Brunklaus, A., Ellis, R., Reavey, E., Forbes, G.H. & Zuberi, S.M. (2012) Prognostic, clinical and demographic features in SCN1A mutation-positive Dravet syndrome. *Brain*, **135**, 2329-2336.

Brunklaus, A. & Zuberi, S.M. (2014) Dravet syndrome - From epileptic encephalopathy to channelopathy. *Epilepsia*, **55**, 979-984.

C

Callén, L., Moreno, E., Barroso-Chinea, P., Moreno-Delgado, D., Cortés, A., Mallol, J., Casadó, V., Lanciego, J.L., Franco, R., Lluis, C., Canela, E.I. & McCormick, P.J. (2012) Cannabinoid receptors CB_1 and CB_2 form functional heteromers in brain. *J Biol Chem*, **287**, 20851-20865.

Camfield, P., Camfield, C. & Nolan, K. (2012) Helping families cope with the devastation of Dravet syndrome. *Eur J Paediatr Neurol*, **16**, S9-S12.

Carlini, E.A., Leite, J.R., Tannhauser, M. & Berardi, A.C. (1973) Letter: Cannabidiol and Cannabis sativa extract protect mice and rats against convulsive agents. *J Pharm Pharmacol*, **25**, 664-665.

Carman, C.V. & Martinelli, R. (2015) T lymphocyte-endothelial interactions: emerging understanding of trafficking and antigen-specific immunity. *Front Immunol*, **6**, 603.

Castillo, P.E., Younts, T.J., Chavez, A.E. & Hashimotodani, Y. (2012) Endocannabinoid signaling and synaptic function. *Neuron*, **76**, 70-81.

Catterall, W.A. (2018) Dravet syndrome: a sodium channel interneuronopathy. *Curr Opin Physiol*, **2**, 42-50.

Catterall, W.A., Kalume, F. & Oakley, J.C. (2010) $Na_V1.1$ channels and epilepsy. *J Physiol*, **588**,1849-1859.

Chávez-Hurtado, P., González-Castañeda, R.E., Beas-Zarate, C., Flores-Soto, M.E. & Viveros-Paredes, J.M. (2020) β-caryophyllene reduces DNA oxidation and the overexpression of glial fibrillary acidic protein in the prefrontal cortex and hippocampus of d-galactose-induced aged BALB/c mice. *J Med Food*, **23**, 515-522.

Cheah, C.S., Westenbroek, R.E., Roden, W.H., Kalume, F., Oakley, J.C., Jansen, L.A. & Catterall, W.A. (2013) Correlations in timing of sodium channel expression, epilepsy, and sudden death in Dravet syndrome. *Channels*, **7**, 468-472.

Cheah, C.S., Yua, F.H., Westenbroek, R.E., Kalume, F.K., Oakley, J.C., Potter, G.B., Rubenstein, J.L. & Catterall, W.A. (2012) Specific deletion of $Na_V1.1$ sodium channels in inhibitory interneurons causes seizures and premature death in a mouse model of Dravet syndrome. *Proc Natl Acad Sci USA*, **106**, 14646-14651.

Chen, L., Wang, Y. & Chen, Z. (2020) Adult neurogenesis in epileptogenesis: an update for preclinical finding and potential clinical translation. *Curr Neuropharmacol*, **18**, 464-484.

Cheng, Y., Dong, Z. & Liu, S. (2014) β-caryophyllene ameliorates the Alzheimer-like phenotype in APP/PS1 mice through CB_2 receptor activation and the PPARγ pathway. *Pharmacology*, **94**, 1-12.

Cho, K.O., Lybrand, Z.R., Ito, N., Brulet, R., Tafacory, F., Zhang, L., Good, L., Ure, K., Kernie, S.G., Birnbaum, S.G., Scharfman, H.E., Eisch, A.J. & Hsieh, J. (2015) Aberrant hippocampal neurogenesis contributes to epilepsy and associated cognitive decline. *Nat Commun*, **6**, 6606.

Choi, H.J., Im, S.J., Park, H.R., Park, S., Kim, C.E. & Ryu, S. (2019) Long-term effects of aripiprazole treatment during adolescence on cognitive function and dopamine D2 receptor expression in neurodevelopmentally normal rats. *Clin Psychopharmacol Neurosci*, **17**, 400-408.

Claes, L., Del-Favero, J., Ceulemans, B., Lagae, L., Van Broeckhoven, C. & De Jonghe, P. (2001) De novo mutations in the sodium-channel gene SCN1A cause severe myoclonic epilepsy of infancy. *Am J Hum Genet*, **68**, 1327-1332.

Coke, C.J., Scarlett, K.A., Chetram, M.A., Jones, K.J., Sandifer, B.J., Davis, A.S., Marcus, A.I. & Hinton, C.V. (2016) Simultaneous activation of induced heterodimerization between CXCR4 chemokine receptor and cannabinoid receptor 2 (CB_2) reveals a mechanism for regulation of tumor progression. *J Biol Chem*, **291**, 9991-10005.

Commission on Classification and Terminology of the International League Against Epilepsy (1989) Proposal for revised classification of epilepsies and epileptic syndromes. *Epilepsia*, **30**, 389-399.

Concannon, R.M., Okine, B.N., Finn, D.P. & Dowd, E. (2016) Upregulation of the cannabinoid CB_2 receptor in environmental and viral inflammation-driven rat models of Parkinson's disease. *Exp Neurol*, **283**, 204-212.

Console-Bram, L., Brailoiu, E., Brailoiu, G.C., Sharir, H. & Abood, M.E. (2014) Activation of GPR18 by cannabinoid compounds: a tale of biased agonism. *Br J Pharmacol*, **171**, 3908-3917.

Covacu, R. & Brundin, L. (2016) Effects of neuroinflammation on neural stem cells. *Neuroscientist*, **23**, 27-39.

Cravatt, B.F., Giang, D.K., Mayfield, S.P., Boger, D.L., Lerner, R.A. & Gilula, N.B. (1996) Molecular characterization of an enzyme that degrades neuromodulatory fatty-acid amides. *Nature*, **384**, 83-87.

Cristino, L., Bisogno, T. & Di Marzo, V. (2020) Cannabinoids and the expanded endocannabinoid system in neurological disorders. *Nat Rev Neurol*, **16**, 9-29.

Cunha, J.M., Carlini, E.A., Pereira, A.E., Ramos, O.L., Pimentel, C., Gagliardi, R., Sanvito, W.L., Lander, N. & Mechoulam, R. (1980) Chronic administration of cannabidiol to healthy volunteers and epileptic patients. *Pharmacology*, **21**, 175-185.

D

da Fonsêca, D.V., da Silva Maia Bezerra Filho, C., Lima, T.C., de Almeida, R.N. & de Sousa, D.P. (2019) Anticonvulsant essential oils and their relationship with oxidative stress in epilepsy. *Biomolecules*, **9**, 835.

Dale, T., Downs, J., Olson, H., Bergin, A.M., Smith, S. & Leonard, H. (2019) Cannabis for refractory epilepsy in children: A review focusing on CDKL5 Deficiency Disorder. *Epilepsy Res*, **151**, 31-39.

Dalla Bernardina, B., Capovilla, G. & Gattoni, M. (1982) Epilepsie myoclonique grave de la première année. *Rev EEG Neurophysiol*, **12**, 21-25.

Davis, M.I., Ronesi, J. & Lovinger, D.M. (2003) A predominant role for inhibition of the adenylate cyclase/protein kinase A pathway in ERK activation by cannabinoid receptor 1 in N1E-115 neuroblastoma cells. *J Biol Chem*, **278**, 48973-48980.

de Oliveira, C.C., de Oliveira, C.V., Grigoletto, J., Ribeiro, L.R., Funck, V.R., Grauncke, A.C., de Souza, T.L., Souto, N.S., Furian, A.F., Menezes, I.R. & Oliveira, M.S. (2016) Anticonvulsant activity of β-caryophyllene against pentylenetetrazol-induced seizures. *Epilepsy Behav*, **56**, 26-31.

De Petrocellis, L., Ligresti, A., Moriello, A.S., Allara, M., Bisogno, T., Petrosino, S., Stott, C.G. & Di Marzo, V. (2011) Effects of cannabinoids and cannabinoid-enriched Cannabis extracts on TRP channels and endocannabinoid metabolic enzymes. *Br J Pharmacol*, **163**, 1479-1494.

Deacon, R.M.J. & Rawlins, N.P. (2006) T-maze alternation in the rodent. *Nat Protoc*, **1**, 7-12.

Devane, W.A., Dysarz, F.A., Johnson, M.R., Melvin, L.S. & Howlett, A.C. (1988) Determination and characterization of a cannabinoid receptor in rat brain. *Mol Pharmacol*, **34**, 605-613.

Devinsky, O., Cilio, M.R., Cross, H., Fernández-Ruiz, J., French, J., Hill, C., Katz, R., Di Marzo, V., Jutras-Aswad, D., Notcutt, W.G., Martinez-Orgado, J., Robson, P.J., Rohrback, B.G., Thiele, E., Whalley, B. & Friedman, D. (2014) Cannabidiol: pharmacology and potential therapeutic role in epilepsy and other neuropsychiatric disorders. *Epilepsia*, **55**, 791-802.

Devinsky, O., Cross, J.H., Laux, L., Marsh, E., Miller, I., Nabbout, R., Scheffer, I.E., Thiele, E.A., Wright, S. & Cannabidiol in Dravet Syndrome Study Group (2017) Trial of cannabidiol for drug-resistant seizures in the Dravet syndrome. *N Engl J Med*, **376**, 2011-2020.

Devinsky, O., Nabbout, R., Miller, I., Laux, L., Zolnowska, M., Wright, S. & Roberts, C. (2019) Long-term cannabidiol treatment in patients with Dravet syndrome: An open-label extension trial. *Epilepsia*, **60**, 294-302.

Devinsky, O., Patel, A.D., Cross, J.H., Villanueva, V., Wirrell, E.C., Privitera, M., Greenwood, S.M., Roberts, C., Checketts, D., VanLandingham, K.E., Zuberi, S.M. & GWPCARE3 Study Group (2018) Effect of cannabidiol on drop seizures in the Lennox-Gastaut syndrome. *N Engl J Med*, **378**, 1888-1897.

Di Marzo, V., Fontana, A., Cadas, H., Schinelli, S., Cimino, G., Schwartz, J.C. & Piomelli, D. (1994) Formation and inactivation of endogenous cannabinoid anandamide in central neurons. *Nature*, **372**, 686-691.

Di Marzo, V. & Piscitelli, F. (2015) The endocannabinoid system and its modulation by phytocannabinoids. *Neurotherapeutics*, **12**, 692-698.

Dinh, T.P., Carpenter, D., Leslie, F.M., Freund, T.F., Katona, I., Sensi, S.L., Kathuria, S. & Piomelli, D. (2002) Brain monoglyceride lipase participating in endocannabinoid inactivation. *Proc Natl Acad Sci USA*, **99**, 10819-10824.

DiSabato, D., Quan, N. & Godbout, J.P. (2016) Neuroinflammation: The devil is in the details. *J Neurochem*, **139**, 136-153.

Dlouhy, B.J., Miller, B., Jeong, A., Bertrand, M.E., Limbrick, D.D. & Smyth, M.D. (2016) Palliative epilepsy surgery in Dravet syndrome: case series and review of the literature. *Childs Nerv Syst*, **32**, 1703-1708.

dos Santos, R.G., Hallak, J.E., Leite, J.P., Zuardi, A.W. & Crippa, J.A. (2015) Phytocannabinoids and epilepsy. *J Clin Pharm Ther*, **40**, 135-143.

Dravet, C. (1978) Les épilepsies graves de l'enfant. *Vie Med*, **8**, 543-548.

Dravet, C. (2011) The core Dravet syndrome phenotype. *Epilepsia*, **52**, 3-9.

Dravet, C., Daquin, G. & Battaglia, D. (2009) Severe myoclonic epilepsy of infancy (Dravet syndrome). In: Nikanorova, M., Genton, P. & Sabers, A. (Eds.), Long-term evolution of epileptic encephalopathies. *John Libbey Eurotext Ltd*, Paris, 29-38.

Dravet, C. & Oguni, H. (2013) Dravet syndrome (severe myoclonic epilepsy in infancy). *Handb Clin Neurol*, **111**, 627-633.

Dressler, A., Trimmel-Schwahofer, P., Reithofer, E., Mühlebner, A., Gröppel, G., Reiter-Fink, E., Benninger, F., Grassl, R. & Feucht, M. (2015) Efficacy and tolerability of the ketogenic diet in Dravet syndrome - comparison with various standard antiepileptic drug regimen. *Epilepsy Res*, **109**, 81-89.

Dudok, B., Barna, L., Ledri, M., Szabó, S.I., Szabadits, E., Pintér, B., Woodhams, S.G., Henstridge, C.M., Balla, G.Y., Nyilas, R., Varga, C., Lee, S.H., Matolcsi, M., Cervenak, J., Kacskovics, I., Watanabe, M., Sagheddu, C., Melis, M., Pistis, M., Soltesz, I. & Katona, I. (2015) Cell-specific STORM super-resolution imaging reveals nanoscale organization of cannabinoid signaling. *Nat Neurosci*, **18**, 75-86.

Dupuis, N. & Auvin, S. (2015) Inflammation and epilepsy in the developing brain: clinical and experimental evidence. *CNS Neurosci Ther*, **21**, 141-151.

Dutta, S. & Sengupta, P. (2016) Men and mice: Relating their ages. *Life Sci*, **152**, 244-248.

Dutton, S.B., Makinson, C.D., Papale, L.A., Shankar, A., Balakrishnan, B., Nakazawa, K. & Escayg, A. (2013) Preferential inactivation of Scn1a in parvalbumin interneurons increases seizure susceptibility. *Neurobiol Dis*, **49**, 211-220.

E

Elahy, M., Jackaman, C., Mamo, J.C., Lam, V., Dhaliwal, S.S., Giles, C., Nelson, D. & Takechi, R. (2015) Blood-brain barrier dysfunction developed during normal aging is associated with inflammation and loss of tight junctions but not with leukocyte recruitment. *Immun Ageing*, **12**, 2.

Elphick, M.R. (2012) The evolution and comparative neurobiology of endocannabinoid signalling. *Philos Trans R Soc Lond B Biol Sci*, **367**, 3201-3215.

ElSohly, M.A. & Slade, D. (2005) Chemical constituents of marijuana: The complex mixture of natural cannabinoids. *Life Sci*, **78**, 539-548.

Encinas, J.M., Michurina, T.V., Peunova, N., Park, J.H., Tordo, J., Peterson, D.A., Fishell, G., Koulakov, A. & Enikolopov, G. (2011) Division-coupled astrocytic differentiation and age-related depletion of neural stem cells in the adult hippocampus. *Cell Stem Cell*, **8**, 566-579.

Escayg, A. & Goldin, A.L. (2010) Sodium channel SCN1A and epilepsy: mutations and mechanisms. *Epilepsia,* **51**, 1650-1658.

Escayg, A., MacDonald, B.T., Meisler, M.H., Baulac, S., Huberfeld, G., An-Gourfinkel, I., Brice, A., LeGuern, E., Moulard, B., Chaigne, D., Buresi, C. & Malafosse, A. (2000) Mutations of SCN1A, encoding a neuronal sodium channel, in two families with GEFS+2. *Nat Genet*, **24**, 343-345.

Espejo-Porras, F., García-Toscano, L., Rodríguez-Cueto, C., Santos-García, I., de Lago, E. & Fernández-Ruiz, J. (2018) Targeting glial CB_2 receptors to delay the progression of the pathological phenotype in TDP-43 (A315T) transgenic mice, a model of amyotrophic lateral sclerosis. *Br J Pharmacol*, **176**, 1585-1600.

F

Fadila, S., Quinn, S., Turchetti Maia, A., Yakubovich, D., Ovadia, M., Anderson, K.L., Giladi, M. & Rubinstein, M. (2020) Convulsive seizures and some behavioral comorbidities are uncoupled in the $Scn1a^{A1783V}$ Dravet syndrome mouse model. *Epilepsia*, **61**, 2289-2300.

Falenski K.W., Blair, R.E., Sim-Selley, L.J., Martin, B.R. & DeLorenzo, R.J. (2007) Status epilepticus causes a long-lasting redistribution of hippocampal cannabinoid type 1 receptor expression and function in the rat pilocarpine model of acquired epilepsy. *Neuroscience*, **146**, 1232-1244.

Falenski, K.W., Carter, D.S., Harrison, A.J., Martin, B.R., Blair, R.E. & DeLorenzo, R.J. (2009) Temporal characterization of changes in hippocampal cannabinoid CB(1) receptor expression following pilocarpine-induced status epilepticus. *Brain Res*, **1262**, 64-72.

Fallah, M.S. & Eubanks, J.H. (2020) Seizures in mouse models of rare neurodevelopmental disorders. *Neuroscience*, **445**, 50-68.

Ferber, S.G., Namdar, D., Hen-Shoval, D., Eger, G., Koltai, H., Shoval, G., Shbiro, L. & Weller, A. (2020) The "entourage effect": terpenes coupled with cannabinoids for the treatment of mood disorders and anxiety disorders. *Curr Neuropharmacol*, **18**, 87-96.

Fernández-Ruiz, J. (2019) The biomedical challenge of neurodegenerative disorders: an opportunity for cannabinoid-based therapies to improve on the poor current therapeutic outcomes. *Br J Pharmacol*, **176**, 1370-1383.

Fernández-Ruiz, J., Galve-Roperh, I., Sagredo, O. & Guzmán, M. (2020) Possible therapeutic applications of cannabis in the neuropsychopharmacology field. *Eur Neuropsychopharmacol*, **36**, 217-234.

Fernández-Ruiz, J., García, C., Sagredo, O., Gómez-Ruiz, M. & de Lago, E. (2010) The endocannabinoid system as a target for the treatment of neuronal damage. *Expert Opin Ther Targets*, **14**, 387-404.

Fernández-Ruiz, J., Moreno-Martet, M., Rodríguez-Cueto, C., Palomo-Garo, C., Gómez-Cañas, M., Valdeolivas, S., Guaza, C., Romero, J., Guzmán, M., Mechoulam, R. & Ramos, J.A. (2011) Prospects for cannabinoid therapies in basal ganglia disorders. *Br J Pharmacol*, **163**, 1365-1378.

Fernández-Ruiz, J., Romero, J., Velasco, G., Tolón, R.M., Ramos, J.A. & Guzmán, M. (2007) Cannabinoid CB_2 receptor: a new target for controlling neural cell survival? *Trends Pharmacol Sci*, **28**, 39-45.

Fernández-Trapero, M., Espejo-Porras, F., Rodríguez-Cueto, C., Coates, J.R., Pérez-Díaz, C., de Lago, E. & Fernández-Ruiz, J. (2017) Upregulation of CB_2 receptors in reactive astrocytes in canine degenerative myelopathy, a disease model of amyotrophic lateral sclerosis. *Dis Model Mech*, **10**, 551-558.

Fezza, F. & Maccarrone, M. (2014) Endocannabinoid biochemistry: What do we know after 50 years? Cannabinoids, John Wiley & Sons, Ltd, 53-94.

Fisher, R.S., Acevedo, C., Arzimanoglou, A., Bogacz, A., Cross, J.H., Elger, J.H., Engel, Jr.J., Forsgren, L., French, J.A., Glynn, M., Hesdorffer, D.C., Lee, B.I., Mathern, G.W., Moshé, S.L., Perucca, E., Scheffer, I.E., Tomson, T., Watanabe, M. & Wiebe, S. (2014) ILAE official report: a practical clinical definition of epilepsy. *Epilepsia* **55**, 475-482.

Fisher, R.S., Boas, W.v.E., Blume, W., Elger, C., Genton, P., Lee, P. & Engel, J. (2005) Epileptic seizures and epilepsy: definitions proposed by the International League Against Epilepsy (ILAE) and the International Bureau for Epilepsy (IBE). *Epilepsia*, **46**, 470-472.

Fisher, R.S., Cross, J.H., French, J.A., Higurashi, N., Hirsch, E., Jansen, F.E., Lagae, L., Moshé, S.L., Peltola, J., Perez, E.R., Scheffer, I.E. & Zuberi, S.M. (2017) Operational classification of seizure types by the International League Against Epilepsy: Position Paper of the ILAE Commission for Classification and Terminology. *Epilepsia*, **58**, 522-530.

Flores-Sanchez, I.J. & Verpoorte, R. (2008) Secondary metabolism in Cannabis. *Phytochem Rev*, **7**, 615-639.

Franco, V., Bialer, M. & Perucca, E. (2021) Cannabidiol in the treatment of epilepsy: Current evidence and perspectives for further research. *Neuropharmacology*, **185**, 108442.

Franco, V. & Perucca, E. (2019) Pharmacological and therapeutic properties of cannabidiol for epilepsy. *Drugs*, **79**, 1435-1454.

Frasier, C.R., Zhang, H., Offord, J., Dang, L.T., Auerbach, D.S., Shi, H., Chen, C., Goldman, A.M., Eckhardt, L.L., Bezzerides, V.J., Parent, J.M. & Isom, L.L. (2018) Channelopathy as a SUDEP biomarker in Dravet syndrome patient-derived cardiac myocytes. *Stem Cell Reports*, **11**, 626-634.

Fredholm, B.B., Chen, J.F., Cunha, R.A., Svenningsson, P. & Vaugeois, J.M. (2005) Adenosine and brain function. *Int Rev Neurobiol*, **63**, 191-270.

Fujiwara, T., Sugawara, T., Mazaki-Miyazaki, E., Takahashi, Y., Fukushima, K., Watanabe, M., Hara, K., Morikawa, T., Yagi, K., Yamakawa, K. & Inoue, Y. (2003) Mutations of sodium channel alpha subunit type 1 (SCN1A) in intractable childhood epilepsies with frequent generalized tonic-clonic seizures. *Brain*, **126**, 531-546.

Fukuma, G., Oguni, H., Shirasaka, Y., Watanabe, K., Miyajima, T., Yasumoto, S., Ohfu, M., Inoue, T., Watanachai, A., Kira, R., Matsuo, M., Muranaka, H., Sofue, F., Zhang, B., Kaneko, S., Mitsudome, A. & Hirose, S. (2004) Mutations of neuronal voltage-gated Na+ channel alpha 1 subunit gene SCN1A in core severe myoclonic epilepsy in infancy (SMEI) and in borderline SMEI (SMEB). *Epilepsia*, **45**, 140-148.

G

Galve-Roperh, I., Ruead, D., Gomez del Pulgar, T., Velasco, G. & Guzman, M. (2002) Mechanism of extracellular signal-regulated kinase activation by the CB(1) cannabinoid receptor. *Mol Pharmacol*, **62**, 1385-1392.

Gambardella, A. & Marini, C. (2009) Clinical spectrum of SCN1A mutations. *Epilepsia,* **50**, 20-23.

Gaoni, Y. & Mechoulam, R. (1964) Isolation, structure, and partial synthesis of an active constituent of hashish. *J Am Chem Soc*, **86**, 1646-1647.

García-Culebras, A., Durán-Laforet, V., Peña-Martínez, C., Moraga, A., Ballesteros, I., Cuartero, M.I., de la Parra, J., Palma-Tortosa, S., Hidalgo, A., Corbí, A.L., Moro, M.A. & Lizasoain, I. (2019) Role of TLR4 (Toll-like receptor 4) in N1/N2 neutrophil programming after stroke. *Stroke*, **50**, 2922-2932.

García-Fuente, A., Vázquez, F., Viéitez, J.M., García Alonso, F.J., Martín, J.I. & Ferrer, J. (2018) CISNE: An accurate description of dose-effect and synergism in combination therapies. *Sci Rep*, **8**, 4964.

Gaston, T.E., Bebin, E.M., Cutter, G.R., Liu, Y., Szaflarski, J.P. & UAB CBD Program (2017) Interactions between cannabidiol and commonly used antiepileptic drugs. *Epilepsia*, **58**, 1586-1592.

Gataullina, S. & Dulac, O. (2017) From genotype to phenotype in Dravet disease. *Seizure*, **44**, 58-64.

Geffrey, A.L., Pollack, S.F., Bruno, P.L. & Thiele, E.A. (2015) Drug-drug interaction between clobazam and cannabidiol in children with refractory epilepsy. *Epilepsia*, **56**, 1246-1251.

Genton, P., Velizarova, R. & Dravet, C. (2011) Dravet syndrome: the long-term outcome. *Epilepsia*, **52**, 44-49.

Gerard, C.M., Mollereau, C., Vassart, G. & Parmentier, M. (1991) Molecular cloning of a human cannabinoid receptor which is also expressed in testis. *Biochem J*, **279**, 129-134.

Gerdeman, G.L., Ronesi, J. & Lovinger, D.M. (2002) Postsynaptic endocannabinoid release is critical to long-term depression in the striatum. *Nat Neurosci*, **5**, 446-451.

Gertsch, J., Leonti, M., Raduner, S., Racz, I., Chen, J.Z., Xie, X.Q., Altmann, K.H., Karsak, M. & Zimmer, A. (2008) Beta-caryophyllene is a dietary cannabinoid. *Proc Natl Acad Sci USA*, **105**, 9099-9104.

Glass, M. & Felder, C.C. (1997) Concurrent stimulation of cannabinoid CB1 and dopamine D2 receptors augments cAMP accumulation in striatal neurons: evidence for a Gs linkage to the CB1 receptor. *J Neurosci*, **17**, 5327-5333.

Godlewski, G., Offertáler, L., Wagner, J.A. & Kunos, G. (2009) Receptors for acylethanolamides-GPR55 and GPR119. *Prostaglandins Other Lipid Mediat*, **89**, 105-111.

Goldman, R.D., Shumaker, D.K., Erdos, M.R., Eriksson, M., Goldman, A.E., Gordon, L.B., Gruenbaum, Y., Khuon, S., Mendez, M., Varga, R. & Collins, F.S. (2004) Accumulation of mutant lamin A causes progressive changes in nuclear architecture in Hutchinson-Gilford progeria syndrome. *Proc Natl Acad Sci USA*, **101**, 8963-8968.

Gómez-Gálvez, Y., Palomo-Garo, C., Fernández-Ruiz, J. & García, C. (2016) Potential of the cannabinoid CB(2) receptor as a pharmacological target against inflammation in Parkinson's disease. *Prog Neuropsychopharmacol Biol Psychiatry*, **64**, 200-208.

Gonçalves, E.C.D., Baldasso, G.M., Bicca, M.A., Paes, R.S., Capasso, R. & Dutra, R.C. (2020) Terpenoids, cannabimimetic ligands, beyond the cannabis plant. *Molecules*, **25**, 1567.

Gonçalves J.T., Schafer, S.T. & Gage F.H. (2016) Adult Neurogenesis in the hippocampus: from stem cells to behaviour. *Cell*, **167**, 897-914.

Gray, R.A., Stott, C.G., Jones, N.A., Di Marzo, V. & Whalley, B.J. (2020) Anticonvulsive properties of cannabidiol in a model of generalized seizure are transient receptor potential vanilloid 1 dependent. *Cannabis Cannabinoid Res*, **5**, 145-149.

Gray, R.A. & Whalley, B.J. (2020) The proposed mechanisms of action of CBD in epilepsy. *Epileptic Disord.* **22**, S10-S15.

Green, H.F., Treacy, E., Keohane, A.K., Sullivan, A.M., O'Keeffe, G.W. & Nolan, Y.M. (2012) A role for interleukin-1beta in determining the lineage fate of embryonic rat hippocampal neural precursor cells. *Mol Cell Neurosci*, **49**, 311-321.

Grueter, B.A., Brasnjo, G. & Malenka, R.C. (2010) Postsynaptic TRPV1 triggers cell type-specific long-term depression in the nucleus accumbens. *Nat Neurosci*, **13**, 1519-1525.

Guindon, J. & Hohmann, A.G. (2008) A physiological role for endocannabinoid-derived products of cyclooxygenase-2-mediated oxidative metabolism. *Br J Pharmacol*, **153**, 1341-1343.

Guo, J. & Ikeda, S.R. (2004) Endocannabinoids modulate N-type calcium channels and G-protein-coupled inwardly rectifying potassium channels via CB_1 cannabinoid receptors heterologously expressed in mammalian neurons. *Mol Pharmacol*, **65**, 665-674.

Guo, K., Mou, X., Huang, J., Xiong, N. & Li, H. (2014) Trans-caryophyllene suppresses hypoxia-induced neuroinflammatory responses by inhibiting NF-κB activation in microglia. *J Mol Neurosci*, **54**, 41-48.

H

Han, S., Tai, C., Jones, C.J., Scheuer, T. & Catterall, W.A. (2014) Enhancement of inhibitory neurotransmission by $GABA_A$ receptors having α2,3-subunits ameliorates behavioral deficits in a mouse model of autism. *Neuron*, **81**, 1282-1289.

Han, S., Tai, C., Westenbroek, R.E., Yu, F.H., Cheah, C.S., Potter, G.B., Rubenstein, J.L., Scheuer, T., de la Iglesia, H.O. & Catterall, W.A. (2012) Autistic-like behaviour in $Scn1a^{+/-}$ mice and rescue by enhanced GABA-mediated neurotransmission. *Nature*, **489**, 385-390.

Hansen, K.B., Rosenkilde, M.M., Knop, F.K., Wellner, N., Diep, T.A., Rehfeld, J.F., Andersen, U.B., Holst, J.J. & Hansen, H.S. (2011) 2-Oleoyl glycerol is a GPR119 agonist and signals GLP-1 release in humans. *J Clin Endocrinol Metab*, **96**, 1409-1417.

Hanuš, L.o. & Hod, Y. (2020) Terpenes/terpenoids in cannabis: are they important? *Med Cannabis Cannabinoids*, **3**, 25-60.

Hattiangady, B., Rao, M.S. & Shetty, A.K. (2004) Chronic temporal lobe epilepsy is associated with severely declined dentate neurogenesis in the adult hippocampus. *Neurobiol Dis*, **17**, 473-490.

Hawkins, N. A., Calhoun, J. D., Huffman, A. M. & Kearney, J. A. (2019) Gene expression profiling in a mouse model of Dravet syndrome. *Exp Neurol*, **311**, 247-256.

Herkenham, M., Lynn, A.B., Johnson, M.R., Melvin, L.S., de Costa, B.R. & Rice, K.C. (1991) Characterization and localization of cannabinoid receptors in rat brain: a quantitative in vitro autoradiographic study. *J Neurosci*, **11**, 563-583.

Hernández-León, A., González-Trujano, M.E., Narváez-González, F., Pérez-Ortega, G., Rivero-Cruz, F. & Aguilar, M.I. (2020) Role of β-caryophyllene in the antinociceptive and anti-inflammatory effects of Tagetes lucida Cav. essential oil. *Molecules*, **25**, 675.

Heyser, C.J. (2004) Assessment of developmental milestones in rodents. *Curr Protoc Neurosci*, **25**, 8.18.1-8.18.15.

Hillard, C.J., Edgemond, W.S., Jarrahian, A. & Campbell, W.B. (1997) Accumulation of N-arachidonoylethanolamine (anandamide) into cerebellar granule cells occurs via facilitated diffusion. *J Neurochem*, **69**, 631-638.

Hofmann, M.E. & Frazier, C.J. (2013) Marijuana, endocannabinoids, and epilepsy: potential and challenges for improved therapeutic intervention. *Exp Neurol*, **244**, 43-50.

Howlett, A.C., Barth, F., Bonner, T.I., Cabral, G., Casellas, P., Devane, W.A., Felder, C.C., Herkenham, M., Mackie, K., Martin, B.R., Mechoulam, R. & Pertwee, R.G. (2002) International Union of Pharmacology. XXVII. Classification of cannabinoid receptors. *Pharmacol Rev*, **54**, 161-202.

Hua, T., Vemuri, K., Pu, M., Qu, L., Han, G.W., Wu, Y., Zhao, S., Shui, W., Li, S., Korde, A., Laprairie, R.B., Stahl, E.L., Ho, J.H., Zvonok, N., Zhou, H., Kufareva, I., Wu, B., Zhao, Q., Hanson, M.A., Bohn, L.M., Makriyannis, A., Stevens, R.C. & Liu, Z.J. (2016) Crystal structure of the human cannabinoid receptor CB_1. *Cell*, **167**, 750-762.e714.

Huntsman, R.J., Tang-Wai, R. & Shackelford, A.E. (2020) Cannabis for pediatric epilepsy. *J Clin Neurophysiol*, **37**, 2-8.

J

Jacob, A. & Todd, A.R. (1940) Cannabis indica. Part II. Isolation of cannabidiol from Egyptian hashish. Observations on the structure of cannabinol. *J Chem Soc*, **1940**, 649-653.

Jansen, F.E., Sadleir, L.G., Harkin, L.A., Vadlamudi, L., McMahon, J.M., Mulley, J.C., Scheffer, I.E. & Berkovic, S.F. (2006) Severe myoclonic epilepsy of infancy (Dravet syndrome): recognition and diagnosis in adults. *Neurology*, **67**, 2224-2226.

Javed, H., Azimullah, S., Haque, M.E. & Ojha, S.K. (2016) Cannabinoid type 2 (CB_2) receptors activation protects against oxidative stress and neuroinflammation associated dopaminergic neurodegeneration in rotenone model of Parkinson's disease. *Front Neurosci*, **10**, 321.

Jensen, F.E. (2002) The role of glutamate receptor maturation in perinatal seizures and brain injury. *Int J Dev Neurosci*, **20**, 339-347.

Johnston, M.V., Fatemi, A., Wilson, M.A. & Northington, F. (2011) Treatment advances in neonatal neuroprotection and neurointensive care. *Lancet Neurol*, **10**, 372-382.

Jones, N.A., Glyn, S.E., Akiyama, S., Hill, T.D., Hill, A.J., Weston, S.E., Burnett, M.D., Yamasaki, Y., Stephens, G.J., Whalley, B.J. & Williams, C.M. (2012) Cannabidiol exerts anti-convulsant effects in animal models of temporal lobe and partial seizures. *Seizure*, **21**, 344-352.

Jones, N.A., Hill, A.J., Smith, I., Bevan, S.A., Williams, C.M., Whalley, B.J. & Stephens, G.J. (2010) Cannabidiol displays antiepileptiform and antiseizure properties in vitro and in vivo. *J Pharmacol Exp Ther*, **332**, 569-577.

K

Kaczocha, M., Hermann, A., Glaser, S.T., Bojesen, I.N. & Deutsch, D.G. (2006) Anandamide uptake is consistent with rate-limited diffusion and is regulated by the degree of its hydrolysis by fatty acid amide hydrolase. *J Biol Chem*, **281**, 9066-9075.

Kadry, H., Noorani, B. & Cucullo, L. (2020) A blood–brain barrier overview on structure, function, impairment, and biomarkers of integrity. *Fluids Barriers CNS*, **17**, 69.

Kalume, F., Westenbroek, R.E., Cheah, C.S., Yu, F.H., Oakley, J.C., Scheuer, T. & Catterall, W.A. (2013) Sudden unexpected death in a mouse model of Dravet syndrome. *J Clin Invest*, **123**, 1798-1808.

Kalume, F., Yu, F.H., Westenbroek, R.E., Scheuer, T. & Catterall, W.A. (2007) Reduced sodium current in Purkinje neurons from $Na_V1.1$ mutant mice: implications for ataxia in severe myoclonic epilepsy in infancy. *J Neurosci*, **27**, 11065-11074.

Kandratavicius, L., Balista, P.A., Lopes-Aguiar, C., Ruggiero, R.N., Umeoka, E.H., Garcia-Cairasco, N., Bueno-Junior, L.S. & Leite, J.P. (2014) Animal models of epilepsy: use and limitations. *Neuropsychiatr Dis Treat*, **10**, 1693-1705.

Kang, J.Q., Shen, W. & Macdonald, R.L. (2006) Why does fever trigger febrile seizures? $GABA_A$ receptor γ2 subunit mutations associated with idiopathic generalized epilepsies have temperature-dependent trafficking deficiencies. *J Neurosci*, **26**, 2590-2597.

Kanner, A. M., Mazarati, A. & Koepp, M. (2014) Biomarkers of epileptogenesis: psychiatric comorbidities (?). *Neurotherapeutics*, **11**, 358-372.

Kanojia, U., Chaturbhuj, S.G., Sankhe, R., Das, M., Surubhotla, R., Krishnadas, N., Gourishetti, K., Nayak, P.G. & Kishore, A. (2021) Beta-caryophyllene, a CB2R selective agonist, protects against cognitive impairment caused by neuro-inflammation and not in dementia due to ageing induced by mitochondrial dysfunction. *CNS Neurol Disord Drug*.

Kaplan, J.S., Stella, N., Catterall, W.A. & Westenbroek, R.E. (2017) Cannabidiol attenuates seizures and social deficits in a mouse model of Dravet syndrome. *Proc Natl Acad Sci USA*, **114**, 11229-11234.

Kaplan, M.S. & Hinds, J.W. (1977) Neurogenesis in the adult rat: electron microscopic analysis of light radioautographs. *Science*, **197**, 1092-1094.

Karanian, D.A., Karim, S.L., Wood, J.T., Williams, J.S., Lin, S., Makriyannis, A. & Bahr, B.A. (2007) Endocannabinoid enhancement protects against kainic acid-induced seizures and associated brain damage. *J Pharmacol Exp Ther*, **322**, 1059-1066.

Kassner, A. & Merali, Z. (2015) Assessment of blood-brain barrier disruption in stroke. *Stroke*, **46**, 3310-3315.

Kawamura, Y., Fukaya, M., Maejima, T., Yoshida, T., Miura, E., Watanabe, M., Ohno-Shosaku, T. & Kano, M. (2006) The CB_1 cannabinoid receptor is the major cannabinoid receptor at excitatory presynaptic sites in the hippocampus and cerebellum. *J Neurosci*, **26**, 2991-3001.

Kearn, C.S., Blake-Palmer, K., Daniel, E., Mackie, K. & Glass, M. (2005) Concurrent stimulation of cannabinoid CB_1 and dopamine D2 receptors enhances heterodimer formation: a mechanism for receptor cross-talk? *Mol Pharmacol*, **67**, 1697-1704.

Kesner, A.J. & Lovinger, D.M. (2020) Cannabinoids, endocannabinoids and sleep. *Front Mol Neurosci*, **13**, 125.

Kim, S.Y., Jin, C.Y., Kim, C.H., Yoo, Y.H., Choi, S.H., Kim, G.Y., Yoon, H.M., Park, H.T. & Choi, Y.H. (2019) Isorhamnetin alleviates lipopolysaccharide-induced inflammatory responses in BV2 microglia by inactivating NF-κB, blocking the TLR4 pathway and reducing ROS generation. *Int J Mol Med*, **43**, 682-692.

Kohno, M., Hasegawa, H., Inoue, A., Muraoka, M., Miyazaki, T., Oka, K. & Yasukawa, M. (2006) Identification of N-arachidonylglycine as the endogenous ligand for orphan G-protein coupled receptor GPR18. *Biochem Biophys Res Commun*, **347**, 827-832.

Kovac, S., Dinkova-Kostova, A.T., Herrmann, A.M., Melzer, N., Meuth, S.G. & Gorji, A. (2017) Metabolic and homeostatic changes in seizures and acquired epilepsy-mitochondria, calcium dynamics and reactive oxygen species. *Int J Mol Sci*, **18**, 1935.

Kralic, J.E., Ledergerber, D.A. & Fritschy, J.M. (2005) Disruption of the neurogenic potential of the dentate gyrus in a mouse model of temporal lobe epilepsy with focal seizures. *Eur J Neurosci*, **22**, 1916-1927.

Kreitzer, A.C. & Regehr, W.G. (2001) Retrograde inhibition of presynaptic calcium influx by endogenous cannabinoids at excitatory synapses onto Purkinje cells. *Neuron*, **29**, 717-727.

Krueger, J. & Berg, A.T. (2015) Incidence of Dravet Syndrome in a US Population. *Pediatr Neurol Briefs*, **29**, 92.

Kuo, F.S., Cleary, C.M., LoTurco, J.J., Chen, X. & Mulkey, D.K. (2019) Disordered breathing in a mouse model of Dravet syndrome. *eLife*, **8**, e43387.

L

Laprairie, R.B., Bagher, A.M., Kelly, M.E.M. & Denovan-Wright, E.M. (2015) Cannabidiol is a negative allosteric modulator of the cannabinoid CB_1 receptor. *Br J Pharmacol*, **172**, 4790-4805.

Lauckner, J.E., Hille, B. & Mackie, K. (2005) The cannabinoid agonist WIN55,212-2 increases intracellular calcium via CB_1 receptor coupling to Gq/11 G proteins. *Proc Natl Acad Sci USA*, **102**, 19144-19149.

Lauckner, J.E., Jensen, J.B., Chen, H.Y., Lu, H.C., Hille, B. & Mackie K. (2008) GPR55 is a cannabinoid receptor that increases intracellular calcium and inhibits M current. *Proc Natl Acad Sci USA*, **105**, 2699-2704.

Laviolette, S.R. & Grace, A.A. (2006) The roles of cannabinoid and dopamine receptor systems in neural emotional learning circuits: implications for schizophrenia and addiction. *Cell Mol Life Sci*, **63**, 1597-1613.

Leweke, F.M., Piomelli, D., Pahlisch, F., Muhl, D., Gerth, C.W., Hoyer, C., Klosterkötter, J., Hellmich, M. & Koethe, D. (2012) Cannabidiol enhances anandamide signaling and alleviates psychotic symptoms of schizophrenia. *Transl Psychiatry*, **2**, e94.

Li, R., Fang, H., Shen, J., Jin, Y., Zhao, Y., Wang, R., Fu, Y., Tian, Y., Yu, H. & Zhang, J. (2021) Curcumin alleviates LPS-induced oxidative stress, inflammation and apoptosis in bovine mammary epithelial cells via the NFE2L2 signaling pathway. *Toxins*, **13**, 208.

Li, X., Hua, T., Vemuri, K., Ho, J.H., Wu, Y., Wu, L., Popov, P., Benchama, O., Zvonok, N., Locke, K., Qu, L., Han, G.W., Iyer, M.R., Cinar, R., Coffey, N.J., Wang, J., Wu, M., Katritch, V., Zhao, S., Kunos, G., Bohn, L.M., Makriyannis, A., Stevens, R.C. & Liu. Z.J. (2019) Crystal structure of the human cannabinoid receptor CB_2. *Cell*, **176**, 459-467.

Librizzi, L., Noè, F., Vezzani, A., de Curtis, M. & Ravizza, T. (2012) Seizure-induced brain-borne inflammation sustains seizure recurrence and blood-brain barrier damage. *Ann Neurol*, **72**, 82-90.

Ligresti, A., De Petrocellis, L. & Di Marzo, V. (2016) From phytocannabinoids to cannabinoid receptors and endocannabinoids: pleiotropic physiological and pathological roles through complex pharmacology. *Physiol Rev*, **96**, 1593-1659.

Lindsey, L.P., Daphney, C.M., Oppong-Damoah, A., Uchakin, P.N., Abney, S.E., Uchakina, O.N., Khusial, R.D., Akil, A. & Murnane, K.S. (2019) The cannabinoid receptor 2 agonist, β-caryophyllene, improves working memory and reduces circulating levels of specific proinflammatory cytokines in aged male mice. *Behav Brain Res*, **372**, 112012.

Liu, F., Peng, J., Zhu, C., Xiao, H., He, F., Yin, F. & Chen, C. (2019) Efficacy of the ketogenic diet in Chinese children with Dravet syndrome: a focus on neuropsychological development. *Epilepsy Behav*, **92**, 98-102.

Liu, H., Song, Z., Liao, D., Zhang, T., Liu, F., Zhuang, K., Luo, K. & Yang, L. (2015) Neuroprotective effects of trans-caryophyllene against kainic acid induced seizure activity and oxidative stress in mice. *Neurochem Res*, **40**, 118-123.

Liu, Z., Wang, S., Liu, J., Wang, F., Liu, Y. & Zhao, Y. (2016) Leukocyte infiltration triggers seizure recurrence in a rat model of temporal lobe epilepsy. *Inflammation*, **39**, 1090-1098.

Lombard, C., Nagarkatti, M. & Nagarkatti, P. (2007) CB2 cannabinoid receptor agonist, JWH-015, triggers apoptosis in immune cells: potential role for CB2-selective ligands as immunosuppressive agents. *Clin Immunol*, **122**, 259-270.

López, A., Aparicio, N., Pazos, M.R., Grande, M.T., Barreda-Manso, M.A., Benito-Cuesta, I., Vázquez, C., Amores, M., Ruiz-Pérez, G., García-García, E., Beatka, M., Tolón, R.M., Dittel, B.N., Hillard, C.J. & Romero, J. (2018) Cannabinoid CB_2 receptors in the mouse brain: relevance for Alzheimer's disease. *J Neuroinflammation*, **15**, 158.

Löscher, W. (2009) Preclinical assessment of proconvulsant drug activity and its relevance for predicting adverse events in humans. *Eur J Pharmacol*, **610**, 1-11.

Löscher, W. (2011) Critical review of current animal models of seizures and epilepsy used in the discovery and development of new antiepileptic drugs. *Seizure*, **20**, 359-368.

Lossin, C. (2009) A catalog of SCN1A variants. *Brain Dev*, **31**, 114-130.

Lozano, I. (2001) The Therapeutic Use of Cannabis sativa (L.) in Arabic Medicine. *J Cannabis Ther*, **1**, 63-70.

Ludányi, A., Eross, L., Czirják, S., Vajda, J., Halász, P., Watanabe, M., Palkovits, M., Maglóczky, Z., Freund, T.F. & Katona, I. (2008) Downregulation of the CB_1 cannabinoid receptor and related molecular elements of the endocannabinoid system in epileptic human hippocampus. *J Neurosci*, **28**, 2976-2990.

Luskin M.B. (1993) Restricted proliferation and migration of postnatally generated neurons derived from the forebrain subventricular zone. *Neuron*, **11**, 173-189.

M

Maa, E. & Figi, P. (2014) The case for medical marijuana in epilepsy. *Epilepsia*, **55**, 783-786.

Machado, K., Islam, M.T., Ali, E.S., Rouf, R., Uddin, S.J., Dev, S., Shilpi, J.A., Shill, M.C., Reza, H.M., Das, A.K., Shaw, S., Mubarak, M.S., Mishra, S.K. & Melo-Cavalcante, A. (2018) A systematic review on the neuroprotective perspectives of beta-caryophyllene. *Phytother Res*, **32**, 2376-2388.

Mackie, K. (2005) Distribution of cannabinoid receptors in the central and peripheral nervous system. *Handb Exp Pharmacol*, **168**, 299-325.

Manda-Handzlik, A. & Demkow, U. (2019) The brain entangled: the contribution of neutrophil extracellular traps to the diseases of the central nervous system. *Cells*, **8**, 1477.

Marchi, N., Granata, T., Ghosh, C. & Janigro, D. (2012) Blood-brain barrier dysfunction and epilepsy: pathophysiologic role and therapeutic approaches. *Epilepsia*, **53**, 1877-1886.

Marini, C., Scheffer, I.E., Nabbout, R., Suls, A., De Jonghe, P., Zara, F. & Guerrini, R. (2011) The genetics of Dravet syndrome. *Epilepsia*, **52**, 24-29.

Marsicano, G., Goodenough, S., Monory, K., Hermann, H., Eder, M., Cannich, A., Azad, S.C., Cascio, M.G., Gutierrez, S.O., van der Stelt, M., Lopez-Rodriguez, M.L., Casanova, E., Schütz, G., Zieglgänsberger, W., Di Marzo, V., Behl, C. & Lutz, B. (2003) CB_1 cannabinoid receptors and on-demand defense against excitotoxicity. *Science*, **302**, 84-88.

Marsicano, G., Wotjak, C.T., Azad, S.C., Bisogno, T., Rammes, G., Cascio, M.G., Hermann, H., Tang, J., Hofmann, C., Zieglgänsberger, W., Di Marzo, V. & Lutz, B. (2002) The endogenous cannabinoid system controls extinction of aversive memories. *Nature*, **418**, 530-534.

Martin, B.R., Compton, D.R., Thomas, B.F., Prescott, W.R., Little, P.J., Razdan, R.K., Johnson, M.R., Melvin, L.S., Mechoulam, R. & Ward, S.J. (1991) Behavioral, biochemical, and molecular modeling evaluations of cannabinoid analogs. *Pharmacol Biochem Behav*, **40**, 471-478.

Martin, M.S., Dutt, K., Papale, L.A., Dubé, C.M., Dutton, S.B., de Haan, G., Shankar A, Tufik, S., Meisler, M.H., Baram, T.Z., Goldin, A.L. & Escayg, A. (2010) Altered function of the SCN1A voltage-gated sodium channel leads to gamma-aminobutyric acid-ergic (GABAergic) interneuron abnormalities. *J Biol Chem*, **285**, 9823-9834.

Martín-Suárez, S., Abiega, O., Ricobaraza, A., Hernandez-Alcoceba, R. & Encinas, J.M. (2020) Alterations of the hippocampal neurogenic niche in a mouse model of Dravet syndrome. *Front Cell Dev Biol*, **8**, 654.

Martínez-Pinilla, E., Reyes-Resina, I., Oñatibia-Astibia, A., Zamarbide, M., Ricobaraza, A., Navarro, G., Moreno, E., Dopeso-Reyes, I.G., Sierra, S., Rico, A.J., Roda, E., Lanciego, J.L. & Franco, R. (2014) CB_1 and GPR55 receptors are co-expressed and form heteromers in rat and monkey striatum. *Exp Neurol*, **261**, 44-52.

Martínez-Pinilla, E., Varani, K., Reyes-Resina, I., Angelats, E., Vincenzi, F., Ferreiro-Vera, C., Oyarzabal, J., Canela, E.I., Lanciego, J.L., Nadal, X., Navarro, G., Borea, P.A. & Franco, R. (2017) Binding and signaling studies disclose a potential allosteric site for cannabidiol in cannabinoid CB_2 receptors. *Front Pharmacol*, **8**, 1-10.

Mashimo, T., Ohmori, I., Ouchida, M., Ohno, Y., Tsurumi, T., Miki, T., Wakamori, M., Ishihara, S., Yoshida, T., Takizawa, A., Kato, M., Hirabayashi, M., Sasa, M., Mori, Y. & Serikawa, T. (2010) A missense mutation of the gene encoding voltage-dependent sodium channel (Nav1.1) confers susceptibility to febrile seizures in rats. *J Neurosci*, **30**, 5744-5753.

Matsuda, L.A., Lolait, S.J., Brownstein, M.J., Young, A.C. & Bonner, T.I. (1990) Structure of a cannabinoid receptor and functional expression of the cloned cDNA. *Nature*, **346**, 561-564.

Mechoulam, R. & Carlini, E.A. (1978) Toward drugs derived from cannabis. *Naturwissenschaften*, **65**, 174-179.

Mechoulam, R., Hanuš, L.O., Pertwee, R.G. & Howlett, A.C. (2014) Early phytocannabinoid chemistry to endocannabinoids and beyond. *Nat Rev Neurosci*, **15**, 757-764.

Mechoulam, R. & Parker, L.A. (2013) The endocannabinoid system and the brain. *Annu Rev Psychol*, **64**, 21-47.

Mechoulam, R. & Shvo, Y. (1963) Hashish-I. The structure of cannabidiol. *Tetrahedron*, **19**, 2073-2078.

Meira, I.D., Romão, T.T., Do Prado, H.J., Krüger, L.T., Pires, M.E. & da Conceição, P.O. (2019) Ketogenic diet and epilepsy: what we know so far. *Front Neurosci*, **13**, 1-8.

Miller, A.R., Hawkins, N.A., McCollom, C.E. & Kearney, J.A. (2014) Mapping genetic modifiers of survival in a mouse model of Dravet syndrome. *Genes Brain Behav*, **13**, 163-172.

Miller, I., Scheffer, I.E., Gunning, B., Sanchez-Carpintero, R., Gil-Nagel, A., Perry, M.S., Saneto, R.P., Checketts, D., Dunayevich, E., Knappertz, V. & GWPCARE2 Study Group (2020) Dose-ranging effect of adjunctive oral cannabidiol vs placebo on convulsive seizure frequency in Dravet syndrome: a randomized clinical trial. *JAMA Neurol*, **77**, 613-621.

Ming, G.L. & Song, H. (2011) Adult neurogenesis in the mammalian brain: significant answers and significant questions. *Neuron*, **70**, 687-702.

Mirza, A.Z., Althagafi, I.I. & Shamshad, H. (2019) Role of PPAR receptor in different diseases and their ligands: Physiological importance and clinical implications. *Eur J Med Chem*, **15**, 502-513.

Mishra, S., Reznikov, V., Maltsev, V.A., Undrovinas, N.A., Sabbah, H.N. & Undrovinas, A. (2015) Contribution of sodium channel neuronal isoform Nav1.1 to late sodium current in ventricular myocytes from failing hearts. *J Physiol*, **593**, 1409-1427.

Molina-Holgado, E., Vela, J.M., Arévalo-Martín, A., Almazán, G., Molina-Holgado, F., Borrell, J. & Guaza, C. (2002) Cannabinoids promote oligodendrocyte progenitor survival: involvement of cannabinoid receptors and phosphatidylinositol-3 kinase/Akt signaling. *J Neurosci*, **22**, 9742-9753.

Montero, C., Campillo, N.E., Goya, P. & Páez, J.A. (2005) Homology models of the cannabinoid CB1 and CB2 receptors. A docking analysis study. *Eur J Med Chem*, **40**, 75-83.

Morales, P., Hurst, D.P. & Reggio, P.H. (2017) Molecular targets of the phytocannabinoids - a complex picture. *Prog Chem Org Nat Prod*, **103**, 103-131.

Moreno, E., Andradas, C., Medrano, M., Caffarel, M.M., Pérez-Gómez, E., Blasco-Benito, S., Gómez-Cañas, M., Pazos, M.R., Irving, A.J., Lluís, C., Canela, E.I., Fernández-Ruiz, J., Guzmán, M., McCormick, P.J. & Sánchez, C. (2014) Targeting CB_2-GPR55 receptor heteromers modulates cancer cell signaling. *J Biol Chem*, **289**, 21960-21972.

Moreno, E., Chiarlone, A., Medrano, M., Puigdellívol, M., Bibic, L., Howell, L.A., Resel, E., Puente, N., Casarejos, M.J., Perucho, J., Botta, J., Suelves, N., Ciruela, F., Ginés, S., Galve-Roperh, I., Casadó, V., Grandes, P., Lutz, B., Monory, K., Canela, E.I., Lluís, C., McCormick, P.J. & Guzmán, M. (2018) Singular location and signaling profile of adenosine A2A-cannabinoid CB_1 receptor heteromers in the dorsal striatum. *Neuropsychopharmacology*, **43**, 964-977.

Morimoto, M., Shimakawa, S., Hashimoto, T., Kitaoka, T. & Kyotani, S. (2017) Marked efficacy of combined three-drug therapy (sodium valproate, topiramate and stiripentol) in a patient with Dravet syndrome. *J Clin Pharm Ther*, **43**, 571-573.

Moya, M.L., Triplett, M., Simon, M., Alvarado, J., Booth, R., Osburn, J., Soscia, D., Qian, F., Fischer, N.O., Kulp, K. & Wheeler, E.K. (2020) A reconfigurable *in vitro* model for studying the blood-brain barrier. *Ann Biomed Eng*, **48**, 780-793.

Muller, C., Morales, P. & Reggio, P.H. (2019) Cannabinoid ligands targeting TRP channels. *Front Mol Neurosci*, **11**, 487.

Munguía-Martínez, M.F., Nava-Ruíz, C., Ruíz-Díaz, A., Díaz-Ruíz, A., Yescas-Gómez, P. & Méndez-Armenta, M. (2019) Immunohistochemical study of antioxidant enzymes regulated by Nrf2 in the models of epileptic seizures (KA and PTZ). *Oxid Med Cell Longev*, **2019**, 1327986.

Munro, S., Thomas, K.L. & Abu-Shaar, M. (1993) Molecular characterization of a peripheral receptor for cannabinoids. *Nature*, **365**, 61-65.

Muro-García, T., Martín-Suárez, S., Espinosa, N., Valcárcel-Martín, R., Marinas, A., Zaldumbide, L., Galbarriatu, L., Sierra, A., Fuentealba, P. & Encinas, J.M. (2019) Reactive disruption of the hippocampal neurogenic niche after induction of seizures by injection of kainic acid in the amygdala. *Front Cell Dev Biol*, **7**, 158.

Murataeva, N., Dhopeshwarkar, A., Yin, D., Mitjavila, J., Bradshaw, H., Straiker, A. & Mackie, K. (2016) Where's my entourage? The curious case of 2-oleoylglycerol, 2-linolenoylglycerol, and 2-palmitoylglycerol. Pharmacol Res, **110**, 173-180.

N

Naidoo, V., Karanian, D.A., Vadivel, S.K., Locklear, J.R., Wood, J.T., Nasr, M., Quizon, P.M., Graves, E.E., Shukla, V., Makriyannis, A. & Bahr, B.A. (2012) Equipotent inhibition of fatty acid amide hydrolase and monoacylglycerol lipase-dual targets of the endocannabinoid system to protect against seizure pathology. *Neurotherapeutics*, **9**, 801-813.

Naidoo, V., Nikas, S.P., Karanian, D.A., Hwang, J., Zhao, J., Wood, J.T., Alapafuja, S.O., Vadivel, S.K., Butler, D., Makriyannis, A. & Bahr, B.A. (2011) A new generation fatty acid amide hydrolase inhibitor protects against kainate-induced excitotoxicity. *J Mol Neurosci*, **43**, 493-502.

Navarro, G., Morales, P., Rodríguez-Cueto, C., Fernández-Ruiz, J., Jagerovic, N. & Franco, R. (2016) Targeting cannabinoid CB_2 receptors in the central nervous system. Medicinal chemistry approaches with focus on neurodegenerative Disorders. *Front Neurosci*, **10**, 406.

Navia-Paldanius, D., Savinainen, J.R. & Laitinen, J.T. (2012) Biochemical and pharmacological characterization of human α/β-hydrolase domain containing 6 (ABHD6) and 12 (ABHD12). *J Lipid Res*, **53**, 2413-2424.

Neumeister, A., Seidel, J., Ragen, B.J. & Pietrzak, R.H. (2015) Translational evidence for a role of endocannabinoids in the etiology and treatment of posttraumatic stress disorder. *Psychoneuroendocrinology*, **51**, 577-584.

Nichol K., Stott C., Jones N., Gray R.A., Bazelot M. & Whalley B.J. (2019) The proposed multimodal mechanism of action of cannabidiol (CBD) in epilepsy: Modulation of intracellular calcium and adenosine-mediated signaling (P5.5-007) *Neurology*, **92**, P5.5-007.

Nicolussi, S. & Gertsch, J. (2015) Endocannabinoid transport revisited. In: *Vitamins and hormones*. pp. 441-485.

Núñez, E., Benito, C., Pazos, M.R., Barbachano, A., Fajardo, O., Gonzalez, S., Tolon, R.M. & Romero, J. (2004) Cannabinoid CB_2 receptors are expressed by perivascular microglial cells in the human brain: an immunohistochemical study. *Synapse*, **53**, 208-213.

O

O'Shaughnessy, W.B. (1843) On the preparations of the Indian hemp, or gunjah (Cannabis indica). *Prov Med J Retrosp Med Sci*, **5**, 363-369.

O'Sullivan, S.E. (2016) An update on PPAR activation by cannabinoids. *Br J Pharmacol*, **173**, 1899-1910.

Oakley, J.C., Kalume, F., Yu, F.H., Scheuer, T. & Catterall, W.A. (2009) Temperature- and age-dependent seizures in a mouse model of severe myoclonic epilepsy in infancy. *Proc Natl Acad Sci USA*, **106**, 3994-3999.

Ogawa, K., Yabe, H., Kitayama, T. & Ito, M. (2016) Locomotor-reducing activity of sesquiterpenes related to zingiber zerumbet essential oil and hexahydrozerumbone derivatives. *Biol Pharm Bull*, **39**, 1077-1080.

Ogino, T., Ohtsuka. Y., Yamatogi, Y. & Ohtahara, S. (1986) Severe myoclonic epilepsy in infancy: clinical-electroencephalographic and long-term follow-up studies. *Brain Dev*, **8**,162.

Ogiwara, I., Iwasato, T., Miyamoto, H., Iwata, R., Yamagata, T., Mazaki, E., Yanagawa, Y., Tamamaki, N., Hensch, T.K., Itohara, S. & Yamakawa, K. (2013) Nav1.1 haploinsufficiency in excitatory neurons ameliorates seizure associated sudden death in a mouse model of Dravet syndrome. *Hum Mol Genet*, **22**, 4784-4804.

Ogiwara, I., Miyamoto, H., Morita, N., Atapour, N., Mazaki, E., Inoue, I., Takeuchi, T., Itohara, S., Yanagawa, Y., Obata, K., Furuichi, T., Hensch, T.K. & Yamakawa, K. (2007) Na(v)1.1 localizes to axons of parvalbumin-positive inhibitory interneurons: a circuit basis for epileptic seizures in mice carrying a Scn1a gene mutation. *J Neurosci*, **27**, 5903-5914.

Oguni, H., Hayashi, K., Awaya, Y., Fukuyama, Y. & Osawa, M. (2001) Severe myoclonic epilepsy in infants - a review based on the Tokyo Women's medical university series of 84 cases. *Brain Dev*, **23**, 736-748.

Ojha, S., Javed, H., Azimullah, S. & Haque, M.E. (2016) β-caryophyllene, a phytocannabinoid attenuates oxidative stress, neuroinflammation, glial activation, and salvages dopaminergic neurons in a rat model of Parkinson disease. *Mol Cell Biochem*, **418**, 59-70.

Oka, S., Toshida, T., Maruyama, K., Nakajima, K., Yamashita, A. & Sugiura, T. (2009) 2-Arachidonoyl-snglycero-3-phosphoinositol: a possible natural ligand for GPR55. *J Biochem*, **145**, 13-20.

Oliveira da Cruz, J.F., Robin, L.M., Drago, F., Marsicano, G. & Metna-Laurent, M. (2016) Astroglial type-1 cannabinoid receptor (CB_1): A new player in the tripartite synapse. *Neuroscience*, **323**, 35-42.

Overton, H.A., Babbs, A.J., Doel, S.M., Fyfe, M.C., Gardner, L.S., Griffin, G., Jackson, H.C., Procter, M.J., Rasamison, C.M., Tang-Christensen, M., Widdowson, P.S., Williams, G.M. & Reynet, C. (2006) Deorphanization of a G protein-coupled receptor for oleoylethanolamide and its use in the discovery of small-molecule hypophagic agents. *Cell Metab*, **3**, 167-175.

P

Pacher, P. & Mechoulam, R. (2011) Is lipid signaling through cannabinoid 2 receptors part of a protective system? *Prog Lipid Res*, **50**, 193-211.

Palazuelos, J., Aguado, T., Pazos, M.R., Julien, B., Carrasco, C., Resel, E., Sagredo, O., Benito, C., Romero, J., Azcoitia, I., Fernández-Ruiz, J., Guzmán, M. & Galve-Roperh, I. (2009) Microglial CB_2 cannabinoid receptors are neuroprotective in Huntington's disease excitotoxicity. *Brain*, **132**, 3152-3164.

Palazuelos, J., Ortega, Z., Díaz-Alonso, J., Guzmán, M. & Galve-Roperh, I. (2012) CB_2 cannabinoid receptors promote neural progenitor cell proliferation via mTORC1 signaling. *J Biol Chem*, **287**, 1198-1209.

Palomo-Garo, C., Gómez-Gálvez, Y., García, C. & Fernández-Ruiz J. (2016) Targeting the cannabinoid CB_2 receptor to attenuate the progression of motor deficits in LRRK2-transgenic mice. *Pharmacol Res*, **110**, 181-192.

Panikashvili, D., Simeonidou, C., Ben-Shabat, S., Hanus, L., Breuer, A., Mechoulam, R. & Shohami, E. (2001) An endogenous cannabinoid (2-AG) is neuroprotective after brain injury. *Nature*, **413**, 527-531.

Parent, J.M., Yu, T.W., Leibowitz, R.T., Geschwind, D.H., Sloviter, R.S. & Lowenstein, D.H. (1997) Dentate granule cell neurogenesis is increased by seizures and contributes to aberrant network reorganization in the adult rat hippocampus. *J Neurosci*, **17**, 3727-3738.

Parker, L.A., Rock, E.M. & Limebeer, C.L. (2011) Regulation of nausea and vomiting by cannabinoids. *Br J Pharmacol*, **163**, 1411-1422.

Patel, D.C., Tewari, B.P., Chaunsali, L. & Sontheimer, H. (2019) Neuron-glia interactions in the pathophysiology of epilepsy. *Nat Rev Neurosci*, **20**, 282-297.

Patra, P.H., Barker-Haliski, M.L., White, H.S., Whalley, B.J., Glyn, S., Sandhu, H., Jones, N., Bazelot, M., Williams, C.M. & McNeish, A.J. (2019) Cannabidiol reduces seizures and associated behavioral comorbidities in a range of animal seizure and epilepsy models. *Epilepsia*, **60**, 303-314.

Pazos, M.R., Mohammed, N., Lafuente, H., Santos, M., Martínez-Pinilla, E., Moreno, E., Valdizan, E., Romero, J., Pazos, A., Franco, R., Hillard, C.J., Alvarez, F.J. & Martínez-Orgado, J. (2013) Mechanisms of cannabidiol neuroprotection in hypoxic-ischemic newborn pigs: role of 5HT(1A) and CB_2 receptors. *Neuropharmacology*, **71**, 282-291.

Pazos, M.R., Sagredo, O. & Fernández-Ruiz, J. (2008) The endocannabinoid system in Huntington's disease. *Curr Pharm Des*, **14**, 2317-2325.

Pertwee, R.G. (2015) Endocannabinoids and their pharmacological actions. *Handb Exp Pharmacol*, **231**, 1-37.

Pertwee, R.G., Howlett, A.C., Abood, M.E., Alexander, S.P., Di Marzo, V., Elphick, M.R., Greasley, P.J., Hansen, H.S., Kunos, G., Mackie, K., Mechoulam, R. & Ross, R.A. (2010) International Union of Basic and Clinical Pharmacology. LXXIX. Cannabinoid receptors and their ligands: beyond CB_1 and CB_2. *Pharmacol Rev*, **62**, 588-631.

Picciolo, G., Pallio, G., Altavilla, D., Vaccaro, M., Oteri, G., Irrera, N. & Squadrito, F. (2020) β-caryophyllene reduces the inflammatory phenotype of periodontal cells by targeting CB_2 receptors. *Biomedicines*, **8**, 164.

Pichler, M. & Hocker, S. (2017) Management of status epilepticus. *Handb Clin Neurol*, **140**, 131-150.

Pineda, J.R. & Encinas, J.M. (2016) The contradictory effects of neuronal hyperexcitation on adult hippocampal neurogenesis. *Front Neurosci*, **10**, 74.

Piomelli, D. (2003) The molecular logic of endocannabinoid signalling. *Nat Rev Neurosci*, **4**, 873-884.

Pisanti, S., Malfitano, A.M., Ciaglia, E., Lamberti, A., Ranieri, R., Cuomo, G., Abate, M., Faggiana, G., Proto, M.C., Fiore, D., Laezza, C. & Bifulco, M. (2017) Cannabidiol: State of the art and new challenges for therapeutic applications. *Pharmacol Ther*, **175**, 133-150.

Pistis, M. & Melis, M. (2010) From surface to nuclear receptors: the endocannabinoid family extends its assets. *Curr Med Chem*, **17**, 1450-1467.

Porter, B.E. & Jacobson, C. (2013) Report of a parent survey of cannabidiol-enriched cannabis use in pediatric treatment-resistant epilepsy. *Epilepsy Behav*, **29**, 574-577.

Press, C.A., Knupp, K.G. & Chapman, K.E. (2015) Parental reporting of response to oral cannabis extracts for treatment of refractory epilepsy. *Epilepsy Behav*, **45**, 49-52.

Puttachary, S., Sharma, S., Stark, S. & Thippeswamy, T. (2015) Seizure-induced oxidative stress in temporal lobe epilepsy. *Biomed Res Int*, **2015**, 745613.

Q

Qu, L., Liu, X., Wu, C. & Leung, L.S. (2007) Hyperthermia decreases GABAergic synaptic transmission in hippocampal neurons of immature rats. *Neurobiol Dis*, **27**, 320-327.

R

Rahimi, V.B., Askari, V.R., Shirazinia, R., Soheili-Far, S., Askari, N., Rahmanian-Devin, P., Sanei-Far, Z., Mousavi, S.H. & Ghodsi, R. (2018) Protective effects of hydro-ethanolic extract of Terminalia

chebula on primary microglia cells and their polarization (M_1/M_2 balance). *Mult Scler Relat Disord*, **25**, 5-13.

Rakhade, S.N. & Jensen, F.E. (2009) Epileptogenesis in the immature brain: emerging mechanisms. *Nat Rev Neurol*, **5**, 380-391.

Remy, S. & Beck, H. (2006) Molecular and cellular mechanisms of pharmacoresistance in epilepsy. *Brain*, **129**, 18-35.

Reynolds, J.R. (1868) Therapeutical uses and toxic effects of Cannabis indica. *Lancet*, **1**, 637-638.

Ricceri, L., Michetti, C. & Scattoni, M.L. (2016) Chapter 7: Mouse behavior and models for autism spectrum disorders. Neuronal and synaptic dysfunction in autism spectrum disorder and intellectual disability. 269-293.

Ricobaraza, A., Mora-Jimenez, L., Puerta, E., Sanchez-Carpintero, R., Mingorance, A., Artieda, J., Nicolas, M. J., Besne, G., Bunuales, M., Gonzalez-Aparicio, M., Sola-Sevilla, N., Valencia, M. & Hernandez-Alcoceba, R. (2019) Epilepsy and neuropsychiatric comorbidities in mice carrying a recurrent Dravet syndrome SCN1A missense mutation. *Sci Rep*, **9**, 14172.

Rimmerman, N., Ben-Hail, D., Porat, Z., Juknat, A., Kozela, E., Daniels, M.P., Connelly, P.S., Leishman, E., Bradshaw, H.B., Shoshan-Barmatz, V. & Vogel, Z. (2013) Direct modulation of the outer mitochondrial membrane channel, voltage-dependent anion channel 1 (VDAC1) by cannabidiol: a novel mechanism for cannabinoid-induced cell death. *Cell Death Dis*, **4**, e949.

Rimmerman, N., Hughes, H.V., Bradshaw, H.B., Pazos, M.X., Mackie, K., Prieto, A.L. & Walker, J.M. (2008) Compartmentalization of endocannabinoids into lipid rafts in a dorsal root ganglion cell line. *Br J Pharmacol*, **153**, 380-389.

Rosenberg, E.C., Patra, P.H. & Whalley, B.J. (2017) Therapeutic effects of cannabinoids in animal models of seizures, epilepsy, epileptogenesis, and epilepsy-related neuroprotection. *Epilepsy Behav*, **70**, 319-327.

Rosenberg, E.C., Tsien, R.W., Whalley, B.J. & Devinsky, O. (2015) Cannabinoids and epilepsy. *Neurotherapeutics*, **12**, 747-768.

Rubinstein, M., Han, S., Tai, C., Westenbroek, R.E., Hunker, A., Scheuer, T. & Catterall, W.A. (2015) Dissecting the phenotypes of Dravet syndrome by gene deletion. *Brain*, **138**, 2219.

Rubio, M., Valdeolivas, S., Piscitelli, F., Verde, R., Satta, V., Barroso, E., Montolio, M., Aras, L. M., Di Marzo, V., Sagredo, O. & Fernández-Ruiz, J. (2016) Analysis of endocannabinoid signaling elements and related proteins in lymphocytes of patients with Dravet syndrome. *Pharmacol Res Perspect*, **4**, e00220.

Russ, S.A., Larson, K. & Halfon, N. (2012) A national profile of childhood epilepsy and seizure disorder. *Pediatrics*, **129**, 256-264.

Russo, E.B. (2011) Taming THC: potential cannabis synergy and phytocannabinoid-terpenoid entourage effects. *Br J Pharmacol*, **163**, 1344-1364.

Russo, E.B., Jiang, H.E., Li, X., Sutton, A., Carboni, A., del Bianco, F., Mandolino, G., Potter, D.J., Zhao, Y.X., Bera, S., Zhang, Y.B., Lü, E.G., Ferguson, D.K., Hueber, F., Zhao, L.C., Liu, C.J., Wang, Y.F. & Li, C.S. (2008) Phytochemical and genetic analyses of ancient cannabis from Central Asia. *J Exp Bot*, **59**, 4171-4182.

Ryberg, E., Larsson, N., Sjögren, S., Hjorth, S., Hermansson, N.O., Leonova, J., Elebring, T., Nilsson, K., Drmota, T. & Greasley, P.J. (2007) The orphan receptor GPR55 is a novel cannabinoid receptor. *Br J Pharmacol*, **152**, 1092-1101.

S

Sagredo, O., González, S., Aroyo, I., Pazos, M.R., Benito, C., Lastres-Becker, I., Romero, J.P., Tolón, R., Mechoulam, R., Brouillet, E., Romero, J. & Fernández-Ruiz, J. (2009) Cannabinoid CB_2 receptor agonists protect the striatum against malonate toxicity: relevance for Huntington's disease. *Glia*, **57**, 1154-1167.

Sagredo, O., Palazuelos, J., Gutierrez-Rodriguez, A., Satta, V., Galve-Roperh, I. & Martínez-Orgado, J. (2018) Cannabinoid signalling in the immature brain: Encephalopathies and neurodevelopmental disorders. *Biochem Pharmacol*, **157**, 85-96.

Santos, P.S., Oliveira, T.C., R Júnior, L.M., Figueiras, A. & Nunes, L. (2018) β-caryophyllene delivery systems: enhancing the oral pharmacokinetic and stability. *Curr Pharm Des*, **24**, 3440-3453.

Sarris, J., Sinclair, J., Karamacoska, D., Davidson, M. & Firth, J. (2020) Medicinal cannabis for psychiatric disorders: a clinically-focused systematic review. *BMC Psychiatry*, **20**, 24.

Satta, V., Alonso, C., Díez, P., Martín-Suárez, S., Rubio, M., Encinas, J.M., Fernández-Ruiz, J. & Sagredo, O. (2021) Neuropathological characterization of a Dravet syndrome knock-in mouse model useful for investigating cannabinoid treatments. *Front Mol Neurosci*, **13**, 602801.

Satta, V., Scherma, M., Giunti, E., Collu, R., Fattore, L., Fratta, W. & Fadda P. (2016) Emotional profile of female rats showing binge eating behavior. *Physiol Behav*, **163**, 136-143.

Scandiffio, R., Geddo, F., Cottone, E., Querio, G., Antoniotti, S., Gallo, M.P., Maffei, M.E. & Bovolin, P. (2020) Protective effects of (E)-β-caryophyllene (BCP) in chronic inflammation. *Nutrients*, **12**, 3273.

Scharfman, H.E., Goodman, J.H. & Sollas, A.L. (2000) Granule-like neurons at the hilar/CA3 border after status epilepticus and their synchrony with area CA3 pyramidal cells: functional implications of seizure-induced neurogenesis. *J Neurosci*, **20**, 6144-6158.

Scheffer, I.E., Halford, J.J., Miller, I., Nabbout, R., Sanchez-Carpintero, R., Shiloh-Malawsky, Y., Wong, M., Zolnowska, M., Checketts, D., Dunayevich, E. & Devinsky, O. (2021) Add-on cannabidiol in patients with Dravet syndrome: Results of a long-term open-label extension trial. *Epilepsia*, **62**, 2505-2517.

Schubert-Bast, S., Wolff, M., Wiemer-Kruel, A., von Spiczak, S., Trollmann, R., Reif, P.S., Pritchard, C., Polster, T., Neubauer, B.A., Mayer, T., Macdonald, D., Kurlemann, G., Kluger, G., Klein, K.M., Kieslich, M., Kay, L., Kalski, M., Irwin, J., Herting, A., Carroll, J. & Strzelczyk, A. (2019) Seizure management and prescription patterns of anticonvulsants in Dravet syndrome: A multicenter cohort study from Germany and review of literature. *Epilepsy Behav*, 98, 88-95.

Schutte, S.S., Schutte, R.J., Barragan, E.V. & o'Dowd, D.K (2016) Model systems for studying cellular mechanisms of SCN1A-related epilepsy. *J Neurophysiol*, **115**, 1755-1766.

Seri, B., García-Verdugo, J.M., McEwen, B.S. & Alvarez-Buylla, A. (2001) Astrocytes give rise to new neurons in the adult mammalian hippocampus. *J Neurosci*, **21**, 7153-7160.

Shapiro, L., Gado, F., Manera, C. & Escayg, A. (2021) Allosteric modulation of the cannabinoid 2 receptor confers seizure resistance in mice. *Neuropharmacology*, **188**, 108448.

Shapiro, L., Wong, J.C, & Escayg, A. (2019) Reduced cannabinoid 2 receptor activity increases susceptibility to induced seizures in mice. *Epilepsia*, **60**, 2359-2369.

Sharma, C., Al Kaabi, J.M., Nurulain, S.M., Goyal, S.N., Kamal, M.A. & Ojha, S. (2016) Polypharmacological properties and therapeutic potential of β-caryophyllene: a dietary phytocannabinoid of pharmaceutical promise. *Curr Pharm Des*, **22**, 3237-3264.

Shen, W., Poliquin, S., Macdonald, R.L., Dong, M. & Kang, J.Q. (2020) Endoplasmic reticulum stress increases inflammatory cytokines in an epilepsy mouse model Gabrg2$^{+/Q390X}$ knockin: A link between genetic and acquired epilepsy? *Epilepsia*, **61**, 2301-2312.

Shirazi-zand, Z., Ahmad-Molaei, L., Motamedi, F. & Naderi, N. (2013) The role of potassium BK channels in anticonvulsant effect of cannabidiol in pentylenetetrazole and maximal electroshock models of seizure in mice. *Epilepsy Behav*, **28**, 1-7.

Shmuely, S., Sisodiya, S.M., Gunning, W.B., Sander, J.W. & Thijs, R.D. (2016) Mortality in Dravet syndrome: A review. *Epilepsy Behav*, **64**, 69-74.

Sierra, A., Martín-Suárez, S., Valcárcel-Martín, R., Pascual-Brazo, J., Aelvoet, S.A., Abiega, O., Deudero, J.J., Brewster, A.L., Bernales, I., Anderson, A.E., Baekelandt, V., Maletić-Savatić, M. & Encinas, J.M. (2015) Neuronal hyperactivity accelerates depletion of neural stem cells and impairs hippocampal neurogenesis. *Cell Stem Cell*, **16**, 488-503.

Silvestro, S., Mammana, S., Cavalli, E., Bramanti, P. & Mazzon, E. (2019) Use of cannabidiol in the treatment of epilepsy: efficacy and security in clinical trials. *Molecules*, **24**, 1459.

Singh, J., Song, Z-H. & Reggio, P.H. (2012) Structure of a cannabinoid receptor subtype 2 homodimer determined by cysteine and homobifunctional crosslinking experiments combined with computational studies. *Biophys J*, **102**, 244a.

Skluzacek, J.V., Watts, K.P., Parsy, O., Wical, B. & Camfield, P. (2011) Dravet syndrome and parent associations: The IDEA League experience with comorbid conditions, mortality, management, adaptation, and grief. *Epilepsia*, **52**, 95-101.

Soltesz, I., Alger, B.E., Kano, M., Lee, S.H., Lovinger, D.M., Ohno-Shosaku, T. & Watanabe, M. (2015) Weeding out bad waves: towards selective cannabinoid circuit control in epilepsy. *Nat Rev Neurosci*, **16**, 264-277.

Sorrells, S.F., Paredes, M.F., Cebrian-Silla, A., Sandoval, K., Qi, D., Kelley, K.W., James, D., Mayer, S., Chang, J., Auguste, K.I., Chang, E.F., Gutierrez, A.J., Kriegstein, A.R., Mathern, G.W., Oldham, M.C., Huang, E.J., Garcia-Verdugo, J.M., Yang, Z. & Alvarez-Buylla, A. (2018) Human hippocampal neurogenesis drops sharply in children to undetectable levels in adults. *Nature*, **555**, 377-381.

Stafstrom, C.E. (2009) Severe epilepsy syndromes of early childhood: the link between genetics and pathophysiology with a focus on SCN1A mutations. *J Child Neurol*, **24**, 15S-23S.

Stamatovic, S.M., Johnson, A.M., Keep, R.F. & Andjelkovic, A.V. (2016) Junctional proteins of the blood-brain barrier: New insights into function and dysfunction. *Tissue Barriers*, **4**, e1154641.

Stamatovic, S.M., Keep, R.F. & Andjelkovic, A.V. (2008) Brain endothelial cell-cell junctions: how to "open" the blood brain barrier. *Curr Neuropharmacol*, **6**, 179-192.

Steel, D., Symonds, J.D., Zuberi, S.M. & Brunklaus, A. (2017) Dravet syndrome and its mimics: Beyond SCN1A. *Epilepsia*, **58**, 1807-1816.

Steinborn, B., Zarowski, M., Winczewska-Wiktor, A., Wójcicka, M., Młodzikowska-Albrecht, J. & Losy, J. (2014) Concentration of Il-1β, Il-2, Il-6, TNFα in the blood serum in children with generalized epilepsy treated by valproate. *Pharmacol Rep*, **66**, 972-975.

Steindel, F., Lerner, R., Häring, M., Ruehle, S., Marsicano, G., Lutz, B. & Monory, K. (2013) Neuron-type specific cannabinoid-mediated G protein signalling in mouse hippocampus. *J Neurochem*, **124**, 795-807.

Stempel, A.V., Stumpf, A., Zhang, H.Y., Ozdogan, T., Pannasch, U., Theis, A.K., Otte, D.M., Wojtalla, A., Racz, I., Ponomarenko, A., Xi, Z.X., Zimmer, A. & Schmitz, D. (2016) Cannabinoid type 2 receptors mediate a cell type-specific plasticity in the hippocampus. *Neuron*, **90**, 795-809.

Sugiura, T. (2008) Biosynthesis of anandamide and 2-arachidonoylglycerol. *Cannabinoids and the Brain*, 15-30.

Sula, A., Booker, J., Ng, L.C.T., Naylor, C.E., DeCaen, P.G. & Wallace, B.A. (2017) The complete structure of an activated open sodium channel. *Nat Commun*, **16**, 14205.

T

Takechi, R., Galloway, S., Pallebage-Gamarallage, M.M., Wellington, C.L., Johnsen, R.D., Dhaliwal, S.S. & Mamo, J.C. (2010) Differential effects of dietary fatty acids on the cerebral distribution of plasma-derived apo B lipoproteins with amyloid-beta. *Br J Nutr*, **103**, 652-662.

Tarragon, E. & Moreno, J.J. (2019) Cannabinoids, chemical senses, and regulation of feeding behavior. *Chem Senses*, **44**, 73-89.

Tchekalarova, J., da Conceição Machado, K., Gomes Júnior, A.L., de Carvalho Melo Cavalcante, A.A., Momchilova, A. & Tzoneva, R. (2018) Pharmacological characterization of the cannabinoid receptor 2 agonist, β-caryophyllene on seizure models in mice. *Seizure*, **57**, 22-26.

Thiele, E.A., Marsh, E.D., French, J.A., Mazurkiewicz-Beldzinska, M., Benbadis, S.R., Joshi, C., Lyons, P.D., Taylor, A., Roberts, C., Sommerville, K. & GWPCARE4 Study Group (2018) Cannabidiol in patients with seizures associated with Lennox-Gastaut syndrome (GWPCARE4): a randomised, double-blind, placebo-controlled phase 3 trial. *Lancet*, **391**, 1085-1096.

Thurman, D.J., Beghi, E., Begley, C.E., Berg, A.T., Buchhalter, J.R., Ding, D., Hesdorffer, D.C., Hauser, W.A., Kazis, L., Kobau, R., Kroner, B., Labiner, D., Liow, K., Logroscino, G., Medina, M.T., Newton, C.R., Parko, K., Paschal, A., Preux, P.M., Sander, J.W., Selassie, A., Theodore, W., Tomson, T. & Wiebe, S. (2011) Standards for epidemiologic studies and surveillance of epilepsy. *Epilepsia*, **52**, 2-26.

Tian, X., Liu, H., Xiang, F., Xu, L. & Dong, Z. (2019) β-caryophyllene protects against ischemic stroke by promoting polarization of microglia toward M2 phenotype via the TLR4 pathway. *Life Sci*, **237**, 116915.

Trinka, E., Cock, H., Hesdorffer, D., Rossetti, A.O., Scheffer, I.E., Shinnar, S., Shorvon, S. & Lowenstein, D.H. (2015) A definition and classification of status epilepticus: report of the ILAE task force on classification of status epilepticus. *Epilepsia*, **56**, 1515-1523.

Tsai, M.S., Lee, M.L., Chang, C.Y., Fan, H.H., Yu, I.S., Chen, Y.T., You, J.Y., Chen, C.Y., Chang, F.C., Hsiao, J.H., Khorkova, O., Liou, H.H., Yanagawa, Y., Lee, L.J. & Lin, S.W. (2015) Functional and structural deficits of the dentate gyrus network coincide with emerging spontaneous seizures in an Scn1a mutant Dravet Syndrome model during development. *Neurobiol Dis*, **77**, 35-48.

Turcotte, C., Blanchet, M.R., Laviolette, M. & Flamand, N. (2016) The CB_2 receptor and its role as a regulator of inflammation. *Cell Mol Life Sci*, **73**, 4449-4470.

V

Valcárcel-Martín, R., Martín-Suárez, S., Muro-García, T., Pastor-Alonso, O., Rodríguez de Fonseca, F., Estivil-Torrús, G. & Encinas, J.M. (2020) Lysophosphatidic acid receptor 1 specifically labels seizure-induced hippocampal reactive neural stem cells and regulates their division. *Front Neurosci*, **14**, 811.

Valdeolivas, S., Sagredo, O., Delgado, M., Pozo, M.A. & Fernández-Ruiz, J. (2017) Effects of a Sativex-like combination of phytocannabinoids on disease progression in R6/2 mice, an experimental model of Huntington's disease. *Int J Mol Sci*, **18**, 684.

Vergnes, L., Péterfy, M., Bergo, M.O., Young, S.G. & Reue, K. (2004) Lamin B1 is required for mouse development and nuclear integrity. *Proc Natl Acad Sci USA*, **101**, 10428-10433.

Verheyen, K., Verbecque, E., Ceulemans, B., Schoonjans, A. S., Van De Walle, P. & Hallemans, A. (2019) Motor development in children with Dravet syndrome. *Dev Med Child Neurol*, **61**, 950-956.

Vezzani, A. (2011) The role of inflammation in epilepsy. *Nat Rev Neurol*, **7**, 31-40.

Vezzani, A., Balosso, S. & Ravizza, T. (2008) The role of cytokines in the pathophysiology of epilepsy. *Brain Behav Immun*, **22**, 797-803.

Vezzani, A., Balosso, S. & Ravizza, T (2019) Neuroinflammatory pathways as treatment targets and biomarkers in epilepsy. *Nat Rev Neurol*, **15**, 459-472.

Vezzani, A. & Granata, T. (2005) Brain inflammation in epilepsy: experimental and clinical evidence. *Epilepsia*, **46**, 1724-1743.

Vilela, L.R., Lima, I.V., Kunsch, É., Pinto, H., de Miranda, A.S., Vieira, É., de Oliveira, A., Moraes, M., Teixeira, A.L. & Moreira, F.A. (2017) Anticonvulsant effect of cannabidiol in the pentylenetetrazole model: Pharmacological mechanisms, electroencephalographic profile, and brain cytokine levels. *Epilepsy Behav*, **75**, 29-35.

Villanueva, V., Carreño-Martínez, M., Gil Nagel-Rein, A. & López-González, F.J. (2021) New therapeutic approach in Dravet syndrome and Lennox-Gastaut syndrome with cannabidiol. *Rev Neurol*, **72**, S1-S10.

Viñals, X., Moreno, E., Lanfumey, L., Cordomí, A., Pastor, A., de La Torre, R., Gasperini, P., Navarro, G., Howell, L.A., Pardo, L., Lluís, C., Canela, E.I., McCormick, P.J., Maldonado, R. & Robledo, P. (2015) Cognitive impairment induced by Delta9-tetrahydrocannabinol occurs through heteromers between cannabinoid CB_1 and serotonin 5-HT2A receptors. *PLoS Biol*, **13**, e1002194.

Viveros-Paredes, J.M., González-Castañeda, R.E., Gertsch, J., Chaparro-Huerta, V., López-Roa, R.I., Vázquez-Valls, E., Beas-Zarate, C., Camins-Espuny, A. & Flores-Soto, M.E. (2017) Neuroprotective effects of β-caryophyllene against dopaminergic neuron injury in a murine model of Parkinson's disease induced by MPTP. *Pharmaceuticals (Basel)*, **10**, 60.

von Rüden, E.L., Bogdanovic, R.M., Wotjak, C.T. & Potschka, H. (2015) Inhibition of monoacylglycerol lipase mediates a cannabinoid 1-receptor dependent delay of kindling progression in mice. *Neurobiol Dis*, **77**, 238-245.

Vučković, S., Srebro, D., Vujović, K.S., Vučetić, Č. & Prostran, M. (2018) Cannabinoids and pain: new insights from old molecules. *Front Pharmacol*, **9**, 1259.

W

Wager-Miller, J., Westenbroek, R. & Mackie, K. (2002) Dimerization of G protein-coupled receptors: CB_1 cannabinoid receptors as an example. *Chem Phys Lipids*, **121**, 83-89.

Wirrell, E.C. (2016) Infantile, childhood and adolescent epilepsies. *Continuum (Minneapolis, Minn.)*, **22** (1, Epilepsy), 60-93.

Wirrell, E.C., Laux, L., Donner, E., Jette, N., Knupp, K., Meskis, M.A., Miller, I., Sullivan, J., Pharm, M.W. & Berg, A.T. (2017) Optimizing the diagnosis and management of Dravet syndrome: recommendations from a North American Consensus Panel. *Pediatr Neurol*, **68**, 18-34.

Wilson, R.I. & Nicoll, R.A. (2001) Endogenous cannabinoids mediate retrograde signalling at hippocampal synapses. *Nature*, **410**, 588-592.

Wirrell, E.C. & Nabbout, R. (2019) Recent advances in the drug treatment of Dravet syndrome. *CNS Drugs*, **33**, 867-881.

Wouters, E., Walraed, J., Banister, S.D. & Stove C.P. (2019) Insights into biased signaling at cannabinoid receptors: synthetic cannabinoid receptor agonists. *Biochem Pharmacol*, **169**, 113623.

Wu, C., Jia, Y., Lee, J.H., Jun, H.J., Lee, H.S., Hwang, K.Y. & Lee, S.J. (2014) Trans-caryophyllene is a natural agonistic ligand for peroxisome proliferator-activated receptor-α. *Bioorg Med Chem Lett*, **24**, 3168-3174.

Wu, Q. & Wang, H. (2018) The spatiotemporal expression changes of CB2R in the hippocampus of rats following pilocarpine-induced status epilepticus. *Epilepsy Res*, **148**, 8-16.

X

Xu, J.Y. & Chen, C. (2015) Endocannabinoids in synaptic plasticity and neuroprotection. *Neuroscientist*, **21**, 152-168.

Y

Yamanaka, G., Morichi, S., Takamatsu, T., Watanabe, Y., Suzuki, S., Ishida, Y., Oana, S., Yamazaki, T., Takata, F. & Kawashima, H. (2021) Links between immune cells from the periphery and the brain in the pathogenesis of epilepsy: a narrative review. *Int J Mol Sci*, **22**, 4395.

Yan, N., Xin-Hua, W., Lin-Mei, Z., Yi-Ming, C., Wen-Hui, L., Yuan-Feng, Z. & Shui-Zhen, Z. (2018) Prospective study of the efficacy of a ketogenic diet in 20 patients with Dravet syndrome. *Seizure*, **60**, 144-148.

Yokubaitis, C.G., Jessani, H.N., Li, H., Amodea, A.K. & Ward, S.J. (2021) Effects of cannabidiol and beta-caryophyllene alone or in combination in a mouse model of permanent ischemia. *Int J Mol Sci*, **22**, 2866.

Youssef, D.A., El-Fayoumi, H.M. & Mahmoud, M.F. (2019) Beta-caryophyllene alleviates diet-induced neurobehavioral changes in rats: The role of CB_2 and PPAR-γ receptors. *Biomed Pharmacother*, **110**, 145-154.

Yu, F.H., Mantegazza, M., Westenbroek, R.E., Robbins, C.A., Kalume, F., Burton, K.A., Spain, W.J., McKnight, G.S., Scheuer, T. & Catterall, W.A. (2006) Reduced sodium current in GABAergic interneurons in a mouse model of severe myoclonic epilepsy in infancy. *Nat Neurosci*, **9**, 1142-1149.

Z

Zaccara, G. & Schmidt, D. (2018) Antiepileptic drugs in clinical development: differentiate or die? *Curr Pharm Des*, **23**, 5593-5605.

Zattoni, M., Mura, M.L., Deprez, F., Schwendener, R.A., Engelhardt, B., Frei, K. & Fritschy, J.M. (2011) Brain infiltration of leukocytes contributes to the pathophysiology of temporal lobe epilepsy. *J Neurosci*, **31**, 4037-4050.

Zelasko, S., Arnold, W.R. & Das, A. (2015) Endocannabinoid metabolism by cytochrome P450 monooxygenases. *Prostaglandins Other Lipid Mediat*, **116-117**, 112-123.

Zhang, H.Y., Bi, G.H., Li, X., Li, J., Qu, H., Zhang, S.J., Li, C.Y., Onaivi, E.S., Gardner, E.L., Xi, Z.X. & Liu, Q.R. (2015) Species differences in cannabinoid receptor 2 and receptor responses to cocaine self-administration in mice and rats. *Neuropsychopharmacology*, **40**, 1037-1051.

Zhang, H.Y., Shen, H., Gao, M., Ma, Z., Hempel, B.J., Bi, G.H., Gardner, E.L., Wu, J. & Xi, Z.X. (2021) Cannabinoid CB_2 receptors are expressed in glutamate neurons in the red nucleus and functionally modulate motor behavior in mice. *Neuropharmacology*, **189**, 108538.

Zoerner, A.A., Gutzki, F.M., Batkai, S., May, M., Rakers, C., Engeli, S., Jordan, J. & Tsikas, D. (2011) Quantification of endocannabinoids in biological systems by chromatography and mass spectrometry: a comprehensive review from an analytical and biological perspective. *Biochim Biophys Acta*, **1811**, 706-723.

Zonis, S., Ljubimov, V.A., Mahgerefteh, M., Pechnick, R.N., Wawrowsky, K. & Chesnokova, V. (2013) p21Cip restrains hippocampal neurogenesis and protects neuronal progenitors from apoptosis during acute systemic inflammation. *Hippocampus*, **23**, 1383-1394

Zoratti, C., Kipmen-Korgun, D., Osibow, K., Malli, R. & Graier, W.F. (2003) Anandamide initiates Ca(2+) signaling via CB2 receptor linked to phospholipase C in calf pulmonary endothelial cells. *Br J Pharmacol*, **140**, 1351-1362.

Zuberi, S.M., Brunklaus, A., Birch, R., Reavey, E., Duncan, J. & Forbes, G.H. (2011) Genotype-phenotype associations in SCN1A-related epilepsies. *Neurology*, **76**, 594-600.

Zurolo, E., Iyer, A.M., Spliet, W.G., Van Rijen, P.C., Troost, D., Gorter, J.A. & Aronica, E. (2010) CB_1 and CB_2 cannabinoid receptor expression during development and in epileptogenic developmental pathologies. *Neuroscience*, **170**, 28-41.

ANNEX

PARTICIPATION IN SCIENTIFIC PUBLICATIONS

Satta, V.*, **Alonso, C.***, Díez, P., Martín-Suárez, S., Rubio, M., Encinas, J.M., Fernández-Ruiz, J. & Sagredo, O. (2021) Neuropathological characterization of a Dravet syndrome knock-in mouse model useful for investigating cannabinoid treatments. *Front Mol Neurosci*, **13**, 602801. *These authors share first authorship.

Alonso, C., Satta, V., Díez, P., Fernández-Ruiz, J. & Sagredo, O. (2021) Preclinical investigation of β-caryophyllene as a therapeutic agent in an experimental murine model of Dravet syndrome. *Neuropharmacology*. Under second review.